EVALUATION OF THE MECHANICAL AND PHYSICAL PROPERTIES OF FIBRE REINFORCED EPOXY COMPOSITES PRODUCED BY MICROWAVE ASSISTED RTM PROCESSING

A thesis submitted to The University of Manchester for the degree of
Doctor of Philosophy
in the Faculty of Engineering and Physical Sciences

2007

DIMITRIOS A. PAPARGYRIS

SCHOOL OF MATERIALS

ProQuest LLC.
789 East Eisenhower Parkway
P.O. Box 1346
Ann Arbor, MI 48106 – 1346

LIST OF CONTENTS

(Word count: 56,732)

LIST OF FIGURES

LIST OF TABLES

ABSTRACT

In this work, microwave heating was incorporated into the resin transfer moulding technique (RTM) and was used to successfully manufacture both carbon fibre and glass fibre epoxy composites. A new moulding tool constructed from Macor, a machinable glass ceramic, was employed in microwave RTM processing as a substitute for the metal mould employed in conventional thermal RTM processing. The LY/HY5052 epoxy-amine resin system was used as matrix, reinforced with woven carbon fibre and woven glass fibre fabric, respectively. Composites were also fabricated conventionally at the same cure temperature as in microwave processing for comparative reasons. The control system maintained a stable cure temperature by adjusting microwave power and achieved uniform heating by varying the excitation frequency between 4 – 8 GHz. The maximum power available in microwave heating was 250 W, as opposed to 4 kW in conventional heating. Through the use of microwave heating, a 50% cure cycle time reduction was achieved.

All fabricated composite panels exhibited minimal thickness variation and were fully cured, achieving a degree of cure of over 99%, while similar T_g values were obtained between conventionally and microwave cured samples. The glass transition, however, appeared to be more intense for the microwave cured LY/HY5052/carbon composites than those cured thermally. Although no difference in the intensity of the lower temperature β-transition was observed between the two types of LY/HY5052/carbon composites, the position of the β-transition peak was shifted by 15°C to a higher temperature for the microwave cured samples. Conversely, the intensities of the glass and β-transition for both thermally and microwave cured LY/HY5052/glass composites were similar. A smaller 4°C shift in the position of the β-transition peak to a higher temperature, however, was observed for the microwave cured samples. The microwave cured LY/HY5052/carbon composites exhibited a higher molecular weight between cross-links and a lower cross-link density than their thermally cured counterparts, while the corresponding values were comparable for both types of glass fibre composites. The intensities of the ether group absorption bands were increased in the IR spectra of the thermally cured LY/HY5052/carbon composites compared to those of their microwave cured counterparts, suggesting that the epoxide-hydroxyl etherification reaction occurred more readily during thermal cure. Nonetheless, this increase appeared to be less prominent between the two types of LY/HY5052/glass composites.

The produced composites exhibited minimal void contents (<2%) and overall defects. The flexural strength and flexural modulus of the microwave cured LY/HY5052/carbon composites were similar to those cured thermally, while their interlaminar shear strength was higher. On the other hand, the flexural properties and interlaminar shear strength were comparable between thermally and microwave cured LY/HY5052/glass composites. These findings were supported by observations of the fracture surface morphology of the composites subjected to mechanical testing via SEM. Furthermore, the dielectric properties of the uncured resin decreased exponentially with time during microwave curing. Both thermally and microwave cured LY/HY5052/carbon and LY/HY5052/glass composites, respectively, exhibited similar dielectric properties, with the exception of a higher dielectric constant for the thermally cured LY/HY5052/carbon composites compared to those cured with microwaves.

DECLARATION

No portion of the work referred to in this thesis has been submitted in support of an application for another degree or qualification of this or any other university or other institute of learning.

COPYRIGHT STATEMENT

DEDICATION

This thesis is solely dedicated to my family,
my father Athanasios, my mother Penelope,
and my sister Sophie

ACKNOWLEDGEMENT

I would like to express my gratitude and appreciation to Dr Richard Day for his supervision and guidance throughout this work.

I would also like to sincerely thank Dr Alan Nesbitt for his valuable help and advice as well as friendship throughout this project.

Thanks are due to all members of the Materials Science Centre and Northwest Composite Centre, who in their own way helped me to complete this research work. I owe special thanks to Poly Crook for her help in DSC and DMTA, Michael Faulkner for his help in SEM and Andy Zardoroshnyj for his technical assistance and help in mechanical testing. I would also like to thank all the technicians in the workshop, and especially Mark Harris and Gary Pickles, for their help in the construction of the ceramic moulding tool used in this study.

Furthermore, I would like to deeply thank all my old and new friends and colleagues who helped me during difficult times and were always there for me. In particular, Dimitrios Tsamakis, Dimitrios Bakavos, Stamatis Oikonomakos, Kostas Stathopoulos, Marek Hejda, Leon Davies, Andrew Sullivan, Kostas Kaifas, Dimitrios Psychogios, Dimitrios Tsivoulas, Ioanna Garefi, Christina Kataki, Irene Malachtari and Eleni Idrioti.

Finally, words can not describe the extent of my gratitude to my father, mother and sister for their encouragement to fulfil my dreams and aspirations as well as their morale and financial support, without which this work would not be possible.

CHAPTER 1

Introduction

1.1 Introduction

Fibre reinforced polymer composites have gained substantial interest over the recent years mainly due to their ability to combine the properties of different materials, which in turn allows them to exhibit very effective and versatile properties. This has led to the use and application of composite materials in several major industries, with the aerospace and automotive industry taking the larger part. The high operational costs of the manufacturing techniques currently employed, however, have restricted wider industrial use of composites hence considerable effort has been made towards finding and developing alternative cost-effective routes for curing composite materials.

One such alternative route is microwave processing, which offers several advantages over conventional thermal processing methods, including rapid, selective and volumetric heating, energy savings, reduced processing time and improved processing control [1-4]. A major limitation in the cost-effective manufacturing of composite materials is the long cure cycle times often involved. In conventional processing, thermal energy is initially deposited on the surface of the resin and is subsequently transferred to the bulk through conduction and convection. Given, however, the very poor thermal conductivity of polymeric materials, this process may not only be time-consuming but also result in thermal gradients through the thickness of the produced composites due to the different energy deposition rates between the surface and the bulk of the resin.

Microwave radiation, on the other hand, has the potential to substantially reduce cure cycle times, since it generates heat internally within the volume of the material rather than relying on heat transfer through conduction and convection. Thus, it is more appropriate to consider microwave heating as conversion of electromagnetic energy to thermal energy instead of heat transfer [5]. Typical cure cycle times are reduced from hours to tens of minutes or even less through microwave heating [2, 6-8]. Hence more economical industrial manufacture of composites can be achieved by means of shorter cure cycles and lower energy consumption due to the more efficient direct deposition of energy in the volume of the material. Nonetheless, there are

certain difficulties involved in microwave processing, arising primarily from the non-uniform distribution of the electromagnetic field within the applicator which can cause variations in the degree of cure across the produced composite panels. Microwave heating can also lead to arcing problems in some types of composites reinforced with carbon and aramid fibres.

Resin transfer moulding (RTM) is a common manufacturing process in which a liquid thermosetting resin is injected into a closed mould tool, previously loaded with a preform consisting of dry fibres, and then heated at a suitable temperature. Upon completion of the curing process, the mould can be opened and the finished part removed. Since conventional RTM relies on thermal curing of the resin inside the mould, it suffers from the same limitations as described earlier. Microwave heating can, thus, be coupled with the RTM technique in an effort to overcome these limitations and exploit the benefits provided by the former.

The aim of this work was to incorporate microwave heating into the RTM technique and develop a new microwave assisted RTM method which would successfully fabricate both carbon fibre and glass fibre reinforced epoxy composites on a laboratory scale. The mechanical and physical properties of the microwave cured composites were compared against those obtained by conventional thermal RTM processing, in order to assess the feasibility and effectiveness of microwave radiation as an alternative power source for curing composites as well as determine any repercussions microwave RTM processing might have on the attained composite properties and structure. Both types of composites were cured at the same curing temperature to accommodate the comparison between the two curing methods.

The mechanical properties of the fabricated composites were assessed through four-point bending and interlaminar shear testing, while the dimensional stability of the produced panels was evaluated in terms of thickness variation. Dynamic mechanical thermal analysis (DMTA) and differential scanning calorimetry (DSC) were used to study the thermal properties of the produced composites. The fibre and void volume fractions of the composites were determined through the hot acid digestion method and optical microscopy. Furthermore, scanning electron microscopy (SEM) was employed to examine the fracture surfaces of the samples subjected to mechanical

testing, while ultrasonic C-scan inspection was used to detect defects in the fabricated panels and assess their overall quality. Density and dielectric measurements were also conducted on the uncured resin and the cured composites. Finally, Fourier transform infrared spectroscopy (FTIR) was employed in order to examine differences in the network structure formed during the curing process between conventionally and microwave cured composite samples.

CHAPTER 2

Literature Review

2.1 Composite Materials

A composite material is a material that consists of two or more constituent materials or phases. The constituents of a composite are arranged so that one or more discontinuous phases are embedded in a continuous phase. The discontinuous phase is known as the *reinforcement* and the continuous phase as the *matrix*. The mechanical and physical properties of composites depend on the properties, geometry and concentration of the constituents. In general, the strength and stiffness of a composite derive from the reinforcement, usually in the form of fibres, while the matrix supports, separates and protects the fibres.

Composite materials are usually categorized according to the type of reinforcement used. The two main types of composites, therefore, are fibrous and particulate. The fibres used in fibrous composites include carbon, glass, boron and aramid. There is also a wide variety of materials that can be used as matrix in composite materials such as carbon, ceramics, glasses, metals or polymers (resins). Polymers or resins are further classified under two types, thermoplastic and thermosetting resins, which will be further discussed below.

2.2 Resin System

The principle role of the matrix in a fibre-reinforced composite is to transfer stresses between the fibres, provide a barrier against an adverse environment and protect the surface of the fibres from mechanical abrasion [9]. Polymers (commonly called plastics) are defined as materials with long chain molecules that contain one or more repeating units of atoms. As mentioned previously, the two main types of polymer materials are thermoplastic and thermosetting resins.

Thermoplastic resins are characterised by a linear structure of individual molecules with no chemical linking between them. These molecules are held together by weak secondary bonds (intermolecular bonds) such as van der Waals and hydrogen bonds. These intermolecular bonds can be temporarily broken upon application of heat and

pressure, thus allowing the molecules to rearrange their positions by moving relative to each other through liquid flow. Once they are cooled, however, the molecules freeze in their new positions by restoring the secondary bonds between them which results in the formation of a new solid shape. In that way, a thermoplastic polymer can be heat softened, melted and reshaped (post formed) as many times as desired [9]. Examples of commonly employed thermoplastic resins are polyvinyl chloride (PVC), polypropylene, polyethylene and polystyrene, while some more recently developed thermoplastic resins are polyphenylene sulfide (PPS), polyether ether ketone (PEEK) and polyether sulfone (PES).

Thermosetting resins, on the other hand, are characterised by a tightly bound and rigid three-dimensional network structure which is formed as a result of chemical cross-linking between the resin molecules. These cross-links are usually achieved by application of heat during the polymerisation process which is also called curing. After these cross-links are formed, the thermosetting resins can not be reshaped or melted by application of heat or pressure, as thermoplastics. Hence thermosets can only be processed once. These characteristics make thermosetting resins a lot more popular in the manufacturing of composite materials compared to thermoplastics. Some of the types of commonly employed thermosetting resins include epoxies, polyesters, vinyl esters and bismaleimides. The resin system used in this work was an epoxy resin with amine hardeners hence the chemical structure and properties of epoxy resins will be extensively discussed below, while those of other thermosetting resins will be briefly mentioned.

2.2.1 Epoxy Resins

2.2.1.1 Structure and Properties

Epoxy resins were first synthesized in Switzerland and the United States in the mid 1930s. Since then epoxy resins, also known as epoxides, are widely used in different applications such as adhesives, coatings and reinforced plastics. They are categorized as thermosetting materials due to the fact that when reaction with a curing agent occurs, a network cross-linked in all three dimensions is formulated. The dense

arrangement of that network is opposed to any movement on behalf of the participating molecules, which in turn results in the transformation of the originally liquid epoxy resins into tough, hard thermoset solids.

The structure of the basic epoxy resin molecule is characterized by the reactive epoxy group (Figure 2.1), which consists of a three-membered ring that includes an oxygen atom attached to two connected carbon atoms:

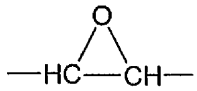

Figure 2.1: *The epoxide group.*

This structure reacts readily with a lot of substances and especially with compounds that possess active hydrogen atoms [10] such as acids:

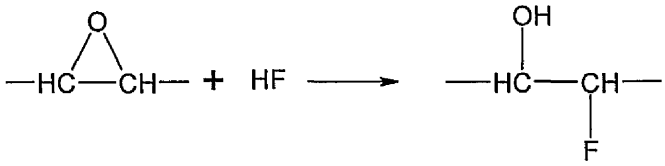

Figure 2.2: *Epoxide reaction with hydrofluoride.*

The properties of a cured epoxy resin depend primarily on the cross-link density which is the distance between successive cross-links. In general, characteristics such as the glass transition temperature, tensile modulus, thermal stability and chemical resistance are enhanced as the cross-link density is increased. The strain-to-failure, however, and the fracture toughness are reduced [9]. The cross-link density can be influenced by several factors such as the chemical structure of the starting material (i.e. the number of epoxide groups per molecule and the spacing between them), the functionality of the curing agent (i.e. the number of active hydrogen atoms) and the curing conditions (i.e. temperature and time).

The major advantages of epoxy resins over the other thermosetting matrices are the wide range of properties, since a large number of starting materials, curing agents, and modifiers are available, the absence of volatiles and the low shrinkage during

cure, the outstanding resistance to solvents and chemicals and the excellent adhesion to a broad range of fibres, fillers and other substrates. On the other hand, epoxy resins are relatively expensive compared to other thermosets and they usually require a long cure time. Some typical properties of cured epoxies are shown below in Table 2.1 [11].

Table 2.1: *Typical properties of cured epoxy resins* [11].

Glass Transition Temperature (°C)	120-190
Maximum Continuous Service Temperature (°C)	130
Specific Gravity	1.11 – 1.14
Thermal Conductivity (W/m.K)	0.88
Coefficient of Linear Thermal Expansion ($1/°K \times 10^{-16}$)	11 - 35
Tensile Modulus (GPa)	2.1 – 5.5
Tensile Strength (MPa)	28 - 90
Compressive Strength (MPa)	240
Water Absorption (vol %)	0.05 – 0.2

2.2.1.2 Synthesis of the Basic Epoxy Resin Molecule

The epoxy molecule, in its simplest form, is represented by the diglycidyl ether of bisphenol A, which is derived from bisphenol A and epichlorohydrin (Figure 2.3). The former is produced from acetone and phenol [12] as follows:

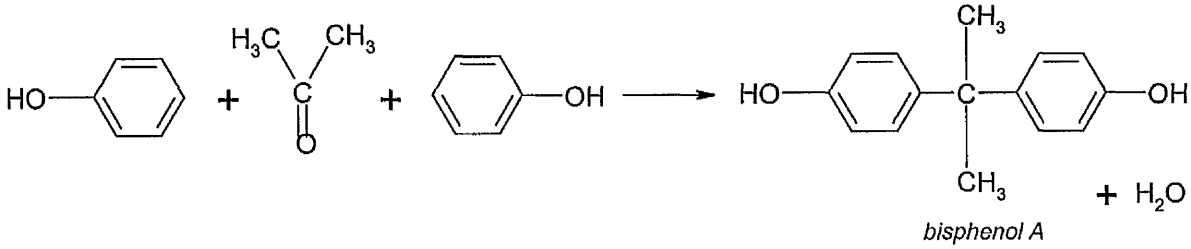

Figure 2.3: *Formation of bisphenol A from the reaction of acetone with phenol.*

The latter is prepared from propylene and chlorine as shown in Figure 2.4:

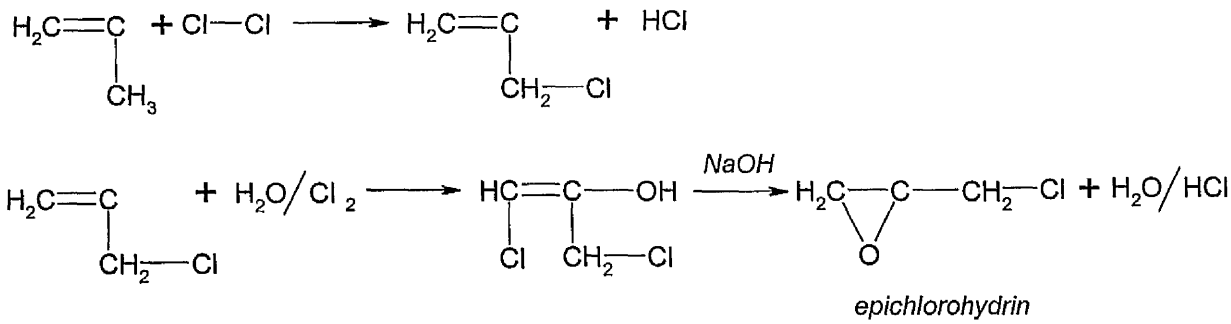

Figure 2.4: *Formation of epichlorohydrin from the reaction of propylene with chlorine.*

The reaction of bisphenol A with epichlorohydrin in the presence of a base (NaOH) results in the formation of the diglycidyl ether of bisphenol A, as shown below in Figure 2.5:

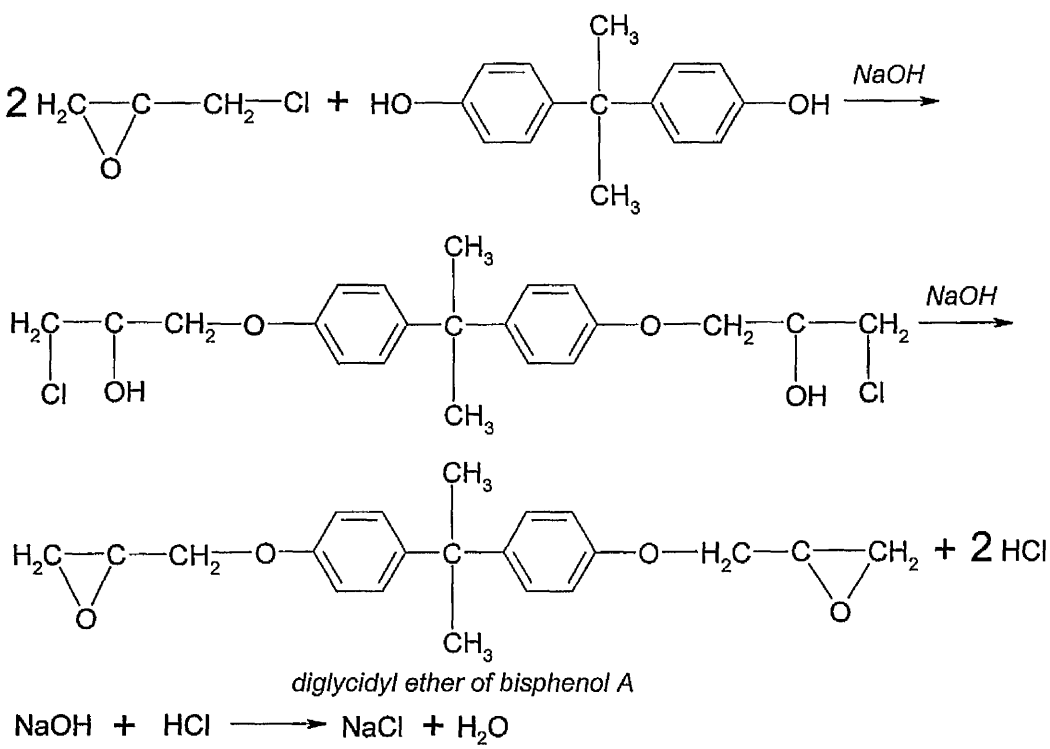

Figure 2.5: *Formation of diglycidyl ether of bisphenol A from the reaction of epichlorohydrin with bisphenol A in a basic environment.*

The purpose of the base is to neutralize the hydrochloric acid produced as a by-product of the dehydrohalogenation and catalyze the polymerization via the epoxy groups. In order to obtain high yields of the monomeric product (70% or more), excess epichlorohydrin should be used. Otherwise, if the stoichiometric ratio 2:1 is followed, the resulting monomeric product will be less than 10% and higher molecular-weight polymerization and condensation products will be also produced.

It is therefore possible to synthesize higher molecular-weight epoxy resins by controlling the degree of polymerization. The general formula for such resins can be written as shown in Figure 2.6:

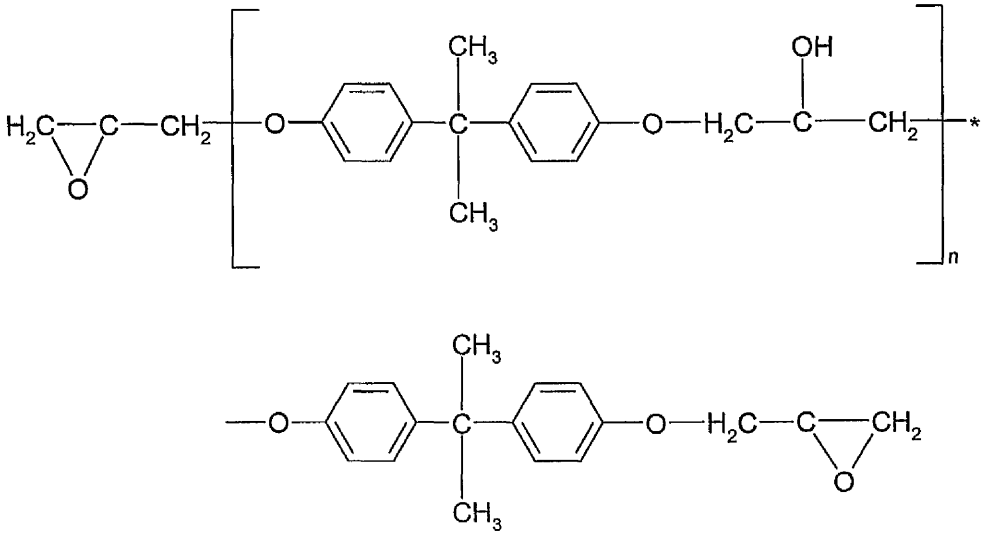

Figure 2.6: *Generalised formula of the epoxy resin molecule.*

where n is the number of repeated units in the resin chain. The molecular weights of commercial epoxy resins differ from 340 to about 4000, with n = 0 and n = 12 respectively.

The degree at which polymerization occurs can be governed by modifying the ratio of epichlorohydrin/bisphenol A in the reaction, while using an excess amount of base than that required to neutralize the produced hydrochloric acid and catalyze the reaction. It is reported though [13, 14] that in practice, there is again a slight excess of epichlorohydrin employed (apparently over the amount defined by the stoichiometric ratio for a given molecular weight).

2.2.1.3 Curing of Epoxy Resins

A curing agent (or hardener or catalyst or activator) is a chemical reagent that initiates the transformation of epoxy resins from a liquid state to rigid and tough materials. This transformation takes place in two stages. First, the liquid resin is transformed to a viscous gel upon addition of the hardener due to the formation of a cross-linked network. This is an irreversible process called gelation. Subsequently, the gelled resin is transformed to a brittle glassy solid, as a three dimensional cross-linked network is formed in a reversible process called vitrification.

The overall process is referred to as the curing process and can be described by the following three reactions [15]:

1. Direct linkage between epoxy groups *(epoxy-epoxy polymerisation also known as homopolymerisation)*
2. Linkage of epoxy groups with aromatic or aliphatic hydroxyl groups *(epoxy-hydroxyl polymerization also known as etherification)*
3. Cross-linkage with the curing agent

The resin remains in the form of a gelled rubber as long as the glass transition temperature T_g stays below the cure temperature T_{cure}. When T_{cure} exceeds the T_g of the epoxy resin, vitrification occurs. In order to attain the ultimate value of T_g and obtain the maximum degree of cross-linking, vitrification should occur after the resin has fully gelled. Otherwise, the full strength and stiffness of the material can not be realised. Therefore, the cure temperature as well as the duration of the curing process should be chosen with much consideration for each resin system. The gelled rubber is also often heated after the main curing process for a certain period of time (post cure) in order to further increase the degree of cross-linking of the resin.

Polymerisation through Epoxy Groups

In the first mechanism, the epoxy group ring may be opened not only by available ions and active hydrogen atoms but also by tertiary amines (R_3N) in the following manner (Figure 2.7):

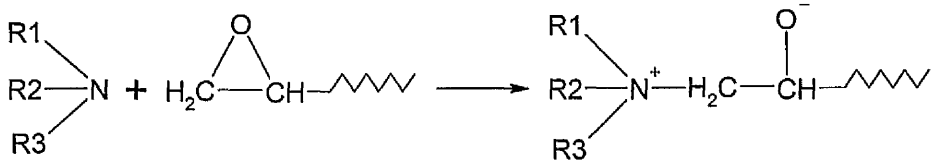

Figure 2.7: *Epoxy group ring opening reaction by tertiary amines.*

The formulated ion can then open up a new epoxy group (Figure 2.8)

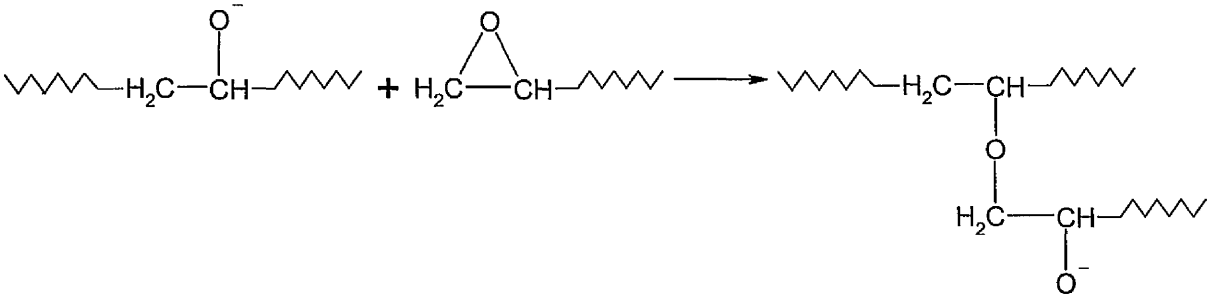

Figure 2.8: *Reaction of the oxygen ion formed upon opening of an epoxy group ring with a new epoxy group.*

and the reaction proceeds as a long chain system is created (Figure 2.9).

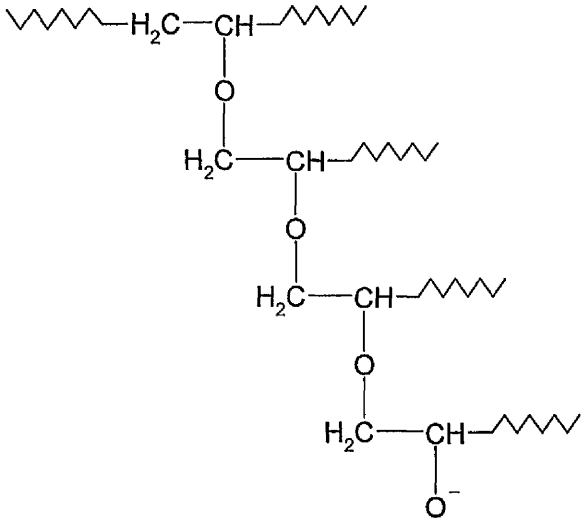

Figure 2.9: *Chain system in epoxy-epoxy polymerisation.*

It is obvious that since the reaction can occur at both ends of the molecule, a three-dimensional cross-linked structure will develop. The termination of the chain building process will randomly occur when the final activated epoxy is blocked off. In particular, as the chain system progresses to enlarge, some epoxy groups will inevitably be trapped between other chains with no groups close enough to react with.

Polymerisation through Hydroxyl Groups

The epoxy groups under suitable conditions can readily react with hydroxyl groups, initiating the epoxy-hydroxyl polymerization reaction (etherification) represented below in Figure 2.10:

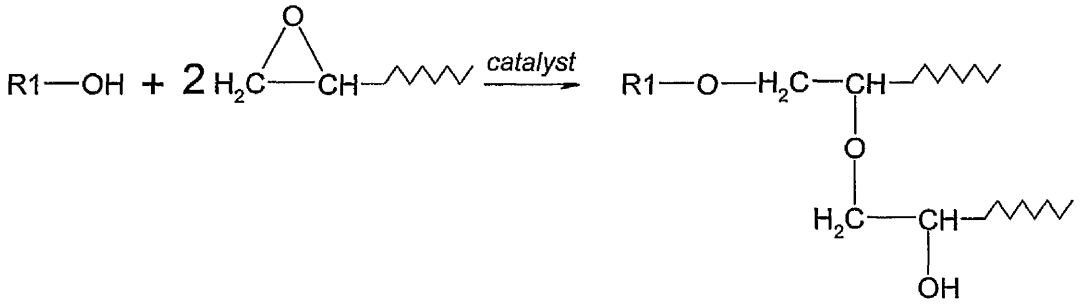

Figure 2.10: *Reaction of a hydroxyl group with an epoxy group in epoxy-hydroxyl polymerisation.*

The created chain structure highly resembles that of the previous polymerization mechanism and as before a high degree of cross-linking is achieved. The presence of a catalyst is essential for the reaction to commence, as noted in the equation. The catalyst can be either an acid or a base. Acid catalysts mainly consist of primary and secondary amines, which will be discussed in the next curing mechanism. The fundamental agents used to catalyze epoxy-hydroxyl reactions are inorganic bases, such as sodium hydroxide (employed in resin synthesis) and tertiary amines (employed in resin cure).

Curing by Cross-linking Agents

The chains of the epoxy resins can also be joined together with the assistance of reactive cross-linking agents (or hardeners), acting as intermediates. The principal reactive cross-linking agents are polyfunctional primary and secondary amines. Organic dibasic acids and acid anhydrides have also been used as second class hardeners. However, polyfunctional phenols such as bisphenol A or resorcinol have been suggested as cross-linking agents as well.

Polyfunctional primary (RNH_2) and secondary (R_2NH) amines have been frequently used for the curing of epoxy resins. Every primary amine is potentially capable of reacting with two epoxy groups through the corresponding two active hydrogen atoms that it possesses (see Figure 2.11).

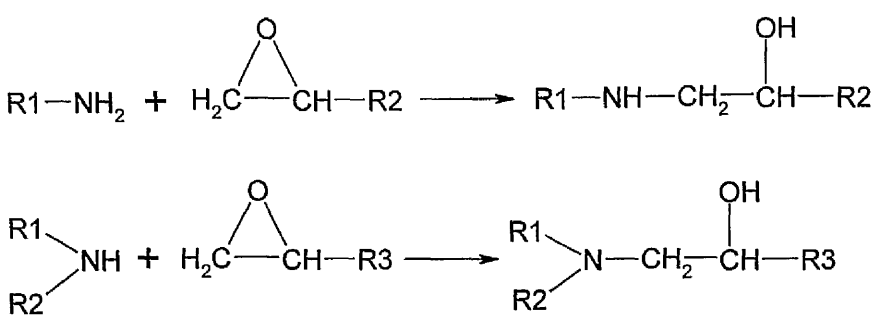

Figure 2.11: *Reactions of primary and secondary amine with epoxy groups.*

The OH adducts formed by the reaction of either primary or secondary amines with epoxy groups can later react with another epoxide ring in an etherification reaction to further cross-link the epoxy resin, as discussed in the previous mechanism [16]. The etherification reactions of the OH adducts with the epoxy groups are shown in Figure 2.12:

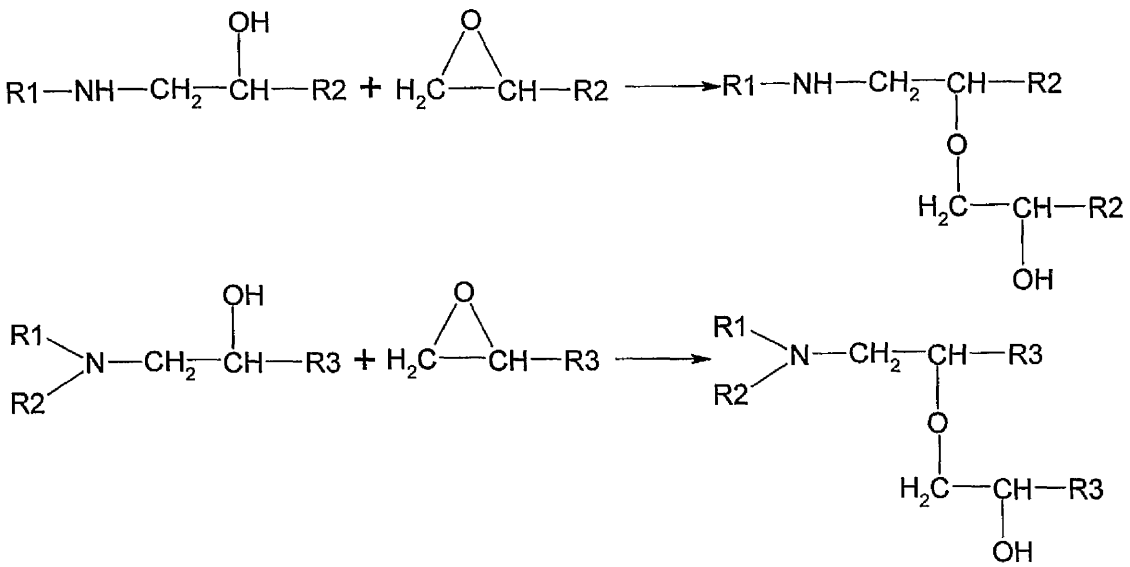

Figure 2.12: *Etherification reaction of the OH adducts formed by the reaction of primary and secondary amines with epoxy groups* [16].

Some of the different types of commercially employed amine hardeners such as diethylenetriamine, triethylenetetramine and other aromatic amines are shown below in Figure 2.13 [17].

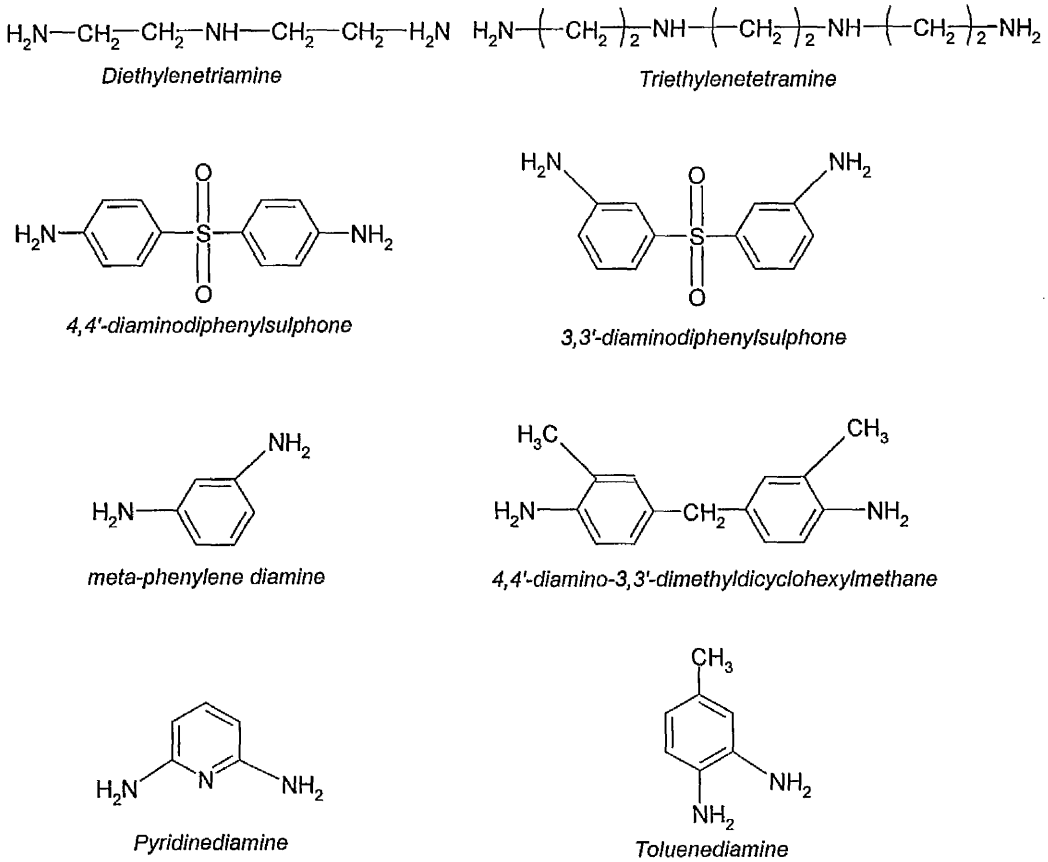

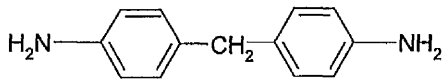

Diaminodiphenylmethane

Figure 2.13: *Chemical structures of commercially employed amine hardeners* [17].

In addition, organic dibasic and polybasic acids such as oxalic acid are used for the esterification of epoxy resins via an epoxy-acid reaction:

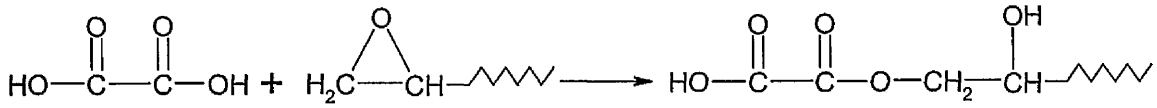

Figure 2.14: *Reaction of oxalic acid with epoxy group.*

Acid anhydrides react in a similar manner, but the first reaction that occurs is the opening of the anhydride ring by an alcoholic hydroxyl (or salt or trace of water). The nascent carboxylic group can then react with an epoxy group, as shown in Figure 2.15. For example in the case of the phthalic anhydride the reaction mechanism can be written as follows:

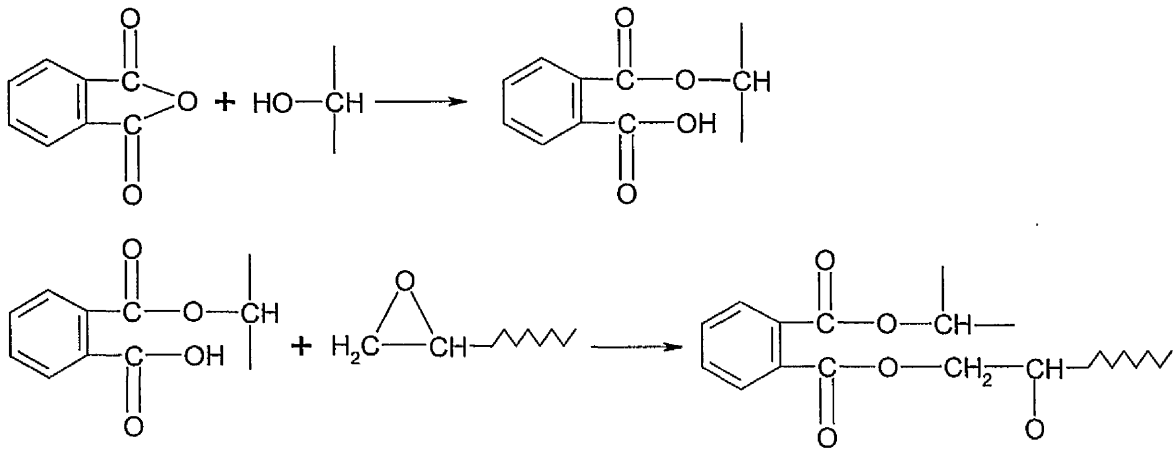

Figure 2.15: *Reaction of phthalic anhydride with epoxy group.*

Besides the amine, acid or acid anhydride curing agents, cross-linking of the epoxy resins may also be accomplished by employing a system that includes both a catalyst

(such as tertiary amines) and a cross-linking agent (such as primary or secondary amines, acid anhydrides or polybasic acids).

2.2.1.4 Diluents, Filers and Modifiers

Diluents are free-flowing liquids used to lower the viscosity of the resin in order to achieve better penetration in casting and to improve the wetting ability of adhesive and laminating formulations. Some of the diluents employed commercially are the following (Figure 2.16):

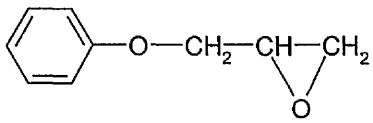

Phenyl glycidyl ether (mol. wt 150)

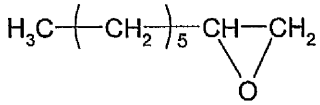

Octylene oxide (mol. wt 128)

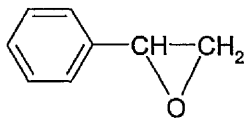

Styrene oxide (mol. wt 120) (little used, toxic)

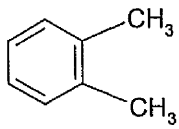

Xylene (mol. wt 98) (non-reactive)

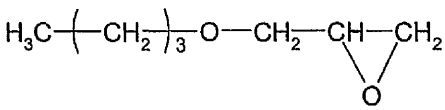

Butyl glycidyl ether (mol. wt 130)

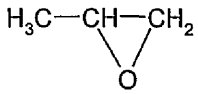

Propylene oxide (mol. wt 56) (little used, volatile)

Figure 2.16: *Chemical structures of commercially employed diluents.*

Diluents generally degrade the physical properties of cured epoxy resins. To be specific, when reactive diluents are employed, the chain building process is repressed due to their lower functionality compared to that of the resin. On the other hand, when the diluents are inert, a portion may be driven off during cure, resulting in increased shrinkage and reduced adhesion. Diluents also reduce hardness as well as heat-distortion temperatures but tend to increase by a considerable value the coefficient of thermal expansion of a resin system [5].

Fillers are organic or inorganic, metallic or nonmetallic substances added to epoxy resins to reduce cost, decrease shrinkage, lower the coefficient of thermal expansion, increase thermal conductivity, reduce exotherms, change surface hardness, improve adhesion and alter the handling characteristics of the resin system in order to achieve the desired flow or thixotropic properties. The main restriction concerning fillers is that they should be neutral or slightly basic and non-reactive with either the curing agent or the resin.

There is also a wide range of synthetic resins that can be used together with epoxy resins in order to modify the properties of the cured system. These synthetic resins are compatible with epoxies and are known as resinous modifiers. Some typical types of modifiers are phenols, polyesters, vinyl esters, polyurethanes and silicone resins. Each type of modifier when used in the original epoxy resin imparts different properties in the overall system. For instance, phenolic resins may be employed to raise heat-distortion temperatures in some systems, when other resins are used to increase impact strength or flexibility. Lower-priced modifiers may also be used in considerable percentages to lower the total cost of the epoxy resin system. In general, the best results are obtained when the employed modifiers are to some extent reactive with the epoxies, rather than acting as inert organic fillers. Polyurethanes and silicone resins are two types of modifiers that have been extensively studied and experimented and will be further discussed below.

Isocyanates (Polyurethanes)

Isocyanates contain the very reactive –N=C=O group, which reacts readily with hydroxyl groups present in the epoxy resin chains providing cross-linking, as presented in the following mechanism (Figure 2.17):

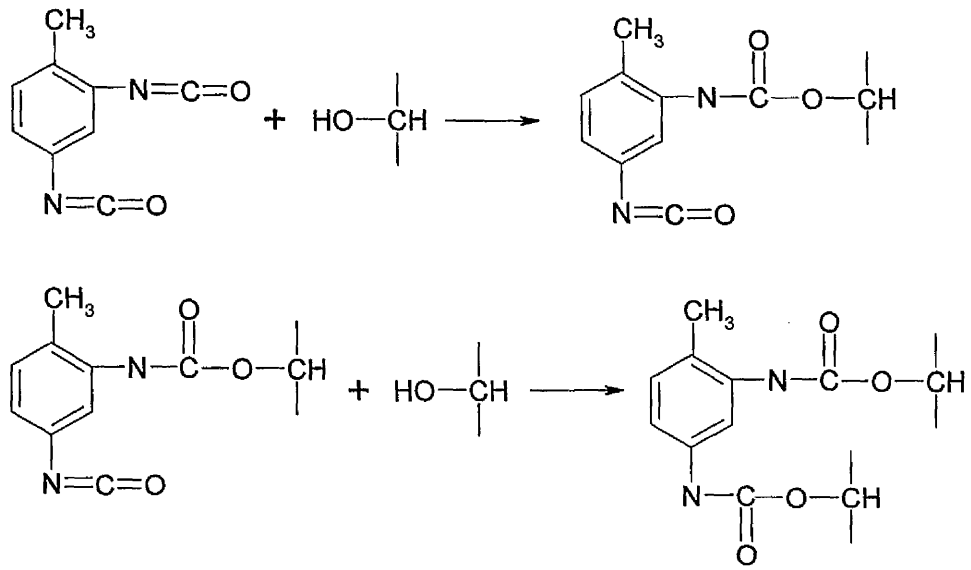

Figure 2.17: *Reaction of isocyanates with the hydroxyl groups of epoxy resins.*

Silicone Resins

Silicone polymers are typically very weak and soft mechanically, but they exhibit high thermal stability and electrical resistance, mainly due to the presence of the silicone atom. The epoxy resins on the other hand, possess good electrical and mechanical properties along with ease of handling. Thus, a combination which exploits the useful properties of both, can offer new materials suitable for coating or high temperature electrical insulation.

2.2.2 Polyester, Vinyl Ester and Bismaleimide Resins

Apart from epoxy resins, other widely used thermosetting resins include polyester, vinyl ester and bismaleimide resins. Their basic properties and chemical structures are briefly discussed below.

Polyester Resins

The chemical structure of a typical unsaturated polyester molecule contains a number of C = C double bonds and results from the reaction of maleic anhydride with ethylene glycol, as shown in Figure 2.18(a). Isophthalic or orthophthalic acids are also added to modify the chemical structure between the cross-linking sites. The resulting polyester liquid is dissolved in a reactive diluent, such as styrene (Figure 2.18(b)), which makes it easier to handle by reducing its viscosity. The diluent also contains C = C double bonds and helps in the cross-linking process by bridging neighbouring polyester molecules without the evolution of any by-products. Polyester resins have a limited storage life, since they will set or gel on their own over a long period of time. For that reason, trace amounts of inhibitors, such as hydroquinone or benzoquinone, are often added to delay premature polymerisation during storage.

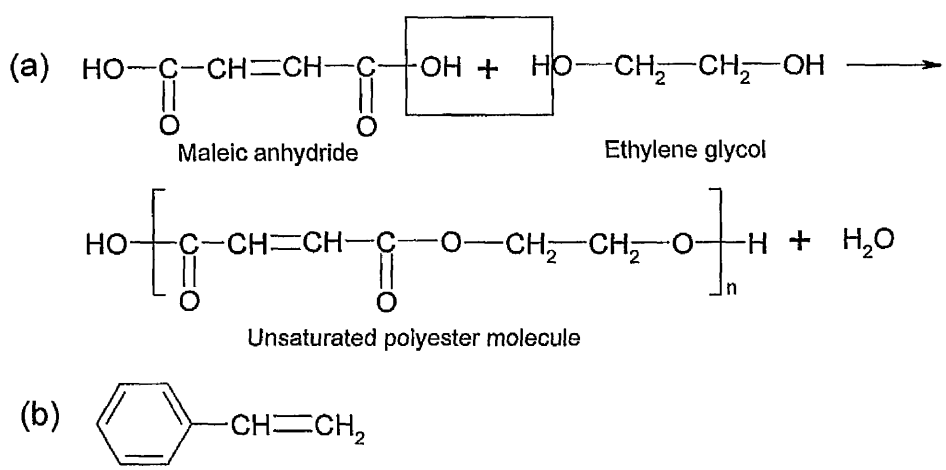

Figure 2.18: *(a) Formation of an unsaturated polyester molecule from the reaction of maleic anhydride with ethylene glycol (n = 3 to 5); (b) Structure of styrene.*

Polyesters are the most widely used resin systems, especially in the marine industry, with a whole range of resins formulated from different acids, glycols and monomers, all exhibiting different properties ranging from hard and brittle to soft and flexible. Their properties, however, are usually lower than those of epoxies. Polyester resins have short cure time, low cost and low viscosity but exhibit high volumetric shrinkage. Although the latter accommodates the removal of the finished parts from the mould, it causes undesirable surface defects or sink marks on the moulded surface.

Vinyl Ester Resins

Vinyl ester resins have a similar molecular structure with that of polyester resins, but differ in the location of their reactive sites (C = C double bonds) which are positioned only at the ends of the molecular chains. Figure 2.19 shows the structure of a typical vinyl ester resin resulting from the reaction of an unsaturated carboxylic acid, such as methacrylic or acrylic acid, with an epoxy resin. Vinyl esters are also dissolved in styrene monomer which lowers their viscosity, just like polyesters.

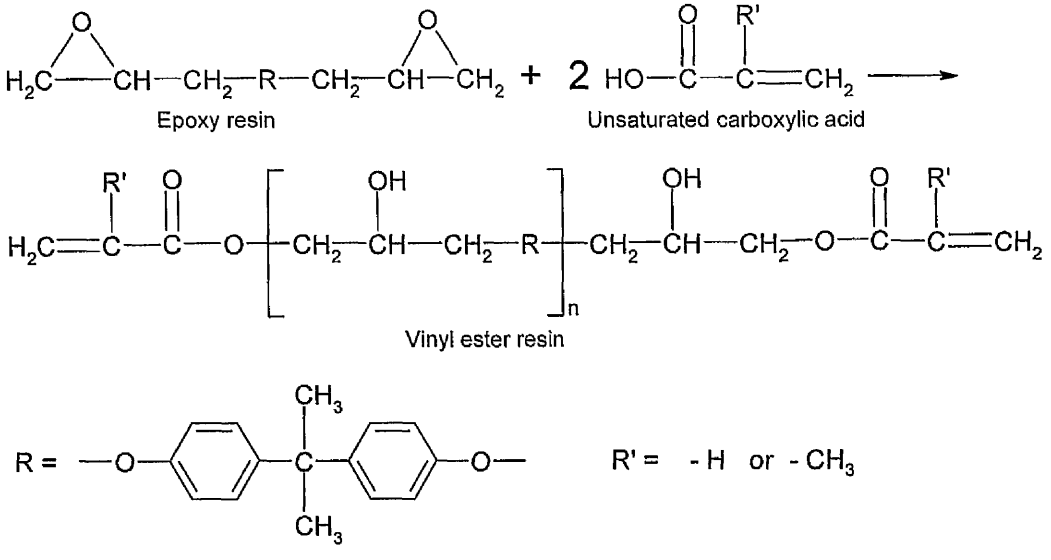

Figure 2.19: *Formation of an unsaturated vinyl ester molecule from the reaction of an unsaturated carboxylic acid with an epoxy resin (n = 1 to 12).*

Vinyl ester resins are more flexible and have higher fracture toughness when cured compared to polyesters due to their fewer cross-links. Furthermore, vinyl esters have fewer ester groups than polyesters hence they exhibit better resistance to water and many other chemicals, as ester groups are generally prone to water degradation by hydrolysis. They also exhibit excellent tensile strength, short cure time and low viscosity. Their volumetric shrinkage, however, is higher than that of epoxy resins.

Bismaleimide Resins

Bismaleimides are thermosetting polyimide resins employed primarily in aircraft composites where operation at higher temperatures is required. Bismaleimide monomers are formulated by the reaction of maleic anhydride with a diamine. Hence a range of resins can be prepared by changing the diamine. The chemical formula of a commercially employed bismaleimide monomer is shown in Figure 2.20.

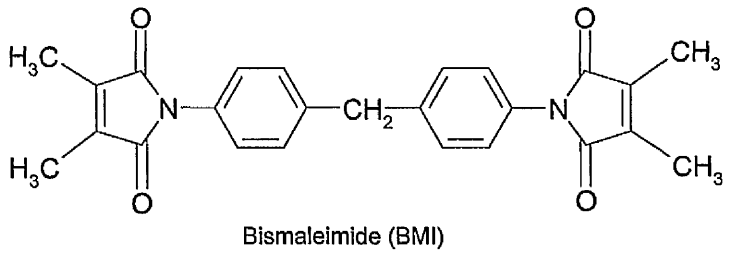

Figure 2.20: *Formula of a commercially employed bismaleimide monomer.*

In order to reduce their viscosity and improve their toughness, bismaleimide monomers are mixed with reactive diluents and other co-monomers, such as vinyl, acrylic and epoxy, respectively. In general, cured bismaleimide and polyimide resins exhibit not only high temperature resistance, but high chemical and solvent resistance as well. The temperature resistance of bismaleimides is 200 – 230°C for continuous exposure and is higher than that of epoxies which is about 150°C [18]. Polyimide resins, however, are very brittle owing to their densely cross-linked molecular structure.

2.3 Reinforcement Materials

The principal role of the reinforcement in a fibre-reinforced composite is to share the major portion of the applied load and provide the composite structure with its greater mechanical strength and stiffness. It can also improve some of the physical properties of a composite, such as its thermal and electrical properties, fire resistance and resistance to abrasion. The reinforcement can be either fibrous or particulate. Fibrous reinforcement can be found in a wide variety of forms, such as continuous bundles of fibres, woven fabrics, mat fabrics, and many others, while particulate reinforcement can be in the form of particles, flakes and whiskers. The most widely used reinforcement in composite materials, however, is in the form of fibres due to the superior strength and stiffness they provide compared to any other form [19].

Regardless of the form in which they are used, the fibres are initially manufactured as bundles of continuous filaments, with each filament usually having a diameter ranging from 5 to 15 μm. The bundle, also known as roving or tow, consists of a large number of filaments (1000 – 10,000). The selection of the fibre reinforcement depends on a number of factors such as low density, good mechanical properties, good compatibility with the matrix, ease of manufacture and handling, adequate permeability and low cost.

The three types of fibres that dominate fibre reinforced polymer composites are: carbon fibres, glass fibres and aramid fibres. Carbon fibres are often utilised in higher performance applications including components for the aerospace industry, where the need for enhanced mechanical properties overshadows the increased cost. Glass fibres, and particularly E-glass, are undoubtedly the most popular choice for the majority of automotive applications, owing to their relatively low cost, while several man-made organic fibres, such as Aramid fibres, are employed in many marine and aerospace applications, where high tensile strength, light weight and impact resistance are essential. Typical properties of commercially employed fibres are included in Table 2.2 [20].

Table 2.2: *Typical properties of commercially employed fibres* [20].

Material	Density (g/cm^3)	Tensile Strength (GPa)	Modulus of Elasticity (GPa)	Ductility (%)	Melting Temp. (°C)	Specific Modulus (10^6 m)	Specific Strength (10^4 m)
E-glass	2.55	3.4	72.4	4.7	<1725	2.90	14
S-glass	2.50	4.5	86.9	5.2	<1725	3.56	18
SiO_2	2.19	5.9	72.4	8.1	1728	3.38	27.4
Al_2O_3	3.95	2.1	380	0.55	2015	9.86	5.3
ZrO_2	4.84	2.1	340	0.62	2677	7.26	4.3
Carbon (High-Strength)	1.50	5.7	280	2.0	3700	18.8	19
Carbon (High-Modulus)	1.50	1.9	530	0.36	3700	36.3	13
BN	1.90	1.4	90	1.6	2730	4.78	7.4
Boron	2.36	3.4	380	0.89	2030	16.4	12
B_4C	2.36	2.3	480	0.48	2450	20.9	9.9
SiC	4.09	2.1	480	0.44	2700	12.0	5.1
TiB_2	4.48	0.10	510	0.02	2980	11.6	0.3
Be	1.83	1.28	300	0.4	1277	19.7	7.1
W	19.4	4.0	410	0.98	3410	2.2	2
Polyethylene	0.97	2.59	120	2.2	147	12.4	27.4
Kevlar 49	1.44	4.5	120	3.8	500	8.81	25.7

The fibre reinforcement used in this work was woven high strength carbon fibre (T300) and woven glass fibre (E-glass) fabric. Woven fabrics consist of two sets of interlaced strands or yarns. The lengthwise set is known as warp and the crosswise set is known as weft. There is a wide variety of weave designs, as shown in Figure 2.21 [21]. The plain weave (Figure 2.21(a)) is the simplest pattern, in which each warp and weft yarn passes over one yarn and under the next one. Plain weave fabrics exhibit excellent stability with almost identical mechanical properties in both warp and weft directions. They have, however, a high level of fibre crimp which can deteriorate the in-plane mechanical properties.

Twill weaves (Figures 2.21(b) and (c)), on the other hand, are characterised by a pattern of diagonal lines on the fibre surface which is produced by crossing warp and weft yarns in a programmed sequence and frequency. Their structure is more packed with a higher degree of drapability compared to that of plain weaves, due to the lower degree of crimp. In satin weave fabrics, such as those used in this study, weft yarns pass over several warp yarns in a programmed order hence the minimum level of interlacing is involved. Satin weaves are further classified according to the associated harness number, which corresponds to the number of warp yarns included in each repetition of the weave pattern [21]. The mechanical properties obtained from satin weave fabrics are greater than those obtained from plain or twill weave fabrics, because their structure allows them to have a high superficial density with a low degree of crimp. Furthermore, satin weaves can be easily draped over complex geometries, owing to their relatively loose fabric structure. The latter, however, can be problematic in terms of handling.

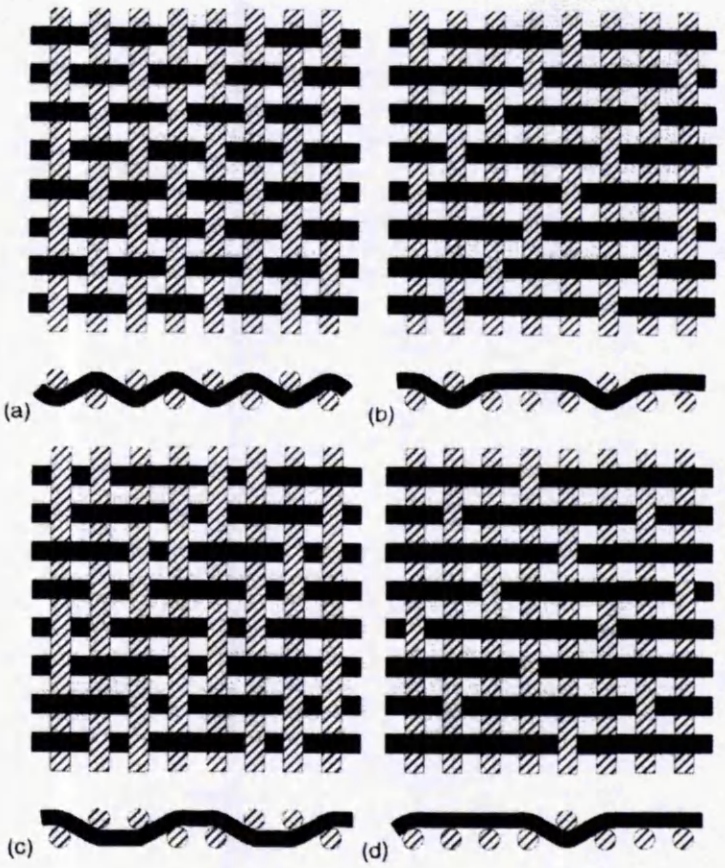

Figure 2.21: *Commonly available weave patterns: a) Plain weave; b) 3 x 1 twill weave; c) 2 x 2 twill weave; d) 5 harness satin weave* [21].

2.3.1 Carbon Fibres

2.3.1.1 Structure and Properties

Carbon fibres are defined as fibres with a minimum of 92 wt.% carbon in their chemical composition [22]. They can be either short or continuous and their structure can be amorphous, crystalline or partly crystalline. The crystalline form has the crystal structure of graphite, as shown in Figure 2.22 [23].

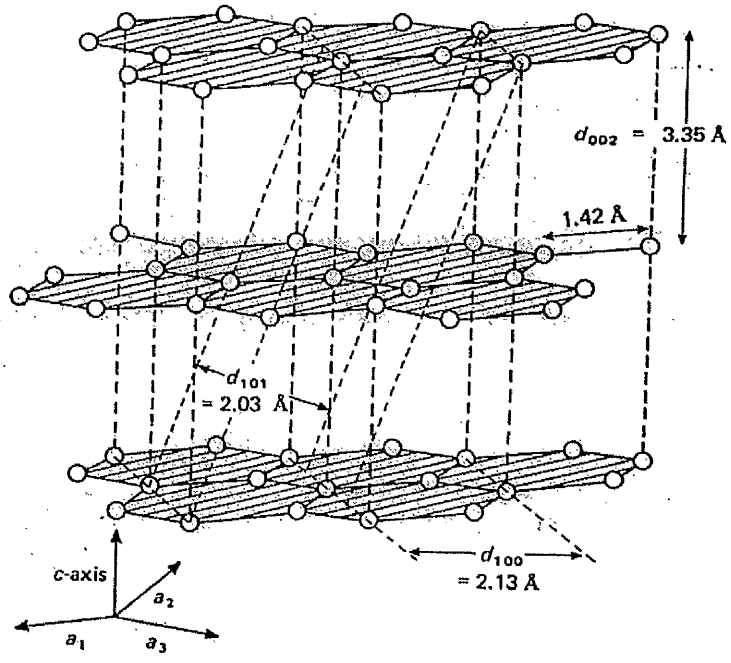

Figure 2.22: *Atomic structure of a perfect graphite crystal* [23].

Graphite consists of sheets of sp^2 hybridized carbon atoms stacked in an AB sequence, such that half of the carbon atoms have atoms straight below and above them in adjacent layers (Figure 2.22). The bonds between the carbon layers are of the weak van der Waals type, allowing them to slide with respect to one another. As a result, the crystal can be easily sheared perpendicular to the plane and the modulus of elasticity in that direction drops dramatically. On the contrary, the bonds between the carbon atoms within a layer are extremely strong, therefore the modulus in the direction parallel to the plane is very high. This consequently means that graphite is highly anisotropic.

In carbon fibres the carbon layers tend to be parallel to the fibre axis. This crystallographic preferred orientation is known as a fibre texture and is responsible for the higher modulus of carbon fibres parallel to the fibre axis as compared to that in the transverse direction. The thermal and electrical conductivities are also higher along the fibre axis, whereas the coefficient of thermal expansion is lower. It is, therefore, evident that the greater the extent in which the carbon layers are aligned parallel to the fibre axis, the higher or lower respectively are the values of the affected physical, mechanical and electrical properties along that axis.

There should also be a distinction between the crystal structure of graphite and that of a carbon fibre. In specific, a carbon fibre can contain graphite regions of size L_c (c-axis crystallite size) perpendicular to the carbon layers and size L_a (a-axis *crystallite size)* parallel to the layers. There can also be crystalline regions where the carbon layers are not stacked according to any particular sequence, although they are of considerable size and parallel to each other. The carbon in these regions is known as turbostratic carbon. Furthermore, another type of carbon that can be found in carbon fibres is amorphous carbon, in which the carbon layers are randomly dispersed and not even parallel to one another. The proportion of graphite in a carbon fibre can vary from 0 to 100%. When that proportion is high, the fibre is said to be graphitic and it is known as graphitic fibre.

Carbon fibres that are used commercially are categorized into three groups, namely general-purpose (GP), high-performance (HP), and activated carbon fibres (ACF). The first group features an amorphous and isotropic structure, low tensile modulus, low tensile strength and low cost. The second group is characterized by high strength and modulus. Depending on the heat treatment of the carbon fibres, those heated to 2500°C are called type I or high-modulus fibres and those heated to 1500°C are called type II or high-strength fibres [24]. In the third group, the activated carbon fibres contain a large number of open micropores, which act as adsorption sites. The amount that can be adsorbed is dependent upon the extent of activation in which the fibres are submitted to.

Referring back to Table 2.1, among the fibres, the high-strength carbon fibres demonstrate the highest strength, whereas the high-modulus fibres demonstrate the highest modulus of elasticity, as expected. Furthermore, the specific modulus (modulus/density ratio) of the high-modulus carbon fibres is remarkably high, due to the low density of the carbon fibres. The polymer fibres, such as polyethylene and Kevlar fibres, also exhibit quite low densities, even lower than that of carbon fibres, but they have low melting temperatures as well. The ceramic fibres, such as Al_2O_3, SiO_2 and SiC fibres, have densities higher than carbon fibres, but the majority of them (except glass fibres) are very expensive and not easily available in a continuous fibre form. The most significant weakness of the carbon fibres in terms of their mechanical properties lies in their low ductility, which is lower than those of SiO_2, glass and Kevlar fibres.

2.3.1.2 Fabrication of Carbon Fibres

Carbon fibres are mainly fabricated from two types of precursors; polymers such as polyacrylonitrile (PAN) or rayon, and pitch. Carbonaceous gases (e.g., acetylene) are also used for the production of carbon fibres, but are not yet commercially available [25]. The present market is dominated by carbon fibres made from polymers (PAN and rayon) because of their good mechanical properties, although the cost of the raw materials used in the fabrication process is much lower in the case of pitch or carbonaceous gases.

The processing routes employed in the production of carbon fibres vary depending on the precursor used. However, the essential features of most processes are quite similar and involve (a) a stabilizing treatment in order to avoid the melting or fusing together of the precursor fibres, (b) a carbonizing treatment to remove the majority of the non-carbon elements and (c) an optional high temperature treatment, known as "graphitizing", in order to enhance the mechanical properties of the final carbon fibres. In fact, the term "graphitizing" is quite misleading because generally care is always taken to avoid the formation of a truly graphitic structure and most of the precursors used for the fabrication of carbon fibres are non-graphitizing.

Nevertheless, the term "graphite" has been used in the literature to describe the turbostratic structure of high-modulus carbon fibres [26].

Carbon Fibres made from Polymers

Carbon fibres can be fabricated from various polymer precursors, namely rayon cellulose, polyvinylidene chloride and most commonly polyacrylonitrile (PAN). This section focuses on the production of carbon fibres from PAN. The acrylonitrile molecule (CH_2=CH–CN) is derived from ethylene by substituting one hydrogen atom for a nitrile group (–C≡N). The nitrile group has a highly polar character which evidently generates a transfer of electrons from the vinyl double bond to itself, leaving the vinyl group with a positive character (Figure 2.23(a)). Polymerisation of acrylonitrile leads to the formation of PAN (Figure 2.23(b)).

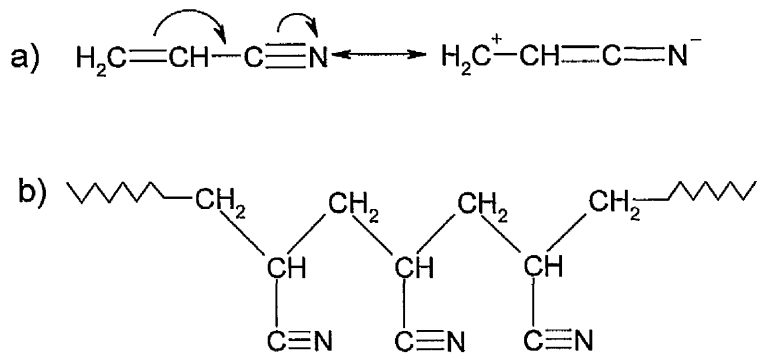

Figure 2.23: *a) Electron transfer in acrylonitrile; b) Polyacrylonitrile (PAN) chain structure.*

The polarity of the nitrile groups produces strong intermolecular dipole/dipole forces, which act as cross-links and do not allow the reorganization necessary for the development of crystallinity. As a result, the material acquires an amorphous structure with the molecular chains assuming a tangled formation and the side groups arranged randomly. Additionally, the polymer is soluble only in the most highly ionizing solvents such as dimethyl formamide, dimethyl sulfoxide and aqueous solutions of inorganic salts, which are able to break the dipole-dipole bonds.

PAN decomposes below its melting temperature, thus it has to be spun by a method relying on the solution of the polymer such as wet or dry spinning. Wet spinning involves the extrusion of the polymer in an organic or inorganic liquid into a coagulating liquid (a mixture of a solvent and a non-solvent). This process precipitates the polymer, which is then drawn out as a fibre. Dry spinning on the other hand, involves the extrusion of the polymer in a volatile organic solvent into a circulating hot gas environment in which the solvent evaporates [25]. The spun PAN fibres typically have a diameter of 11-19 μm, a tensile modulus of 8 GPa, and a tensile strength of 0.5 GPa [27].

The conversion of PAN fibres to carbon fibres requires stabilization and carbonization. Graphitization can also be employed after carbonization of the fibres, in order to further increase their modulus. The stabilization process is essential to the increase of the carbon yield, following carbonization at 400-1500°C. In stabilization, the PAN fibres are heated at about 220°C under tension in an oxidizing atmosphere. This results to the conversion of the PAN into a cyclic compound that can endure high temperatures during carbonization, through linking of the nitrile groups (cyclisation). The cyclized structure is called a ladder polymer (Figure 2.24).

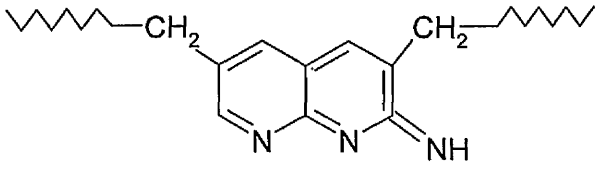

Figure 2.24: *PAN ladder polymer chain structure.*

In addition to cyclisation, stabilization results in dehydrogenation and three-dimensional cross-linking of the parallel molecule chains by oxygen bonds, which helps the chains to remain straight and parallel to the fibre axis. Furthermore, oxygen is responsible for the formation of some oxygen containing groups (such as −OH, −COOH, >C=O) in the backbone of the ladder polymer. These groups subsequently help in fusion of the ladder chains during carbonization. Fully stabilized fibres usually contain 8-12 wt.% oxygen and develop a shiny black color [28].

After stabilization the fibres are carbonised or pyrolyzed by heating in an inert atmosphere (nitrogen) at 400°C-1500°C. During carbonization about 50% by weight of the fibre is lost in the form of gases such as H_2O, NH_3, HCN, CO, CO_2, H_2, N_2 and possibly CH_4. The heating rate at the beginning of the carbonization is quite slow (5°C/min up to 600°C), so that the release of gases does not create pores or surface irregularities in the fibres. After 600°C is being reached, higher heating rates can be employed, leaving only carbon (>92 wt.%) and nitrogen (<6 wt.%). The temperature is then raised again for the final heat treatment called graphitization (optional). In graphitization, the fibres are heated at 1500°C-3000°C in an inert atmosphere, which consists of nitrogen up to 2000°C and argon above 2000°C. Nitrogen can not be used above 2000°C because it reacts with hydrogen and carbon, forming the toxic cyanogen. During graphitization, the crystallite size is increased and the preferred orientation is improved, thus the structure of the fibres becomes more graphitic. A similar process is being developed, when rayon fibres are used as the precursor. Figure 2.25 shows a schematic of the overall manufacturing processes.

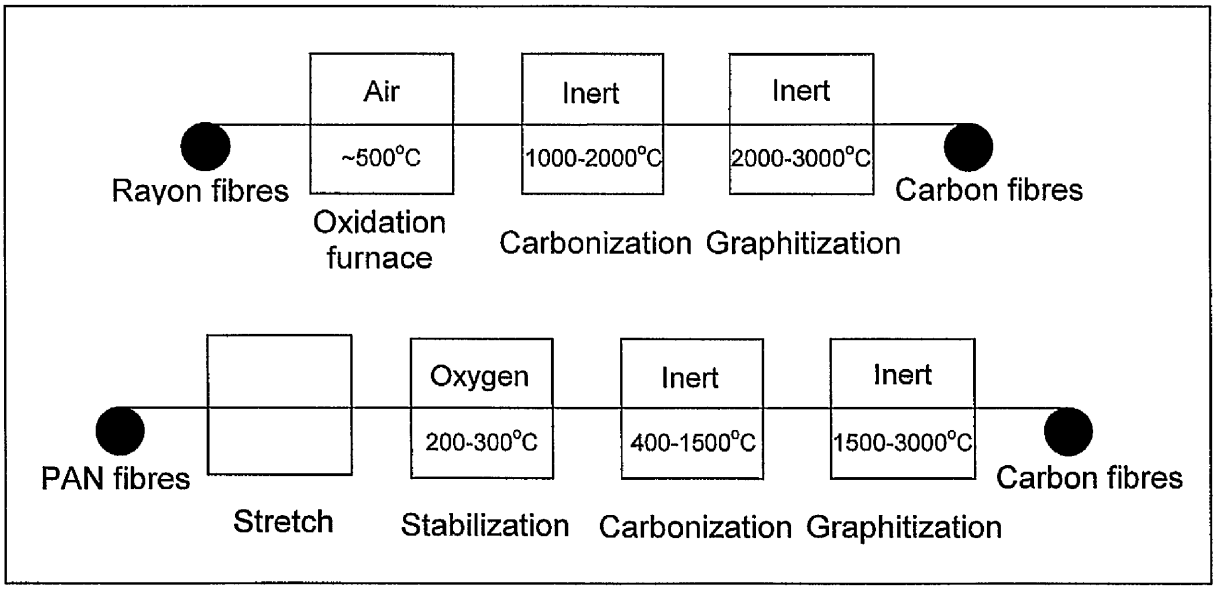

Figure 2.25: *Schematic representation of the production of carbon fibres from rayon and PAN fibres.*

Carbon Fibres made from Pitch

Another type of precursor used for the production of carbon fibres is pitch. Of the various sources of pitch, the most commonly employed in the manufacture of carbon fibres are petroleum pitch and coal tar pitch. Pitch is a thermoplastic material and so it melts upon heating. The molten pitch can be spun to form pitch fibres. The pitch fibres are then subjected to a stabilization process, which enables them to maintain their shape during the subsequent carbonization step. Stabilization involves air oxidation at 250-400°C. It is believed that during stabilization the pitch molecules are attacked by oxygen, resulting into the formation of ketone, carbonyl and carboxyl groups. The introduction of polar CO groups leads to intermolecular hydrogen bonding between adjacent molecules, which in turn prevents softening and deformation of the pitch fibres upon heating.

If isotropic pitch is used as the precursor, the graphitization heat treatment which takes place at the end of the manufacturing process has to be carried out while the fibres are stretched. This process helps to improve the preferred orientation in the fibres, but is quite expensive. On the other hand, if anisotropic pitch is used, stretching is not necessary during graphitization, due to the inherently preferred orientation of the anisotropic pitch molecules. Therefore, the isotropic pitch is converted to anisotropic pitch by heating at 350-400°C for a couple of hours. The anisotropy is due to the formation of a liquid crystalline phase, called "mesophase". The mesophase is in the form of small droplets that consist of large planar molecules. The droplets gradually grow in size and merge into larger spheres, resulting into the formation of anisotropic regions upon heating. The so-called mesophase pitch contains both an isotropic pitch and the mesophase.

The mesophase pitch is formed into fibres usually by melt spinning. Melt spinning involves extrusion of the melted pitch into a gaseous atmosphere (e.g., Ar or N_2) through a spinneret, which is a steel disc that contains a large number of small holes. The extruded fibres are then cooled and solidified. Depending on the spinning conditions (spinning temperature, spinneret diameter, number of holes etc.), different types of orientation of the planar molecules and therefore different microstructures of the resulting fibres can be achieved (Figure 2.26).

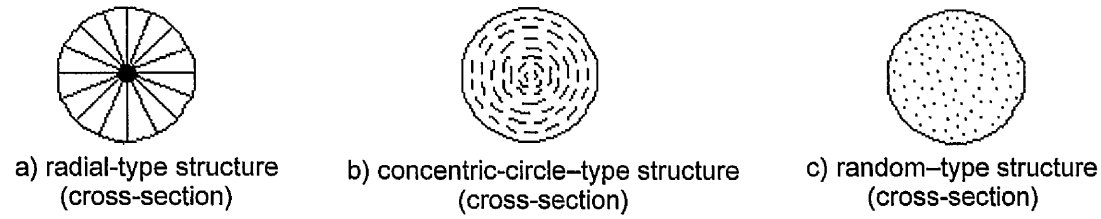

Figure 2.26: *Microstructures of carbon fibres obtained by spinning.*

After stabilization, the pitch fibres are carbonized by heating at 1000-2000°C in an inert atmosphere, so as to prevent oxidation of the resulting carbon fibres. During carbonization, the non-carbon elements are removed as gases, such as CH_4 and H_2. The fibre microstructure developed during fibre formation is retained and high-strength carbon fibres are produced after the carbonization process. Finally, graphitization of the carbon fibres is optionally carried out by heating in an inert atmosphere at 2500-3000°C, if high-modulus carbon fibres are desired. A schematic of the overall manufacturing process of carbon fibres from pitch is presented in Figure 2.27.

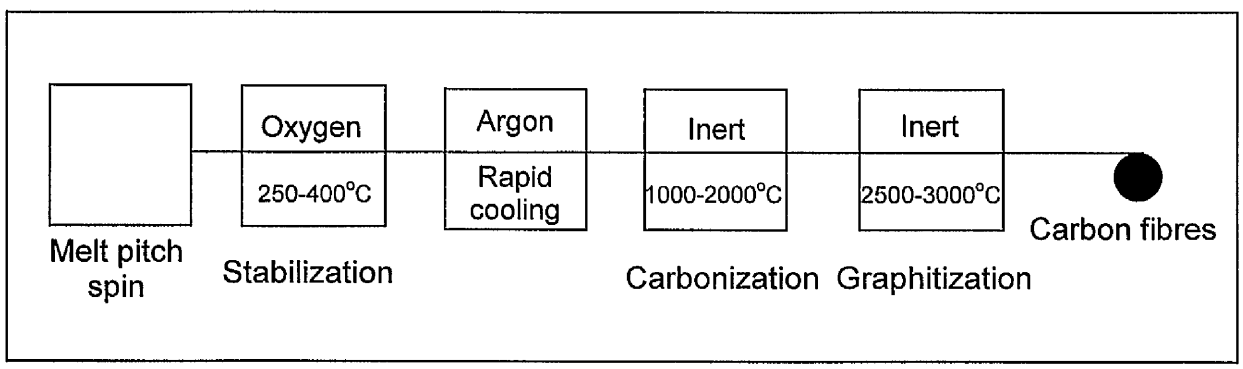

Figure 2.27: *Schematic representation of the production of carbon fibres from pitch.*

2.3.1.3 Surface Treatment of Carbon Fibres

Surface treatments of carbon fibres are necessary for the enhancement of the adhesion between the fibres and the matrix in carbon fibre reinforced composites. Depending on the matrix material, which can be polymeric, metallic, carbon or ceramic, different types of surface treatments may be employed. In specific, when polymers are used as matrix, oxidation using liquid agents (nitric acid, potassium permanganate, etc.), gaseous oxidation, electro-chemical oxidation and plasma techniques are applied. These treatments help mainly to remove any weak surface layers from the carbon fibres and to enhance the mechanical interlocking between the fibres and the matrix, by roughening the fibre surface. Furthermore, they result in the formation of carbonyl, carboxyl, and hydroxyl groups on the fibre surface, almost doubling the surface concentration of oxygen. These chemical active groups significantly contribute to a better fibre-matrix adhesion.

In addition to the oxidation treatments, the adhesion between the fibres and the matrix, the handleability of the fibres and their wetting by the polymer is extensively improved by the use of coupling agents, wetting agents and chemical coatings, known as "sizings". Coupling agents [29], consist mainly of short-chain hydrocarbon molecules, which have the form X-R. One end of the hydrocarbons (R) is either compatible or interacts with the polymer, while the other end (X) interacts with the fibre. A type of coupling agent that is widely used to improve the bonding between carbon fibres and thermosetting polymers is organotitanates. Their general formula is shown below in Figure 2.28, where R is usually a short-chain hydrocarbon chain (such as C_8H_{17}) and X is a group that can interact with the fibre.

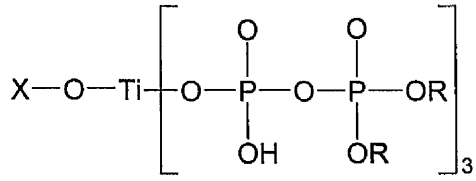

Figure 2.28: *General chemical formula of organotitanates.*

Wetting agents are molecules with high polarity that have one end attracted to the polymer and the other to the fibre. The agent accommodates the adhesion between the fibre and the matrix by allowing more efficient impregnation of the polymer on the fibre. The main difference between a wetting and a coupling agent is that the latter forms a chemical bond with the fibre. Chemical coatings or sizings are often applied to carbon fibres in order to prevent fibre abrasion and to improve fibre handleability and adhesion between the fibres and the matrix. The selection of the suitable sizing depends on the employed polymer system. Materials that are used as sizings include prepolymers/polymers, carbon, SiC and metals, with the polymers (fully or partially cured) being the most popular among them, due to the relative ease of application.

2.3.2 Glass Fibres

2.3.2.1 Structure and Properties

Glass fibres are the most common fibre reinforcement among polymer matrix composites. They are silica (SiO_2) based compounds with a variety of metallic oxides. The internal structure of glass fibres is a long three-dimensional network of silicon, oxygen, and other atoms arranged randomly. As a result of this random atom configuration, glass fibres are amorphous (non-crystalline) and isotropic (equal properties in both axial and transverse directions). The most well known types of glass are E-glass, S-glass and C-glass. The designations E, S and C stand for electrical, strength and chemical, respectively, indicating the distinct properties of each type of glass which allow them to be tailored to different applications. In specific, E-glass fibres have the lowest cost of all commercially employed fibres, which is the main reason for their widespread use in the composite industry, while having good electrical insulation properties in addition to providing adequate mechanical properties. S-glass, originally developed for aircraft components and missile casings, has the highest tensile strength of all the other types of glass. Owing, however, to its higher manufacturing cost and compositional difference, S-glass is more expensive than E-glass. C-glass is used in chemical applications where a greater corrosion resistance to acids than that provided by E-glass is required. Its

strength, however, is lower than that of E-glass. Typical compositions of the different types of glass fibres are shown in Table 2.3 [30].

The principal advantages of glass fibres are low cost, excellent insulating properties, high tensile strength and high chemical resistance (except in alkaline conditions). On the other hand, glass fibres have low tensile modulus, relatively high specific gravity and are sensitive to abrasion with handling, which often decreases their tensile strength. This is one of the main disadvantages of glass fibres. Strength degradation is increased as the surface flaws expand under cyclic loads. The latter also expand in the presence of water, as water removes the alkalis from the fibre surface and deepens the pre-existing surface flaws. Furthermore, glass fibres have relatively low resistance to fatigue and high hardness which causes excessive wear on moulding dies and cutting tools [9].

Table 2.3: *Typical glass fibre compositions (% by weight)* [30].

	E-glass	C-glass	S-glass
Silicon oxide	54.3	64.6	64.2
Aluminium oxide	15.2	4.1	24.8
Ferrous oxide	-	-	0.21
Calcium oxide	17.2	13.2	0.01
Magnesium oxide	4.7	3.3	10.27
Sodium oxide	0.6	7.7	0.27
Potassium oxide	-	1.7	-
Boron oxide	8.0	4.7	0.01
Barium oxide	-	0.9	0.2

2.3.2.2 Fabrication of Glass Fibres

Glass fibres are usually fabricated by a high temperature process in which various raw materials (usually borosilicates) are melted together in order to form a homogeneous melt which is then transformed into glass fibres. In specific, the various raw ingredients in the glass composition (silica, feldspar, sodium sulphate,

anhydrous borax, boric acid and others) are first dry mixed and melted in a high temperature furnace at 1500 - 1700°C. The molten glass is fed under gravity through several hundreds of small holes contained in a platinum bushing and rapidly drawn into filaments of diameters in the range of 5-24 μm. The diameter of the filaments is dictated by the reservoir pressure, the temperature and viscosity of the molten glass and the diameter of the holes in the platinum bushing. The individual filaments are then cooled with water and a surface finish or protective coating, often referred to as 'size', is applied on them prior to being gathered together into strands and wound on to a forming package or 'spincake'. The size is usually applied in the form of an aqueous solution and is a combination of several different components. Further details regarding the surface treatment of glass fibres are given in the next section. A schematic of the overall manufacturing process of glass fibres is shown in Figure 2.30 [21].

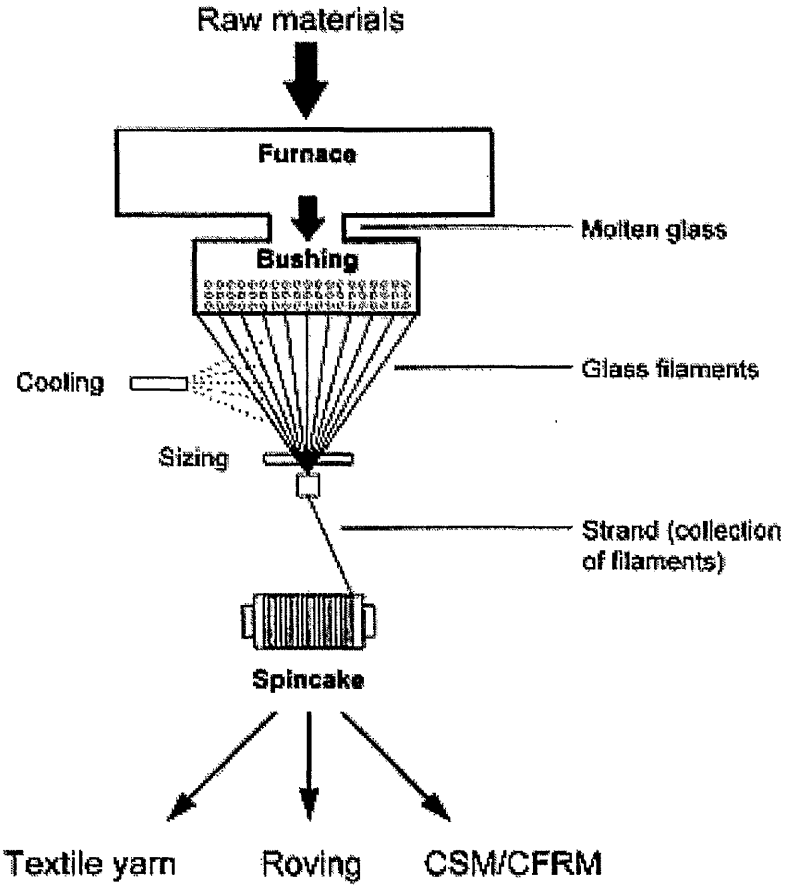

Figure 2.29: *Schematic representation of the manufacture of glass fibres* [21].

The basic commercial form of continuous glass fibres is a strand, which is a bundle of approximately 204 or more parallel filaments. Other available forms of glass fibres are rovings, mats, and woven fabrics. Rovings are groups of untwisted parallel strands wound on to a cylindrical forming package. They can also be preimpregnated with a layer of polymeric resin to produce prepregs. Furthermore, chopped strand mats can be produced by mixing chopped strands with a resinous binder and spreading them in a random two-dimensional way. These mats are primarily used for hand lay-up mouldings and exhibit equal properties in all directions in the plane of the structure. Glass fibres are also produced in woven form, such as woven cloth or woven roving. Woven cloth is weaved from twisted continuous strands, while woven roving is woven from continuous rovings into a rough drapable fabric. Both types of glass fibres are woven in two equally perpendicular directions, providing bidirectional properties that depend on the weave pattern as well as the relative fibre counts in each direction.

2.3.2.3 Surface Treatment of Glass Fibres

The interface between matrix and fibre reinforcement is a critical factor in the production of a composite system, since the applied load must be transferred from the matrix to the fibres through the matrix/fibre interface if the desired level of strength and modulus are to be achieved. Most reinforcement fibres, however, can not form direct chemical bonds with the resin system. Thus, the use of coupling agents, which are chemically reactive with both the matrix and the fibres and/or can chemically modify the surfaces of the system components involved in order to promote adhesion, is required. In addition, a good interface can not only influence the mechanical properties of the composite but also its stability and durability in external factors, such as temperature and moisture. Hence untreated fibres will probably degrade and lose their mechanical strength during their use.

Glass fibres are coated with a multi-component size during the manufacturing process. The size usually takes up to 1% by mass of the fibres and its main components can be summarised as follows [21]:

1. A coupling agent to promote adhesion between the fibres and the resin matrix. This will typically be an organofunctional silane, and may form up to 5% by mass of the size.
2. A polymeric film-forming agent to bind the filaments together into strands and prevent abrasion during further processing. The film former is likely to take up to 90% by mass of the size and is selected so as to be compatible with the resin system used.
3. Other components such as lubricants to prevent abrasion between the filaments and antistatic agents to reduce static friction between the filaments during subsequent processing operations.

Since direct interfacial bonding between glass fibres and the polymer matrix is not possible, it is necessary to use coupling agents in order for the resin to form a strong interface with the glass fibres. The most effective and commonly used coupling agents are the organofunctional silanes. Research on epoxy and polyester laminates indicated that their effectiveness depends on the process, the substrate, the type of silane used and the thickness of the silane layer [31]. Silanes offer considerable resistance to water and utilise molecules with one group functional to the resin and the other functional to the glass fibre. Their typical structure is $Y\text{-}Si\text{-}(OX)_3$, where Y is a covalently bonded organic group tailored to cross-link with the resin during the curing process and OX is an ionic group that can be hydrolised forming silanols. The latter can bond with the silicon ions on the glass fibre surface enhancing the strength of the fibre-matrix interface.

The main factors affecting the nature of the interface in glass fibre reinforced polymer composites are [32]: a) the chemical reactivity of the functional groups of the silane in terms of covalent bonding with the polymer matrix; b) the formation of primary or secondary chemical bonds at the glass interface and c) the diffusion ability of the matrix into the siloxane interface. The interface is generally considered as a region of finite thickness close to surface of the fibres and is more correctly referred to as the interphase. The concept of a polymer/siloxane/glass interphase is demonstrated in Figure 2.30 [32]. Furthermore, it has to be noted that the other components of the size formulation, such as the film former which takes up most of the size mass, should also be taken into account when examining the interfacial

properties of composites. Depending on several factors such as the temperature and the time available for fibre wet-out, the film former is dissolved to a certain degree in the matrix during impregnation, forming chemical bonds between the fibres and the resin which in turn can significantly affect the properties of the resulting interphase [21].

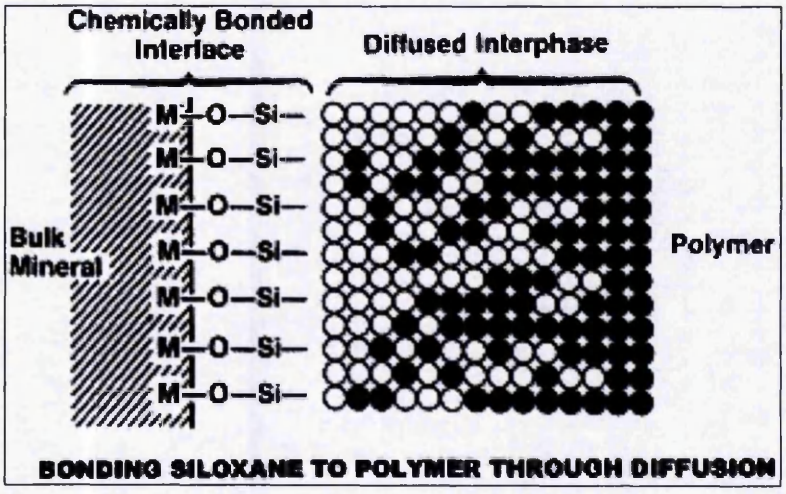

Figure 2.30: *Bonding siloxane to polymer through diffusion* [32].

2.3.3 Aramid Fibres

2.3.3.1 Structure and Properties

Aramid fibres are a synthetic range of highly crystalline organic fibres known as aromatic polyamides. Their structure consists of long aligned polymer chains which provide outstanding longitudinal mechanical properties. Aramid fibres were produced commercially by Du Pont in the early 1970s under the trade name of Kevlar, thus since then this name is synonymous with aramid fibres. More recently, however, similar materials have been introduced by other manufacturers such as Teijin and Akzo. The chemical structure of aromatic polyamide fibres is shown in Figure 2.31 [33]. In aramid fibres, at least 85% of the amide linkages are attached directly to two aromatic rings [34]. This provides the aromatic polyamide molecules with superior chain stiffness (modulus), chemical and thermal stability compared to other conventional polyamides such as nylons.

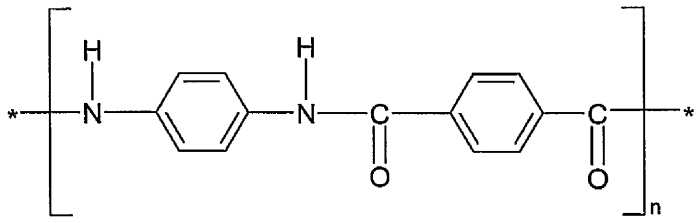

Figure 2.31: *Chemical structure of aromatic polyamide fibres* [33].

Aramid fibres have the highest level of tensile strength-to-weight ratio and the lowest specific gravity among the other types of fibres. They also exhibit a high degree of impact resistance, a negative coefficient of thermal expansion in the longitudinal direction and exceptional dimensional stability. They do not melt or support combustion but will start to carbonize at about 427°C. Due to their structure, however, which is characterised by strong covalent bonds in the fibre direction and relative weak hydrogen bonds in the perpendicular direction, the mechanical properties of aramid are highly anisotropic.

In specific, the longitudinal tensile properties are considerably higher than those in the transverse direction. Their compressive properties are quite poor in both directions with the compressive strength only 20% of the tensile strength [21], while their shear properties are lower than both tensile and compressive properties. Other disadvantages include moisture sensitivity and difficulty in cutting and machining due to their high toughness. Aramid fibres are employed in many marine and aerospace applications where high strength and low weight are essential. They are also found in soft lightweight body armours and helmets for the police and the military due to their superior damage tolerance, as well as in other applications, such as industrial gloves, ropes and cables, pipes, skis and tennis rackets.

2.3.3.2 Fabrication of Aramid Fibres

The precursor from which Kevlar fibres are manufactured is a liquid crystalline polymer known as poly paraphenylene terephthalamide (PPD-T), which is produced from a condensation reaction of paraphenylene diamine and terephthaloyl chloride [21]. In order to produce continuous filaments, a solution of PPD-T is extruded through a spinneret at 200°C and drawn through an air gap. During the drawing process, the aramid molecules become highly oriented in the direction of flow. As a result, the produced filaments are highly anisotropic since their structure consists of long, straight, polymer chains oriented parallel to the fibre axis. Kevlar fibres are commercially available as yarns, consisting of 25 – 1000 filaments, rovings or even woven fabrics. Among many different grades of Kevlar fibres used in composite applications are Kevlar 49 and Kevlar 29. Kevlar 49 is the most widely used and is believed to be compatible with a wide range of resin systems, while Kevlar 29 is employed in applications that demand high damage tolerance owing to its high toughness.

2.3.3.3 Surface Treatment of Aramid Fibres

In order to achieve maximum reinforcement, a good interface between the matrix and the aramid fibres is required. The adhesion, however, between aramid fibres and most thermosetting matrices is inherently poor due to the high crystallinity, relatively smooth surface and chemical inertness of the former. For that reason, a considerable amount of research has been carried out to assess the quality and nature of the interfacial adhesion between the matrix and aramid fibres subjected to different surface treatments such as plasma treatment [35, 36], chemical modification [37] and treatment with a coupling agent [38]. These treatments change the topography and chemical composition of the surface of the fibres, while introducing functional groups on their surface. In this way, improved chemical bonding between the fibres and the matrix and maximum fibre wettability are achieved, thus resulting in better interlaminar properties for the produced composites.

2.4 Composite Manufacturing Techniques

2.4.1 General

Fibre reinforced polymer composites can be manufactured by a wide range of techniques. The main processes currently in use are hand lay-up, spray-up, vacuum bag/autoclave moulding, compression moulding, filament winding, pultrusion and resin transfer moulding (RTM). Each of these techniques has different advantages and limitations and thus may be restricted to specific types of composite structures. In this work, the composite panels were manufactured using resin transfer moulding.

2.4.2 Hand Lay-Up

Hand lay-up is a very simple yet widely used method for the production of large one-piece composite structures such as boat hulls, tanks and building panels. It involves the manual placement of a mat or fabric reinforcement and a resin on the mould surface. To ensure that the mould gives a good surface finish and has satisfactory release properties, the surface of the mould is initially coated with a gel coat and subsequently with a chemical release agent. After the gel coat has hardened sufficiently, the reinforcement is laid on the mould, one layer at a time. The resin is then painted into the reinforcement using a brush or a roller (Figure 2.32) [39]. This process is repeated for each layer of reinforcement until the desirable thickness is achieved. The laminate is then left to cure inside the mould at or above room temperature at low pressure, usually atmospheric pressure. The fibre contents attained with the hand lay-up technique vary from 25% to 40% and the moulds employed in the process are commonly made from glass reinforced plastic, while low cost materials such as wood, metal and plaster can also be used. After completion of the curing process the composite part is removed from the mould and can receive the final trimming or finish.

The operational and tooling costs involved in the hand lay-up process are quite low. The technique allows great flexibility in the shape and the design of the produced laminates. A wide range of obtained physical properties can also be achieved depending on the resin type and the amount and type of the reinforcement used. Furthermore, large and complex parts can be produced, while the materials employed are relatively inexpensive. On the other hand, the hand lay-up process suffers from high labor cost and longer curing times, since room temperature catalysts are used. The produced composite parts have only one moulded surface and their dimensions are not always consistent. In addition, the quality and uniformity of each part depends greatly on the operator's skill.

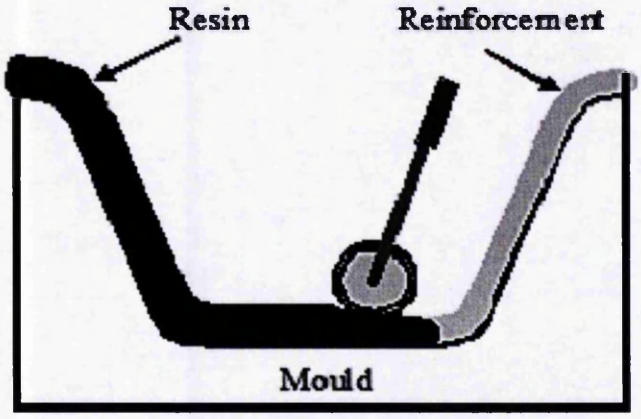

Figure 2.32: *Schematic diagram of the hand lay-up technique* [39].

Spray-up is a variation of the hand lay-up technique, which incorporates the use of a special type of spray gun. In specific, the spray-up gun chops glass fibre into specific lengths, mixes it with catalyzed liquid resin and projects it against the mould surface, which is usually pre-coated with gel coat. In order to achieve sufficient consolidation of the fibre and the resin, compaction between successive passes (layers) is often required. The method is susceptible to a high degree of automation and thus faster production rates can be achieved, although the operational cost is higher than for hand lay-up and the quality of the overall product may again be dependant upon the operator's expertise.

2.4.3 Vacuum Bagging / Autoclave Moulding

Vacuum bagging is basically an extension of the hand lay-up process described previously, where pressure is applied to the laminate once laid up inside the mould. The laminates used in the technique are usually in the form of pre-preg sheets, which consist of unidirectional or woven fabric fibres in a partially cured resin, and the mould, often made of aluminium or graphite, is designed to have high thermal resistance.

The surface of the mould is initially coated with a release agent, which can be a liquid release coating, a wax or even a Teflon tape. The pre-preg sheets are subsequently laid on a single sided mould, building up to 20 mm or more of thickness. The stack of fibre layers is then covered with a porous poly(tetrafluoroethylene) (PTFE) release film, allowing air and excess resin to escape during the process. Furthermore, a bleeder cloth designed to absorb the excess resin generated, is placed on top of the porous PTFE release film. A non-porous PTFE film and a plastic breather are also added. The entire assembly is covered by a thin heat resistant plastic bag, which has sealant tape around its periphery. After sealing the edges, a vacuum is drawn by evacuating the air inside the bag, either through a connection fitted to the mould or a fastening in the bag itself. The atmospheric pressure (1 atm) achieved accommodates the compaction of the laminates and the whole assembly is afterwards submitted to heating, which initiates the curing of the resin.

Increasing the pressure inside the bag increases the compaction between the fibre layers and thus improves the quality of the produced laminates. For that reason, the assembly can be placed in an autoclave, so that after evacuation and heating, the curing process can take place under pressure higher than atmospheric (up to 10 bar). A schematic diagram of the vacuum bagging technique is presented below in Figure 2.33 [9].

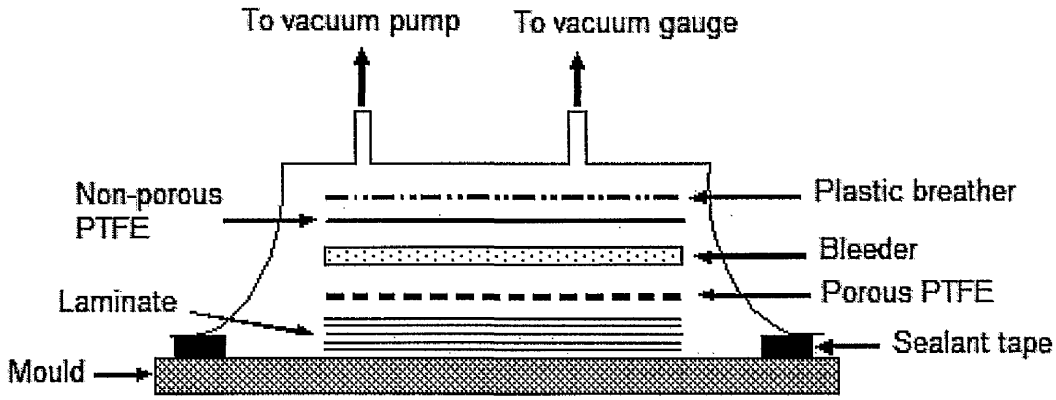

Figure 2.33: *Schematic diagram of the vacuum bagging process* [9].

Vacuum bagging results in the production of laminates with higher fibre content and lower void content compared to standard hand lay-up techniques. The applied pressure involved in the process, significantly improves resin flow and fibre wet-out. In addition, vacuum bagging is a quite safe technique, as the presence of the vacuum bag minimizes the amount of volatiles released during the curing process. The higher quality of the manufactured composites, however, reflects upon the overall cost of the technique, due to the increased labor cost involved and the use of pre-pregs and disposable bagging bags. A higher level of skill and expertise is also required by the operator.

2.4.4 Compression Moulding

Compression moulding is a technique primarily used for the processing of temperature-activated thermosetting plastics, such as phenolic, amino and epoxy resins, as well as unsaturated polyesters. The produced composite parts are generally limited to simple designs; ribs, holes, flanges, bosses and threads are possible. A large number of compression moulded thermoset components are found in electrical and electronic applications, as thermosets are good electrical insulators. In addition, the process is used for the manufacture of several automotive parts.

Compression moulding involves the pressing of a deformable material charge between the two halves of a mould, under conduction heating (Figure 2.34). After the charge is placed inside the bottom half of the mould, the top half is lowered at a

constant rate until a specific pressure is applied to the charge. The combination of applied mould pressure and heating increases the flow of the material which starts to soften and fills the cavity, expelling the air enclosed both inside the mould and the charge. As a result, after sufficient curing has been achieved, the material is transformed into a solid product, acquiring the desirable shape. The mould is then opened and the component is released, often with the help of ejector pins.

The temperature and pressure used in the process are defined by the complexity of the design, the fibre content and the type of the resin. Typically, compression moulding temperatures vary from 130-160°C, whereas moulding pressures are often in the range 1-35 MPa. The most common types of thermoset-based materials used in compression moulding are bulk moulding compounds (BMC) and sheet moulding compounds (SMC). BMC result from the mixing of chopped glass fibres and a thick resin system in a blade-type mixer. The compound is in the form of dough and can flow well into fairly intricate shapes. On the other hand, SMC consist of about 25% by weight of fairly long chopped glass fibres (1-5 cm) and a high viscosity polyester resin. They are produced as sheets in a continuous operation and the rolled material can be stored or shipped for subsequent moulding [40].

Compression moulding can be reasonably good for large scale production of simple shaped components, although the mould cycles can sometimes be long. However, rejected or scrap parts cannot be reprocessed, due to the nature of thermosets and equipment and tooling costs are moderate to high, especially if large presses are employed.

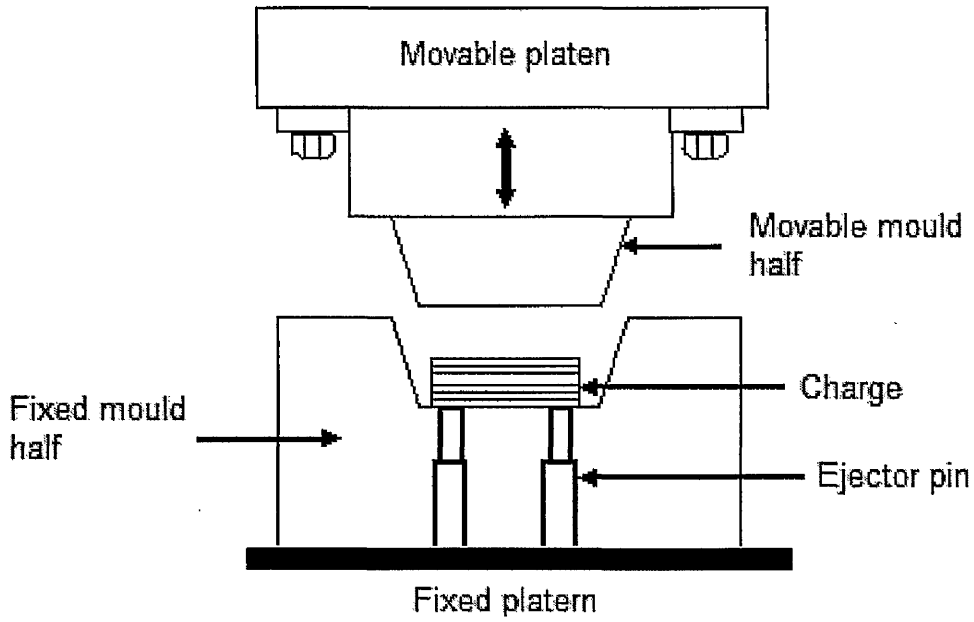

Figure 2.34: *Schematic diagram of the compression moulding process* [9].

2.4.5 Filament Winding

Filament winding is a continuous fabrication method primarily used for the production of hollow, usually circular or oval shaped components, such as pipelines, tanks and pressure vessels. Figure 2.35 shows a schematic diagram of the filament winding process [41].

The basic elements of a filament winding machine include a number of fibre creels, a resin bath tank, a wiping device, a carriage-mounted guide and a mandrel. In specific, a large number of fibre rovings (filaments or strands gathered together in a bundle) are pulled from a selection of fibre creels and are immersed into a resin bath tank that contains liquid resin, catalyst and other ingredients. The resin-impregnated fibres are subsequently pulled through a wiping device, in order to remove the excess resin and regulate the thickness of the received resin coating around each roving. After sufficient impregnation and wiping is achieved, the rovings are gathered together in a flat band with the help of a guide positioned on the carriage and are wrapped over the mandrel.

The mandrel rotates on the horizontal axis, while the carriage moves back and forth parallel to the mandrel, placing fibres in a predetermined configuration. Therefore, the winding angle depends on the relative speeds of the mandrel and the carriage and so by modifying them the desired fibre orientation and thickness can be obtained. After winding and curing the composite material (room temperature, oven, or autoclave), the mandrel can either remain in place as part of the product or it can be removed. Cylindrical or tapered mandrels are removed from the part with mandrel extraction equipment. Some mandrels are also collapsible, inflatable or built from several smaller disassembled parts, while others are made of soluble material and can be easily dissolved and washed out of the product.

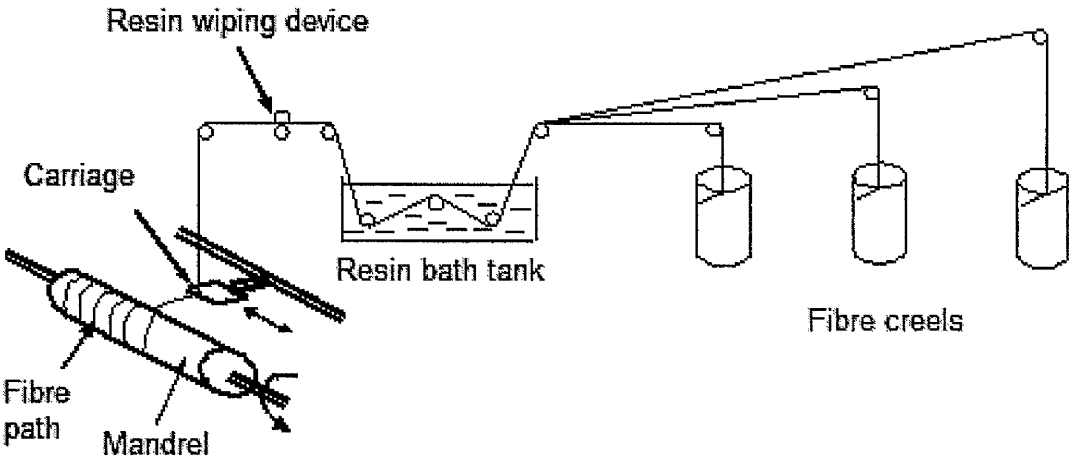

Figure 2.35: *Schematic diagram of the filament winding process* [41].

Filament winding is a fast, automated and repeatable process suitable for the production of large size components. The material costs involved are relatively low, especially since the fibres are not required to be converted into fabric before the actual process. Furthermore, when complex winding patterns of the straight fibres are employed, the manufactured laminates exhibit very good structural properties. On the other hand, filament winding is restricted to the production of convex shaped components. The end sections of the windings are inevitably cut off, due to the mandrel being pulled out at the end of the process. In addition, the external surface of the fabricated components is unmoulded.

2.4.6 Pultrusion

Pultrusion is another continuous manufacturing technique used for the production of composites with uniform cross-section and outstanding longitudinal strength and rigidity. The reinforcing materials (carbon, Kevlar and mostly glass fibres) are in the form of unidirectional tows, continuous mats or other types of fabrics, while the resin systems employed include primarily polyester resins; epoxy and phenolic resins are also used. Common applications of pultrusion include cylindrical products such as rods and golf clubs, rectangular products such as sail battens, channel profiles such as ladder rails, cable trays and hollow products such as ladder rungs and windmill blades [40].

The fibres are initially drawn from a variety of creel boards and are pulled though a resin bath. These resin impregnated fibres are then carefully guided through a pre-shaping station (preformer), for the purpose of removing the excess resin and uniformly distributing the fibre bundles. Subsequently, they are pulled through a long preheated die, in which the resin matrix cures at high temperature under pressure to accommodate compaction and form the final shape of the component. The pull off device features two or more pairs of contoured clamps mounted on endless tracks, sequentially pulling a distance, releasing and returning. The duration of the curing process is thus determined by the length and temperature of the die, as well as the pulling speed. For that reason, the fibre-resin stream should exit the die only after sufficient curing has been achieved. Finally, after cooling with air or water, the resulting profile is pulled past a saw, where it is cut into pre-determined lengths. A schematic diagram of the pultrusion process is presented in Figure 2.36 [42].

Pultrusion is a fast, continuous, automated and cost effective process for high volume production of constant cross-sectional components. The manufactured laminates exhibit very good structural properties, since straight fibres are being used and high fibre volume fractions can be obtained. In addition, the presence of the die, in which the curing of the composites takes place, considerably limits the amount of released volatiles.

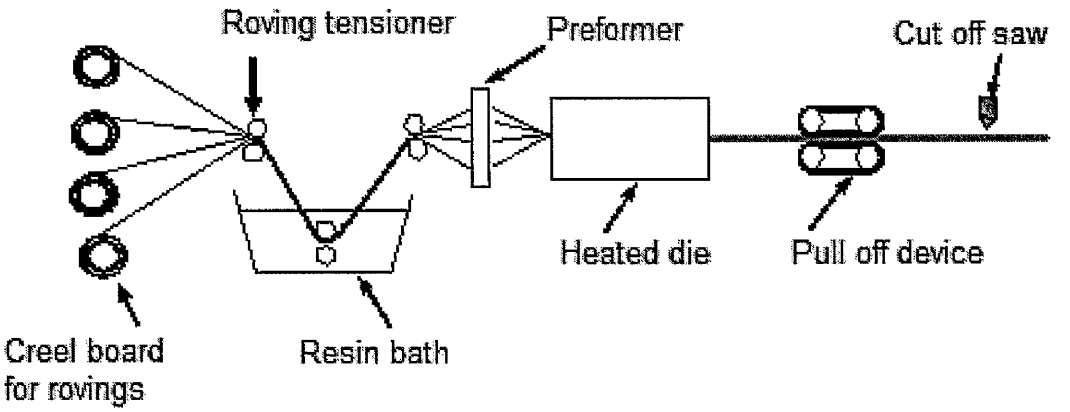

Figure 2.36: *Schematic diagram of the pultrusion process* [42].

The most significant disadvantage of pultrusion is the fact that it is generally restricted to straight components with a uniform cross-section. However, modifications of the basic process can be made in order to produce slightly curved or twisted parts. In specific, the technique referred to as "pulforming" is a variation of pultrusion, in which a heated but not fully cured component is formed in suitable moulds. The cross-sectional area of the product is still almost uniform along its length, but the cross-sectional shape can be considerably altered [40].

2.4.7 Resin Transfer Moulding (RTM)

2.4.7.1 General

Resin transfer moulding, also known as "resin injection moulding", is a closed-mould process that was initially introduced in the early 1950's for aerospace applications [43]. Since then, RTM continues to retain a great interest among the aerospace industries, mainly due to its ability to produce high-performance complex composite parts in relatively low costs. A lot of automotive industries have also acknowledged resin transfer moulding as one of the most promising processes to overcome certain difficulties encountered in the manufacturing of composites, such as the high cost of materials, the increased labour demand and the emission of volatiles (for example styrene when polyesters or some vinyl esters are used), just to name a few.

The main advantages of RTM over other composites processing techniques are summarized below:

1. Both sides of the produced components have a moulded surface.
2. The emission of volatiles is reduced, due to enclosure of the resin.
3. High fibre volume laminates (up to 70%) with relatively low void content (less than 1% void content) can be obtained.
4. Production times are very short compared to the hand lay-up process.
5. Large and complex composite parts can be manufactured.
6. Labour and material costs are low.

On the other hand, the basic drawbacks of RTM are:

1. Tooling is relatively expensive, as the closed moulds need to be matched to prevent leaking.
2. Cycle times can sometimes be long, thus increasing energy requirements.
3. Fibre reinforcement may be displaced during resin injection.

2.4.7.2 Process Description

Resin Transfer Moulding (RTM) incorporates the use of a two-part closed mould tool and pressure (or vacuum) to inject a low viscosity resin into the mould. The characteristic features of RTM when compared to other composite manufacturing techniques are:

1. The two-sided moulded surface of the parts, due to the closed mould.
2. The low pressure applied to transfer the resin.
3. The manual placement of the fibre reinforcement prior to resin injection.

The RTM process involves the initial placement of fibrous reinforcement inside the cavity of a mould tool. The fabric material can be in the form of continuous or chopped strand fibre mat and is either pre-cut or preformed to easily fit into the shape of the mould. A second mould tool is then clamped over the first and a resin is injected into the cavity, usually through an injection point located at the bottom part of the mould. Low pressure (generally less than 0.7 MPa) is applied during the injection to assist the transfer of the resin system throughout the mould. As the resin is injected into the cavity, excess air is forced out through air vents positioned at the uppermost part of the mould, while impregnating the porous preform. The moment the first amount of resin exits the vent tubes, the injection is shut off and the mould filling process has finished. The injection tubes and the air vent holes must then be plugged to avoid any resin leakage.

The mould temperature is afterwards raised in order to initiate the curing process, with the curing temperature being dictated by the employed resin system. After the material has fully cured, the clamps are loosened and the part is removed from the mould, which can then be cleaned and prepared for the next moulding session. The component can be subsequently trimmed or subjected to any necessary post-moulding operations. The separate steps of the RTM process are shown in Figure 2.37 [44].

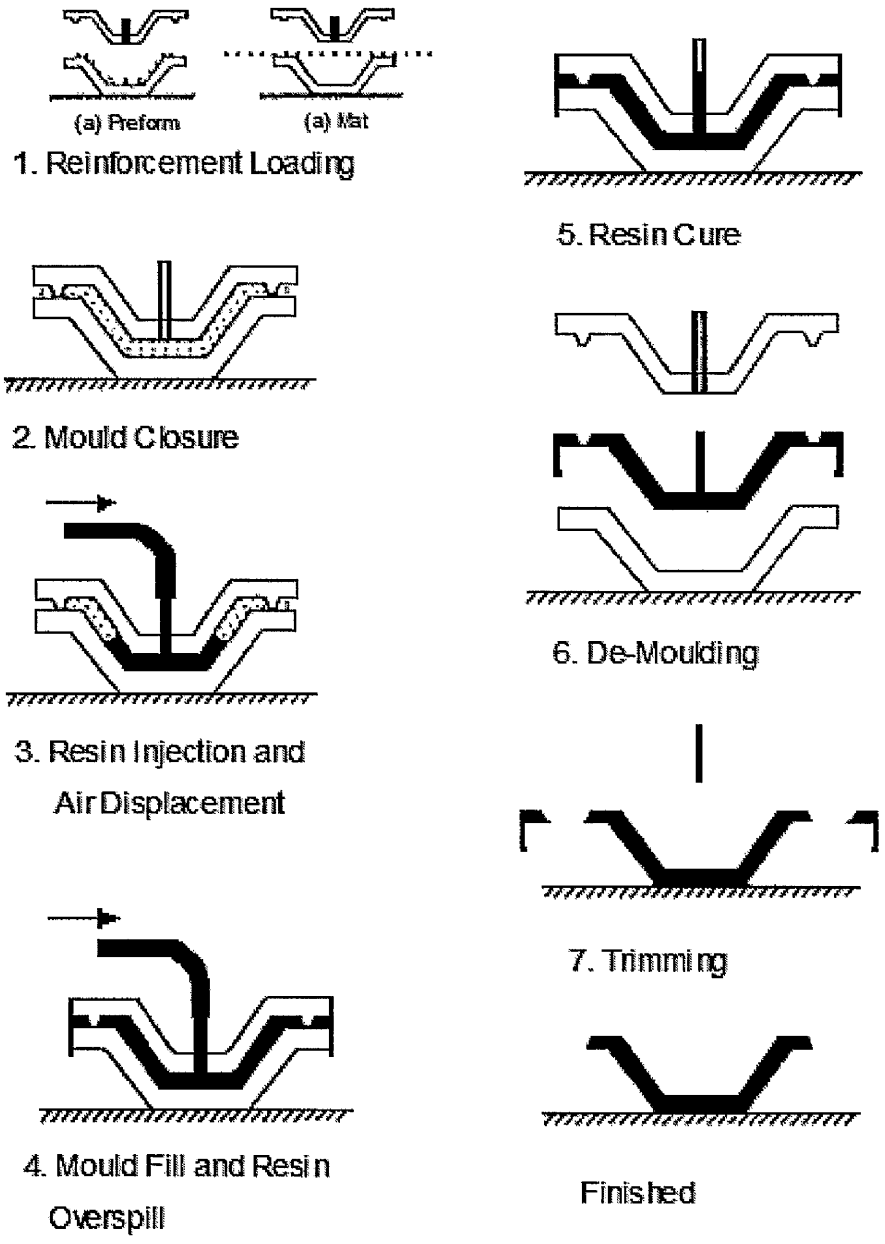

Figure 2.37: *Schematic diagram of the separate steps of an RTM cycle* [44].

2.4.7.3 Fundamentals and Influencing Factors

Resin Systems

RTM can utilize a large number of different types of resin systems, such as epoxy resins, polyesters, vinyl esters, phenolic or high-temperature bismaleimide resins. Nevertheless, there are several factors that need to be considered before a resin system is effectively used in an RTM process. In specific, viscosity, compatibility, void formation, and cure time are the most critical ones.

The employed resin system has to maintain a sufficiently low viscosity to accommodate the injection process and allow good fibre wet-out. The latter has shown to be greatly influencing the mechanical properties of the produced composites. Highly viscous resins require higher injection pressure which can lead to fibre displacement or poor fibre wet-out, inevitably degrading the quality of the finished parts. It is also essential that the resin is compatible with the other materials used in the RTM process, otherwise undesirable side reactions may occur. Furthermore, the resin system should not emit volatiles or generate gaseous by-products while being inside the mould during the curing stage, so as to minimize the formation of voids. Degassing is usually carried out prior to injection as well, to ensure that the resin is free of air bubbles. Finally, the curing of the resin must take place in the shortest time possible in order to enable high productivity and short cycle times.

Fibre Reinforcement

All of the common types of fibres such as E-glass, S-glass, carbon, graphite or Kevlar fibres can be used in the RTM process. The selection of the fibre reinforcement, however, depends primarily on the desired mechanical properties of the finished component and the employed resin system. Therefore, the sizings applied to the fibres to increase fibre-matrix adhesion and improve fibre wet-out must be compatible with the resin used; if not air entrapment would be more likely to

occur. The fibres are usually in the form of continuous or chopped strand fibre mats, although any type of woven or stitched material can be used.

The permeability and architecture of the fibre reinforcement used in the RTM process have a significant influence on the mechanical properties and microstructure of the fabricated laminates. Pearce and co-workers [45] tried to relate variations in permeability and in the laminate mechanical properties, to differences in microstructure. Four types of carbon-fibre fabrics, three of which had been modified by including varying proportions of 3k tows in place of 6k tows in the weft direction, were woven and used to manufacture carbon fibre/epoxy plates by RTM. Mechanical testing showed that the compression strengths were unaffected by the changes in fabric architecture, but the tensile and compressive moduli in the weft direction were lower than the warp direction. Microstructural image analysis also confirmed the results from the mechanical testing and the permeability measurements.

In addition, Karbhari and Slotte [46] investigated the effects of combinations of different fibre architectures on the performance and manufacturability of a stiffened plaque using RTM. The preform used consisted of a five-unit E-glass fibre stamped preform, two wrapped and or/braided foam PVC cores that were placed in a hat-stiffener section, and a four-layer thick continuous strand mat (CoSM) sheeting placed on top of the configuration. The injected resin was vinyl ester. Flow front studies also yielded interesting results mainly regarding the higher volume fractions at the corners and the use of unidirectional fibres as flow conduits.

Pressure

Pressure within the mould in an RTM process can be generated by two sources, namely injection pressure and pressure caused by compaction of the fibre preform. The pressures involved in RTM are generally low; however considerable separating forces between the two halves of the mould can still be generated, inevitably affecting the desired fibre volume fraction. For that reason, the moulds must be sufficiently rigid and stiff in order to withstand the created deflection pressures. Onur Kas and Kaynak [47] used C-scan and microscopic analysis to correlate the mechanical properties of epoxy resin/carbon fibre composites with the microvoids

formed during RTM processing. Three different injection pressures were used (2, 3, and 4 atm) and 3-point bending and impact tests were also carried out. The results showed that as the injection pressure increased the amount of microvoids also increased, thus the specimens moulded under 2 atm injection pressure had the highest mechanical properties. Good agreement between the results of the C-scan analysis and the mechanical tests was reported.

Furthermore, Lebrun and co-workers [48] recorded the through-thickness temperature profiles in the mould cavity for a flat steel preheated RTM mould at different locations and under different moulding conditions. Results showed that lower pressures, higher fibre contents and higher mould temperatures, increased the resin temperatures. A large temperature difference was observed between the mid-thickness and the mould surface during the filling and heating phases, resulting into faster resin flow at the mould surface and thus entrapment of air at mid-thickness during the impregnation.

Mould Filling and Void Formation

In order to manufacture composite laminates with good overall properties, higher fibre volume fractions (>50%) and lower void contents must be achieved. In that case, the permeability of the fibre preform is significantly reduced and hence lower flow rates are possible. During mould filling, the resin will follow the path of least resistance. This means that the resin chooses to penetrate the spaces around the fibre tows (porespace) rather than within the fibre tows. Therefore, if the injection rate is relatively high, the flow between the tows (channel flow) will lead that within the tows (capillary flow), resulting into a non-uniform flow front and increased voidage.

Pearce and co-workers [49] studied the effects of convergent flow fronts on the properties of epoxy resin composites reinforced with carbon fibres of three different weave styles (twill, 5 harness satin and 5 harness satin Injectex), produced by RTM. Ultrasound C-scanning, image analysis and interlaminar shear strength testing showed that in the areas where flow fronts meet there was an increase in void content and incident decrease in ILSS. Finally, differences in fabric architecture appeared to have a far greater effect on ILSS than on void content variation.

Bickerton *et al.* [50] investigated whether corners of different radii would have any significant effect on the progress of the resin flow front and the injection pressure within a mould cavity. Flow visualization studies were performed for five moulds of varying radii and three different preform styles (continuous strand random mat, woven carbon fibre fabric and stitched fiberglass fabric). Results showed that increased injection pressures were required to fill the moulds with the lowest corner radii. Flow front progression, however, was not significantly affected by different corner radii.

The formation of voids has also shown to reduce the interlaminar shear strength (ILSS), the longitudinal and transverse flexural modulus, the longitudinal and transverse tensile strength and modulus, the compressive strength and modulus, the fatigue resistance and the high temperature resistance of composites, as Judd and Wright [51] indicated with an extensive review of the findings of 47 papers. Additionally, Varna and co-workers [52] studied the effect of void content and geometry on the mechanical behaviour of unidirectional glass-fibre/vinylester fabric laminates produced by RTM under transverse tensile loading. Laminates with the highest average void content had the highest content of large spherical voids and a transverse strain to failure as high as 2%, while low void content laminates failed at 0.3%. A few large and well-defined transverse cracks were formed in low void content laminates before final failure, whereas multiple transverse cracks and various smaller cracks were created in the high void content laminates.

Gate Position, Venting and Sealing

The position of the gate is probably the most important part in the design of a mould used in RTM, as it can influence the shape of the resin flow front and thus prevent fibre wash-out as well as minimize air entrapment during injection. Usually, the gate is placed near the geometric centre of the lower part of the mould in order to allow the resin to get in contact with all the reinforcement and minimize the resin path length. The resin, initially, fills up the gate and then starts to flow over into the mould, slowly progressing throughout the mould area until impregnation of every part of the fibre reinforcement is achieved.

A good venting and sealing system is also necessary in the RTM process, so as to allow the air inside the cavity to escape and reduce the amount of resin spill. In vacuum assisted resin injection process (VARI), a high quality seal is placed around the mould and the air inside the cavity is removed by applying a vacuum. A soluble in the resin gas or vapour can also be used to remove the air inside the mould prior to injection, provided a seal is properly positioned. The mould is usually sealed using "O-rings", which are placed inside a retaining wall around its periphery. In addition, vent ports are located opposite the injection point to allow air to escape. The position of the vent ports and the injection point must be carefully selected to prevent the formation of local regions of enclosed air within the mould. After the mould has been completely filled with resin, both the injection gate and the vent ports are sealed in order to sustain mould pressure and prevent resin leakage.

2.5 Microwave Processing

2.5.1 General

Microwave technology and several microwave applications were first developed during and just before World War II, in an effort to design and manufacture microwave radar, navigation and communications equipment for military purposes. Although, the initial research was meant to fulfil only military needs, many other microwave applications were developed after World War II, such as industrial microwave processing systems and most importantly domestic microwave ovens. In the past 20 years, the microwave oven has become a necessary appliance in most homes, due to faster cooking times and significantly lower energy requirements. It is, therefore, evident that the use of microwave heating in materials processing can offer similar benefits.

2.5.2 Microwaves

Microwaves belong to the portion of the electromagnetic spectrum with frequencies usually considered to range from 300 Megahertz (MHz) to 300 Gigahertz (GHz) and corresponding wavelengths of 1 m to 1 mm. This portion of the electro-magnetic

spectrum covers frequencies that are used for cellular phones, radar and television satellite communications. For that reason, the Federal Communications Commission (FCC) has reserved two frequencies for industrial, scientific and medical (ISM) purposes. The two most commonly used frequencies for microwave heating are 0.915 and 2.45 GHz and are widely known as the ISM bands [5]. Most of the domestic microwave ovens operate at 2.45 GHz frequency. The position of microwaves with respect to the overall electromagnetic spectrum is shown in Figure 2.38 [53].

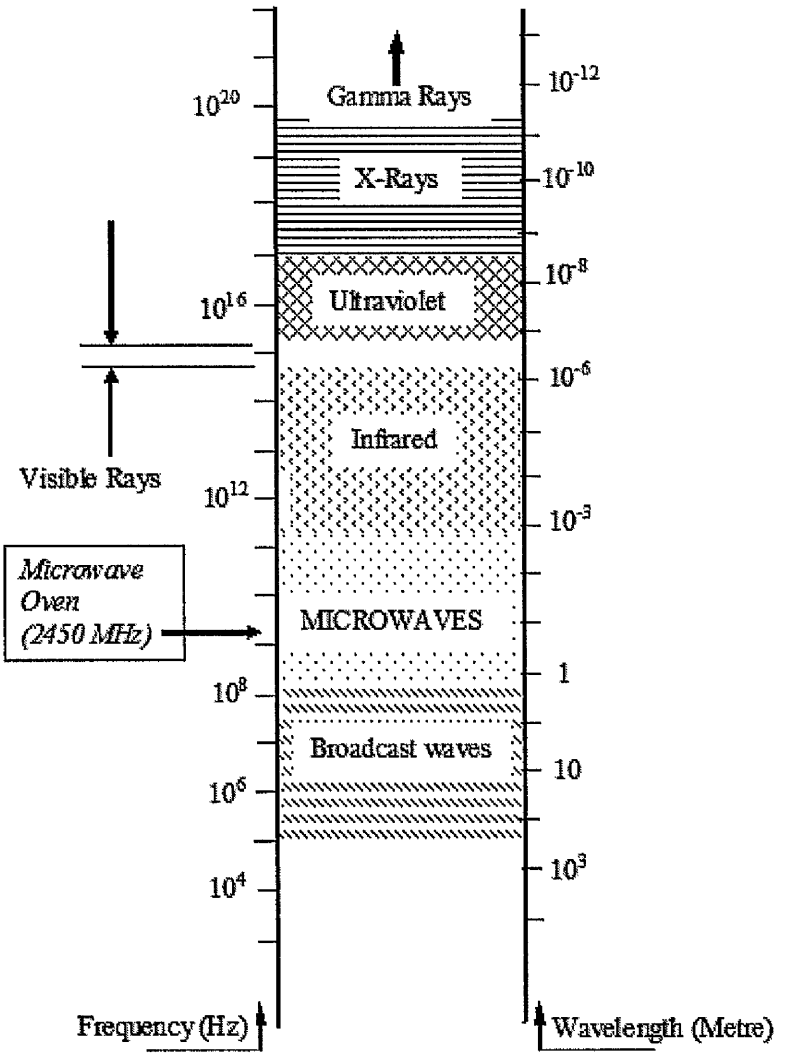

Figure 2.38: *Electromagnetic spectrm* [53].

Microwaves can be transmitted through hollow metallic tubes and can be focused into beams using high gain antennas. They propagate through free space at the speed of light and the relationship between wavelength and frequency is expressed by Equation 2.1:

$$\lambda_o = c/f \qquad \text{(Equation 2.1)}$$

where λ_o is the wavelength in free space in centimeters, c is the speed of light ($3x10^{10}$ cm/sec) and f is the frequency in Hertz (cycles/sec). Thus, for a domestic microwave oven operating at 2.45 GHz frequency, the wavelength, λ_o, is 12.25 cm.

2.5.3 Fundamentals of Microwave Heating

2.5.3.1 Dielectric Properties

When a dielectric material is under the influence of an external electric field, the internal bound charges within the material are redistributed according to its direction, resulting in the polarization of the material. Therefore, in order to measure the response of a material to an external electric field the dielectric permittivity, ε, is introduced. If the external electric field is alternating (ac), the dielectric response of the material follows it, but with some lag behind the field changes [4]. The dielectric permittivity in that case is expressed as a complex number:

$$\varepsilon^* = \varepsilon' - i \cdot \varepsilon'' \qquad \text{(Equation 2.2)}$$

where ε^* is the complex dielectric permittivity, ε' is the dielectric constant and ε'' is the dielectric loss factor.

The real component of the complex permittivity, the dielectric constant (ε'), determines how much of the electrical energy is absorbed and how much is reflected, whereas the imaginary component, the dielectric loss factor (ε''), expresses the ability of the material to convert the incoming electrical energy into heat. Due to a certain amount of the incident electromagnetic energy being absorbed, the

electromagnetic field attenuates as it penetrates the material. The dissipation of the electromagnetic energy is commonly described by the loss tangent, tanδ:

$$\tan\delta = \frac{\varepsilon''}{\varepsilon'} \qquad \text{(Equation 2.3)}$$

The loss tangent, tanδ, represents the extent to which a material can be penetrated by an external electric field and can convert electrical energy to heat. The attenuation of the electromagnetic field can also be expressed by a penetration depth (or skin depth), which is defined as the distance from the sample surface where the absorbed power is 1/e of the absorbed power at the surface. The penetration depth is given by the following equation:

$$d = \frac{\lambda \cdot \sqrt{\varepsilon'}}{2\pi \cdot \varepsilon''} \qquad \text{(Equation 2.4)}$$

where d is the penetration depth in millimeters, λ is the wavelength of the electromagnetic wave in millimeters, ε' is the dielectric constant and ε'' is the dielectric loss factor. The knowledge of the penetration depth is very important especially when processing thick materials, because if the penetration depth is much less than the actual thickness of the material only the surface is heated.

Materials with high dielectric loss factors have consequently low penetration depth and thus are considered reflectors. On the other hand, materials that exhibit low dielectric loss factors have very large penetration depth. As a result, the material is transparent to microwave energy, absorbing a very small amount of energy. Due to this behaviour, microwave energy is more effectively transferred to materials that have dielectric loss factors somewhere in the middle of those two extremes [5]. In addition, the dielectric properties of a material are not constant. They are functions of temperature, frequency, and for reacting systems, degree of reaction, mainly because they depend on the mobility of the polar molecules within the material's structure. For that reason, the extent to which a material absorbs microwave energy varies during processing.

2.5.3.2 Microwave Heating Mechanisms

In conventional heating, thermal energy is transferred to the material mainly through convection, conduction and radiation of heat from its layers. In contrast, microwave radiation generates heating throughout the volume of the material, as a result of its interaction with the electromagnetic field. Microwave heating is, therefore, conversion of electromagnetic energy to thermal energy, rather than heat transfer [5]. As a result, rapid, uniform and volumetric heating of materials can be achieved through effective use of microwaves.

It is generally considered that there are three qualitative ways in which a material can be categorized in terms of its interaction with the microwave field [54]:

1. Transparent (low dielectric loss materials), where microwaves penetrate with little, if any, attenuation.
2. Opaque (conductors), where microwaves are reflected and do not pass through.
3. Absorbing (high dielectric loss materials), where microwave energy is absorbed to a certain degree based on the value of the dielectric loss factor.

There is also a fourth type of material-microwave interaction, that of a mixed absorber. Mixed absorbers are composites or multi-phase materials where one of the phases is a high-loss dielectric material, while the other is a low-loss material. The microwaves, therefore, pass through the low-loss material with little attenuation and are absorbed by the high-loss component, taking in that way advantage of one of the significant characteristics of microwave heating, that of selective heating. This selective heating process can not be achieved through conventional heating methods.

As microwaves are absorbed by a dielectric material, energy is transferred from the microwaves to the material, consequently increasing its temperature. The two main mechanisms by which microwaves generate heat in dielectric materials are ionic polarization and dipole orientation [55].

Ionic polarization takes place when ions in solution move under the influence of an electric field. The ions being electrically charged are accelerated by the electric field,

which provides them with the necessary kinetic energy. Due to collision of ions with other ions, the kinetic energy is converted into heat and hence the temperature of the dielectric material is raised. Therefore, the frequency of the collisions depends on the concentration of the solution. When the electric field is alternating at microwave frequencies, a large amount of heat is produced due to several collisions taking place. Ionic polarization can occur in cellular fluids and is less significant as a heating mechanism compared to dipole rotation.

Dipole rotation depends on the existence of polar molecules (dipoles) within a material. Polar molecules are randomly oriented under normal conditions (Figure 2.39(a)). In the presence of an external electric field, however, the dipoles orient themselves according to the polarity of the field (Figure 2.39(b)). When a microwave field is applied, the polarity of the field varies at the rate of the microwave frequency (e.g. at 2.45 GHz frequency, the polarity changes 2.45×10^9 cycles per second) and the dipoles try to maintain alignment with the rapidly changing field (Figure 2.39(c)). As a result, heat is generated due to friction with the surrounding medium during rotation of the dipoles. The initial random orientation of the molecules is restored upon removal of the field. However, as the temperature of the material increases, the dipoles tend to align with the field and return to the random state more rapidly. Additionally, microwave heating can be influenced by other factors such as the shape, size, properties and physical state of the material.

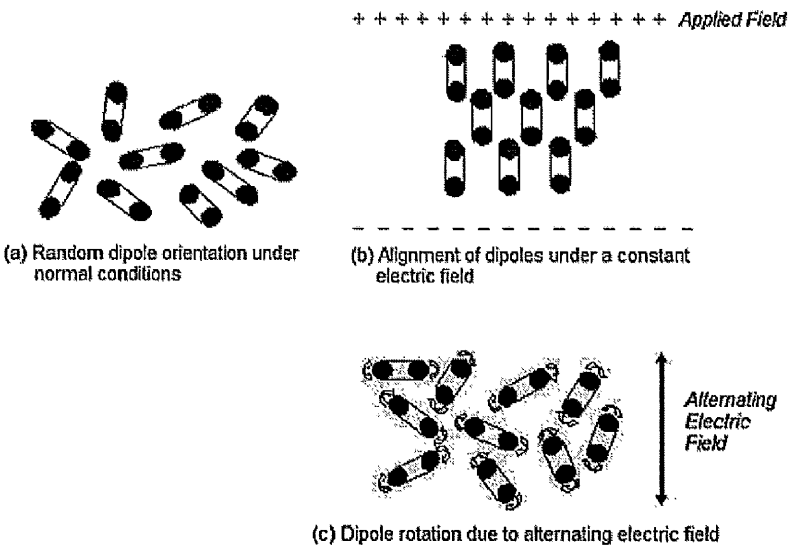

Figure 2.39: *Orientation of dipoles.*

2.5.3.3 Conversion of Microwave Energy into Heat

The dielectric properties of the materials combined with the applied electromagnetic fields result in the conversion of microwave energy into heat. If the electric field is assumed to be uniform throughout the volume, an approximation of the absorbed power per unit volume can be obtained by the following equation:

$$P = 2\pi \cdot f \cdot E^2 \cdot \varepsilon_o \cdot \varepsilon'' \qquad \text{(Equation 2.5)}$$

where P is the absorbed power (Watt/m^3), f is the applied frequency (Hz), E is the electric field strength (Volt/metre), ε_o is the dielectric permittivity of free space (8.854×10^{-12} Farad/metre) and ε'' is the dielectric loss factor of the material. As can be seen from Equation 2.5, a small increase in the electric filed strength increases significantly the absorbed power, since the relationship involves a squared term.

The relationship between microwave power and the temperature raise (ΔT) in a material for a given period of time (Δt) is:

$$\frac{\Delta T}{\Delta t} = \frac{2\pi \cdot f \cdot E^2 \cdot \varepsilon_o \cdot \varepsilon''}{\rho \cdot C_p} \qquad \text{(Equation 2.6)}$$

where ρ is the density and C_p is the specific heat capacity of the material. It is evident from Equation 2.6 that there are no structural parameters involved, as they are assumed to be accounted for by changes in the dielectric loss factor (ε'') of the material.

2.5.4 Microwave Sources

The principal factors that determine the microwave source employed in a certain application are the power and frequency [56]. The required power levels vary significantly, from less than a watt continuous wave for local communication systems to megawatts pulse power for an early warning radar, while the frequency

spectrum in use extends from less than 1 GHz to 90 GHz, continually extending to higher frequencies [57]. The majority of the devices used to achieve high power and frequencies are vacuum electron tubes. Typical examples of vacuum electron tubes that have been used for microwave heating include klystrons, magnetrons and travelling wave tubes (TWTs).

2.5.4.1 Klystrons

Klystrons are electron beam modulated vacuum tubes also called velocity modulated tubes or linear beam tubes. They consist of an electron gun and a resonator, which usually comprises of two or more circular cavities. A schematic view of a high-power klystron is shown in Figure 2.40. The operating principle of the klystron can be described as follows. An electron beam, produced from a heated cathode, passes through two or more resonant cavities and is finally collected on a 'collector' electrode. The first cavity is coupled to an external oscillating electric field which alternately slows down and accelerates the electrons within the beam. This causes some electrons to travel faster than average and some slower. As the beam propagates through the body of the tube called the drift section, the faster moving electrons bunch with the slower ones, so that they travel in groups or bunches. Changes in the amount of bunching represent modulation, which is further increased by intermediate cavities (buncher cavities) as electrons travel through them. Ultimately, the electron beam excites the final cavity (output cavity) at maximum bunching hence promoting the strongest or most amplified oscillations which are removed in the form of RF output power. The remaining electrons pass through the collector and then return to the cathode by means of an external power supply circuit.

Klystrons can generate high power and thus are extensively used in communications, radar, television and scientific research. They are mainly used as amplifiers due to the purity of spectrum (free of undesired side bands), flexibility over a broad frequency range and distortion free modulated signals that they provide. Despite the fact that klystrons of 50 kW output or more at 2.45 GHz have been available for

industrial use for over 20 years [58], they have not been extensively employed in industrial applications owing to their high cost.

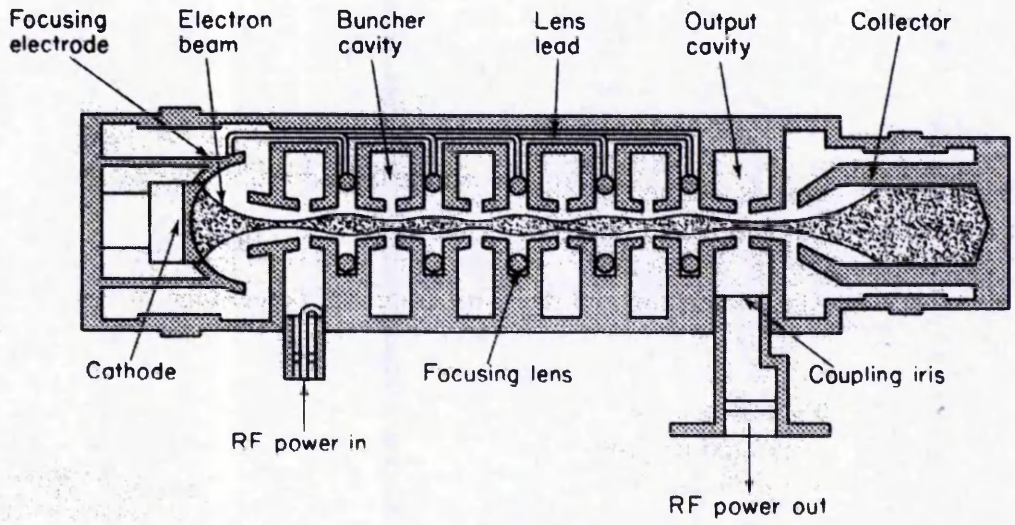

Figure 2.40: *Schematic view of a high-power klystron* [59].

2.5.4.2 Magnetrons

Magnetrons are compact self-oscillating devices, capable of producing high power. They consist of a cylindrical cathode surrounded at a specific spacing by a cylindrical anode. The anode consists of a number of resonant cavities, extending out radially from the centre of the cathode-anode structure. The space between the anode and cathode is called the interaction space. Figure 2.41 shows a typical magnetron cavity arrangement. By applying a potential difference between the anode and cathode, a strong electric field is created in the interaction space and the cathode is heated in order for the loosely bound electrons to be emitted. These electrons are accelerated towards the anode due to the electric field. The whole arrangement is also immersed in a strong axial magnetic field which is perpendicular to the electric field. This causes an additional circumferential force to be applied on the electrons as they are accelerated towards the anode. As a result, the electrons are suspended somewhere in the interaction space, moving in a spiral direction and forming a cloud of electrons which continuously circles around the cathode. The resonant cavities generate oscillations in the electron cloud, the frequency of which is determined by

the physical dimensions of the cavities. The generated energy is then transformed to electromagnetic energy (RF output power) and coupled from the resonant cavities to the transmission lines through a waveguide or coaxial line.

The magnetron was one of the early microwave power generators used in radar and communication telemetry. Since then, it has been used to cover a very wide range of frequencies, from 0.5 to 100 GHz, in a wide range of power outputs for radar and microwave heating. Its space factor and simplicity of auxiliary-control apparatus give structural advantages over klystrons and TWTs in many applications [59]. The single greatest application of the magnetron in terms of production is the domestic microwave oven (operating at 2.45 GHz). Magnetron tubes are nowadays produced in large numbers and so they are very cheap. In addition, they are compact in size, light, highly efficient and able to provide high power which makes them suitable for material processing applications. Magnetrons, however, use resonant cavities to generate the electromagnetic field, thus they are only capable of producing a fixed frequency electromagnetic field.

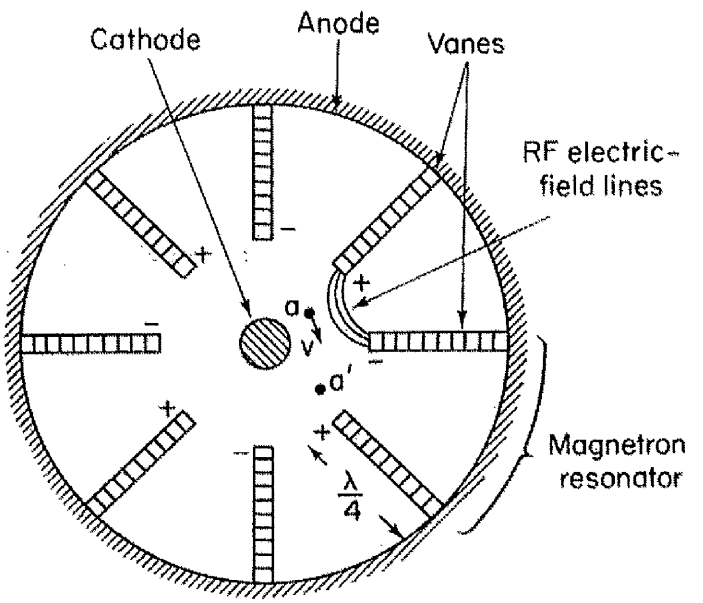

Figure 2.41: *Schematic view of a typical magnetron cavity arrangement* [59].

2.5.4.3 Travelling Wave Tubes (TWTs)

Unlike magnetrons, travelling wave tubs (TWTs) are used only as amplifiers. The microwave signal, usually produced by a voltage-controlled oscillator, is sent to the TWT for amplification, with the frequency of the signal being dictated by the input voltage of the oscillator. TWTs comprise of an electron gun and a helical transmission line. The latter consists of a single-wire helix, an attenuator winding integrated to the helix, RF input-output devices and a collector. The whole arrangement is enclosed in a glass envelope and surrounded by a focusing magnet. Figure 2.42 shows a schematic view of the basic construction of a TWT. The electron gun produces an electron beam which is focused by an external magnetic field through a control grid and accelerated towards the electron gun anode. The collector at the end of the helix is also of positive potential so as to give a final acceleration to the electron beam, while the attenuator windings are used to prevent reflections from passing back down to the helix.

The helix itself serves as a type of delay line which slows the velocity of the applied RF wave along the axis of the coiled wire (phase velocity) to about one tenth the velocity of light. The wave velocity is determined by the diameter and pitch of the helix. Thus, as the microwave signal travels along the helix, its longitudinal component interacts with the electron beam, causing acceleration and deceleration of electrons within the beam. At certain points where the velocity of the electromagnetic wave is roughly equal to the velocity of the beam, more electrons are being decelerated than accelerated which in turn produces electron grouping or bunching. As a result, the microwave signal is amplified due to energy being transferred from the electron beam to the RF wave travelling down the helix.

The main advantages of the TWT are the light weight and the low-noise amplifier performance over a very broad range of frequencies, since there are no resonant structures. TWTs are used to generate the electromagnetic field in variable frequency microwave ovens. They are not, however, high-powered devices hence they rarely have been used above the low-kilowatt range due to the difficulty in coupling to the helix [59].

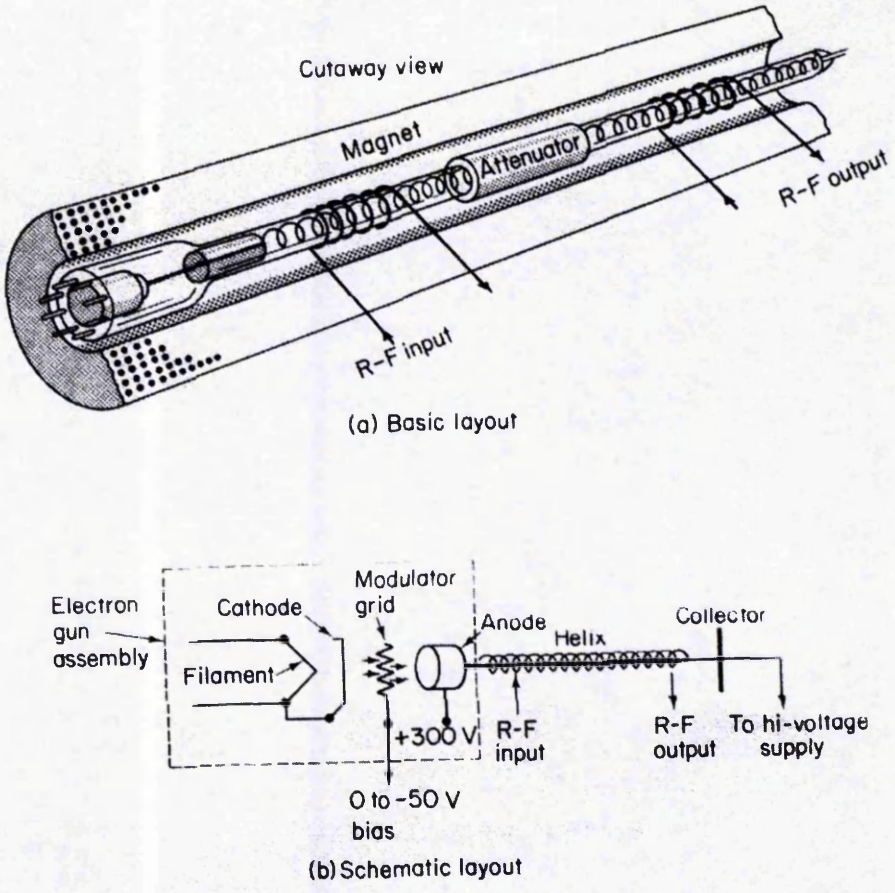

Figure 2.42: *Basic construction of a travelling wave tube; a) basic layout and b) schematic layout* [59].

2.5.5 Transmission Lines

Transmission lines are parallel structures used to continuously transfer the energy produced by the microwave source throughout their length from one point to another. The transmission lines employed for low power systems are usually coaxial cables, while at high frequencies and output power waveguides are preferred.

Coaxial cables are two-wire cables used to transfer microwave power from the source to the applicator. Their structure consists of an outer conductor which shields the inner conductor by means of solid insulation. Waveguides, on the other hand, are hollow metallic tubes which allow the propagation of electromagnetic waves [5]. Their cross-section is usually rectangular, although waveguides of circular cross-

section are also used. They consist of a single conductor and the field configurations (also known as modes) during propagation of the electromagnetic waves have an axial component of either electric or magnetic field. Hence the fields are divided into two classes: *transverse electric* (TE), for which the axial electric field is zero, and *transverse magnetic* (TM) for which the axial magnetic field is zero [57].

2.5.6 Microwave Applicators

The applicator is the component of a processing system responsible for the transfer and deposition of microwave energy to the material. In order to focus and transfer microwave energy efficiently into the material load, accurate impedance matching needs to be provided. The latter is influenced by the geometry (size and shape) of the applicator which is specifically tailored for a given application and relies on several factors, such as the complex dielectric permittivity of the material (ε^*), the material size and shape, the position of the material inside the applicator and the type of processing (batch or continuous). A wide range of applicators are currently employed in the industry [55]. The most common applicators for material processing are resonant cavities such as single-mode, multi-mode applicators and waveguides.

2.5.6.1 Single-Mode Applicators

Single-mode applicators are rectangular or cylindrical cavities designed to support only one resonant mode. This means that the electric field distribution within single-mode applicators is non-uniform, but predictable, and is usually characterised by one 'hot spot' in which the field strength is high. As a result, power concentrations in certain areas within the volume of the processed material might occur. The efficiency of single-mode applicators, however, is higher compared to multi-mode or travelling wave applicators and despite the non-uniformity of the produced field patterns, mode switching can be achieved via changing the physical dimensions of the applicator or regulating the frequency of the microwave source.

Zhou and Hawley [60] used a cylindrical single-mode applicator to investigate the adhesive bonding of polymers and composites under microwave heating. In order to achieve a time-averaged uniform heating regime within the single-mode applicator, two different modes were employed by varying the applied frequency. In specific, the TM_{020} mode, corresponding to a frequency of 2.845 GHz, was used to heat the centre of the adhesive and the TM_{212} mode, corresponding to a frequency of 3.383 GHz frequency, was used to heat the edges. The results indicated that the temperature gradient across the adhesive was significantly reduced from as high as 60°C to 10°C when using a combination of two different modes instead of one. Furthermore, Fellows and Hawley [61] used the mode switching technique to process composite materials in a cylindrical single-mode cavity by changing the length of the cavity and the depth of the coupling probe. The composite samples had complex geometries and were autoclaved for microwave curing studies. Their research revealed that the mode-switching technique produced uniform temperature profiles during microwave processing of the composite samples. Single-mode applicators have also been used for the microwave processing of thermosetting resins in other studies [62-64].

2.5.6.2 Multi-Mode Applicators

As suggested by the relevant term, multi-mode applicators are applicators that are capable of sustaining a number of high order modes at the same time [58]. The presence of different modes results in multiple hot spots within the microwave cavity, which in turn may cause localised overheating. In order to improve the electromagnetic field uniformity and reduce the effect of hot spots, larger cavities and/or higher operating frequencies can be employed. Nevertheless, the penetration depth of microwaves is higher at lower frequencies (for example 2.45 GHz) than at higher frequencies hence considerable amount of effort has been directed towards achieving more uniform heating inside smaller cavities at 2.45 GHz. A typical example of such efforts is the domestic microwave oven, which is usually equipped with a rotating turntable so that the product is passed through a series of hot and cold spots to balance out heating during operation.

The field uniformity can be also improved by a technique called mode stirring. Mode stirrers are reflectors, much like fans, which rotate within the cavity near the waveguide input [5]. This causes continuous redistribution of the electromagnetic field, as the mode stirrers 'mix up' the modes by reflecting waves off their irregularly shaped blades. In addition, variable frequency processing systems have been recently developed for materials research. These systems utilize travelling wave tubes (TWTs) to sweep a wide range of microwave frequencies, thus achieving greater field uniformity. Variable frequency microwave processing has been shown to evenly cure large amounts of resin [65] as well as thick composite laminates [66]. Multi-mode applicators have also been employed for the microwave processing of thermosetting resins in other studies [67, 68]. Finally, another method to achieve more uniform heating is hybrid heating [5]. Hybrid heating is a combination of microwave and conventional thermal heating so that heat is transferred through radiation, convection and conduction.

2.5.6.3 Waveguides

Waveguides are hollow conducting metallic tubes with either a rectangular or circular cross-section. The microwave field inside a waveguide is fundamentally different to that inside either a single-mode or multi-mode applicator. While in both single-mode or multi-mode applicators microwaves are reflected off the walls and combined with incident microwaves forming standing waves, in waveguides microwaves are travelling waves. As microwaves travel through the waveguide, some portion of the microwave energy is absorbed by the processed material, while the remaining portion is directed to a terminating load. Fu and Hawley [69] used a circular waveguide in the TE_{111} resonant mode at 2.45 GHz frequency to cure epoxy resins by means of both continuous-power and pulsed-power microwave heating. The results indicated that the temperature variation was lower during continuous-power than pulsed-power curing. Furthermore, higher reaction rates and ultimate extents of cure were observed in continuous-power than in pulsed-power microwave curing. Waveguides have also been used for the microwave processing of thermosetting resins in other studies [8, 70].

2.5.7 Potential of Microwave Processing

One of the main advantages of microwave heating is the significantly lower energy consumption during processing, due to the direct deposition of energy in the volume of the material. Heating the walls of the furnace or reactor, its components and heat carriers is no longer necessary, resulting into considerable energy savings. The overall energy efficiency in industrial microwave processing is 50-70%; a Canadian source also estimated that the energy savings in drying and firing of ceramics using microwave energy is 80% compared to its conventional rival, while in alumina sintering the energy savings can be as high as 90%, as summarized in [3]. In addition, the rapid and volumetric heating achieved in microwave processing also reduces the time needed for the completion of a process. Nonetheless, microwave processing equipment is usually more expensive than its conventional counterpart.

Microwave heating can also be selective, due to the interdependence between the deposited microwave power and the absorption properties of the processed materials. In specific, the temperature distribution in a composite material during microwave heating is determined by the distribution of the individual components within the material, as well as their absorption properties. It is possible, therefore, to obtain materials with the desired microstructure and overall properties. This selectivity of microwave heating is used to fabricate composites, fabricate and join ceramics and synthesize materials that have inhomogeneous microstructures and gradient functional properties, known as functionally graded materials (FGM) [4].

Furthermore, depending on the material and the frequency of the applied microwave radiation, the penetration depth can be small enough to enable the absorption of microwave energy only in the near-surface area of the material. In that way, microwave heating can also be considered as another method for the surface treatment of materials, such as electron and ion beams, plasma processing and laser irradiation. Additionally, many high-temperature multistage processes involve the succession of various steps which replace each other, as the temperature of the material rises. Some of these stages may have a detrimental effect on the quality and properties of the final product. The use of microwaves can provide, therefore, rapid

and efficient heating, eliminating the need for undesired intermediate stages in the process. An example of such a multistage process is the sintering of ceramics.

2.5.8 Microwave Curing of Epoxy Resins

Vulcanization of rubber was the first successful commercial application of microwave processing for polymers. The process was characterized by increased throughput, reduced operational costs, product uniformity, reduced scrap parts, improved automation and process control, continuous vulcanization, improved cleanliness and environmental stability [3]. Since then, there have been many attempts to explain and understand the effects of microwave processing on the kinetics and physical properties of polymers.

The acceleration of cure kinetics of thermosetting resins is probably one of the most commonly reported "microwave effect". By using microwave radiation instead of conventional heating methods, a drastic reduction in the duration of the curing process is achieved. However, the existence of the microwave effect in thermosetting resins is quite controversial, as some researchers have shown favourable results while others have reported the opposite. So far, there are two proposed models for the chemical mechanism of microwave induced reaction enhancement chemistry in the literature. The first one assumes that while the reaction time is significantly reduced in a microwave induced reaction, the kinetics or mechanism of the reaction is not changed. Microwave irradiation results in a drastic enhancement of the system temperature, and thus the rate of the reaction, simply due to thermal dielectric heating [71]. The alternative proposal suggests that the reaction rate enhancement is a result of a specific activation effect due to microwave radiation in addition to the previously mentioned dielectric heating (the latter is also referred to as the non-thermal microwave effect) [71].

Wei and co-workers [72-74] studied the reaction kinetics and glass transition temperatures of microwave and thermally cured DGEBA (diglycidyl ether of bisphenol A) epoxy resins using two different curing agents, DDS (diaminodiphenyl sulfone) and mPDA (meta phenylene diamine) respectively. Higher ultimate extents

of cure and reaction rates were observed in the microwave cured samples compared to their thermally cured counterparts. Furthermore, higher T_g values were obtained in the microwave cured samples compared to those cured thermally after gelation. The increase in the T_g values and reaction rates, however, was much more prominent for the DGEBA/DDS than the DGEBA/mPDA system, suggesting that the magnitude of the acceleration induced by microwave heating is also influenced by the curing agent employed.

A strong dependence of microwave curing on the curing agent was also suggested by Boey *et al.* [75] who investigated the effect of three different curing agents (4,4'-DDS, 4,4'-diaminodipheyl methane (DDM) and mPDA) on the rate enhancement during both microwave and thermal curing of a DGEBA resin system. The microwave power used to cure the resins varied between 200 W and 600 W. Similar degrees of cure were reported for both curing methods, while the duration of the curing process was significantly reduced when using microwaves for all systems. This was consistent with the work of Zhou *et al.* [1] who showed that the curing time and curing temperature of the E44 epoxy resin could be decreased by approximately two-thirds and 15 – 20°C, respectively, when using microwave radiation. They also found that the amount of maleic anhydride hardener consumed was 5% less during microwave curing than thermal curing.

Furthermore, Lewis and co-workers [76] studied the curing of a DGEBA/DDA epoxy resin system, while continuously monitoring the resin temperature by means of a fibre-optic probe. Their results revealed an 8 – 10 fold decrease in cure time for 100% completion of the reaction in the microwave cure compared to the thermal cure at a comparable temperature. The observed rate enhancement of microwave irradiation was attributed to a localised superheating effect. This group also examined epoxy resin systems where a large degree of hydrogen bonding is known to take place involving both oxygen-hydrogen and nitrogen-hydrogen bonds, and attributed microwave induced curing acceleration in epoxy systems to interaction of the microwave radiation with the hydrogen-bonded networks [77].

In agreement with the results reported by the previous researchers, Marand and co-workers [16, 78], who studied the reaction mechanisms of DGEBA/DDS epoxy resin

systems undergoing thermal and microwave cure via *in situ* measuring their dielectric properties, showed that the rate of the curing reaction was much higher in the samples cured by microwave radiation than in those cured thermally. Particularly at higher temperatures, the induced rapid cross-linking rates created a rigid network which was believed to have led to entrapment of unreacted amine and epoxy groups within the resin matrix, resulting to lower overall degree of cure in the microwave cured samples. Furthermore, Wallace and co-workers [79] studied an epoxy/amine resin system cured by conventional and microwave heating, using several methods such as Differential Scanning Calorimetry (DSC), Dynamic Mechanical Thermal Analysis (DMTA), Infrared Spectroscopy (IR), Solid state NMR Spectroscopy and dielectric measurements. Their results showed that the reaction path is slightly different in the two cases. In specific, the epoxy-amine reaction was found to be dominating the epoxy-hydroxyl reaction in the microwave cured resin, compared to the thermally cured one. This conclusion was affirmed by the results derived from the majority of the employed methods, except from the dielectric measurements. The discrepancy in that case was attributed to a less significant impact of the involved chemical groups on the dielectric properties.

These findings, however, are contradictory to the work of Mijovic and Wijaya [67, 80, 81] who conducted a comparative calorimetric study of cure of an epoxy/amine (DGEBA/DDS) formulation by microwave and thermal energy and observed that at a given temperature cure proceeds slightly faster in the thermal field. In addition, a broader glass transition temperature (T_g) range was observed in microwave cured samples, suggesting a possible difference in the cure mechanism in thermal and microwave fields. In their more recent work, Mijovic *et al.* [82] used an in-situ method to investigate the cross-linking of several different materials including epoxies, polyimides and bismaleimides. They concluded that the mechanisms and rates of isothermal kinetics in the reactive systems studied were identical in both thermal and microwave fields and that the claims of accelerated cure kinetics due to a "microwave effect" are unfounded.

Similar findings were also reported by Hill and co-workers [83] who investigated the microwave and thermal curing of the DGEBA/DDS and DGEBA/DDM epoxy/amine systems by means of FT-NIR spectroscopy. Their results revealed no

evidence of any microwave induced specific effect on the cure kinetics, as the reactions rates of both primary amines and secondary amines were found to be comparable between the two curing methods. No change in the reaction kinetics between microwave and thermally cured DGEBA/DDS resin systems was also reported in [84]. In addition, Rogers *et al.* [85] conducted comparative kinetic studies of the thermal and microwave curing reactions of two epoxy systems, MY721/DDS and MY721/DDM, using FT-NIR spectroscopy. Microwave curing was carried out in both rectangular and cylindrical microwave cavities. The reaction rates during microwave curing of both resin systems in the rectangular cavity were found to be about 30% faster than those observed for thermal cure in a heated aluminium block. This result, however, was not reproduced using the cylindrical cavity, for which the microwave curing reactions proceeded more slowly than the comparable thermal curing process under the same conditions. The authors concluded that the differences in the reaction kinetics between the conducted experiments were caused by temperature gradients within the microwave cavity rather than real mechanistic differences.

Many researchers also compared the mechanical properties between thermally and microwave cured epoxy resins. Several studies suggested that microwave curing could be beneficial to the mechanical performance of the resin systems, while some other reported no significant differences in the mechanical properties of resins produced using both conventional and microwave curing methods. In specific, Zhou *et al.* [1] investigated the mechanical properties of an epoxy/maleic anhydride resin system cured both by microwave and thermal energy. Their results indicated that microwave curing of an epoxy resin can increase the compressive and flexural strength of the epoxy resin. All of these beneficial effects were believed to be induced by a series of media polarization taking place in the epoxy resin, while subjected to microwave radiation. More than 10% higher Young's modulus for a microwave cured commercial epoxy resin system, AY103/HY991, was also reported by Karmazsin *et al.* [70, 86]. The cure cycle employed for microwave curing was 10 min at less than 100°C in a TE_{10} waveguide, as opposed to 1 h at 100°C in a conventional resistance furnace for thermal curing.

Additionally, Bai and co-workers [87] compared the mechanical behaviour between a DGEBA/3DCM epoxy resin system cured by microwaves and one cured thermally. Tensile testing showed that the tensile strength and Young's modulus were slightly higher in the microwave cured samples. This difference was considered to be attributed to the greater homogeneity of the microwave cured resin, due to fewer created microvoids compared to the thermally cured resin. After ageing in water, the microwave cured samples maintained their advantage of the mechanical properties over the thermally cured ones. The tensile strength and modulus of both resins increased with the increasing strain rate and decreased with higher ageing temperature and longer ageing duration. The fracture surfaces also showed some significant mechanisms of rupture and of an ageing effect.

Singer and co-workers [7] compared the values of the tensile strength and Young's modulus of an epoxy-amine system (DGEBA/DDS) cured by microwave irradiation in a cylindrical brass cavity and by thermal means. Their results indicated that the tensile strength of the microwave cured samples below 80% degree of cure was considerably lower compared to their thermally cured counterparts. As the extent of cure increased, however, the tensile strength of the microwave cured samples increased rapidly, exceeding that of their thermally cured counterparts. The lower strength at lower degrees of cure was attributed to the restricted alignment of the dipoles during microwave cure, which in turn resulted to a lower entanglement in the molecular structure of the formed network. Nevertheless, the mechanical properties of the fully cured samples produced under microwave irradiation were comparable to those produced thermally.

Other researchers, however, claimed that the mechanical properties of the resins were not affected by microwave irradiation. Jordan *et al.* [88] investigated the effect of a microwave cure of a DGEBA epoxy resin with 3DCM (4,4'–diamino-3,3'–dimethyldicyclohexylmethane) amine curing agent, as compared to a standard thermal cure. Their results showed that under microwave curing, it was not possible to obtain fully cured DGEBA/3DCM networks and no direct influence of microwave curing on the mechanical properties of the network was established. However, the only parameter that influenced the mechanical properties was the extent of reaction, as the compression modulus increased for lower extent of cure. Furthermore, Surrett

et al. [65] used variable frequency microwave processing to cure an epoxy resin system (ERL-2258/mPDA) in a multimode cavity capable of producing 200 W of power. It was reported that the microwave samples were not fully cured due to their large size. After post-cure treatment, however, the hardness and degree of cure values obtained were comparable between microwave and thermally cured resin samples. Finally, Tanrattanakul and TiSaw [89], who carried out research on the tensile, impact resistance and flexural properties of epoxy-anhydride resins cured with both conventional and microwave heating, showed that equivalent or better properties were obtained through the use of microwaves. Microwave curing also resulted in an equivalent degree of conversion at a shorter cure time, while the glass transition temperatures obtained by means of dynamic mechanical thermal analysis were found to be comparable between microwave and thermally cured resin samples.

2.5.9 Microwave Curing of Epoxy Matrix Composites

The difficulties related to the curing of thermosetting composite laminates are well known and are often magnified in the case of thick laminates. Conventional thermal curing of composites relies on conduction and convection of heat throughout the thickness of the material. Therefore, to achieve efficient cure the material must be heated at a slow rate. In addition, the exothermic chemical reactions occurring during the curing process generate internal heat that is dissipated slowly through conduction. As a result, a complex temperature distribution is observed within the composite laminate, capable of causing non-uniform cure, thermal degradation, uncontrolled solidification and process-induced stresses. All of these effects reflect negatively upon the quality and overall properties of the finished component. Microwave curing has the potential to minimize some of these difficulties, as it realizes uniform and volumetric heating of the material [5].

A considerable amount of research has been carried out on the microwave curing of fibre reinforced composites. The primary objective of this study is microwave curing of epoxy resins reinforced with both glass and carbon fibres. Most of the literature reported so far is devoted to the investigation of the properties of microwave cured glass-fibre reinforced composites. This is reasonable considering the relatively easy

processing conditions involved during microwave curing, since most glasses are transparent to microwave energy. Glass has a significantly low dielectric loss factor which allows microwave energy to be absorbed predominantly by the resin during the curing process. Hence microwave heating can be readily achieved in these systems. Application of microwave energy in the processing of carbon fibre/epoxy composites, however, has always been more complicated owing to the high dielectric loss and conductive nature of carbon fibres at microwave frequencies.

Lee and Springer [90], who were among the first to carry out a fundamental investigation of microwave curing of composite materials, developed a numerical model and compared the derived data with experimental results for the same conditions. They reported that although glass fibre reinforced composites were capable of efficient curing by microwave radiation, in the case of carbon fibre reinforced composites curing would only be achieved in thin unidirectional laminates. This was due to the high dielectric loss of carbon fibre. In angle ply laminates, the reflectance of the first few layers was too high to achieve efficient heating of thick laminates. In addition, the presence of highly conductive carbon fibres may result in the formation of local hot spots. Boey and Lee [91] investigated the effect of curing time and power rating of the radiation source, on the gelation time and the glass transition temperature during microwave curing of a glass-fibre reinforced epoxy (DEBGA-type) resin composite. The results showed that maximum gelation was achieved faster at the higher power rating, although full gelation occurred within about 8 minutes for all ratings. The glass transition temperatures obtained for all the microwave cured specimens were practically identical.

Furthermore, Mooteri and co-workers [92] investigated the mechanical behaviour of glass fibre-epoxy composites cured by microwaves in a custom-built microwave oven by means of tensile, compression and flexural strength tests. The results demonstrated that the associated mechanical properties of the microwave cured composites were equivalent (and sometimes superior) to those of their thermally cured counterparts, while significant reductions in the cure cycle time and power consumption were achieved through microwave processing. Day and Nightingale [93] compared the mechanical properties of two types of carbon fibre/epoxy composites. The first one consisted of a resin and a hardener with considerably

higher dielectric loss factors than those of the second one. The composites were cured by: autoclave curing, partial microwave followed by microwave post-curing and microwave curing. The results showed that the autoclave cured composites had the best flexural and interlaminar shear strength properties, with system 1 prevailing system 2. The microwave cured composites followed with the properties in both systems being similar. The microwave post-cured composites had the worst flexural and ILSS properties, with system 2 dominating system 1 in terms of properties. The void content of the microwave cured composites was high, compared with the autoclave cured and microwave post-cured composites.

Qiu and Hawley [94] developed an automated microwave processing system comprising of a single mode cavity and a variable frequency power source, able to fully utilize the benefits of microwaves via uniform heating. The material used in their study was a graphite/epoxy prepreg. The control parameters were microwave frequency and power. Several modes with complementary heating patterns were alternatively excited, providing uniform heating. As a result, the mode-switching heating method significantly improved the temperature distribution within the cavity, thus the flexural properties of the product were found to be improved. In addition, Liu et al. [95] examined the microwave curing of polyimide precursors with and without glass and glass-graphite cloth at 2.45 GHz frequency in a microwave oven using a multi-step heating cycle. They found that the addition of chopped carbon fibre accelerated substantially the curing process. It was also noted that electrically conducting fibres, such as graphite and carbon fibres, absorb microwave energy more efficiently compared to other non-conducting materials hence microwave processing may enhance the interfacial bonding between resin matrix and fibres. Higher flexural and interlaminar shear strengths for the microwave cured carbon fibre/polyimide composites compared to those cured conventionally were also reported by Fang and Scola [96].

Wei and co-workers [97] investigated the microwave curing of thick cross-ply carbon fibre/epoxy composites (Hercules AS4/3501-6) using a tuneable resonant microwave cavity. It was shown that the extent and uniformity of cure varied according to the resonant mode used for processing. Study of the flexural strength and modulus of the produced composites indicated that the microwave cured

composites yielded better mechanical properties compared to those cured thermally under similar processing conditions. Nevertheless, the resonant heating mode and hence the temperature uniformity inside the cavity were found to influence the flexural strength of the composites. The mechanical properties of the microwave cured unidirectional composites also appeared to rely significantly on the fibre orientation in the stacking sequence. Lye and Boey [98] also reported considerably superior mechanical properties of glass fibre laminates cured by microwaves in an autoclave compared to those cured thermally. Additionally, the duration of the curing process was found to be shorter in microwave processing than in thermal processing [98].

Microwave processing is also claimed by some researchers to have improved the interfacial strength of the produced composites, resulting in a stronger interface between the matrix and the fibres. Bai and Djafari [99] studied the mechanical behaviour of a microwave cured unidirectional continuous E-glass fibre/epoxy composite by *in situ* transverse tensile loading and short-beam tests which were carried out in the interior of a scanning electron microscope (SEM). The mechanisms of rupture were also analyzed. By comparing the results for the microwave and thermally cured composites, it was found that more voids exist in microwave cured composites. This difference was attributed to the shorter time and lower applied pressure involved in microwave curing. However, the fibre-matrix interface of microwave cured composites appeared to be stronger than that of thermally cured composites, as suggested by the results of transverse tensile and 4-point bending tests and observations of the damage and rupture process.

Similar findings were also reported by Boey and Yue [100] who examined the interfacial strength of a glass-fibre reinforced epoxy composite (DGEBA/DDS) microwave cured for different radiation times, at increasing power ratings. The maximum interfacial strengths of the specimens obtained for all of the power ratings were higher compared to those of the thermally cured ones. However, for the specimens cured at higher microwave power (400 and 500 W) a drastic drop of the interfacial strength after a certain curing time was observed, indicating that overheating and thus degradation by charring had occurred. Improved interfacial properties of microwave cured aramid fibre/epoxy composites compared to those of

their conventionally cured counterparts were also reported by Day and Yau [101], as indicated by Raman spectroscopy.

Furthermore, Rao *et al.* [102] investigated the effect of thermal and microwave curing on the thermo-mechanical properties of 3 mm thick glass fibre epoxy-amine laminates (the fibre weight fraction of the latter was 62.2%). The results indicated that the tensile and interlaminar shear strengths (ILSS) of the microwave cured composites were similar or superior to those cured by thermal means. It was also reported that substantial energy savings and reduced cycle times were achieved through microwave processing, while the degree of cure across the produced panels was found to be uniform. The glass transition temperatures (T_g) of the composites cured with microwaves were slightly superior to those of their thermally cured counterparts (120°C to 112°C and 165°C to 160°C for the low and high curing temperature cycles, respectively).

Hook *et al.* [103, 104] investigated the effects of microwave processing on the chemical interactions taking place between an epoxy-amine resin matrix and the carbon fibre surface by examining the produced composite samples through X-ray Photoelectron Spectroscopy (XPS). Their research indicated that the extent of chemical bonding of the epoxy-amine resin matrix to the carbon fibre surface was increased by more than 5% in microwave heating compared to conventional thermal heating. In specific, an increased population of carbon oxide species, indicating a higher percentage of oxygen, was observed in the case of microwave processing. Furthermore, the extent of chemical interaction between the carbon fibre surface and the epoxy and amine reactants was shown to have doubled when using microwaves, while very small interaction was observed between the hydroxyl group adduct and the fibre surface regardless of the curing method employed.

Nevertheless, the effect of microwave processing on the mechanical properties of composites is disputed by other researchers. In specific, Boey and Lee [105] used a vacuum bagging method to fabricate a glass-fibre/epoxy composite via microwave curing. They reported that optimum curing was achieved at a considerably faster time under microwave energy compared to a conventional thermal process. In addition, the highest flexural strength achieved in microwave curing was close to

that achieved for thermal curing, whilst the flexural modulus was significantly higher. Furthermore, Yue and Looi [106] examined and determined the mechanical and interfacial properties of a glass-fibre/epoxy composite cured under both thermal and microwave energy, from analysis of experimental data gathered from pull-out tests. The results suggested that thermal processing of a glass-fibre/epoxy system leads to composites with higher strength and higher toughness compared to microwave processing. This difference was due to the higher matrix shrinkage pressure (P_o) on the fibre developed in thermal processing. The test method adopted, however, had a strong influence on the measured interfacial bond strength (τ_i), as the compression lap shear test indicated higher interfacial bond strength of the microwave cured composites compared to the thermally cured ones.

Agrawal and Drzal [6] assessed the matrix-fibre interface of a microwave cured epoxy resin system reinforced with glass fibres, aramid fibres and carbon fibres by means of a single fibre critical length test. Their results indicated that the interfacial shear strength was decreased by 15% for the microwave cured glass fibre/epoxy and aramid fibre/epoxy composites, respectively, compared to those cured thermally. The interfacial shear strength of the microwave cured carbon fibre/epoxy composites, however, was found to be 70% higher than that of their thermally cured counterparts. This enhancement in the interfacial properties was attributed to the selective heating of carbon fibres during microwave processing. In specific, due to the dielectric properties of carbon fibres, a large amount of microwave power is thought to be absorbed as heat by the fibres during the curing process. Thus, heat is transferred from the fibre surface to the bulk resin, possibly resulting in a stress-free interphase with a better fibre-matrix adhesion.

In other studies, however, similar properties have been observed between microwave and thermally cured composites. Paulaskas and Meek [107] carried out research on the microwave and thermal processing of two types of thermoset prepreg (unidirectional and multidirectional carbon fibre/epoxy and glass fibre/epoxy). They found that the ultimate tensile strength was comparable between both types of microwave and conventionally cured laminates. Additionally, it was reported that the cure cycle time for microwave curing of both unidirectional and multidirectional glass fibre laminates and unidirectional carbon fibre laminates was drastically

reduced. Microwave radiation at 2.45 GHz, however, was proven to be unable to directly cure the multidirectional carbon fibre laminates hence reduction of the cure cycle time to one third of that required for thermal curing was achieved by means of hybrid heating. Furthermore, Day and Samoladas [108] evaluated the micro-mechanical properties of single fibre model carbon/epoxy composites cured and post-cured using both microwave and conventional heating. Raman spectroscopy showed that the interfacial shear strengths of both cured and post-cured composite samples were similar amongst the two curing methods.

2.5.10 Microwave RTM Processing of Composites

The coupling of microwave radiation with the resin transfer moulding process (RTM) as a means of manufacturing microwave-cured composite laminates, has been scarcely reported throughout literature. Johnson *et al.* [109] used an in-line cylindrical applicator to preheat the resin by microwaves prior to injection. As a result, thermal quench at the injection gate and resin viscosity was reduced, leading to considerably reduced cure cycle times. Furthermore, Rahmat [110] studied the microwave curing of aramid fibre reinforced polyester resin composites using a PTFE mould and a commercial microwave oven operating at 2.45 GHz. The power supply of the microwave oven was modified so that the accelerating voltage supplied to the magnetron, and thus the microwave power, was controlled during the curing process. Neat polyester resin samples were also cured both thermally and with microwaves. The results showed that the cure cycle time required to cure neat resin and composite samples in a microwave oven was reduced compared to a conventional oven. The flexural modulus and strength, transverse tensile modulus and strength, and interlaminar shear strength of the microwave cured composites were higher than those cured thermally. This was partly attributed to the presence of holes within the structure of the microgels formed during the early stages of cure, as observed by SEM. These holes are thought to facilitate more styrene monomers and polyester chains diffusing into the microgels, thus resulting in microwave cured resin and composite samples with higher crosslink density. Both thermally and microwave cured samples had similar NMR spectra.

Finally, Yusoff [17] investigated the microwave curing of carbon fibre/epoxy composites using both microwave assisted and conventional thermal RTM processing. Study of the thermal characteristics as the curing progressed revealed that polymerisation occurred faster during microwave curing than thermal curing, while similar glass transition temperatures and ultimate degrees of cure were obtained for both microwave and thermally cured samples. The void contents, however, were higher for the microwave cured composites compared to their thermally cured counterparts. In addition, the tensile, flexural and compressive properties were similar for both conventionally and microwave cured composites, while the interlaminar shear strength of the microwave cured samples were slightly higher than their thermally cured counterparts. The densities and dielectric properties of the composite samples produced using both curing methods were similar.

CHAPTER 3

Materials and Processing Methods

Introduction

This chapter provides details regarding the raw materials and the processing methods used in this work. The separate stages in both conventional and microwave resin transfer moulding (RTM) processing together with the preparation of the samples and the relevant tooling involved in the fabrication of the composite panels are described.

Materials

Resin System

The epoxy resin used in this study was the Araldite LY5052/Aradur HY5052 resin system (manufactured by Huntsman). The LY5052 epoxy resin consisted of 60-70% epoxy phenol novalak resin and 34-42% butanedioldiglycidyl ether. The HY5052 hardener consisted of three amine cross-linking agents. Two difunctional primary amines, 50-60% 2,2-dimethyl-4,4-methylenebis (cyclohexylamine) and 35-45% isophore diamine, and an aromatic tertiary amine, 1-5% 2,4,6-tris(dimethyl-aminomethyl)phenol. The chemical structures of all the components in the LY5052/HY5052 epoxy resin system are shown in Figures 3.1 and 3.2.

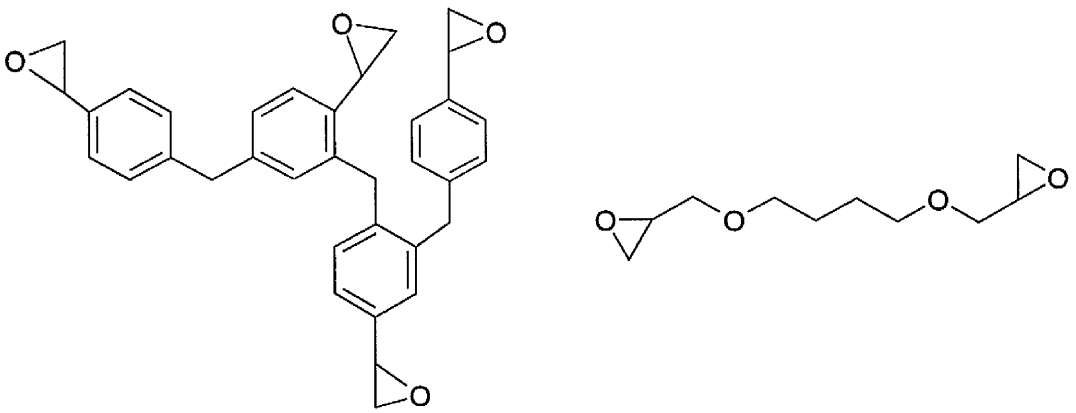

(i) Typical epoxy phenol novalak resin (ii) Butanedioldiglycidyl ether

Figure 3.1: *Chemical structures of the Araldite LY5052 epoxy resin components* [111].

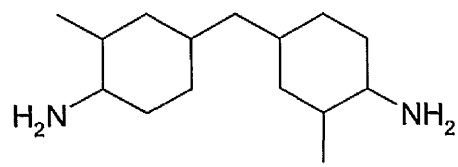

i) 2,2 dimethyl-4,4-methylenebis (cyclohexylamine)

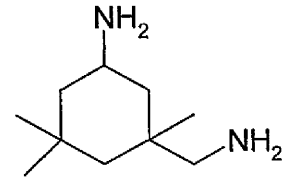

ii) Isophorone diamine

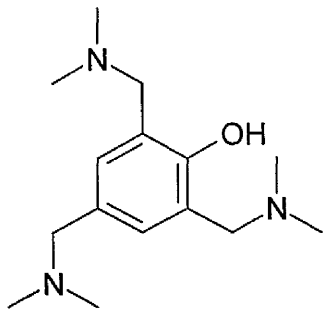

iii) 2,4,6-tris(dimethyl-aminomethyl)phenol

Figure 3.2: *Chemical structures of the Aradur HY5052 hardener components* [111].

The ether is a reactive diluent added to the phenol novalak resin to reduce the viscosity of the epoxy resin and make it easier to handle. The primary amines in the hardener would cross-link with the resin and produce a rigid three dimensional network, while the tertiary amine help to chain extend and cross-link the resin furthermore via a catalytic mechanism. The relevant cross-linking reactions are described in Chapter 2.

Fibre Reinforcement

The reinforcements used in this work were woven carbon fibre and woven glass fibre fabrics. The carbon fabric consisted of high strength T300 carbon fibre and was supplied by Hexcel Composites Ltd. The weave design was a balanced 50/50 warp and weft 5-harness satin. The glass fabric was very similar in weave; it consisted of E-glass and had a balanced 50/50 warp and weft 4-harness satin weave design. The glass fabric was supplied by Fothergill Engineered Fabrics Ltd. The weave designs for both types of fibre reinforcement are illustrated in Figure 3.3. The harness number used in the designation (4 or 5) corresponds to the total number of fibres

crossed and passed under, before the pattern is repeated. Satin weaves are very flat, allow a high degree of drape, have a good wet-out and provide good mechanical properties. Both carbon and glass fibre fabrics were surface treated for epoxies. Details regarding the surface treatment used for the carbon fibre fabric were not disclosed by Hexcel due to reasons of confidentiality. The surface finish, however, was compatible with epoxy resins. The surface finish used for the glass fibre fabric was methacrylato chromic chloride (also known by the trade name Volan), which is a coupling agent for glass fibre reinforced unsaturated polyester, epoxy resin and other polymer composites.

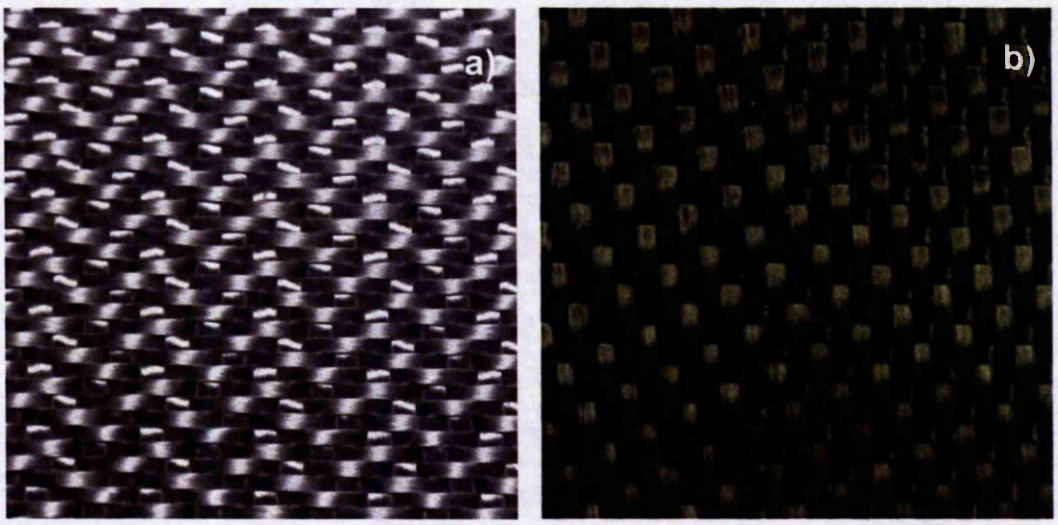

Figure 3.3: *Weave designs for; a) glass fibre fabric (4-harness satin) and b) carbon fibre fabric (5-harness satin).*

Sample Preparation

LY5052/HY5052 resin samples were prepared by mixing the LY5052 resin with the HY5052 hardener at a ratio of 100:38 by weight, as recommended by the manufacturer. Based on the work of Yusoff [17] and preliminary DSC analysis on the uncured resin system, the cure cycle employed for conventional thermal RTM processing was 100°C for 3 hours. Determination of the cure cycle for microwave RTM processing was based on the dielectric properties of the uncured resin, as measured using the cavity perturbation technique described in Section 4.11. A cure cycle of 90 minutes at 100°C was employed for the microwave curing of the

composite samples and the selection was based on the dielectric data of the uncured resin. The cure cycle determination for both conventional thermal and microwave curing are discussed in detail later in Section 5.4.

The carbon fibre and glass fibre fabric were cut to specific dimensions in order to fit inside the mould cavity. A metal moulding tool was used in conventional thermal RTM, whereas a ceramic moulding tool suitable for use inside the microwave field was specifically manufactured for microwave RTM (see Section 5.2). The mould dimensions in both cases are given later in this chapter. Seven layers of reinforcement were used for each laminate panel.

Resin Transfer Moulding (RTM) Processing

As described in Chapter 2, RTM is a common composite manufacturing process which involves injection of a liquid resin into a closed mould tool loaded with a fibre reinforcement. When the curing stage has been completed, the mould tool can be opened and the finished component removed. Composites were produced by both conventional thermal and microwave resin transfer moulding (RTM) for the purpose of comparison.

Conventional Thermal RTM Processing

Conventional thermal RTM processing was based on the Hypaject Mark II RTM Injection system (Plastech T.T), as illustrated schematically in Figure 3.4. The system comprised of an RTM control unit, an inlet valve, a homogenizer, a pneumatic resin injection valve and a two part metal mould.

The fibres were initially placed inside the mould cavity (200 x 300 x 3 mm dimensions) and the metal mould was inclined at 45° from horizontal in a steel stand to minimize air entrapment during the injection. Apart from regulating the injection pressure, the Hypaject control unit generated an internal vacuum which allowed the resin to be drawn into the homogenizer through the inlet valve. The resin was left

under vacuum for 10-15 minutes to remove any air bubbles created at the resin-hardener mixing stage. The resin was then injected at room temperature and under low pressure (0.5 Bar) into the mould through the inlet located at its lower corner.

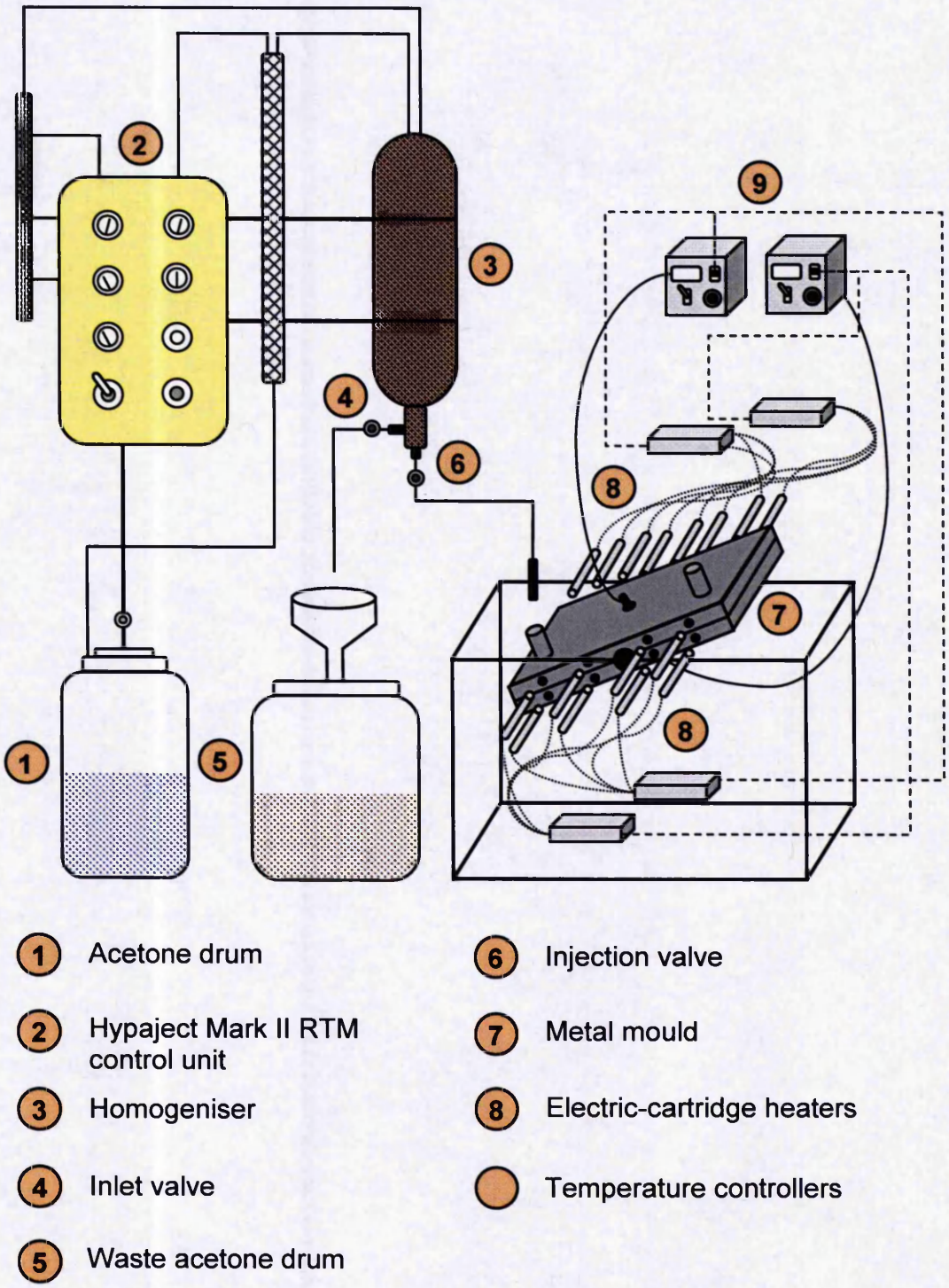

Figure 3.4: *Schematic diagram of conventional resin transfer moulding processing.*

Prior to the placement of the fabric, the mould surfaces were treated with release agent to prevent bonding of the produced composite panels to the mould surfaces and facilitate the removal of the composites from the mould. More specifically, the metal mould was coated with 5 layers of Frekote 44-NC release agent; the ceramic mould was initially coated with 2 layers of Chemlease C15 sealer followed by 4 coats of Chemlease PMR release agent. 15 - 20 minutes were left to elapse between applying each coating to allow sufficient time for the sealer and the release agent to set.

On completion of the injection process, the resin-loaded mould was heated using 16 electric-cartridge heaters (8 for each mould part) which gave a total power output of 4 kW. The mould temperature was monitored using two K-type thermocouples, located at the centre of each mould part, while the desired cure temperature was maintained via two PID temperature controllers. At the end of the injection process, the whole apparatus was washed through with acetone to prepare it for further production.

Microwave RTM Processing

Microwave RTM processing differed from conventional thermal RTM processing in how the resin and fibre loaded mould was heated after the injection stage. Instead of traditional thermal heating, microwave radiation was used in order to cure the composites. This required a different moulding tool to be employed during microwave heating, since standard metal moulds were not suitable for use inside the microwave field. The new moulding tool was manufactured from a ceramic material called Macor, which was supplied by Precision Ceramics. The fibres were placed inside the Macor mould cavity (200 x 200 x 3 mm dimensions) and the injection of the resin in microwave RTM processing was carried out using the Hypaject Injection system with the moulding tool inclined at 45° from horizontal, as described previously in Section 3.4.1.

The microwave RTM heating equipment comprised of a network analyser (NA) (Hewlett Packard HP8720ET) used as the power source, a travelling wave tube

(TWT) amplifier, a multi-mode microwave applicator (brass cavity) and four fluoroptic probes (Luxtron Corp.) connected to a Luxtron 790 fluoroptic thermometer. A photograph of the microwave RTM system set-up is shown in Figure 3.6. The microwave signal generated from the NA was amplified by the TWT amplifier and then fed to the microwave applicator. The maximum amplifier output power that could be used in this configuration was 250 W. The microwave applicator comprised of a 440 x 340 x 160 mm multimode brass cavity and two N series coaxial input ports located at the centre of each half of the cavity. The input ports were connected to the internal coupling probes via semi-rigid coaxial cables. Microwave power and frequency were adjusted via a General Purpose Interface Bus (GPIB) connection between the computer and the NA. A control schematic diagram for microwave RTM processing is illustrated in Figure 3.5 (solid arrows indicate microwave power flow; dotted arrows indicate process control / temperature measurements).

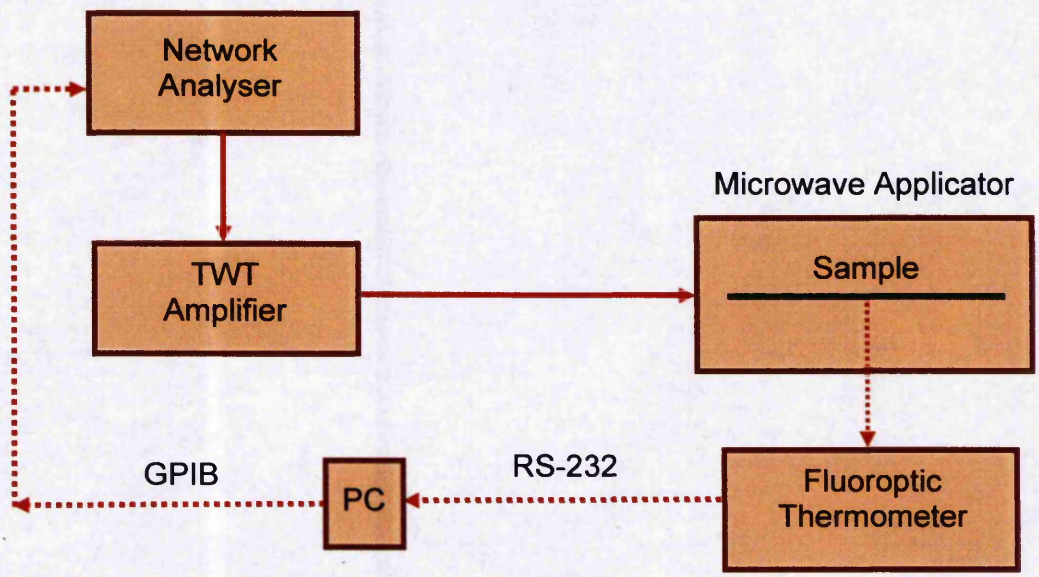

Figure 3.5: *Control schematic diagram for microwave RTM processing.*

1. Network analyser
2. Fluoroptic thermometer
3. Uninterruptible power supply (UPS)
4. Macor mould
5. Microwave applicator
6. PC
7. TWT amplifier

Figure 3.6: *Microwave RTM processing equipment.*

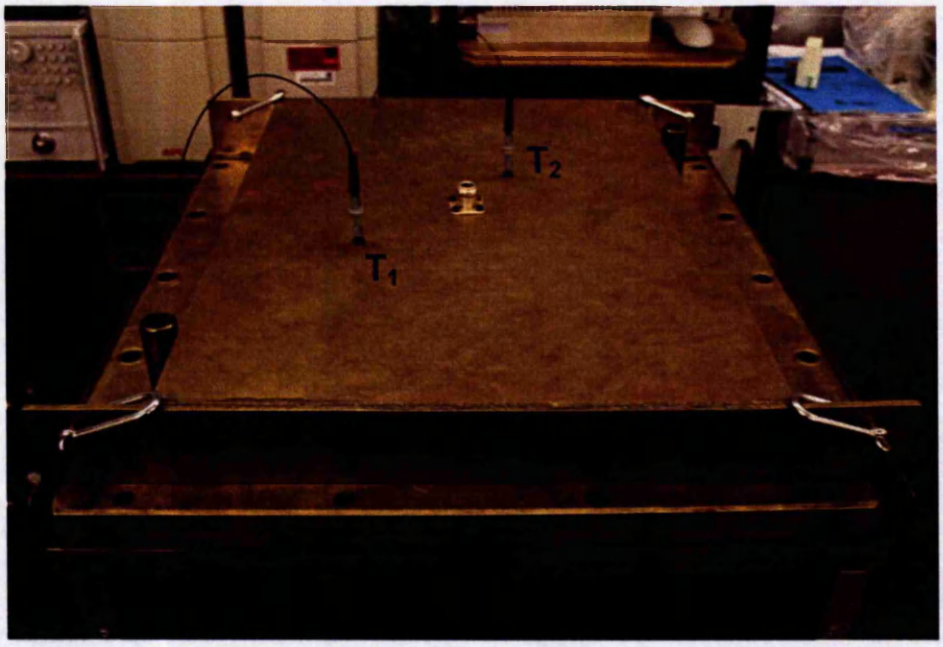

Figure 3.7: *Surface temperature probes (T_1 and T_2) placed in contact with the Macor moulding tool through the top half of the microwave applicator.*

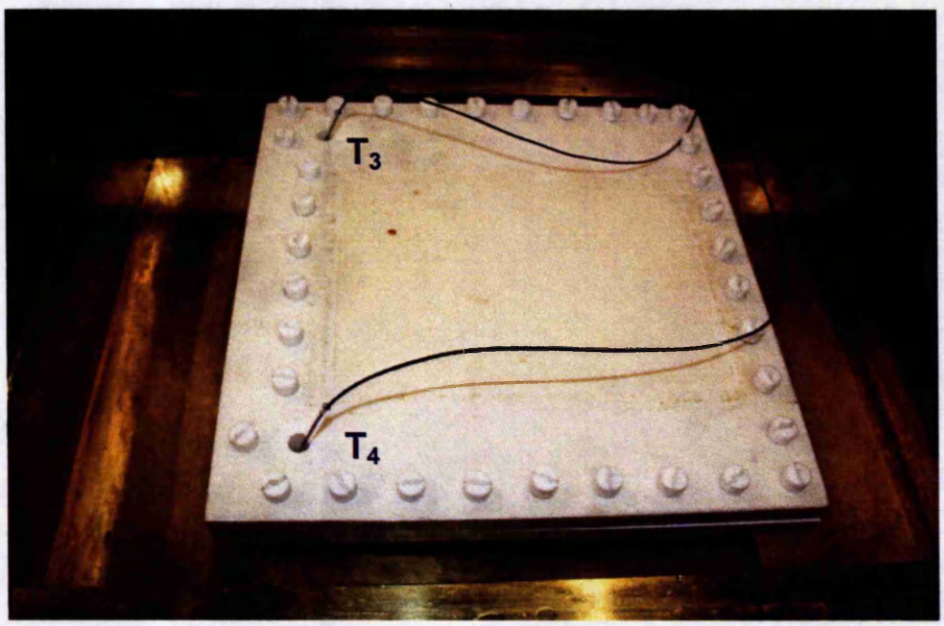

Figure 3.8: *Immersion probes (T_3 and T_4) inserted at the inlet and outlet of the Macor moulding tool inside the lower half of the microwave applicator.*

Yusoff [17] observed low heating rates when the microwave signal was fed to the applicator via two input ports. This was probably the result of power loss in the external transmission line due to a T-connector used to split the coaxial cable from the amplifier to the two input ports, as well as poor coupling of microwave power from the external transmission line via the internal antenna into the sample. For those reasons, only one input port, located at the top cavity half, was used during microwave processing of the composite panels.

The sample temperature was measured using four fluoroptic probes and was constantly monitored by the computer via a serial connection (RS-232) with the fluoroptic thermometer. Two fluoroptic temperature probe configurations, surface and immersion, were used for measuring the sample temperature. The four temperature probes were placed at four different places. Figures 3.7 and 3.8 show the surface and immersion temperature probes respectively, as they were positioned during microwave RTM processing. Two surface temperature probes were placed in contact with the mould surface (T_1 and T_2) and two immersion probes were inserted in the resin at the mould inlet and outlet (T_3 and T_4). The immersion probes were inserted inside thin wall capillary tubes before being placed into the resin for protection, while the surface temperature probes were placed in contact with the mould surface through two small holes located at the top half of the microwave applicator.

CHAPTER 4

Characterisation Techniques

4.1 Introduction

This chapter presents and describes the experimental techniques employed for the characterization of the uncured resin and the fabricated composites involved in this work. The dimensional stability of the composite panels was evaluated in terms of thickness variation, while their mechanical performance was assessed through four-point bending and interlaminar shear testing. Dynamic mechanical thermal analysis (DMTA) was used to study the thermal properties and determine the glass transition temperatures (T_g) of the produced laminates. Differential scanning calorimetry (DSC) was carried out to verify that the composite samples were fully cured and a water displacement method was used to measure the density of the samples. Furthermore, the fibre volume fractions of the produced composites were determined through the hot acid digestion method and optical microscopy. Defects in the composite panels, as well as their overall quality, were assessed using C-scan and optical microscopy, while scanning electron microscopy (SEM) was employed to study the fracture surfaces of samples subjected to mechanical testing. In addition, differential scanning calorimetric, dielectric and rheological measurements of the uncured epoxy resin were performed. The dielectric properties of the cured composites were also determined. The cross-linking reaction mechanisms for both thermally and microwave cured composites were investigated using Fourier transform infrared spectroscopy (FTIR).

4.2 Thickness Variation

The dimensional stability of the produced composite panels was assessed by means of thickness variation. Digital electronic calipers were used to measure the thickness of the panels in different points equally distributed across their surface. Approximately 100 measurements were taken for each panel.

4.3 Mechanical Testing

Mechanical testing involves a series of experimental methods used for the evaluation of the mechanical performance of a material, by measuring the amount of deformation (strain) introduced to the material when subjected to a given load (stress). Flexural tests (four-point bending) and interlaminar shear tests (short beam test) were carried out on the fabricated composite panels. The mechanical data were recorded with the help of the Instron Automated Materials Tester software. The specimens were cut from the panels using a fine band saw and their edges were polished with P600 silicon carbide paper. For each composite panel, a minimum of ten specimens were tested and an average value was taken. The specimens were taken from different locations in the composite panels to ensure good representativity of the results.

4.3.1 Four-Point Bending

The use of flexural tests to determine the mechanical properties of resins and laminated fibre composite materials is widespread throughout industry owing to the relative simplicity of the test method, instrumentation and equipment required [112]. The two methods most commonly used for the determination of flexural properties of laminates are the three-point and four-point bending tests.

In this work, the flexural modulus and flexural strength of the composites were measured by means of four-point bending. A schematic diagram of the four-point bending test is illustrated in Figure 4.1. The sample is supported close to its ends by two cylindrical rollers and is loaded by two loads placed symmetrically between the supports. The tests were conducted according to the ASTM D 6272 standard [113]. The apparatus used was an Instron 4301 equipped with a four-point bend jig and a 1 kN load cell. The selected support span was 60 mm, providing a span-to-thickness ratio of 16:1, while the load span was set at one half of the support span. The tests were carried out at a cross-head speed of 2 mm/min. The composite samples were flat and rectangular with dimensions of 80 mm (length) x 15 mm (width) x 3.3 – 3.7 mm (thickness).

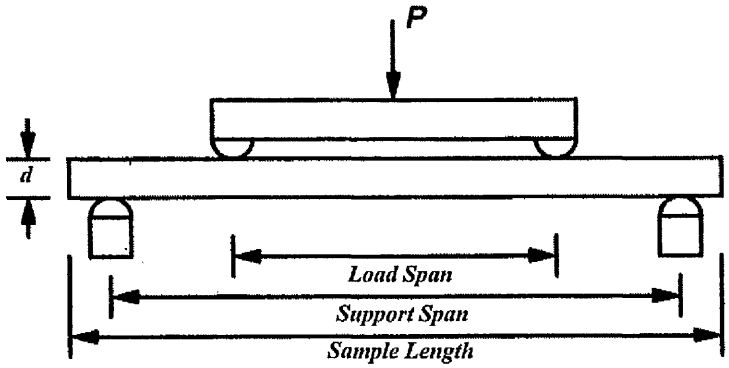

Figure 4.1: *Schematic diagram of four-point bending test* [112].

The flexural modulus of elasticity, E_B, (MPa) was derived from Equation 4.1 [113]:

$$E_B = \frac{0.17L^3m}{bd^3} \qquad \text{(Eqn. 4.1)}$$

where L is the support span (mm), m is the slope of the tangent to the initial straight-line of the load-deflection curve, b is the width of the sample (mm) and d is the thickness of the sample (mm).

The flexural strength, S, (MPa) was calculated according to Equation 4.2 [113]:

$$S = \frac{3PL}{4bd^2} \qquad \text{(Eqn. 4.2)}$$

where S is the maximum stress throughout the load span (MPa), L, b, d are the same as for Equation. 4.1 and P is the load at failure (N).

It can be seen from Equations 4.1 and 4.2 that small deviations in the measured values of the support span and sample thickness can result in significantly different values of flexural modulus and flexural strength, due to the cubed and squared terms involved. Thus, much care was taken in the preparation and accurate measurement of the sample dimensions and the support span.

4.3.2 Interlaminar Shear Strength Test

Interlaminar shear strength (ILSS) is the strength of a material when subjected to shear stresses parallel to the plane of lamination and is associated with the interface between the matrix and the fibre. The test is very similar to three-point bending, as it consists of a short rectangular sample supported by two cylindrical rollers and loaded through a central roller located midway between the supports. The only difference is that a smaller span-to-thickness ratio is employed to encourage interlaminar shear failure in the test samples by increasing the level of shear stress relative to the flexural stress. A schematic diagram of the interlaminar shear strength test is shown in Figure 4.2 [112].

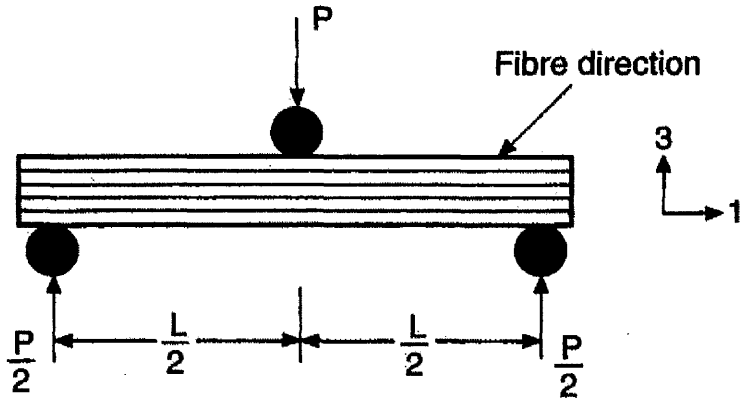

Figure 4.2: *Schematic diagram of interlaminar shear strength test* [112].

The tests were carried out on an Instron 4301 equipped with a three-point bending jig and a 1 kN load cell, according to the ASTM D 2344/D 2344M standard [114]. The support span used was 14 mm, providing a span-to-thickness ratio of 4:1, while the cross-head speed was set at 1 mm/min. The composite sample dimensions were 20 mm (length) x 7 mm (width) x 3.3 - 3.7 mm (thickness).

The interlaminar shear strength, *ILSS*, (MPa) was derived from Equation 4.3 [114]:

$$ILSS = 0.75\frac{P_m}{bd} \qquad \text{(Eqn. 4.3)}$$

where P_m is the load at failure (N), b is the sample width (mm) and d is the sample thickness (mm).

4.4 Dynamic Mechanical Thermal Analysis (DMTA)

Dynamic mechanical thermal analysis (DMTA) is a technique in which a mechanical property of a material is monitored as a function of temperature, while a periodic stress is imparted to the material. DMTA can be used to measure the mechanical properties of polymers and composites and obtain information on their ability to store and dissipate mechanical energy upon deformation.

While liquids display viscous flow when a force is applied, solid materials can behave elastically, plastically, if the force exceeds an elastic limit, and finally viscoelastically. This technique is based on the fact that when a viscoelastic material is subjected to a force it will exhibit both elastic and viscous behaviour. Beyond the elastic limit the material undergoes plastic deformation and any further increase in load will eventually cause fracture. The elastic behaviour is determined by the potential energy stored in the sample, which may be completely recovered on removal of the stress. On the other hand, the viscous behaviour is due to energy lost in distortion of the structure of the material. DMTA can be employed to measure, through the effect of temperature on the microstructure, the viscoelastic properties of a material, since the viscoelastic behaviour is determined by molecular movement which is consequently determined by the microstructure.

In DMTA, a small sinusoidal oscillating stress is applied to a sample producing a corresponding oscillating strain. If the material is elastic, the strain will be in phase with the stress. In the case of viscoelastic materials, however, the measured strain will lag behind the imparted stress by a phase difference (δ) shown in Figure 4.3. The ratio of peak stress to peak strain gives the complex modulus (E^*) which consists of an in-phase component or storage modulus (E') and a 90° out-of-phase component or loss modulus (E'').

The storage modulus (E' is used for stretching deformations and G' for twisting or torsional deformations) represents the energy stored during deformation and is related to the elastic portion of the material, while the loss modulus (E'' is used for stretching deformations and G'' for twisting or torsional deformations) represents the energy lost, usually as heat, during deformation and is related to the viscous portion of the material.

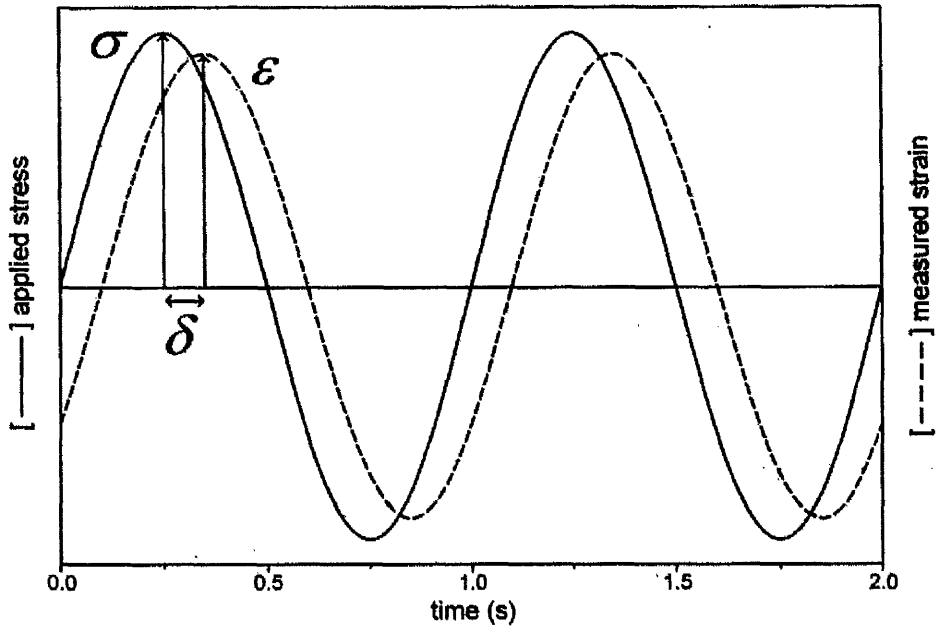

Figure 4.3: *Stress and strain as a function of time for viscoelastic materials during a dynamic mechanical test* [115].

The ratio between the loss and storage moduli (E''/E') gives the quantity known as mechanical damping factor or loss tangent (tan δ) which represents the ability of the material to dissipate deformational energy. The relationship between these quantities can be better understood through an Argand diagram, as shown in Figure 4.4.

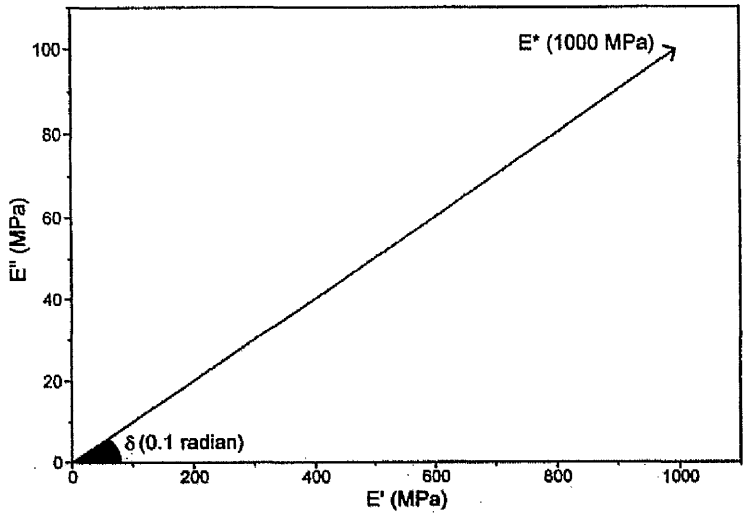

Figure 4.4: *Argand diagram showing the relationship between complex modulus (E*) and its components* [115].

The complex modulus is a vector quantity characterised by angle (δ) and magnitude (E^*), while E' and E'' represent the real and imaginary parts of this vector, thus:

$$E^* = E' + iE'' \qquad \text{(Eqn. 4.4)}$$

where $i = \sqrt{-1}$, so that:

$$E' = E^* \cos\delta \qquad \text{(Eqn. 4.5)}$$

and

$$E'' = E^* \sin\delta \qquad \text{(Eqn. 4.6)}$$

Since the values of the moduli will change with temperature, detection of even small changes in molecular structure in a material is possible, by monitoring the parameter $\tan\delta$ as a function of temperature and/or frequency of applied stress. In practice, this technique is very sensitive to small molecular transitions and thus lends itself to determining secondary transitions, such as the β transition which may occur at temperatures below T_g in some polymeric materials and which may influence properties such as impact strength.

In this work, dynamic mechanical thermal analysis was carried out on a TA Instruments DMA Q800 to obtain the glass transition temperatures for both thermally and microwave cured composites. A schematic representation of the DMA Q800 analyser is illustrated in Figure 4.5 [116]. The Q800 uses a non-contact drive motor to provide the required oscillatory or static force, which is transmitted directly to a rectangular air bearing slide. A high resolution optical encoder is used to measure displacement, while the sample is heated under a controlled temperature profile inside the furnace. Liquid nitrogen is used to cool the samples to sub ambient temperatures. A variety of sample clamps can be employed providing multiple modes of deformation. In this study, the samples were tested under three-point bending mode, which is ideal for high modulus composite materials. The storage modulus, loss modulus and tan δ of the composite samples with dimensions 60 mm (length) x 8 mm (width) x 3.3 – 3.7 mm (thickness) were obtained in the temperature range of -150°C to 250°C at 2°C/min, while the frequency of the applied oscillating stress was 1 Hz. For each composite panel, a minimum of six samples taken from different locations in the panel were tested.

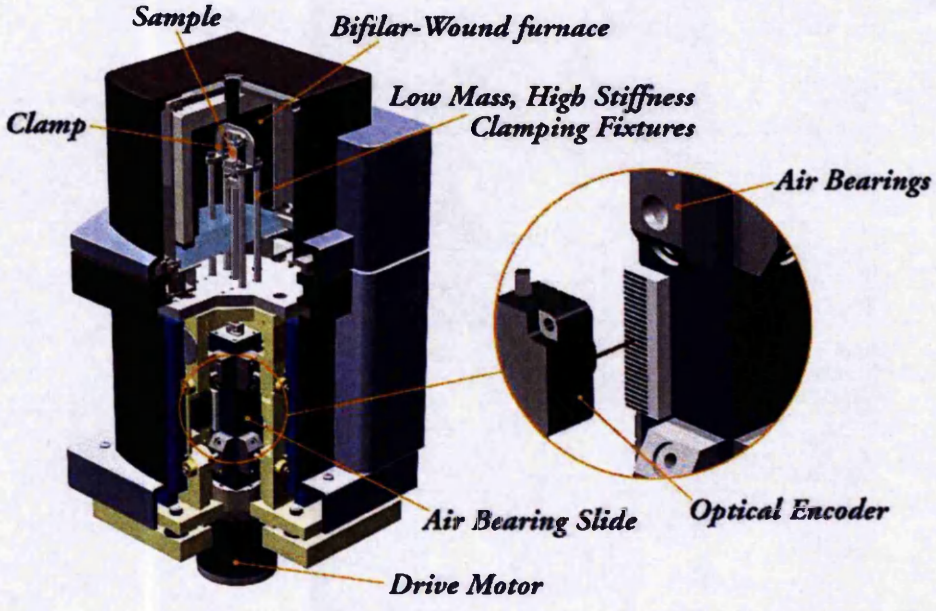

Figure 4.5: *Schematic representation of the DMA Q800 analyser* [116].

4.5 Differential Scanning Calorimetry (DSC)

Differential scanning calorimetry is a technique in which the difference in heat flow (power) between a sample (pan) and a reference (pan) is monitored against time or temperature, while the temperature of the sample, in a specified atmosphere, is programmed [117]. DSC is based on the principle that when a substance is subjected to heating it undergoes physical or chemical changes, which in turn reflect upon the enthalpy of the system.

The main parts of a DSC apparatus are shown schematically in Figure 4.6 [115]. The sample and the reference are contained in the DSC cell, along with the temperature sensors and heating elements. A computer unit monitors and operates the various control functions, such as the atmosphere and temperature control, as well as the data capture and analysis.

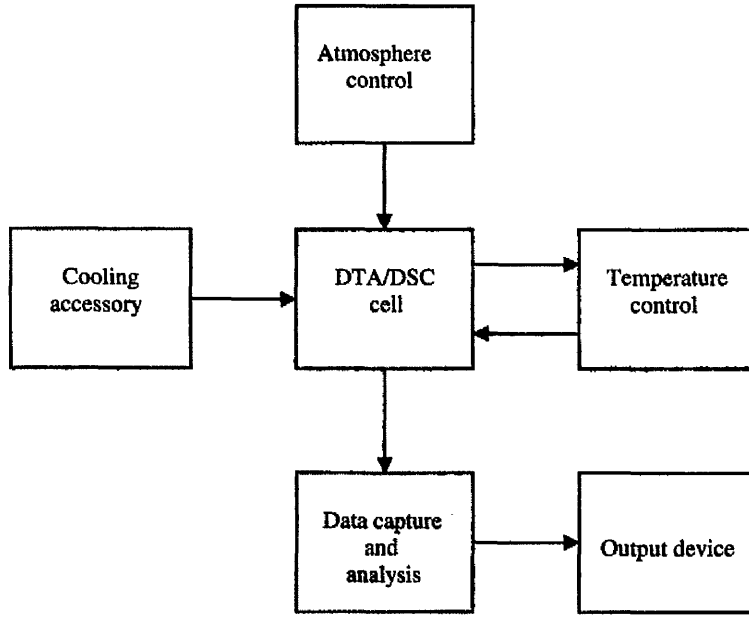

Figure 4.6: *Schematic representation of the main parts of a DSC instrument* [115].

Depending on the operating principle, there are two types of differential scanning calorimeters:

1. *Power-compensated DSC*, where the sample and the reference are heated by separate heaters and the difference in electrical power ($\Delta P = d(\Delta Q/dt)$), which is needed to keep a zero temperature difference (ΔT) is monitored (Fig. 4.7a).
2. *Heat flux DSC*, where the sample and the reference are heated by the same heater and the temperature difference (ΔT) is measured and converted to power difference (ΔP) using the calorimetric sensitivity (Fig. 4.7b).

A schematic diagram showing the difference between the two types of calorimeters is shown in Figure 4.7 [115].

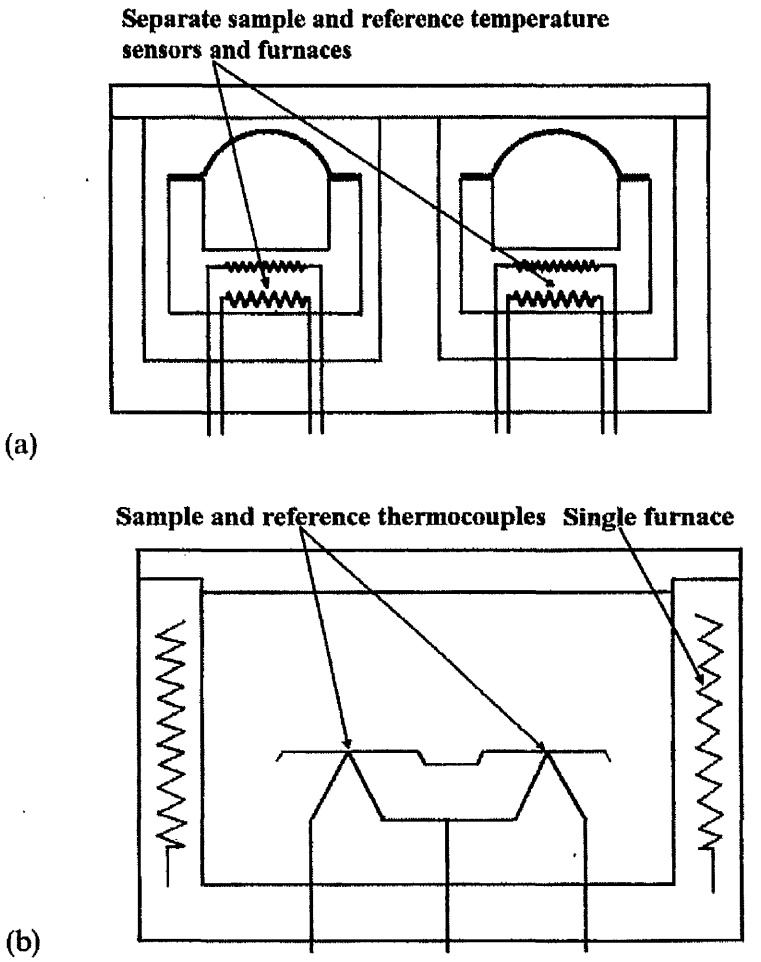

Figure 4.7: *(a) Power-compensated differential scanning calorimeter. (b) Heat flux differential scanning calorimeter* [115].

DSC is one of the most popular techniques used for the analysis of polymers. If a transition takes place in the sample, a characteristic excursion in the DSC curve can then be related to the energy associated with the transition. The DSC curve obtained represents the actual amount of electrical energy supplied to the system and so the area under the peak is a direct measure of the heat of transition. DSC can be used for the investigation of physical changes and measurements (e.g. heat capacity, glass transitions, phase changes, thermal conductivity) and also of chemical reactions (e.g. polymer curing, polymer degradation). DSC can detect changes in heat capacity which are caused by phase transitions or chemical reactions in the sample. The knowledge of the position and the magnitude of these transitions can give valuable information about the polymer and its performance in a given use. Since DSC measures directly the heat flow, the calculations of the energy involved in a given transition are relatively easy. Among the advantages of DSC are its relative simplicity and its capability of giving information regarding reaction kinetics, energetics and thermal properties. Figure 4.8 shows an example of a DSC trace of polyethylene terephthalate (PET) in which various transitions (glass transition, cold crystallisation and melting) are detected.

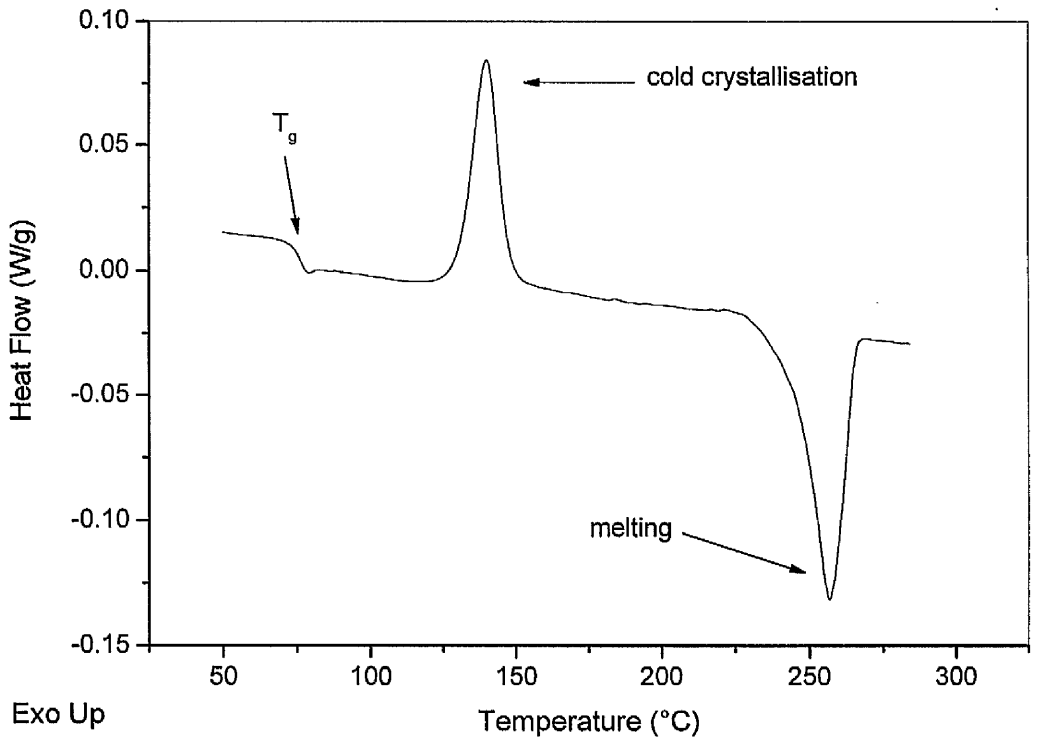

Figure 4.8: *Example of a DSC trace of polyethylene terephthalate (PET).*

In this work, differential calorimetric studies were carried out on a heat flux TA Instruments DSC Q100 mainly for the purpose of ensuring that the fabricated composite panels were fully cured. Small size samples in the range of 5 – 10 mg were sealed in aluminium pans and were heated from 20°C to 250°C at 10°C/min in an inert nitrogen atmosphere, while an empty pan was used as a reference. The samples were taken from different locations in the composite panels and for each composite panel a minimum of ten samples were tested. In some cases, however, conventional DSC was unable to determine accurately the residual degree of cure, due to the exothermic peak of the residual reaction overlapping with the changes in the heat flow in the vicinity of the glass transition temperature. For that reason, temperature modulated DSC (TMDSC) was employed. TMDSC uses a sinusoidal modulation in the temperature profile applied to the sample, which allows the DSC heat flow to be separated into reversible (glass transition event) and non-reversible (kinetic thermal event) heat flows. Thermoset cure is a non-reversible event; hence any residual cure can be calculated from the area under the exothermic transition in the non-reversible heat flow curve. TMDSC measurements were performed on the fabricated composite samples in the temperature range of 20°C to 250°C at 3°C/min using a modulation amplitude of ±1°C every 60 seconds. Furthermore, DSC measurements were performed on the uncured epoxy resin at different heating rates and isothermally to establish the characteristics of the curing cycle used throughout this work. DSC traces of the neat resin were obtained at scan rates of 2°C/min, 5°C/min and 10°C/min from 20°C to 250°C and isothermally at 100°C for 4 hours.

4.6 Density Measurements

The density of the resin and the composite samples was measured using a water displacement method according to the Airbus ABT 1-0018 test specification [118]. Ten samples were taken from different locations in each composite panel to ensure representativity of the results. The samples were initially suspended from a balance hook using a fine wire and their weight plus that of the supporting wire was measured (M_1). They were subsequently suspended in fresh distilled water contained in a 100 ml beaker and were weighed at room temperature (M_2). The samples were

then removed and the weight of the wire immersed to the same depth as before in the water was measured (M_3). The wire was then dried and weighted in air (M_4).

Taking the density of water to be 0.997 g/cm^3, the sample density was calculated as follows:

Weight of specimen in air, M_c, (g): $M_c = M_1 - M_4$ (Eqn. 4.7)

Weight of specimen in water, M_w, (g): $M_w = M_2 - M_3$ (Eqn. 4.8)

Density of specimen, ρ_c, (g/cm^3): $\rho_c = \frac{M_c}{(M_c - M_w)} \cdot 0.997$ (Eqn. 4.9)

4.7 Fibre and Void Volume Fraction

The percentage fibre volume fraction (V_f) and percentage void volume fraction (V_v) were determined using matrix digestion with nitric acid in a microwave oven according to the ASTM D 3171 standard [119]. Ten samples with dimensions 20 mm (length) x 10 mm (width) x 3.3 - 3.7 mm (thickness) taken from different locations in each composite panel were tested. The density of the samples was initially determined according to Airbus ABT 1-0018 test method, described previously in Section 4.6. The samples were then weighed (sample sizes approximately 0.5 g) and placed inside Teflon reaction vessels together with approximately 10 ml of 70% nitric acid solution. The reaction vessels were sealed in pressure sleeves and placed inside the microwave oven. The samples were heated under pressure (<20 Bar) to 140°C and held at this temperature until the matrix was fully digested. The contents of the vessels were then filtered under vacuum using pre-weighed sintered glass crucibles. After filtration, the fibres were thoroughly washed with distilled water to remove the nitric acid. A final wash with acetone also followed to improve drying times. The crucibles with the fibres were placed in an oven at 100°C for approximately 2 hours to dry and then left inside a desiccator to cool down before the final weighing of the fibres took place.

The fibre volume fraction, V_r, (%) of the samples was calculated using the following equation:

$$V_r = \left(\frac{M_f}{M_i}\right) \cdot 100 \cdot \left(\frac{\rho_c}{\rho_r}\right) \quad \text{(Eqn. 4.10)}$$

where M_i is the initial mass of the sample (g), M_f is the mass of the fibres (g), ρ_c is the density of the sample (g/cm^3) and ρ_r is the density of the reinforcement (g/cm^3). The matrix volume fraction, V_m, (%) was calculated according to:

$$V_m = \left(\frac{M_i - M_f}{M_i}\right) \cdot \left(\frac{\rho_c}{\rho_m}\right) \cdot 100 \quad \text{(Eqn. 4.11)}$$

where M_i, M_f, ρ_c are the same as for Equation 4.10 and ρ_m is the density of the matrix (g/cm^3). The void volume fraction V_v (%) was calculated using the equation:

$$V_v = 100 - (V_r + V_m) \quad \text{(Eqn. 4.12)}$$

4.8 C-scan

The basic principle of C-scan lies in the fact that mechanical vibrations can be propagated in solids, liquids and gases. Each particle of matter oscillates about a mean position, causing similar vibrations to be taken up by the neighbouring particles. If the mechanical movement of the particles have a regular motion, the vibrations can be assigned a frequency in cycles per second, measured in hertz (Hz), where 1 Hz = 1 cycle per second [120]. The human ear can only detect mechanical vibrations of frequencies in the range of 10 to 20.000 Hz, where the sound is audible; above 20,000 Hz, the 'sound' waves are referred to as 'ultrasound' or 'ultrasonic' [120]. Ultrasonic waves travel at different speeds through different materials, depending on the elastic properties of the material. If the particle vibration is sinusoidal, the wave velocity, V, is given by the equation:

$$V = f \cdot \lambda \qquad \text{(Eqn. 4.13)}$$

where V is the wave velocity (m/s), f is the wave frequency (Hz) and λ is the wavelength (m). The latter represents the distance travelled by the sound wave during one cycle of vibration. The characteristic ultrasonic velocities in a selection of materials are shown in Table 4.1 [120].

Table 4.1: *Ultrasonic velocities (mean values)* [120].

Material	Relative density	Velocity (m s^{-1})	
		Compressional	Shear
Aluminium	2.70	6300	3080
Mild steel	7.85	5900	3230
Magnesium	1.70	5770	3050
Copper	8.90	4700	2260
Titanium	4.51	6000	3000
Polythene	1.20	2000	540
Perspex (Lucite)	1.18	2700	1300
Water	1.00	1490	—
Air	—	344	—

The propagation of vibrational energy within any medium takes place as the oscillation of a particle of solid, liquid or gas is passed onto the neighbouring particles by means of longitudinal (compressional) or transverse (shear) waves. Compressional waves propagate parallel to direction of the particle motion and exist in solids, liquids and gases because they all have elasticity. On the other hand, shear waves propagate in a direction perpendicular to the particle motion and are only found in solids, since liquids and gases have zero resistance to shear. The velocity of compressional waves, V_c, and shear waves, V_s, in a bulk material can be calculated using the following equations [120]:

$$V_c = \sqrt{\frac{E(1-\sigma)}{\rho(1+\sigma)(1-2\sigma)}} \qquad \text{(Eqn. 4.14)}$$

$$V_S = \sqrt{\frac{E}{2\rho(1+\sigma)}} \qquad \text{(Eqn. 4.15)}$$

where V_c is the compressional wave velocity, V_s is the shear wave velocity, E is the Young's modulus (N/m^2), ρ is the density of the material and σ is the Poisson's ratio.

When a propagating ultrasonic wave encounters a plane boundary between two media, such as an interface between two materials or a defect or internal flaw within a material, some portion of the ultrasonic energy is transmitted through the interface and some is reflected back. Assuming normal incidence, the portion of energy transmitted through the boundary depends on the specific acoustic impedance, Z, of the two media, which is defined as [120]:

$$Z = \rho \cdot V \qquad \text{(Eqn. 4.16)}$$

where Z is the specific acoustic impedance of the material, ρ is the density of the material and V is the wave velocity.

The sound waves reflected or scattered due to an internal discontinuity or flaw within a material are detected by a transducer and the amplitude of these waves is proportional to the size of the discontinuity or flaw, while the interval of time between the transmitted and reflected waves is proportional to the distance of the discontinuity or flaw from the surface of the material.

In this study, defects in the fabricated composite panels were examined by a Midas NDT jet probe inspection ultrasonic C-scan used in through transmission mode (Figure 4.9). The system uses two axes of movement to scan across the area of the component. A transducer transmits ultrasound waves along a column of water and into the component. The sound waves then travel through a secondary water column and are collected and evaluated by a secondary transducer on the other side of the component. The separation between the two jets must remain constant without any variation in their alignment so that a constant sound level, set as a maximum signal level, is established between them. Thus, any reductions in the maximum signal level can only be caused by sound losses due to defects in the component. The computer

software (Zeus version 3.0) then reads the entire range of the signal attenuation throughout the component in a single inspection and plots it as a colour C-scan. All composite panels were scanned at 50 mm/sec speed using a 5 MHz probe so that the two-dimensional attenuation maps constructed would be directly comparable.

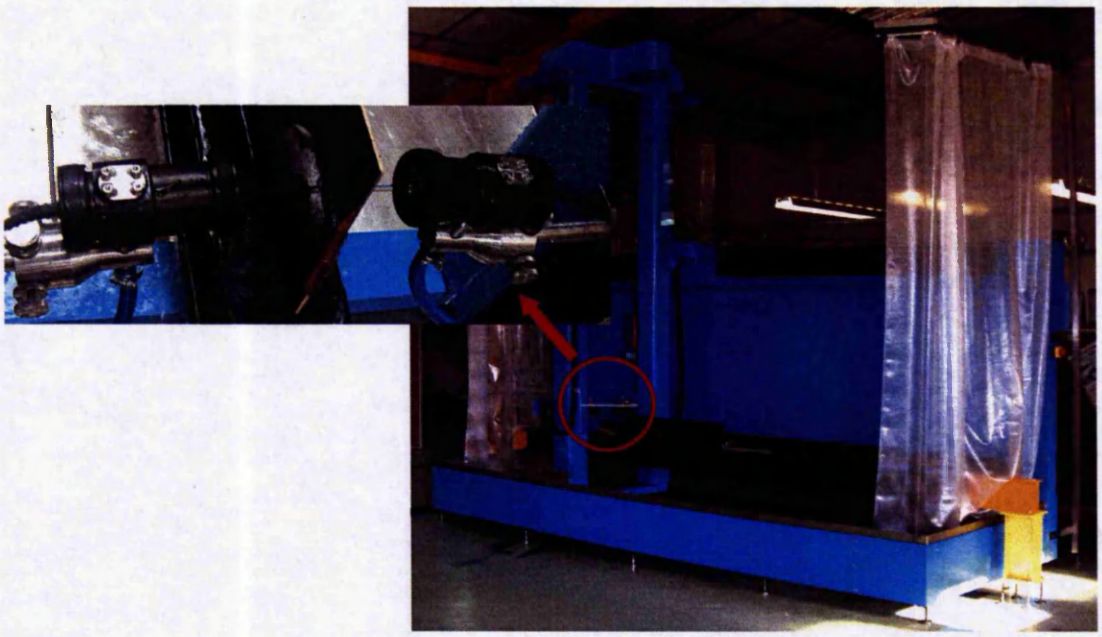

Figure 4.9: *Midas NDT jet probe inspection ultrasonic C-scan.*

4.9 Optical Microscopy

Optical microscopy is a simple technique where visible light is focused through a combination of lenses in order to produce magnified images of small objects or samples. In this work, optical microscopy was employed for the cross-sectional visualisation and void content determination of the composite samples. High resolution optical micrographs of the composite samples (20 x 10 x 3 mm) were taken at x10 and x20 magnification using an Olympus BH2 optical microscope coupled with a video camera. The specimens were initially mounted in polyester resin and ground with SiC grinding paper discs of successively finer grades (P120, P400, P600 and P1200). The samples were then polished using a Bueller Metaserve Universal polisher. The polishing cloths fixed on the rotating wheels of the polisher

were impregnated with diamond pastes of successively smaller particle size (6 μm, 1 μm and 1/4 μm), enabling a fine sample surface finish of 1/4 μm to be achieved at the end of the polishing stage.

Ten samples taken from different locations in each composite panel were examined and the void content was determined using a Java-based image processing software (ImageJ). Voids were selected by adjusting the threshold level and the void content was calculated by dividing the area of the selected voids by the total area of the image at a given magnification. Ten random locations distributed across the sample were examined in each micrograph and an average void content value was calculated. The results from optical microscopy were compared against those obtained from the hot acid digestion method.

4.10 Scanning Electron Microscopy (SEM)

In scanning electron microscopy (SEM), an electron gun produces electrons and accelerates them to an energy ranging from about 2 keV to 40 keV. Two or three condenser lenses then demagnify the electron beam so by the time it reaches the sample surface it may have a diameter of only 2-10 mm. The fine electron beam is scanned across the sample with the help of scan coils, while a detector measures the number of low energy secondary electrons and back-scattered electrons given off from each point on the sample surface. Simultaneously, the spot of a cathode ray tube (CRT) is scanned across the screen, while the brightness of the spot is adjusted according to the amplified current from the detector. The pattern in which both the electron beam and CRT spot are scanned is similar to that of a television receiver and is known as a 'raster', which is a rectangular set of straight lines [121]. The intensities of secondary and back-scattered electrons are very sensitive to the angle at which the incident electron beam encounters the surface of the sample, which is the main reason why SEM is mainly used to study the surface features or topography of a sample. The main components of a scanning electron microscope are shown in Figure 4.10 [121]. SEM has several advantages over traditional microscopy. Owing to its larger depth of field, SEM allows more of the specimen to be in focus at one time, while its much higher resolution enables specimens to be magnified at much

higher levels. Furthermore, the specimen chamber in SEM is large enough to accommodate samples from few millimetres to several centimetres in size, while the sample preparation is relatively easy and straightforward.

In this study, SEM was used to investigate the fracture surfaces of composite samples after they were subjected to four-point bending and interlaminar shear testing. From the appearance of the surfaces in an SEM micrograph it was possible to draw valuable information regarding the interfacial properties of the composites. The composite samples were examined using a Philips XL30 FEG SEM microscope. Sample preparation involved cutting of small sections of the fracture surfaces from test samples and placing them on metal stubs using double-sided carbon tabs. The stubs with the fracture surfaces were then coated with a very thin layer of gold using Edwards S150B sputter coater in order to make them electrically conductive.

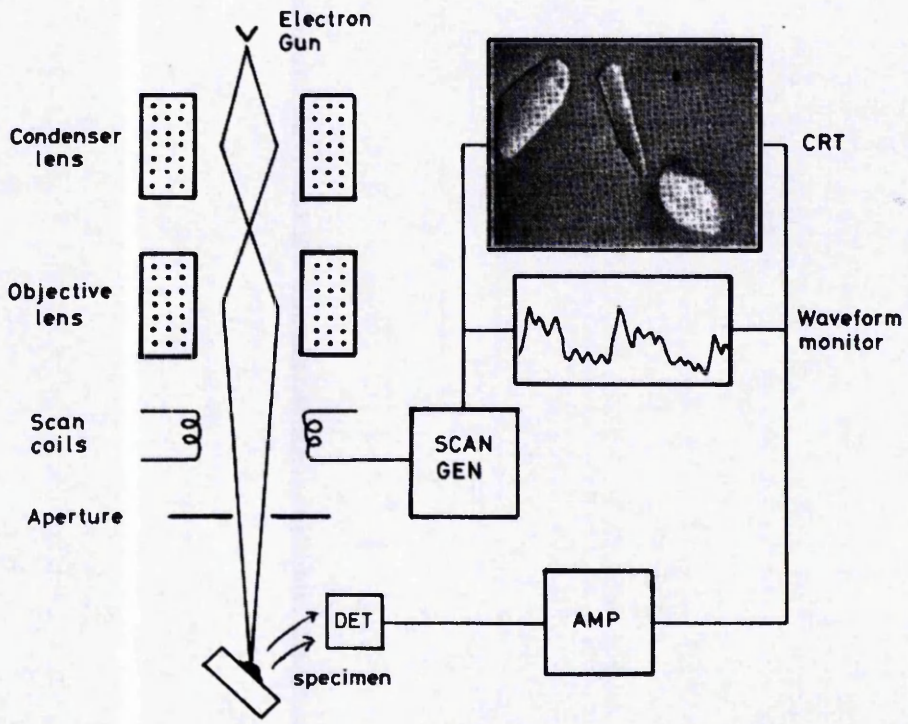

Figure 4.10: *Schematic diagram showing the main components of a scanning electron microscope* [121].

4.11 Dielectric Measurements

The dielectric properties of both the uncured epoxy resin and the produced composites were determined using the cavity perturbation method. The principle behind the resonant cavity perturbation method rests on the fact that it is possible to calculate the values of the dielectric constant (ε') and dielectric loss (ε'') of a material by measuring the values of the resonant frequency (f) and quality factor (Q) of a resonant cavity before and after insertion of a sample material. The dielectric properties can be calculated using the following equations [122]:

$$\varepsilon' = 1 + A \cdot \frac{(f_c - f_s)}{f_c} \cdot \frac{V_c}{V_s} \qquad \text{(Eqn. 4.17)}$$

$$\varepsilon'' = B \cdot \left(\frac{1}{Q_s} - \frac{1}{Q_c} \right) \cdot \frac{V_c}{V_s} \qquad \text{(Eqn. 4.18)}$$

where ε' is the dielectric constant and ε'' is the dielectric loss of the material, f_c and f_s are the unperturbed and perturbed resonant frequencies, respectively, Q_c and Q_s are the unperturbed and perturbed unloaded quality factors, respectively, and V_c and V_s are the volumes of the cavity and the sample, respectively. The parameters A and B depend on the cavity and sample geometries and the resonant mode of the cavity and not on the dielectric properties of the sample material. Thus, their values can be obtained by calibration using materials with known dielectric properties. For the cavity used in this study A and B were found to be 0.5 and 0.25, respectively.

In this work, the dielectric properties of the uncured epoxy resin were measured as a function of time during microwave heating, whereas for the cured composites only dielectric measurements at room temperature were performed. The system set-up comprised of a cylindrical cavity, a network analyser (Hewlett Packard HP8714ET), a narrow-band (2.3 – 2.5 GHz) solid state amplifier (Microwave Amplifier Ltd, AM81 series), a power meter (Anritsu ML2438A) connected to the power sensors (Anritsu ML2438A) and a temperature controller (FISO Technologies) connected to a fibre optic temperature sensor (FISO Technologies, FOT-H model), as shown in

Figure 4.11. The single mode cylindrical brass cavity (radius 58mm, height 77mm) was used as the heating cell and was operated in the TE_{111} mode at a resonant frequency of 2.45 GHz. The *E* field vectors in the TE_{111} mode were perpendicular to the cavity axis with the maximum electric field magnitude at the centre of the cavity [122].

The microwave signal, generated by the network analyser, was amplified and then fed to the microwave cavity through a directional coupler, which allowed the signal reflected from the cavity to be monitored. The transmission signal was also monitored by the network analyser in order to determine the dielectric properties during heating. The reflection and transmission powers were measured from the power meter via the power sensors. The temperature control system used a feedback loop between the sample temperature and the source power and the desired heating rate was achieved by varying the amplifier gain. The sample (< 0.5g) was contained inside a 10 mm diameter test tube and was inserted into the cavity through a 12.5 mm diameter hole located at the top. The sample tube was held in place using a PTFE support and was placed so that the sample was at the centre of the cavity, where the magnitude of the electric field was at the maximum. The sample temperature was monitored via a fluoroptic temperature probe, which was inserted inside a thin wall capillary tube before coming in contact with the sample for protection reasons. The dielectric loss and dielectric constant of the uncured epoxy resin were measured at heating rates of 5°C/min and 10°C/min from room temperature to 200°C and also isothermally at 100°C. The dielectric properties of the fabricated composites were only measured at room temperature.

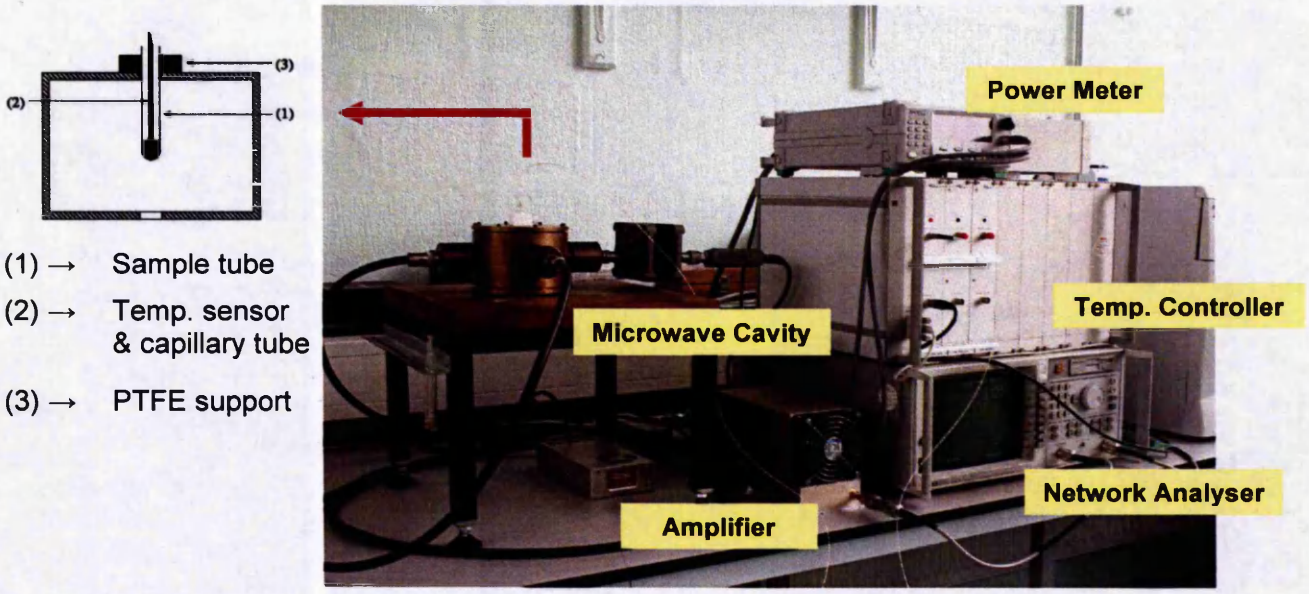

Figure 4.11: *Dielectric measurements using the cavity perturbation method.*

4.12 Rheological Measurements

Rheological characterization of the uncured epoxy resin employed in this study was carried out using a Rheometric Scientific RMS 800 analyser equipped with a 50 mm diameter parallel plate measurement system and a torque transducer. The fixed upper plate was connected to the transducer, while the neat resin was placed on the lower moveable plate, which was rotated clockwise and anti-clockwise in relation to the upper plate at 1 Hz oscillating frequency. The torque values recorded by the transducer were then converted into viscosity data during different heating regimes. The viscosity of the neat resin was measured at 2°C/min, 5°C/min and 10°C/min from room temperature until gelation occurred.

4.13 Fourier Transform Infrared Spectroscopy (FTIR)

Infrared spectroscopy (IR) is a technique which studies the interaction of electromagnetic radiation with a chemical substance. All the atoms in molecules are in a state of continuous vibration with respect to each other, with the main types of

molecular vibration being stretching and bending. When the frequency of the IR radiation directed on the molecule coincides with the frequency of a specific vibration, the molecule absorbs the radiation resulting in vibrations of increased amplitude. The frequencies of absorbed radiation are unique for each molecule, since different functional groups absorb characteristic frequencies of IR radiation. These characteristic absorption bands provide the basis for the structural determination of organic compounds by simple inspection and reference to generalised charts of characteristic IR group frequencies.

Infrared radiation refers to the part of the electromagnetic spectrum with wavenumbers from roughly 13,000 to 10 cm^{-1}, or wavelengths from 0.78 to 1,000 μm. The mid IR region ranging from 4,000 to 400 cm^{-1} (2.5 to 25 μm) is more frequently used, since the absorption bands for most organic and inorganic compounds are found in that region. Band positions in IR spectra are generally presented either as wavenumbers, $\bar{\nu}$ (cm^{-1}), or wavelengths, λ (μm). Wavenumbers can be converted to wavelengths according to the following equation:

$$cm^{-1} = \frac{1}{\mu m} \cdot 10^4 \qquad \text{(Eqn. 4.19)}$$

Any absorption band can be described by the wavelength at which maximum absorption occurs and the intensity of absorption at this wavelength. In an IR absorption spectrum, the intensity of the band, which is proportional to the number of molecules observed, is depicted on the y-axis, while the wavenumber or wavelength is depicted on the x-axis. Band intensities are expressed either as transmittance or absorbance. Transmittance (T) or percent transmittance ($\%T$) is the ratio of the radiant power or intensity (I) transmitted by a sample to the incident intensity (I_o) and can be expressed as shown in Equations 4.20 and 4.21, respectively. Absorbance (A) is the logarithm, to the base of 10, of the reciprocal of the transmittance (Eqn. 4.22) [123].

$$T = \frac{I}{I_o} \qquad \text{(Eqn. 4.20)}$$

$$\%T = 100\frac{I}{I_o} \qquad \text{(Eqn. 4.21)}$$

$$A = \log_{10} \frac{I_o}{I} = \log_{10} \frac{1}{T} \qquad \text{(Eqn. 4.22)}$$

Most commercial instruments use either dispersive or Fourier transform spectrometers to obtain the IR spectra of chemical substances. Dispersive spectrometers were first introduced in the mid 1940's and have been replaced by Fourier transform spectrometers, due to the superior speed and sensitivity of the latter. Fourier transform spectrometers consist of three basic components: (1) a continuous IR radiation source, (2) an interferometer, and (3) a sensitive detector of IR radiation. The interferometer divides and recombines radiant beams such that the recombined beams produce a wavelength-dependent interference pattern or an interferogram. A mathematical operation known as Fourier transformation is then used to convert the interferogram, which displays intensity versus time as a time domain spectrum, to the IR spectrum in its final form, displaying intensity versus frequency as a typical frequency domain spectrum.

In this study, Fourier transform infrared spectroscopy was employed for the identification of the characteristic functional groups in conventional and microwave cured composite samples, as well as the uncured epoxy resin. The apparatus used was a Nicolet 5700 FTIR spectrometer manufactured by Thermo Electron Corporation. A top view of the optical layout of the spectrometer is shown in Figure 4.12 [124]. The IR spectra of composite samples cured by both methods as well as that of the uncured resin were collected at room temperature in the wavenumber range of 600 to 4000 cm^{-1} at a resolution of 4 cm^{-1}. 20 scans at random sample locations were averaged in order to avoid any absorbance variations due to sample topography. The intensity of each peak in the spectra of the cured composites was normalised against the intensity of the aliphatic band at approximately 2920 cm^{-1}. Aliphatic hydrocarbon groups are not involved in any of the cure reactions, thus their band intensity remains constant during the curing process.

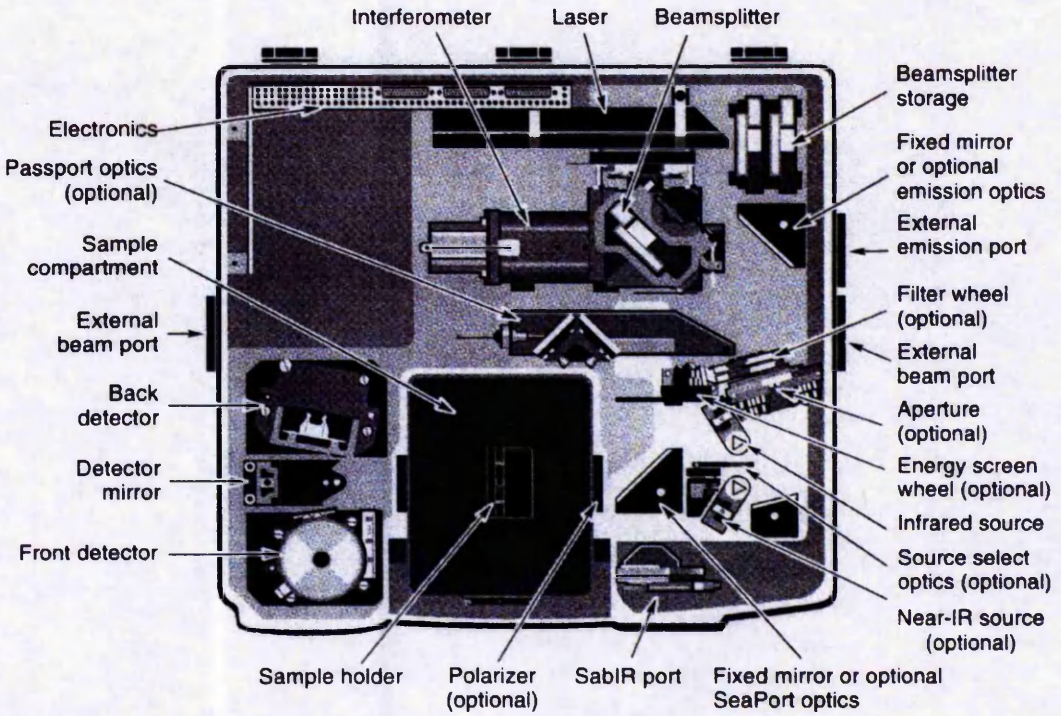

Figure 4.12: *Nicolet 5700 FTIR spectrometer manufactured by Thermo Electron Corporation* [124].

CHAPTER 5

Development of Microwave RTM Processing

5.1 Introduction

In this chapter, the development of microwave resin transfer moulding (RTM) processing is discussed with an emphasis given on the moulding tool employed in this work. The resonant frequencies used in order to achieve a uniform electric field distribution within the microwave applicator during processing for both LY/HY5052/carbon and LY/HY5052/glass composite systems are tabulated. DSC analysis of the uncured resin system was performed in order to determine the cure cycle in conventional thermal RTM processing. The cure cycle for microwave RTM processing was based on measurement of the dielectric properties of the uncured resin system. Furthermore, the computer control system responsible for maintaining a stable cure temperature and achieving uniform heating is described in detail, while the temperature profiles recorded during microwave curing of both composite systems are presented and discussed. Finally, the average thickness across the surface of the composite panels fabricated under conventional and microwave RTM processing is measured and compared against each other.

5.2 Moulding Tool Development

Resin transfer moulding (RTM) is a closed-mould process in which the moulding tool plays a fundamental role in the manufacturing of polymer composites, as it dictates the shape of the finished component once the curing stage has been completed. Conventional RTM usually employs a metal moulding tool for curing composites because of its strength, rigidity and high thermal conductance. Despite all these useful properties for conventional RTM processing, a metal moulding tool could not be used for curing composites via microwave heating, given that metals reflect microwave energy. Thus, it was imperative that a different moulding tool made of a material suitable for use inside the microwave field was manufactured.

In previous work by Yusoff [17], a polytetrafluoroethylene (PTFE) moulding tool was employed to cure flat composite panels under microwave radiation. Although PTFE exhibited suitable dielectric properties, it failed to provide sufficient

dimensional stability. This resulted in composite panels with a significantly uneven thickness variation across their surface; the panel thickness varied from 3.2 mm at the edges and up to 6.5 mm in the middle, albeit the mould cavity was designed to produce composites of approximately 3 mm thickness. As a consequence, the mechanical properties of the fabricated composites were degraded, since their fibre volume fractions were substantially lower in the middle of the panels. For that reason, a moulding tool constructed from Macor, a machinable glass ceramic, was used in microwave RTM processing. A photograph of the Macor moulding tool is shown in Figure 5.1. The two parts of the moulding tool were fastened together using PTFE screws.

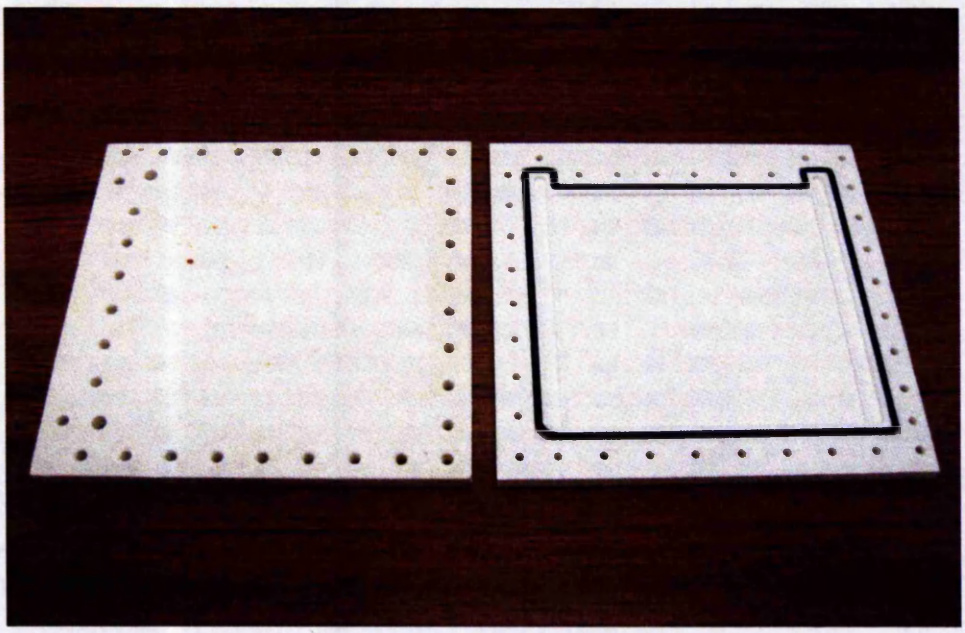

Figure 5.1: *Macor moulding tool used in microwave RTM processing.*

Macor is a machinable glass ceramic with good dielectric properties, exhibiting at room temperature a loss tangent and a dielectric loss of 7.1×10^{-3} and 4×10^{-2} at 8.5 GHz, and 4.7×10^{-3} and 2.8×10^{-2} at 1 kHz, respectively, as can be seen in Table 5.1. The lower the dielectric loss, and thus the loss tangent, the more transparent the material appears to be inside the microwave field. Based on the values of the dielectric properties of Macor, it is reasonable to assume that microwave energy was absorbed predominantly by the resin and not the mould material during microwave curing.

Furthermore, the mechanical properties of Macor provided sufficient stiffness to withstand the temperature and pressure built-up during microwave processing and ensured the required dimensional stability. Some of the properties of Macor are summarised below in Table 5.1 (the values are given by the supplier).

Table 5.1: *Electrical, mechanical and thermal properties of Macor* [119, 125].

Macor Properties	SI / Metric
Dielectric Constant (25°C) 1 kHz 8.5 GHz	 6.03 5.67
Dielectric Loss Tangent (25°C) 1 kHz 8.5 GHz	 4.7×10^{-3} 7.1×10^{-3}
Density	2.52 g/cm
Porosity	0%
Poison's Ratio	0.29
Young's Modulus (25°C)	66 GPa
Shear Modulus (25°C)	25.5 GPa
Compressive Strength (25°C)	345 MPa
Flexural Strength (25°C)	94 MPa
Continuous Operating Temperature	800°C
Maximum No Load Temperature	1000°C

5.3 Excitation Frequencies

The excitation frequencies used for microwave processing were selected in order to minimise the power reflected from the microwave applicator and therefore maximise the power available for heating. These frequencies were dictated by the microwave response of the applicator loaded with the moulding tool, resin and fibre reinforcement. The values were obtained by connecting the loaded microwave applicator directly to the NA before curing and measuring the frequencies corresponding to the minimum reflection peaks.

Modelling of the electric field within the microwave applicator, carried out by Dr Alan Nesbitt in previous work by Yusoff [17], indicated that localisation of the electric field was more pronounced at lower excitation frequencies (f_i = 2 - 4 GHz), thus more uniform electric field distributions could be obtained at higher frequencies (f_i = 4 - 8 GHz). Additionally, epoxy resin and carbon fibre/epoxy composite samples processed using fixed and variable frequency revealed differences in the uniformity of cure. In particular, fixed frequency processing showed evidence of hot spots i.e. burning of samples. Hence, in this work excitation frequency sweeping using a multi-mode applicator was employed in order to generate a time averaged uniform electric field distribution within the microwave applicator.

For each composite system, ten different excitation frequencies ranging from 4 – 8 GHz were used for processing. After the selection of the excitation frequencies, a pre-run was carried out for each excitation frequency to obtain the NA output power value that would produce a maximum amplifier output power of 250 W. It was noted that the selected excitation frequencies did not shift more than 3% from run to run when using different composite samples of the same type of fibre reinforcement. The average excitation frequencies and NA output power values for both LY/HY5052/cabon and LY/HY5052/glass composite systems are summarised in Table 5.2 and Table 5.3, respectively.

Table 5.2: *Average excitation frequency and corresponding NA output power values for achieving maximum amplifier power output (250 W) for the LY/HY5052/carbon composite system.*

Excitation Frequency (GHz)	NA Output Power (dBm)
$f_1 = 4.389$	- 7.02
$f_2 = 4.745$	- 7.16
$f_3 = 4.980$	- 7.26
$f_4 = 5.025$	- 8.28
$f_5 = 5.175$	- 8.65
$f_6 = 5.998$	- 6.89
$f_7 = 6.741$	- 4.57
$f_8 = 7.575$	- 3.33
$f_9 = 7.84$	- 2.55
$f_{10} = 7.945$	- 1.7

Table 5.3: *Average excitation frequency and corresponding NA output power values for achieving maximum amplifier power output (250 W) for the LY/HY5052/glass composite system.*

Excitation Frequency (GHz)	NA Output Power (dBm)
$f_1 = 4.095$	- 5.91
$f_2 = 4.325$	- 6.24
$f_3 = 4.637$	- 7.18
$f_4 = 5.025$	- 7.82
$f_5 = 5.164$	- 8.66
$f_6 = 5.386$	- 8.09
$f_7 = 6.405$	- 5.66
$f_8 = 7.036$	- 3.56
$f_9 = 7.221$	- 3.79
$f_{10} = 7.565$	- 4.17

5.4 Cure Cycle Determination

The cure cycle employed in conventional RTM processing was based on differential scanning calorimetric studies performed on the uncured LY/HY5052 resin system. DSC traces of the uncured resin were obtained at scan rates of 2°C/min, 5°C/min and 10°C/min from 20°C to 250°C. The results are presented in Figure 5.2.

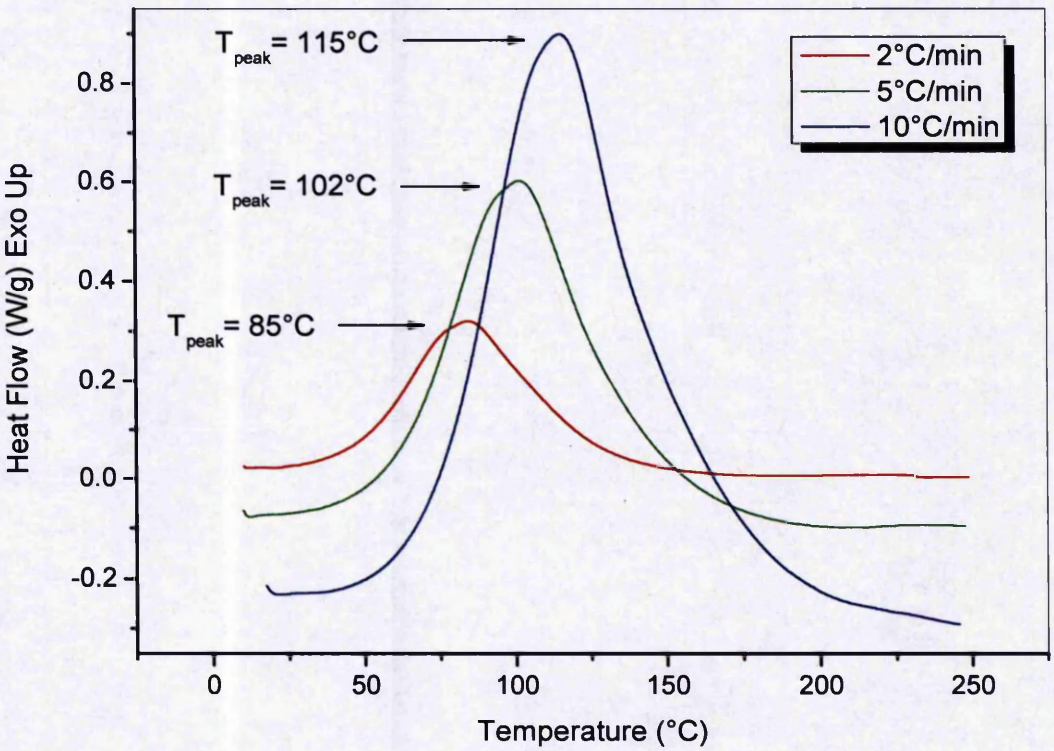

Figure 5.2: *DSC curves of the uncured LY/HY5052 resin system at scan rates of 2°C/min, 5°C/min and 10°C/min from 20°C to 250°C.*

Depending on the heating rate, the shape of the exothermic peak of the uncured epoxy resin changed. Specifically, as the heating rate increased, the exothermic peak became narrower whilst its height increased. This had a direct effect on the peak exotherm temperature (T_{peak}), which increased with increasing heating rate. At 2°C/min heating rate the peak exotherm temperature was 85°C, at 5°C/min heating rate it increased to 102°C and at 10°C/min heating rate it reached 115°C (Figure 5.2). The cure temperature selected for the LY/HY5052 resin system in this work was 100°C. Due to its high chemical reactivity, however, the curing reactions of the specific resin system initiate even at ambient temperature.

In order to establish the duration of the curing cycle, an isothermal DSC run of the neat LY/HY5052 epoxy resin system was performed at 100°C for an extended period of time. The results indicated that the resin was fully cured after about 3 hours at the selected temperature, as can be seen in Figure 5.3. Hence the cure cycle for conventional RTM processing was 3 hours at 100°C. This was also the cure cycle used in previous work by Yusoff [17].

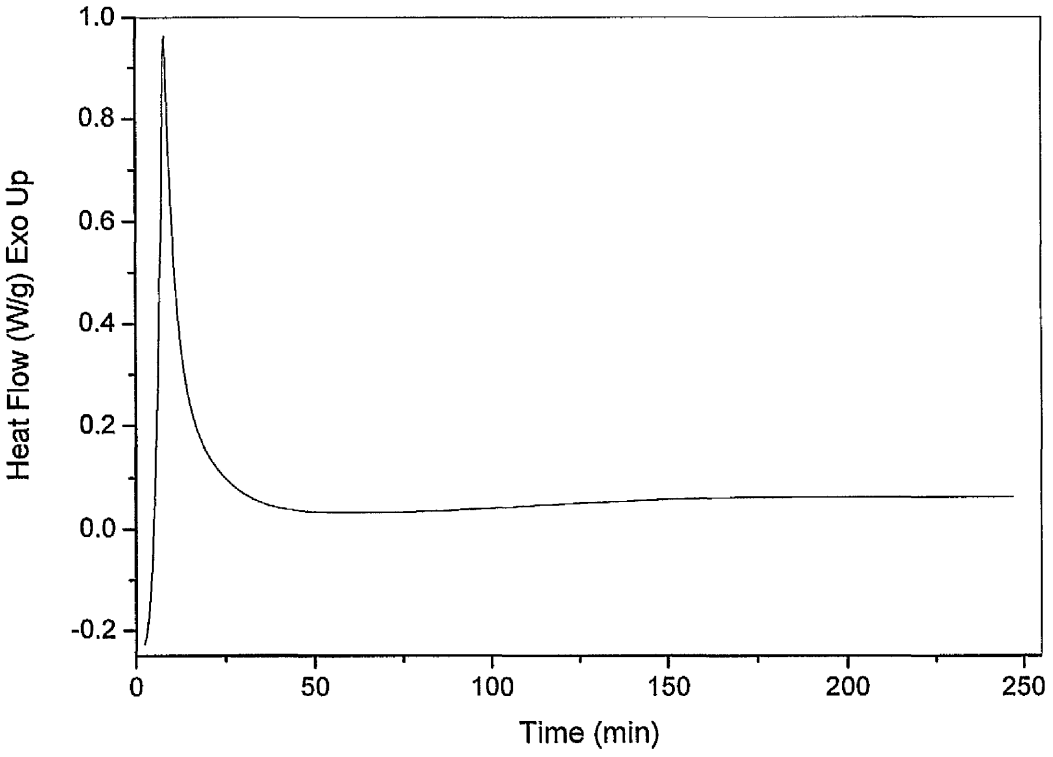

Figure 5.3: *Isothermal DSC curve of the uncured LY/HY5052 resin system at 100°C.*

Determination of the cure cycle for microwave RTM processing was based on in-situ measurements of the dielectric properties of the LY/HY5052 resin system during cure. The measurement of the dielectric properties was carried out at a set frequency of 2.45 GHz using the cavity perturbation technique (see Section 4.11). The dielectric properties changed as the cure reaction proceeded and it was assumed that the cure was complete when no further change in properties was observed. Despite the fact that the dielectric properties were determined for the resin system without taking into account the effect of the fibre reinforcement, they should be indicative of the dielectric response of the composite system at the desired curing temperature.

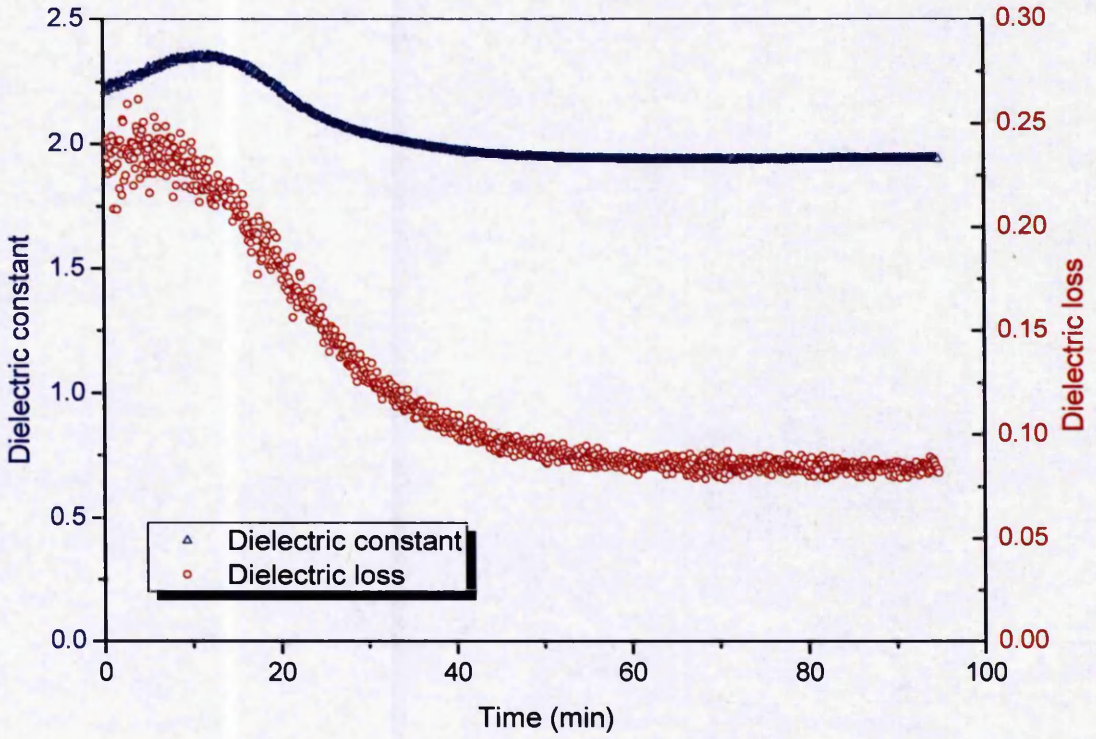

Figure 5.4: *Dielectric constant and dielectric loss of the uncured LY/HY5052 resin system measured at 100°C and 2.45GHz versus time.*

Figure 5.4 shows the evolution of the dielectric loss and dielectric constant of the uncured resin at 100°C and 2.45 GHz as a function of time. As is evident from the graph, the dielectric loss stabilised after about 90 minutes, thus the cure cycle employed for microwave processing was 90 minutes at 100°C. A similar cure cycle was also employed in previous work [17]. DSC analysis of the composite panels produced by microwave RTM under the selected cure cycle, presented later in Chapter 6, showed that the samples were fully cured, indicating sufficient cure cycle time as well as uniform microwave field distribution inside the applicator. Hence a 50% cure cycle time reduction between conventional and microwave RTM processing was achieved. The key question, therefore, is whether this substantial cutback in the duration of the cure cycle of the microwave cured composites would have any detrimental effect on their overall mechanical and physical properties.

5.5 Process Control and Temperature Profiles

A computer control system was employed to ensure both a uniform heating and maintain a stable cure temperature. Microwave power, excitation frequency and sample temperature were used as the process control parameters. Temperature stability was achieved by adjusting the microwave power, while uniformity of the electric field distribution within the applicator was provided by varying the excitation frequency. The computer control system was designed in such way that the NA would continuously step through the excitation frequencies, while simultaneously regulating the microwave power in order to maintain the desired cure temperature. The program code was developed by Dr Alan Nesbitt and was written in Visual C++ (Version 6, Microsoft Visual Studio). Hewlett Packard Standard Instrument Control Library (SICL) commands were used to communicate with the NA and the temperature controller. The control system regulated the microwave power according to a quadratic algorithm based on that of Wei *et al.* [126]:

$$Power \propto \left[\frac{T_{cure} - T}{T_{cure} - T_{\min}}\right]^2 \qquad \text{(Eqn. 5.1)}$$

where T was the maximum of the measured sample temperatures (T_1, T_2, T_3, T_4), T_{cure} was the cure temperature and T_{min} was a pre-set temperature limit.

As can be seen from the above parabolic relationship, the output power of the amplifier was proportional to the square of the difference between the set cure temperature and the actual temperature. The amplifier output power was adjusted by changing the output power of the NA; hence in practice the control algorithm was used to regulate the output power of the NA. During the initial heating stages ($T < T_{min}$), the NA output power was set to P_{max}. When the sample temperature exceeded the temperature limit ($T > T_{min}$), the power was gradually decreased by adjusting the NA output power according to the following equation:

$$P_{NA} = P_{\min} + (P_{\max} - P_{\min}) \cdot \left[\frac{T_{cure} - T}{T_{cure} - T_{\min}}\right]^2 \qquad \text{(Eqn. 5.2)}$$

where P_{min} was the power required to maintain the sample at T_{cure} and P_{max} the power required to rapidly heat until T_{min} was reached. At the curing temperature ($T = T_{cure}$) the power was set to P_{min}.

The sample temperature was monitored via four fluoroptic probes, as described in detail in Section 3.4.2. Two surface temperature probes (T_1 and T_2) were in contact with the mould surface, while two immersion probes (T_3 and T_4) were inserted in the resin at the mould inlet and outlet. Figures 5.5 and 5.6 show the temperature profiles with time at four different places during microwave processing of the LY/HY5052/carbon and the LY/HY5052/glass composite system, respectively. It has to be noted that due to the position of the temperature probes during microwave processing, the recorded temperature readings have to be considered as basic process control parameters necessary for achieving temperature stability and avoiding temperature overshoots rather than accurate resin or mould temperatures.

Furthermore, uniform heating was achieved and maintained during microwave processing of both composite systems, as verified by the high degrees of cure of the produced composite samples presented in Chapter 6. A larger variation between the resin and the mould temperatures was observed in the microwave curing of the LY/HY5052/carbon composite system compared to that of its glass fibre counterpart. The resin reached the required cure temperature slightly faster in the case of the carbon fibre composite system. The time required for the resin to reach a plateau was approximately 27 minutes in the carbon fibre composite system as opposed to 37 minutes in its glass fibre equivalent. This is attributed to the presence of the carbon fibre, as the resin system and the microwave power output were the same for both composites. Carbon fibres, having a substantially higher dielectric loss than glass fibres, absorbed more microwave energy which in turn was dissipated as heat via conduction into the surrounding resin. The additional heat enhanced the exothermic cross-linking reactions taking place within the epoxy resin, resulting into a faster increase of the resin temperature. This was also confirmed by the fact that the mould temperatures measured during microwave curing of the LY/HY5052/glass fibre composite system reached a plateau earlier (~ 43 min) than those of its carbon fibre counterpart (~ 54 min), suggesting that the mould itself was heated faster in the first case due to more microwave energy being available.

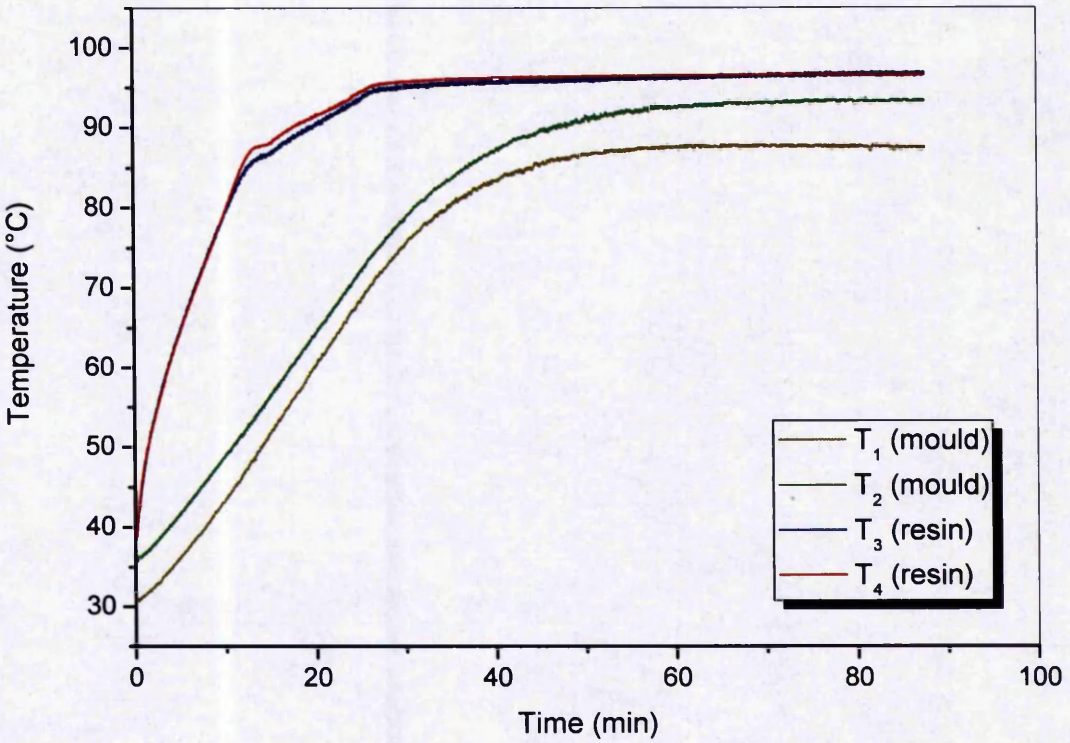

Figure 5.5: *Variation of the sample temperature against time at four different places during microwave processing of the LY/HY5052/carbon composite system.*

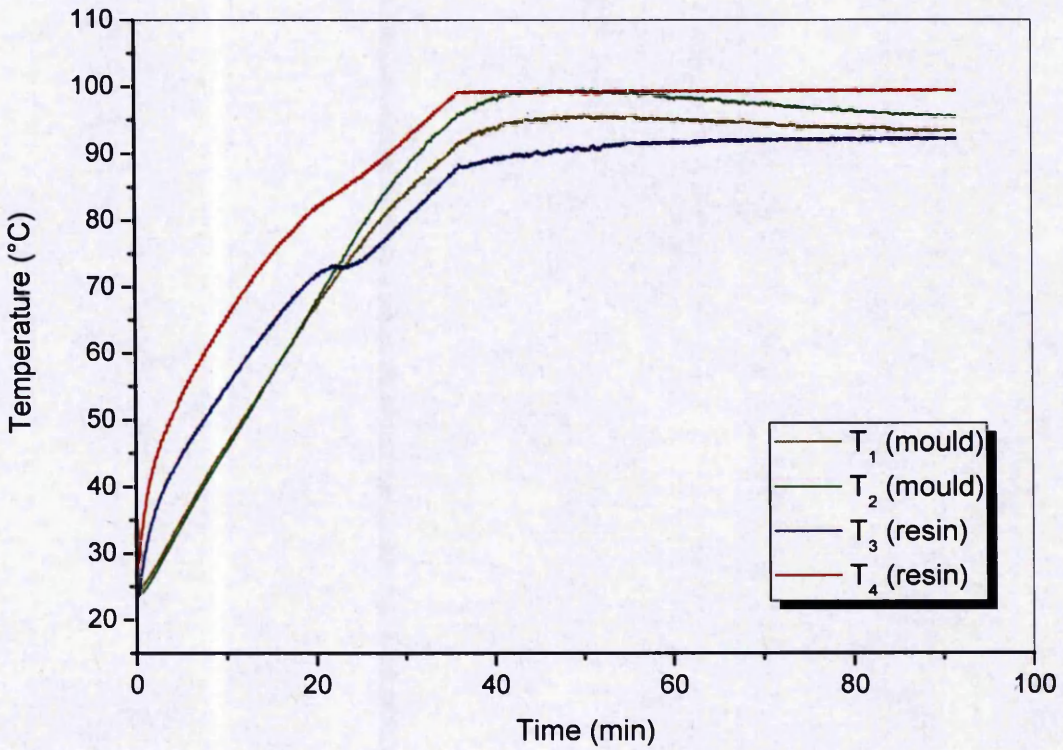

Figure 5.6: *Variation of the sample temperature against time at four different places during microwave processing of the LY/HY5052/glass composite system.*

5.6 RTM Composite Panels

A photograph of the LY/HY5052/carbon and LY/HY5052/glass composite panels produced by conventional thermal and microwave RTM processing is shown in Figure 5.7.

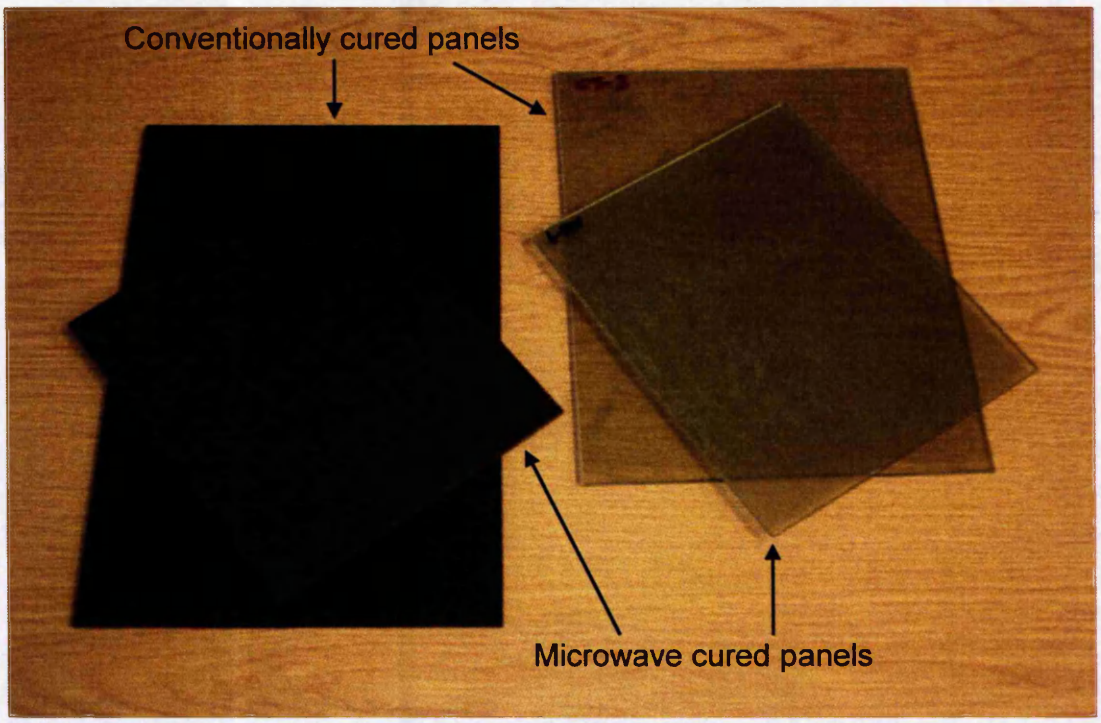

Figure 5.7: *LY/HY5052/carbon and LY/HY5052/glass composite panels produced by conventional thermal and microwave RTM processing.*

The average panel thickness of the composites manufactured using both processing methods is tabulated in Table 5.4. The results revealed minimal thickness variation across the surface of the fabricated composite panels, ensuring adequate dimensional stability. The latter is an important prerequisite in order to produce composites with good mechanical properties, as it directly affects their fibre volume fractions. A large thickness variation was an inherent weakness of the PTFE mould employed for the microwave curing of carbon fibre composites in previous work by Yusoff [17]. Furthermore, careful examination of the values presented in Table 5.4 showed that the average panel thickness of the microwave cured panels was slightly higher compared to those cured conventionally. This was due to small dimensional differences of the Macor mould cavity with that of the metal mould attained at

machining. Nevertheless, when comparing the average thickness between composite panels manufactured under the same processing method, the values are very similar.

Table 5.4: *Average thickness of the LY/HY5052/carbon and the LY/HY5052/glass composite panels produced by both conventional thermal and microwave RTM processing.*

Composite System	Average Panel Thickness (mm)	
	Manufacturing Method	
	Conventional Thermal RTM	Microwave RTM
LY/HY5052/carbon	3.38 ± 0.08	3.74 ± 0.1
LY/HY5052/glass	3.33 ± 0.03	3.79 ± 0.07

5.7 Summary

A new moulding tool constructed from a machinable glass ceramic material called Macor was used in microwave RTM processing as a substitute for the metal mould used in conventional thermal RTM processing. A computer control system was employed in order to sustain a stable cure temperature and achieve uniform heating of the composite samples during microwave processing. Temperature stability and uniformity of the electric field distribution within the applicator were provided by adjusting the microwave power and varying the excitation frequency, respectively.

Ten excitation frequencies ranging from 4 to 8 GHz were employed for microwave curing of both LY/HY5052/carbon and LY/HY5052/glass composite samples. These frequencies were dictated by the microwave response of the loaded applicator before curing each composite sample and were within 3% from run to run when using different composite samples of the same type of fibre reinforcement. Dynamic and isothermal DSC analysis on the uncured LY/HY5052 resin indicated that the optimal cure cycle for conventional RTM processing was 3 hours at 100°C. On the other hand, the cure cycle employed for microwave RTM processing was determined to be 90 minutes at 100°C based on measurements of the dielectric properties of the uncured resin. Hence, a 50% cure cycle time reduction was achieved via microwave

heating. The temperature profiles recorded during microwave processing of the composite samples confirmed that there was good temperature control and uniform heating. In addition, the composite panels produced by both processing methods exhibited minimal thickness variation across their surface. The average thickness of the microwave cured composites was higher than those cured conventionally, due to the cavity of the Macor mould being slightly deeper than that of the metal mould employed in conventional thermal RTM processing.

CHAPTER 6

Curing Characteristics of Composite Systems

Introduction

This chapter is concerned with the curing characteristics, thermal and dynamic mechanical properties and network structure of both thermally and microwave cured composites. The degrees of cure across the fabricated composite panels were determined using temperature modulated differential scanning calorimetry (TMDSC), while the effect of the curing method on the dynamic mechanical properties of the produced composites such as the storage modulus (E'), the loss modulus (E'') and the loss tangent (tan δ) was investigated by means of dynamic mechanical thermal analysis (DMTA). The molecular weight between cross-links (M_c) and cross-link density (v_e) of both thermally and microwave cured composites were calculated in order to examine variations in the network structure. Differences in the final network structure obtained between conventionally and microwave cured composite samples were also studied using Fourier transform infrared spectroscopy (FTIR).

Degree of Cure

In order to assess the effectiveness of microwave RTM processing, it was essential to determine whether the produced composites were fully cured. The degree of cure is an important factor that affects the properties of a composite, as it controls the cross-link density and the overall network structure of the resin system formed throughout the curing process. In addition, when microwave processing is concerned, a consistent degree of cure across the composite panel would be direct evidence of a uniform electric field distribution within the microwave applicator. The degree of cure for both microwave and conventionally cured samples was obtained using temperature modulated differential scanning calorimetry (TMDSC) instead of conventional differential scanning calorimetry (DSC), due to the exothermic peak of the residual reaction overlapping with the changes in the heat flow in the vicinity of the glass transition temperature (T_g). TMDSC is a more sensitive method compared to conventional DSC in which the heat flow is separated into reversible and non-reversible heat flows. Typical reversing events in TMDSC include glass transitions

and melting, while typical non-reversing events include thermoset cure, evaporation and decomposition. TMDSC scans were performed on the fabricated composite samples from 20°C to 250°C at 3°C/min using a modulation amplitude of ±1°C every 60 seconds. The samples were taken from various locations in the composite panels and for each panel ten samples were tested to ensure the accuracy of the results. Furthermore, DSC measurements were performed on the uncured LY/HY5052 resin system to determine the total heat released by the exothermic curing reaction.

Figure 6.1 shows the DSC trace obtained for the uncured LY/HY5052 resin system. The total heat of the curing reaction (ΔH_{unc}) was 437 J/g, as calculated from the area under the exothermic transition. This value was higher than that reported by Suckley [111] (389 J/g), but very similar to the value reported by Montserrat et al. [127] (440 J/g). The difference is probably due to the high reactivity of the specific resin system and the broad range of the exothermic transition region, which makes it difficult to determine the exact value of ΔH_{unc}. The exothermic transition was characterised by a starting temperature for polymerisation (T_1 = 40 ± 10°C), an exothermic peak temperature (T_{peak} = 115 ± 3°C) and a final temperature (T_2 = 220 ± 5°C) at which the reaction was completed.

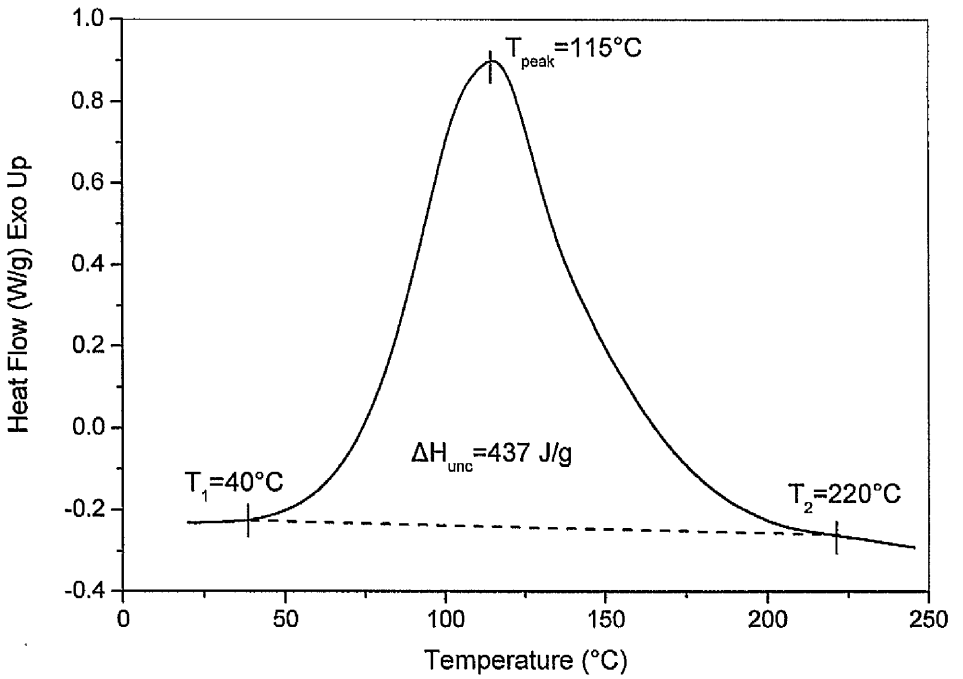

Figure 6.1: *DSC trace of the uncured LY/HY5052 resin system.*

The degree of cure (α) was calculated according to the following equation:

$$\alpha = 1 - \frac{\Delta H}{\Delta H_{unc}} \qquad \text{(Eqn. 6.1)}$$

where ΔH and ΔH_{unc} is the total heat released by the exothermic reaction for the composite and the uncured resin system, respectively.

LY/HY5052/carbon Composite System

Figure 6.2 shows the non-reversible, reversible and standard heat flow curves obtained from TMDSC for a typical LY/HY5052/carbon composite sample produced by conventional RTM processing. Thermoset cure is a non-reversible event; hence any residual cure can be calculated from the area under the exothermic transition in the non-reversible heat flow curve. The heat of the residual reaction for the composite sample in Figure 6.2 was 3.71 J/g. Thus, by using Equation 6.1 the degree of cure was calculated at 99.1 %. Similarly, in Figure 6.3 the heat flow curves obtained from TMDSC for a typical microwave cured LY/HY5052/carbon composite sample are presented. The heat of the residual reaction for the microwave cured sample was 3.17 J/g, which corresponded to a 99.3% degree of cure.

The degrees of cure obtained throughout the LY/HY5052/carbon composite panels manufactured using both conventional thermal and microwave RTM processing were averaged, giving overall values of α = 99.6 ± 0.3 % and α = 99.3 ± 0.2 %, respectively. The calculated values for the two different processing methods are very similar and close to 100 %, indicating that the produced composite panels in both cases were fully cured. This was expected for the thermally cured composites, since conventional RTM is a common manufacturing method. Microwave RTM processing, however, had yet to be assessed regarding its efficiency in curing composites. The degree of cure for the microwave cured composites was found to be consistent throughout the panels, as shown by the small standard deviation from the average degree of cure value, verifying that the electric field distribution within the microwave applicator was uniform.

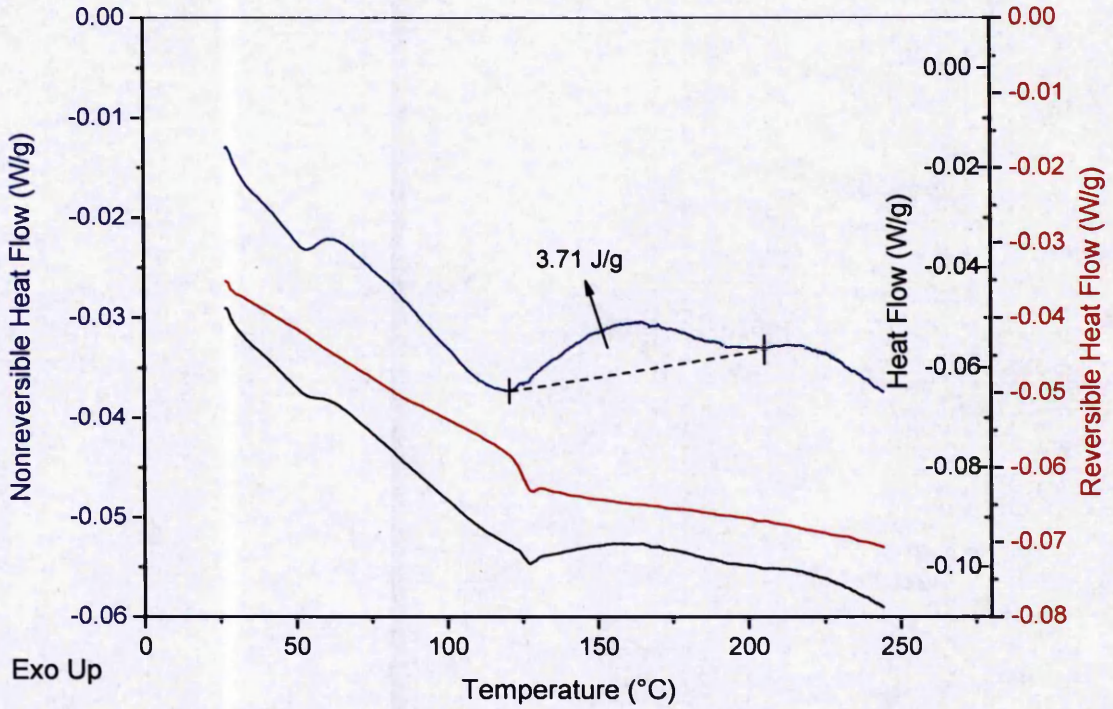

Figure 6.2: *Non-reversible, reversible and standard heat flow curves obtained from TMDSC for a typical LY/HY5052/carbon composite sample cured using conventional thermal RTM processing.*

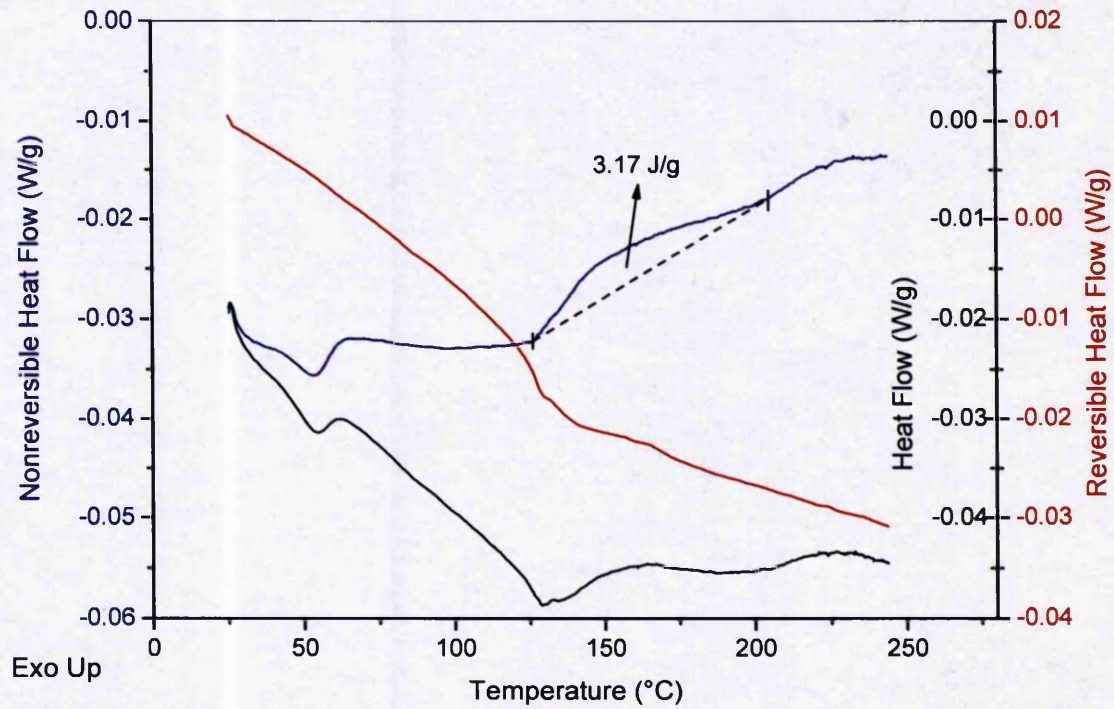

Figure 6.3: *Non-reversible, reversible and standard heat flow curves obtained from TMDSC for a typical LY/HY5052/carbon composite sample cured using microwave RTM processing.*

LY/HY5052/glass Composite System

TMDSC was also performed on the LY/HY5052/glass composite panels produced by both conventional thermal and microwave RTM processing. The non-reversible, reversible and standard heat flows for the two types of composite samples are shown in Figures 6.4 and 6.5. The heat released by the residual curing reaction for a typical thermally cured LY/HY5052/glass composite sample was 3.37 J/g, which according to Equation 6.1 corresponded to a 99.2 % degree of cure. On the other hand, the heat of the residual reaction for a typical microwave cured LY/HY5052/glass sample was measured at 2.02 J/g, giving a 99.5 % degree of cure.

The degrees of cure for both thermally and microwave cured LY/HY5052/glass composite samples, taken from different locations on the fabricated panels, were averaged. The overall degree of cure values were α = 99.4 ± 0.2 % for the composites produced using conventional thermal RTM processing and α = 99.5 ± 0.1 % for those produced using microwave RTM processing. As with the carbon fibre composites, the calculated values are very similar. The high average value of the degree of cure for the microwave cured LY/HY5052/glass composite samples confirmed that the composite panels manufactured using microwave RTM processing were fully cured, while the small standard deviation verified that a uniform electric field distribution was achieved during the curing process.

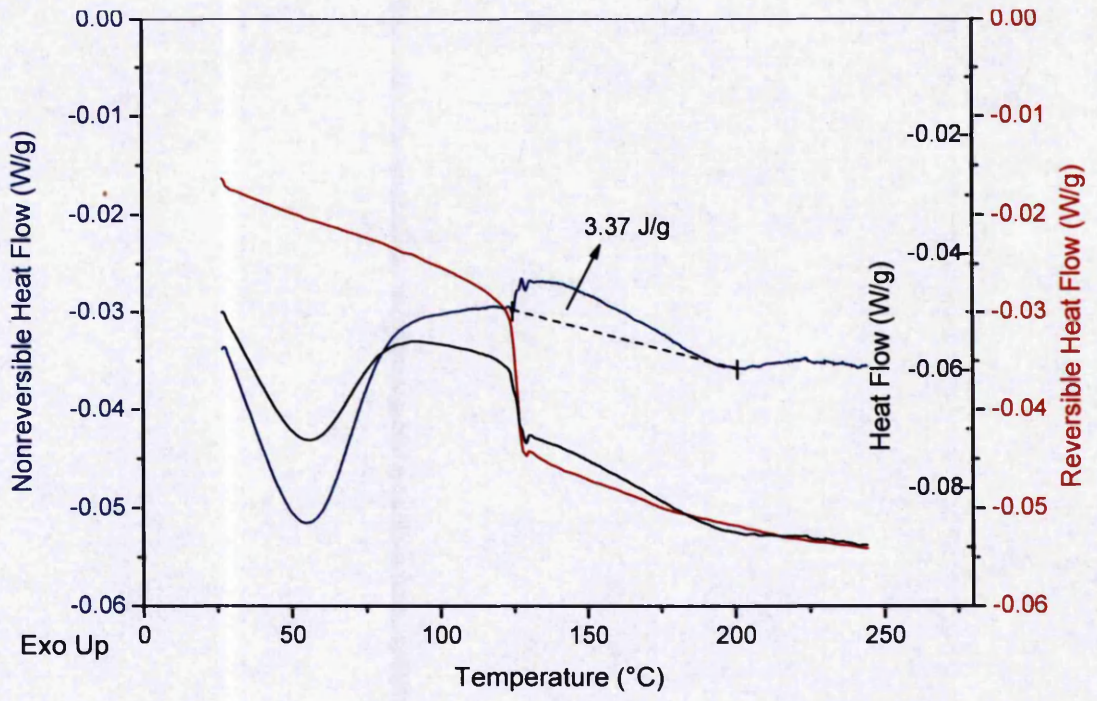

Figure 6.4: *Non-reversible, reversible and standard heat flow curves obtained from TMDSC for a typical LY/HY5052/glass composite sample cured using conventional thermal RTM processing.*

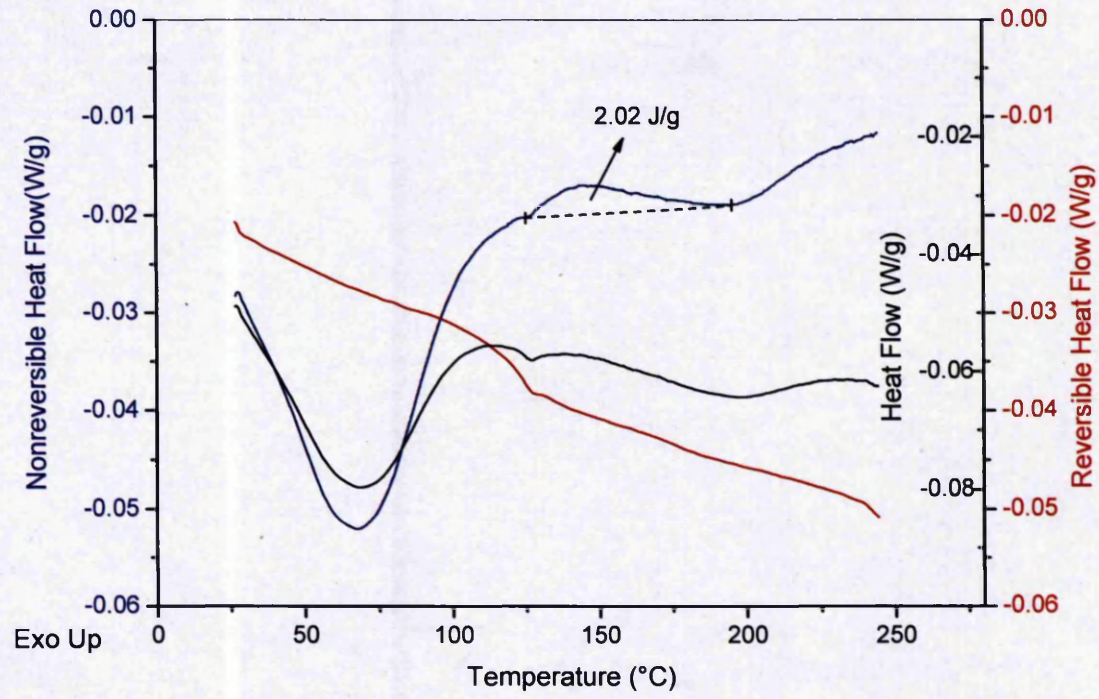

Figure 6.5: *Non-reversible, reversible and standard heat flow curves obtained from TMDSC for a typical LY/HY5052/glass composite sample cured using microwave RTM processing.*

Summary of Degree of Cure Data

The average values of the degree of cure for the LY/HY5052/carbon and LY/HY5052/glass composite panels manufactured using both processing methods are summarised below in Table 6.1.

Table 6.1: *Average values of the degree of cure for the LY/HY5052/carbon and LY/HY5052/glass composite panels produced using both conventional thermal and microwave RTM processing.*

Composite System	Average Degree of Cure (%)	
	Manufacturing Method	
	Conventional Thermal RTM	Microwave RTM
LY/HY5052/carbon	99.6 ± 0.3	99.3 ± 0.2
LY/HY5052/glass	99.4 ± 0.2	99.5 ± 0.1

6.3 Dynamic Mechanical Properties

Dynamic mechanical thermal analysis (DMTA) was used in this study to evaluate the effect of the curing method on the dynamic mechanical properties of the produced composites. Dynamic mechanical properties such as the storage modulus (E'), the loss modulus (E'') and the loss tangent (tan δ) were measured for both thermally and microwave cured composites in the temperature range of -150°C to 250°C at 2°C/min heating rate and 1 Hz oscillating stress frequency. For each composite panel, six samples taken from different locations in the panel were tested to ensure good representativity of the results. The glass transition temperatures (T_g) of the manufactured composites were also determined and compared against each other, since changes in the T_g suggest different network morphologies between conventional thermal and microwave curing processes. In addition, the low temperature secondary relaxation (or β-transition) was investigated for both types of composite systems in order to identify any differences in the reaction path followed due to the curing method employed.

6.3.1 LY/HY5052/carbon Composite System

The storage modulus (E'), loss modulus (E'') and tangent Delta (tan δ) curves obtained from DMTA for a typical LY/HY5052/carbon composite sample produced by conventional thermal RTM processing are presented in Figure 6.6. In this study, the glass transition temperature (T_g) was taken from the maximum peak in the tan δ curve. The measured T_g values from all the tested samples were averaged, giving an overall T_g value of 128 ± 2°C for the conventionally cured LY/HY5052/carbon composites. Similarly, Figure 6.7 shows the DMTA curves for a typical microwave cured composite sample. The average T_g value, as calculated from all the tested samples, for the LY/HY5052/carbon composites produced by microwave RTM processing was 130 ± 1°C. The results indicated that no significant difference in the T_g existed between the two types of composites.

As can be seen in Figures 6.6 and 6.7, although the general trend for E' and E'' was similar between the two types of composites, the actual values obtained for the conventionally cured LY/HY5052/carbon composites were higher than those obtained for their microwave cured counterparts. This is attributed to the higher average fibre volume fraction of the conventionally cured composites (33 %) compared to those cured using microwave heating (27 %). The fibre volume fraction results will be presented in detail later in Chapter 7. As mentioned in Section 5.6, the cavity of the Macor mould was slightly deeper than that of the metal mould employed in conventional thermal processing, which resulted in the microwave cured panels being thicker than those cured thermally. Hence the difference in the fibre volume fraction of the produced composite samples, given that the same number of carbon fibre layers was used to manufacture composites with both methods. However, since tan δ represents the ratio between the loss and storage moduli (E''/E'), it can be used in order to compare the dynamic mechanical properties of the two types of composites.

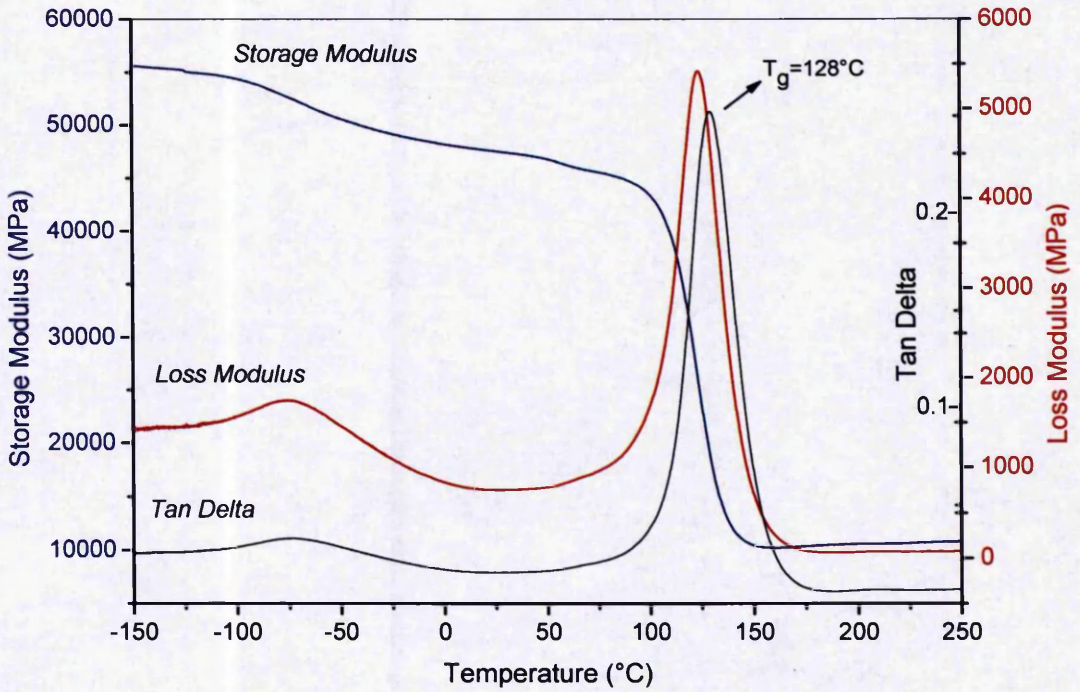

Figure 6.6: *Storage modulus, loss modulus and tangent Delta obtained from DMTA for a typical LY/HY5052/carbon composite sample cured using conventional thermal RTM processing.*

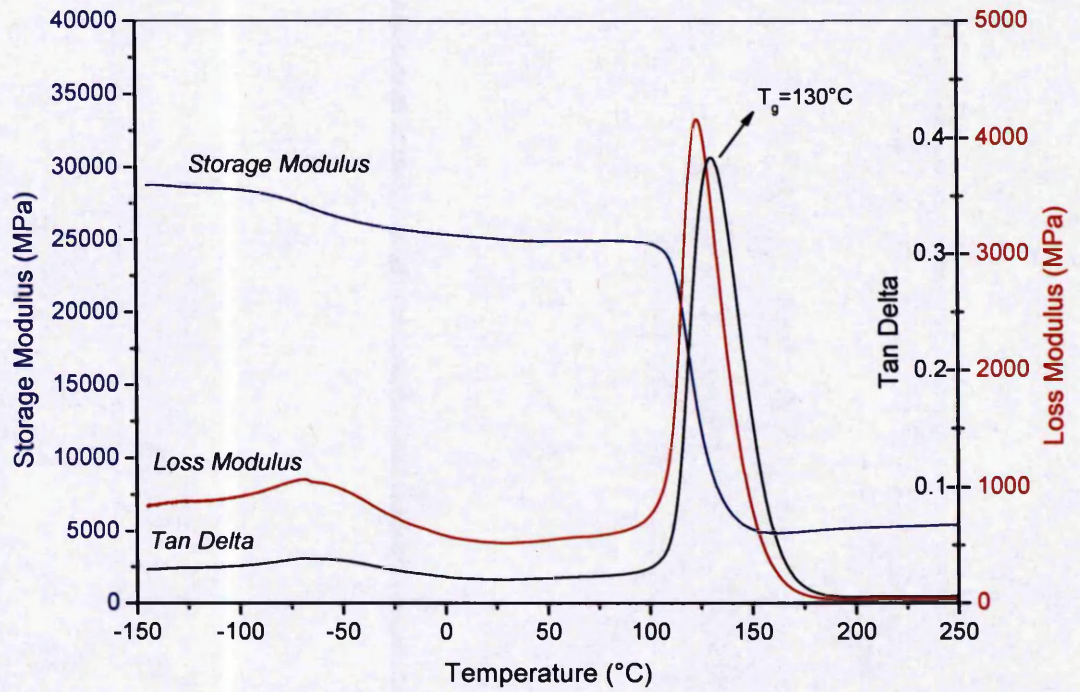

Figure 6.7: *Storage modulus, loss modulus and tangent Delta obtained from DMTA for a typical LY/HY5052/carbon composite sample cured using microwave RTM processing.*

Murayama and Bell [128] suggested that the height of the tan δ peak is related to the distance between cross-links, M_c. The increase in tan δ_{max} with increasing M_c reflects the increasing ability of the polymer to absorb energy, as the molecular constraints are reduced and the mobility of the chain segments becomes greater [128]. For that reason, the height of the glass transition peak in the tan δ curve was measured for both conventionally and microwave cured LY/HY5052/carbon composite samples. The average values were 0.24 ± 0.002 and 0.36 ± 0.010 for the thermally and microwave cured composites, respectively. It appears that although similar T_g values were obtained for both types of composites, the glass transition for the microwave cured samples was more intense compared to their conventionally cured counterparts, which in turn suggests that a less packed network structure with a larger distance between cross-links was formed during microwave processing. Figure 6.8 shows a comparison of the tan δ curves obtained for both conventionally and microwave cured LY/HY5052/carbon composites, in which the difference in the glass transition peak height is portrayed.

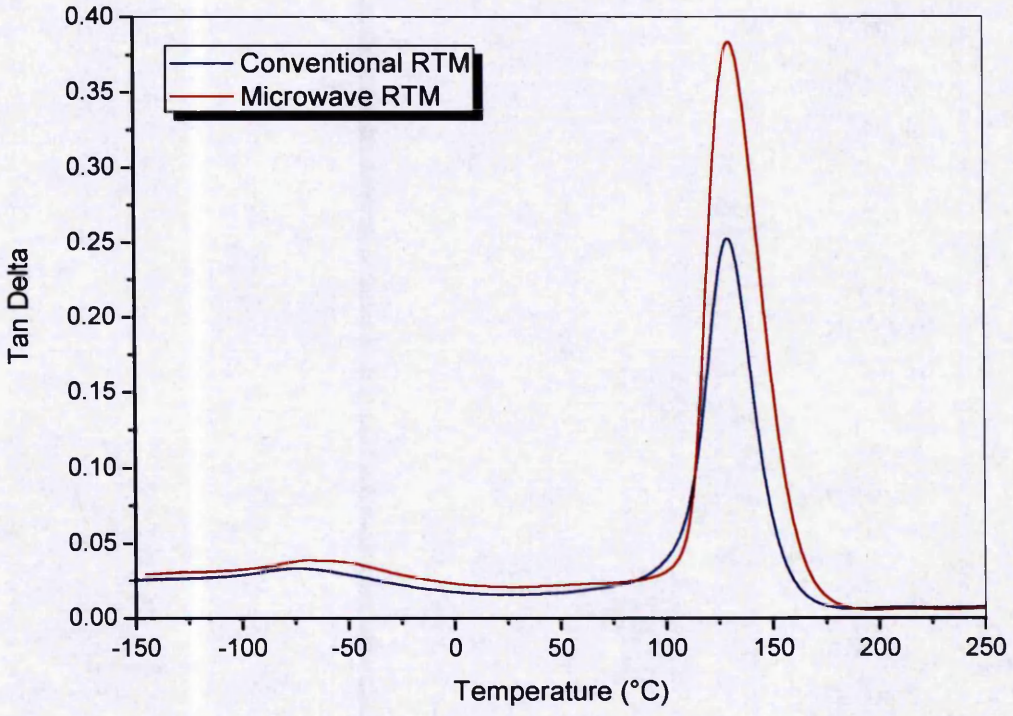

Figure 6.8: *Comparison of the tan δ curves obtained for both conventionally and microwave cured LY/HY5052/carbon composites.*

The β-transition of the produced composites was also investigated based on the tan δ curves measured by DMTA. The low temperature β-transition in epoxy systems has been observed between -80°C to -40°C [129-132]. More specific in epoxy-amine curing, low temperature relaxations have been shown to be related to the molecular motion of the hydroxyether portion ($-CH_2-CH(OH)-CH_2-O-$) of the polymer network [133, 134], which is generated by the reaction between epoxide and hydroxyl groups. Both thermally and microwave cured LY/HY5052/carbon composites exhibited a β-transition of similar intensity, with an average peak height value of 0.01 ± 0.001 as calculated from all the tested samples. A 15°C difference, however, in the position of the β-transition peak was detected between the two types of composites. The maximum of the β-transition peak was observed at -72 ± 3°C for the thermally cured composites, as opposed to -57 ± 3°C for those cured using microwave heating.

This shift in the position of the β-transition peak to a higher temperature may be caused by a different molecular structure of the polymer chain formed during the curing process, possibly resulting from an alteration in the cross-linking path followed between the two processing methods. Figure 6.9 shows an expansion of the tan δ versus temperature curves in the β-transition temperature range for the two types of composites. Gong [135] who studied the dynamical behaviour of short fibre-reinforced epoxy resin composites observed a similar shift of the β-transition to a higher temperature. He suggested that this phenomenon is due to interactions between the macromolecules of the epoxy resins and the molecules along the surface of the fibres. Some segments of the epoxy macromolecules could not move in the way they normally would and had to be mobilised with greater energy or, in other words, at a higher temperature. The amount of energy required could depend on the intensity of the interaction between the polymer segments and the fibre surface molecules as well as the distance between them [135].

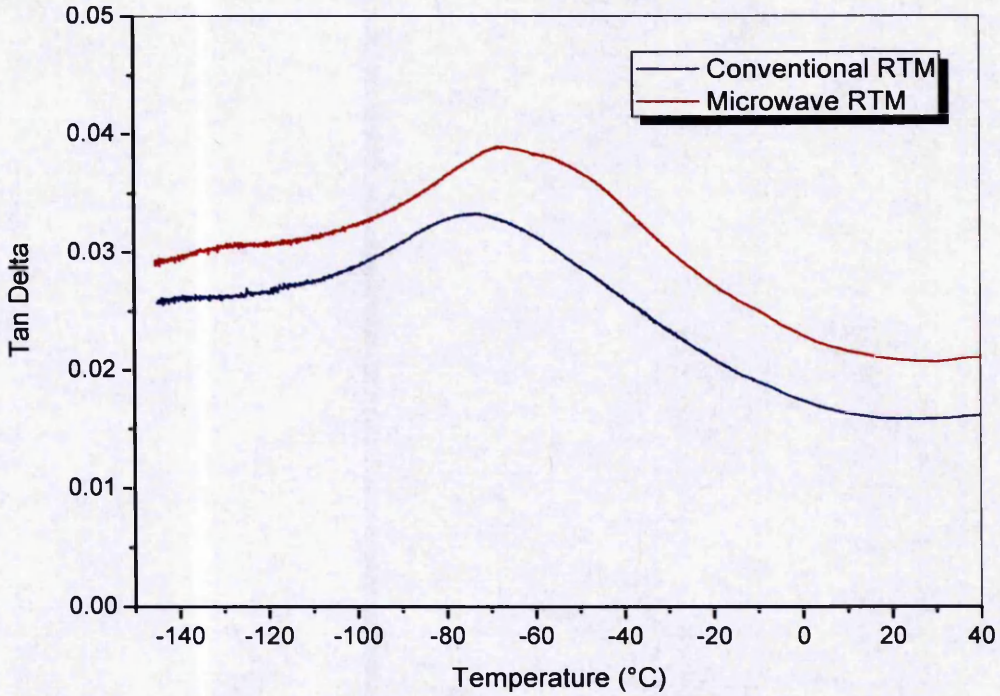

Figure 6.9: *Expansion of the tan δ versus temperature curves in the β-transition temperature range for both conventionally and microwave cured LY/HY5052/carbon composites.*

6.3.2 LY/HY5052/glass Composite System

The storage modulus, loss modulus and tan δ curves obtained from DMTA for the LY/HY5052/glass composite samples produced by both conventional and microwave RTM processing are presented in Figures 6.10 and 6.11, respectively. The measured T_g values from all the tested samples were averaged. The thermally cured composites yielded an overall T_g value of 125 ± 1°C, while those cured using microwave heating yielded an overall T_g value of 126 ± 1°C. Similar to the carbon fibre composites, the results showed no significant difference in the T_g between the two types of composites. The values for E' and E'', however, were found to be comparable even though, for reasons described previously in Section 6.3.1, the thermally cured LY/HY5052/glass fibre composites had higher fibre volume fractions (26 %) than those cured using microwave heating (20 %). Glass fibres have a considerably lower tensile modulus (~ 70 GPa) than carbon fibres (~ 230 GPa) hence their contribution to the mechanical stiffness of the composites produced was less significant.

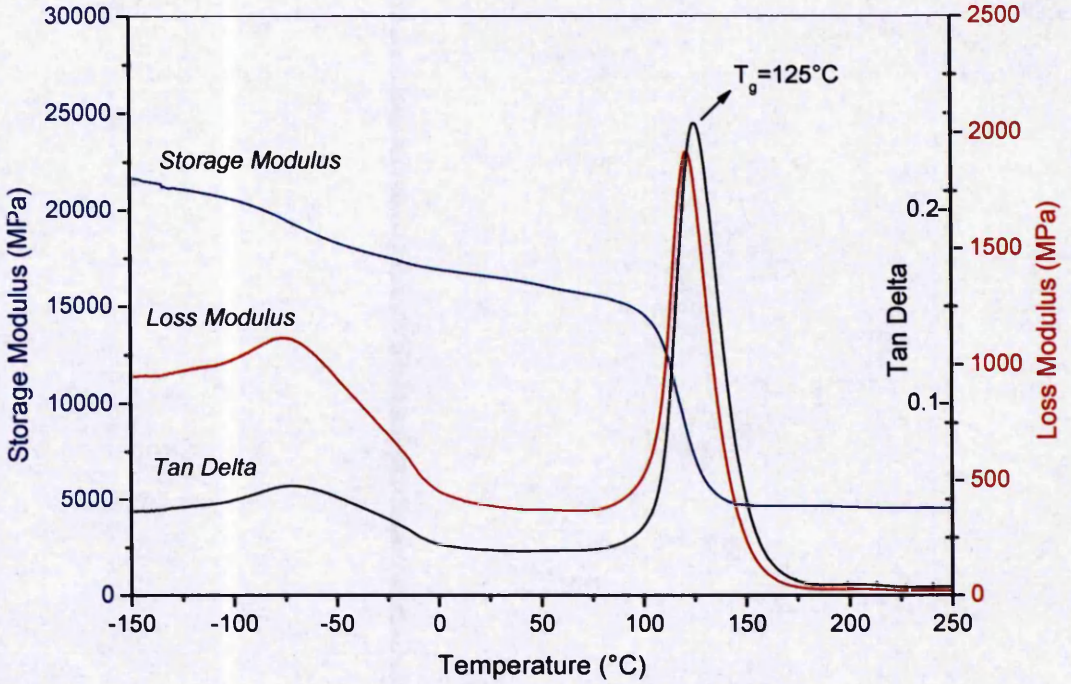

Figure 6.10: *Storage modulus, loss modulus and tangent Delta obtained from DMTA for a typical LY/HY5052/glass composite sample cured using conventional thermal RTM processing.*

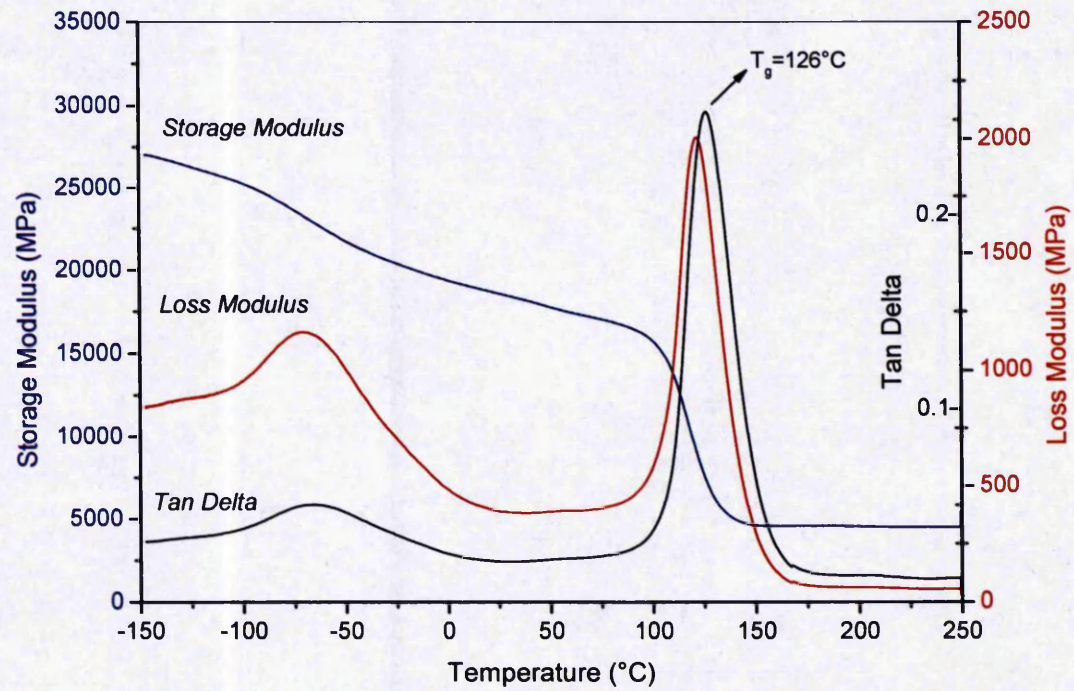

Figure 6.11: *Storage modulus, loss modulus and tangent Delta obtained from DMTA for a typical LY/HY5052/glass composite sample cured using microwave RTM processing.*

The intensity of the glass transition was investigated for both types of composites in terms of peak magnitude. The height of the glass transition peak in the tan δ curve was measured at peak maximum for both conventionally and microwave cured composite samples. The average values were 0.22 ± 0.007 for the conventionally cured LY/HY5052/glass composites and 0.24 ± 0.008 for those cured using microwave heating. The results revealed that the average peak height value of the glass transition for the microwave cured composites was higher than that of their thermally cured counterparts, but only to a small extent. In contrast with the carbon fibre composites, the difference in the intensity of the glass transition between the glass fibre composites produced conventionally and by microwave processing was less prominent. This is probably due to the presence of the glass fibres which absorbed less amount of microwave energy than carbon fibres, thus allowed the cross-linking reactions to progress further producing a denser network structure. A comparison of the tan δ curves obtained for the composites manufactured using both curing methods is shown in Figure 6.12.

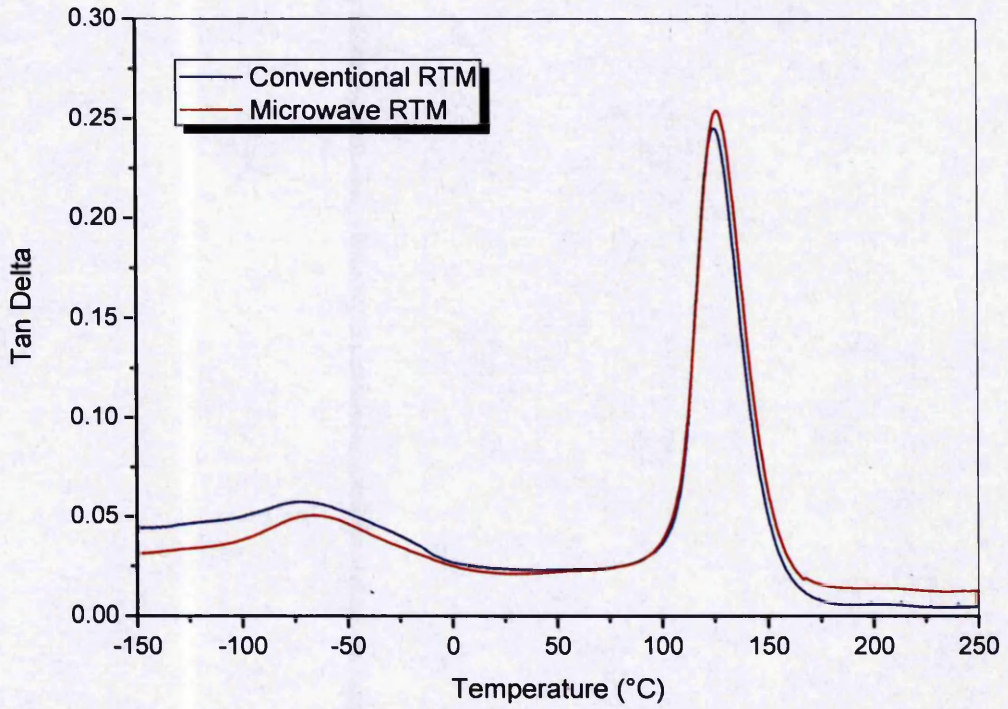

Figure 6.12: *Comparison of the tan δ curves obtained for both conventionally and microwave cured LY/HY5052/glass composites.*

The temperature at which β-transition occurred for both types of composites was determined from the maximum peak in the tan δ curve in the -150°C to 0°C temperature range. The position of the β-transition peak, as calculated from all the tested samples, was – 68 ± 2°C and – 64 ± 1°C for the thermally and microwave cured LY/HY5052/glass composites, respectively. The results indicated a 4°C shift in the position of the β-transition peak to a higher temperature for the microwave cured LY/HY5052/glass composites compared to those cured thermally. This shift, however, was not as distinct as with the carbon fibre composites. Furthermore, the intensity of β-transition for both types of LY/HY5052/glass composites was found to be similar. The average peak height values were 0.016 ± 0.002 and 0.017 ± 0.004 for the conventionally and microwave cured composites, respectively. Figure 6.13 shows an expansion of the tan δ versus temperature curves in the β-transition temperature range for the two types of composites.

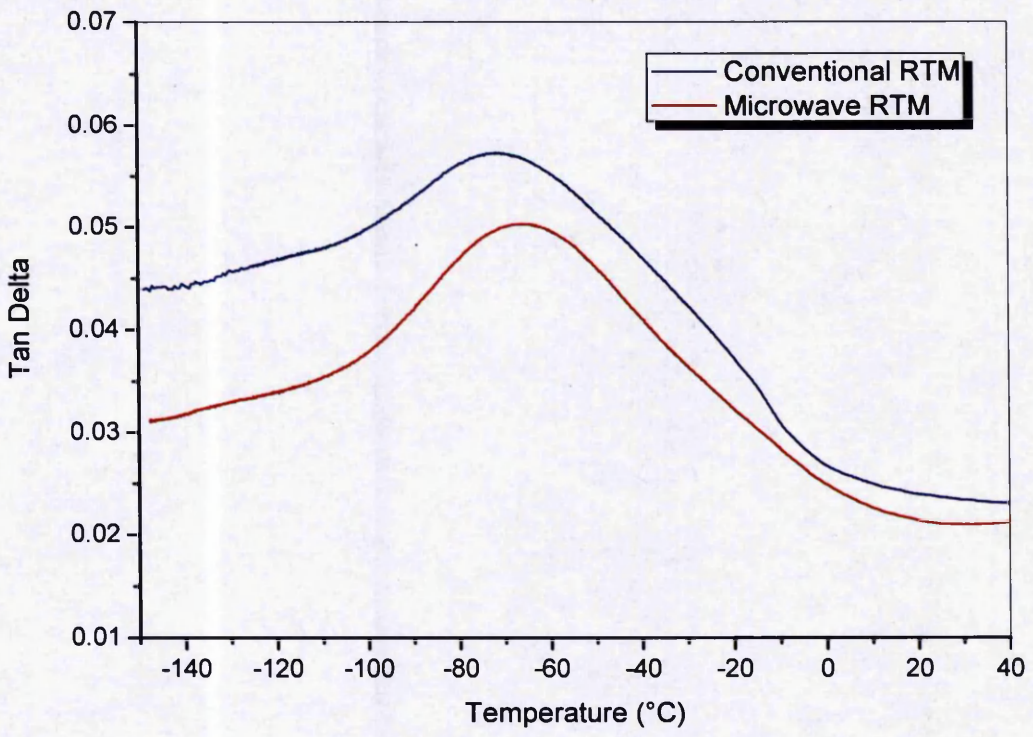

Figure 6.13: *Expansion of the tan δ versus temperature curves in the β-transition temperature range for both conventionally and microwave cured LY/HY5052/glass composites.*

6.3.3 Summary of DMTA Data

The overall results derived from the DMTA analysis of the LY/HY5052/carbon and LY/HY5052/glass composite samples manufactured using both conventional thermal and microwave RTM processing are summarised in Table 6.2.

Table 6.2: *Average temperature and peak height values of the glass transition and β-transition for the LY/HY5052/carbon and LY/HY5052/glass composites manufactured using both conventional thermal and microwave RTM processing.*

Composite System	Glass Transition		β-Transition	
	Temperature T_g (°C)	Peak Height	Temperature T_β (°C)	Peak Height
CT-LY/HY5052/carbon	128 ± 2°C	0.24 ± 0.002	− 72 ± 3°C	0.01 ± 0.001
MW-LY/HY5052/carbon	130 ± 1°C	0.36 ± 0.010	− 57 ± 3°C	0.01 ± 0.001
CT-LY/HY5052/glass	125 ± 1°C	0.22 ± 0.007	− 68 ± 2°C	0.016 ± 0.002
MW-LY5052/glass	126 ± 1°C	0.24 ± 0.008	− 64 ± 1°C	0.017 ± 0.004

(CT = Conventional Thermal RTM Processing; MW = Microwave RTM Processing)

6.4 Molecular Weight Between Cross-links and Cross-link Density

When fully cured, epoxies form highly cross-linked three-dimensional networks characterised by a closely packed nature, which provides the basis for their superior properties. As a consequence, the mechanical properties of an epoxy system are often linked directly to its cross-link density and so changes in cross-link density inevitably lead to changes in ultimate properties. For that reason, the molecular weight between cross-links (M_c) and cross-link density (v_e) of both thermally and microwave cured composite samples were calculated in order to examine any variations in the network structure induced by the curing method employed. The M_c and v_e of a thermoset can be measured using a number of methods, the most common of them being the measurement of the elastic modulus of the thermoset in its rubbery

regime (i.e. $T >> T_g$) by means of dynamic mechanical thermal analysis (DMTA) [136]. Other methods include swelling and T_g measurements [136].

In this study, the M_c of the produced composites was obtained from DMTA measurements of the elastic modulus in the rubbery plateau region. According to the theory of network elasticity and assuming that at temperatures much higher than the T_g epoxy thermosets exhibit rubbery behaviour, the relationship between molecular weight between cross-links (M_c) and shear modulus (G') for a polymer system is described by the following equation [137]:

$$M_c = \frac{\rho RT}{G'} \qquad \text{(Eqn. 6.1)}$$

where ρ is the density of the resin (g/cm^3), R is the universal gas constant (8.314 J/mol.K) and T and G' are the absolute temperature (K) and shear modulus (Pa), respectively measured in the rubbery plateau region generally taken at T_g + 40°C [128] to ensure that the asymptotic value of the modulus is measured well away from the transition region. At this level the storage modulus changes only slightly with temperature. Given that the relationship between shear modulus and Young's modulus or storage modulus (E') is $G' = E'/3$ [128], Equation 6.1 can be written as follows:

$$M_c = \frac{3\rho RT}{E'} \qquad \text{(Eqn. 6.2)}$$

The above equation can be used to calculate the average molecular weight between cross-links of polymer systems and so it does not take into account the effect of the fibres on the storage modulus. Hence a correction term needs to be introduced before it can be applied for composite systems. Karhbari [138] suggested that the use of a simple rule of mixtures is admissible to take into account the fibre effect with the transverse direction being representative of the resin effect,

$$E_R = \frac{E_m E_f}{V_f E_m + (1 - V_f) E_f} \qquad \text{(Eqn. 6.3)}$$

where E_f, V_f and E_m, V_m are the moduli and volume fractions of the fibre and matrix, respectively.

Combining Equations 6.2 and 6.3 and assuming that $E_f >> E_m$, the relationship between molecular weight between cross-links and rubbery modulus is modified to:

$$M_c \approx \frac{3\rho RT}{(1-V_f)E_R} \qquad \text{(Eqn. 6.4)}$$

The molecular weight between cross-links of the LY/HY5052/carbon and LY/HY052/glass composite samples fabricated using both conventional and microwave RTM processing was calculated according to Equation 6.4 by measuring E' and T in the rubbery plateau region of the corresponding dynamic mechanical spectra. In order to determine the density of the neat resin, resin samples were prepared under both curing methods. The density of the resin was obtained in both cases using a water displacement method (Section 4.6), while the fibre volume fraction of both types of composites was determined using matrix digestion with nitric acid (Section 4.7). It has to be noted, however, that the calculations based on Equation 6.4 use simplifications and assumptions and thus the absolute values of M_c should not be considered as being very accurate, although the orders of magnitude are quite reasonable. Furthermore, Fraga et al. [139] pointed out that the storage modulus in the rubbery state depended inversely on the molecular weight between cross-links and directly on the cross-linking density, which is in agreement with the simplified formula in Equation 6.4.

Alternatively, an empirical equation proposed by Nielsen [137] was also employed for the calculation of the molecular weight between cross-links of the produced composite samples. This equation was obtained by averaging the data in the literature, thus is claimed to have good agreement with the experimental results for materials with high degree of cross-linking such as epoxies. The Nielsen equation is given below:

$$\log_{10} G' = 7 + \frac{293\rho}{M_c} \qquad \text{(Eqn. 6.5)}$$

where G' is the shear modulus (dyn/cm^2), ρ is the density of the resin (g/cm^3) and M_c is the molecular weight between cross-links (g/mol). For calculations based on the empirical equation, it was assumed that $G' = E'/3$.

The overall average results for the molecular weight between cross-links of both conventionally and microwave cured LY/HY5052/carbon and LY/HY5052/glass composite samples are presented in Table 6.3.

Table 6.3: *Overall average results for the molecular weight between cross-links of the LY/HY5052/carbon and LY/HY5052/glass composite panels manufactured using both conventional thermal and microwave RTM processing.*

Composite System	Molecular Weight Between Cross-links, M_c (g/mol)	
	Eqn. 6.4	Eqn. 6.5
CT-LY/HY5052/carbon	1839 ± 27	624 ± 4
MW-LY/HY5052/carbon	3115 ± 12	1226 ± 5
CT-LY/HY5052/glass	3566 ± 15	1648 ± 16
MW-LY/HY5052/glass	3555 ± 26	1646 ± 15

(CT = Conventional Thermal RTM Processing; MW = Microwave RTM Processing)

The absolute values for the M_c of the manufactured composites calculated using Equation 6.4 and Equation 6.5, respectively, are significantly different. In specific, all the M_c values calculated by Equation 6.4 are higher than those calculated by Equation 6.5. The general trends, however, depicted by both sets of values are very much alike. The thermally cured carbon fibre composites exhibited the lower M_c values, with both thermally and microwave cured glass fibre composites exhibiting the highest M_c values. Regarding the LY/HY5052/carbon composite system, there is a significant difference in the M_c between conventionally and microwave cured panels. The microwave cured LY/HY5052/carbon composites exhibited a higher M_c than their thermally cured counterparts, which in turn suggests that a less packed network structure with a larger distance between cross-links was produced during the curing process. This is in agreement with the results from the DMTA, which showed a higher glass transition peak in the tan δ versus temperature curve for the

microwave cured composites compared to those manufactured using conventional thermal RTM processing (Figure 6.8). On the other hand, comparing the M_c values calculated for the LY/HY5052/glass composite system, it appears that the produced network structure was similar regardless of the curing method employed. Both microwave and thermally cured LY/HY5052/glass composites exhibited similar M_c values. The results from the DMTA verify this finding, since the intensity of the glass transition in the tan δ versus temperature curve for both types of composites was found to be similar (Figure 6.12).

The cross-link density (v_e) is defined as the effective number of cross-linked chains per unit volume [137]. The relationship between the cross-link density and storage modulus in the rubbery plateau region is described by the following equation:

$$v_e = \frac{E'}{3RT} \qquad \text{(Eqn. 6.6)}$$

If Equations 6.6 and 6.2 are combined, it becomes apparent that the cross-link density is inversely proportional to the molecular weight between cross-links (M_c), as shown below:

$$v_e = \frac{\rho}{M_c} \qquad \text{(Eqn. 6.7)}$$

As the curing progresses and more three-dimensional cross-links are formed, there is a gradual increase in the cross-link density and a gradual decrease in the molecular weight between cross-links. The overall results for v_e of both conventionally and microwave cured LY/HY5052/carbon and LY/HY5052/glass composite samples are summarised in Table 6.4. The density of the LY/HY5052 resin cured both thermally and by microwave heating was obtained using a water displacement method. The results indicated similar ρ values (in g/cm^3); the average density of the thermally cured resin was 1.17 ± 0.01, while that of the microwave cured resin was 1.18 ± 0.01. The v_e values of the fabricated composites were calculated based on the corresponding M_c values obtained from Equations 6.4 and 6.5, thus both sets of values are included in Table 6.4. In correspondence with the M_c results, the

thermally cured LY/HY5052/carbon composites had a higher cross-link density than their microwave cured counterparts, while a similar extent of molecular packing was observed in the network structure of both thermally and microwave cured LY/HY5052/glass fibre composites, as indicated by the comparable v_e values obtained.

Table 6.4: *Overall average cross-link density results for the LY/HY5052/carbon and LY/HY052/glass composite panels manufactured using both conventional thermal and microwave RTM processing.*

Composite System	Cross-link Density, v_e (mol/cm^3)	
	M_c from Eqn. 6.4	M_c from Eqn. 6.5
CT-LY/HY5052/carbon	$6.36 \times 10^{-4} \pm 9.2 \times 10^{-6}$	$1.87 \times 10^{-3} \pm 1.25 \times 10^{-5}$
MW-LY/HY5052/carbon	$3.79 \times 10^{-4} \pm 1.5 \times 10^{-6}$	$9.62 \times 10^{-4} \pm 4.13 \times 10^{-6}$
CT-LY/HY5052/glass	$3.28 \times 10^{-4} \pm 1.36 \times 10^{-6}$	$7.1 \times 10^{-4} \pm 7 \times 10^{-6}$
MW-LY/HY5052/glass	$3.33 \times 10^{-4} \pm 1.54 \times 10^{-6}$	$7.23 \times 10^{-4} \pm 6.58 \times 10^{-6}$

(CT = Conventional Thermal RTM Processing; MW = Microwave RTM Processing)

6.5 Network Structure

In order to detect differences in the network structure formed during the curing process between conventionally and microwave cured composite samples, Fourier transform infrared spectroscopy (FTIR) was employed. As described in Section 4.13, infrared spectroscopy is a helpful analytical tool which allows the identification of the characteristic functional groups of a chemical substance by exciting these groups through IR radiation and assigning them based on the excitation frequencies recorded. The frequencies at which functional groups absorb IR radiation are characteristic for each group, thus valuable information regarding the structure of an organic molecule can be obtained by examining its IR absorption spectrum.

Prior to investigating whether any differences existed in the curing path followed between thermal and microwave RTM processing, it is essential to remember the

reaction mechanism for the polymerisation of an epoxy/amine system. As mentioned in Chapter 2, the polymerisation mechanism of an epoxy/amine system is believed to take place by means of three fundamental reactions: a) the primary amine-epoxy ring opening reaction which results in the formation of a secondary amine and a hydroxyl group; b) the secondary amine-epoxy reaction which results in the formation of a tertiary amine and a second hydroxyl group; c) an etherification reaction, in which one of the pendant hydroxyl groups reacts with the epoxide functionalities in the epoxy resin [83]. The extent to which each of these competing reactions takes place determines the final network structure of the cured epoxy system. These reactions, however, can be incomplete due to diffusion or steric restrictions as well as due to the presence of side reactions like the homopolymerisation of the epoxide group [140]. For comparative reasons, the intensity of each peak in the IR spectra of all the fabricated composite samples was normalised against the intensity of the aliphatic hydrocarbon group band at approximately 2920 cm^{-1}. This peak was selected as an internal standard because it is known that the aliphatic hydrocarbon groups do not participate in any of the chemical reactions that take place during curing of the epoxy resin. Thus, their concentration in the curing mixture should remain constant as the cure progresses.

Figure 6.14 shows the IR spectrum of the uncured LY/HY5052 resin system. The chemical structures of the LY5052 resin and the HY5052 hardener, which would help to understand the assignment of the most prominent IR absorption peaks, are given in Chapter 3. The peaks at 2918 cm^{-1} and 2870 cm^{-1} are assigned to aliphatic hydrocarbon groups. The absorption at 1610 cm^{-1} is assigned to the NH_2 deformation in primary amines, while the peaks at 1585 cm^{-1} and 1508 cm^{-1} are indicative of the benzene ring in aromatic compounds. Furthermore, the absorption at 1452 cm^{-1} is attributed to CH_2 groups in aliphatic compounds and the bands at 1240 cm^{-1} and 912 cm^{-1} are both associated with the epoxide ring. Finally, the presence of the ether group is confirmed by the two absorption peaks at 1107 cm^{-1} and 1034 cm^{-1}, while the bands at 837 cm^{-1} and 754 cm^{-1} are assigned to substituted benzene rings.

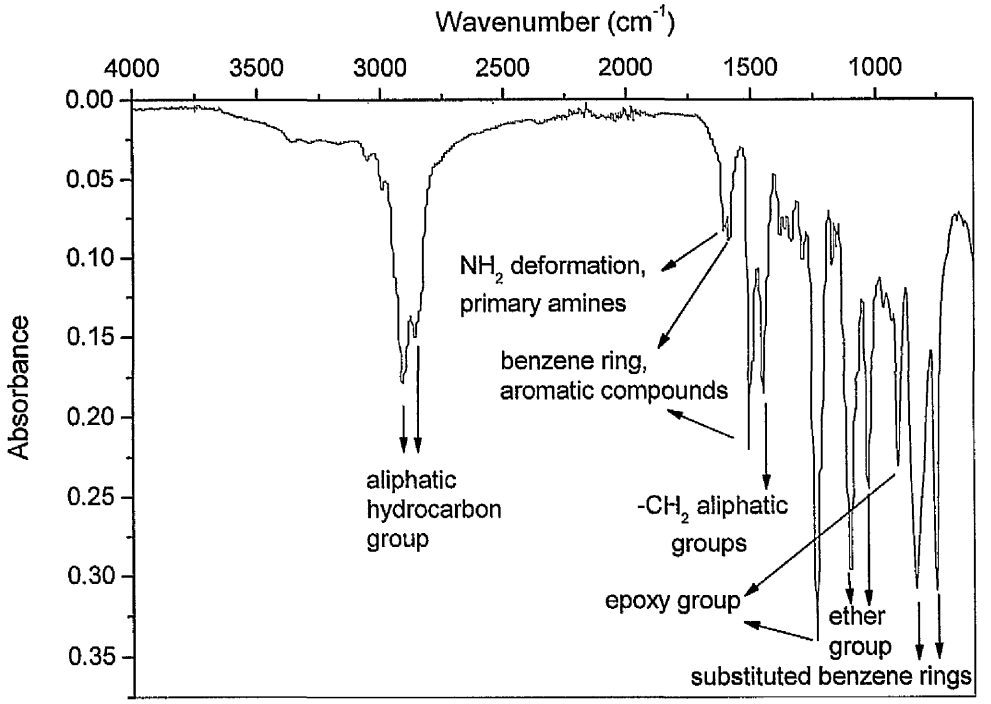

Figure 6.14: *Infrared spectrum of the uncured LY/HY5052 resin system.*

6.5.1 LY/HY5052/carbon Composite System

The aim of the FTIR study in this work was to compare the final network structure of the cured composites rather than investigate the evolution of the chemical species during curing. For that reason, the normalised IR spectrum of the uncured LY/HY5052 resin was superimposed on the normalised spectra of the thermally and microwave cured LY/HY5052/carbon composites, respectively, as shown in Figures 6.15 and 6.16. During the curing process, the amine groups of the HY5052 hardener react with the epoxide groups of the LY5052 novalak resin, resulting in a decrease in the epoxide concentration of the curing mixture and hence the intensity of the peak corresponding to the epoxide ring. At the same time, the opening of the epoxide ring produces hydroxyl groups, leading to an increase in the intensity of the hydroxyl peak since the hydroxyl concentration of the curing mixture increases as the curing process progresses.

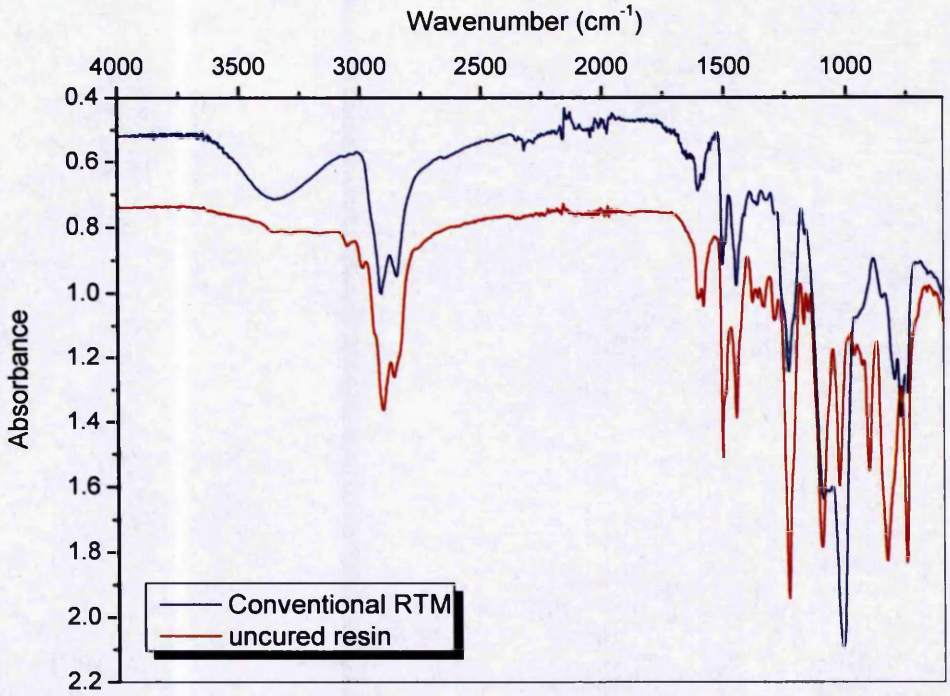

Figure 6.15: *Normalised IR spectra of the conventionally cured LY/HY5052/carbon composites and the uncured LY/HY5052 resin system. The spectrum corresponding to the uncured resin is shifted for clarity.*

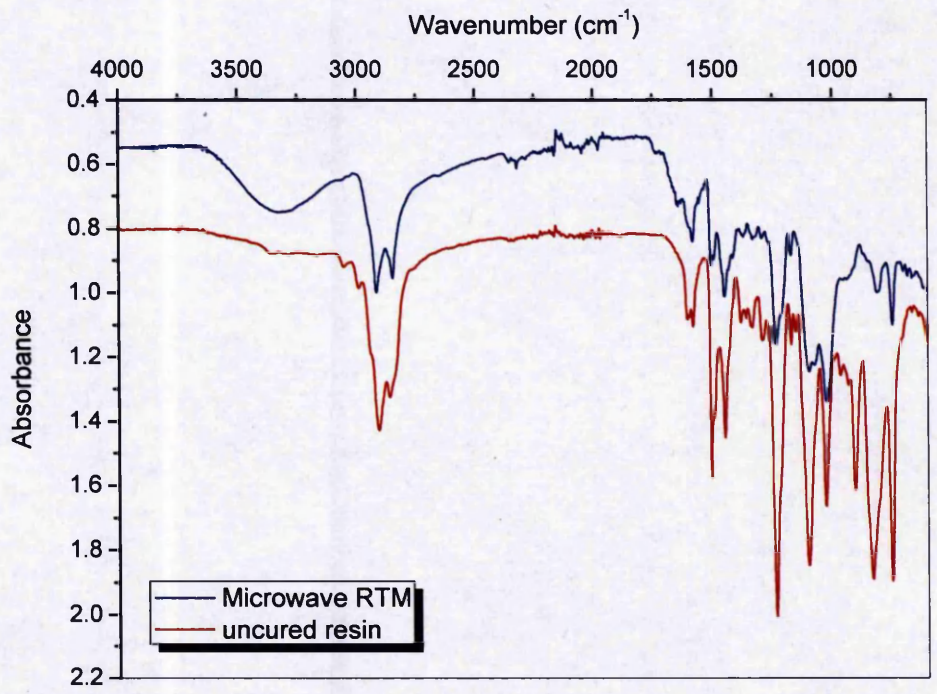

Figure 6.16: *Normalised IR spectra of the microwave cured LY/HY5052/carbon composites and the uncured LY/HY5052 resin system. The spectrum corresponding to the uncured resin is shifted for clarity.*

An initial examination of the obtained spectra revealed a broad peak at 3350 cm^{-1} corresponding to the hydroxyl functional group. Since hydroxyl groups are products of polymerisation their appearance is expected in the spectra of the cured composites. Despite the fact that amine peaks are typically observed in the 3520 – 3320 cm^{-1} region, no well defined amine peaks were observed in the IR spectra of both composite types. This is due to them being obscured by the broad hydroxyl band at 3350 cm^{-1}. Amine bands also appear at lower frequencies in the spectrum at approximately 1600 cm^{-1}. The assignment of these amine bands, however, was not achievable, owing to the complex chemical structure of the HY5052 hardener which contained a mixture of amine compounds. The absorption at 912 cm^{-1}, assigned to the epoxide ring, decreased in the spectra of the cured composites and appeared as a small shoulder in the absorption of the ether group at 1026 cm^{-1}, due to the consumption of the epoxide molecules during polymerisation. The peak at 1244 cm^{-1} was still visible but significantly decreased as well compared to that of the uncured resin.

Figure 6.17 shows the normalised infrared spectra of the LY/HY5052/carbon composites cured by both conventional thermal and microwave RTM processing. The scale in the spectrum corresponding to the microwave cured composites is shifted for clarity. Comparing directly the spectra of the cured composites, the main appearance was found to be similar. Differences, however, in the intensity of some peaks were observed. In specific, the relative peaks heights at 1103 cm^{-1} and 1024 cm^{-1}, assigned to the ether group, were considerably increased in the thermally cured composites compared to those cured using microwave heating. This would suggest that the epoxide-hydroxyl etherification reaction occurred more readily during thermal curing than microwave curing of the LY/HY5052/carbon composites, thus leading to a higher concentration of ether groups in the final network structure. Furthermore, the peaks in the 820 – 750 cm^{-1} wavenumber region, assigned to substituted benzene rings, were higher and slightly shifted in the conventional cured composites compared to those cured using microwave radiation, providing further evidence of differences in the network structure obtained between the two types of composites.

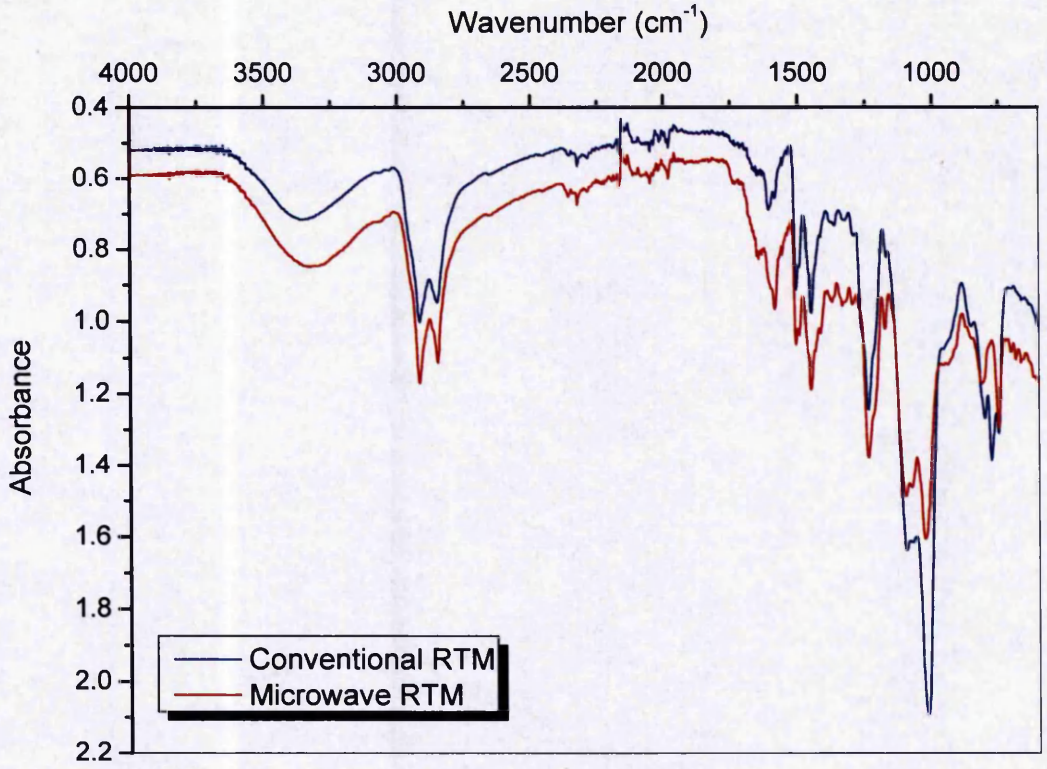

Figure 6.17: *Normalised infrared spectra of both conventionally and microwave cured LY/HY5052/carbon composites. The spectrum corresponding to the microwave cured composites is shifted for clarity.*

It has been reported in the literature that the etherification reaction becomes much more significant when the epoxy resin is in excess (2:1) than when stoichiometric quantities of epoxide/amine are used (1:1) [141]. The occurrence of etherification in a curing system may vary the structure and associated macroscopic properties of the cured product, as a result of an increase in the number of possible branches created [141, 142]. Given, therefore, that the LY5052 epoxy resin to HY5052 hardener ratio used in this study was 100:38 by weight (Chapter 3), it can be assumed that the etherification reaction was responsible to some extent for the network structure of the cured composites. In thermal curing, ether linkages are believed to form during the later stages of the cure reactions after the primary amine has reacted with the epoxide molecules. Microwave curing, on the other hand, appears to have favoured the epoxide-amine reaction over the epoxide-hydroxyl etherification reaction at some stage of the curing process, resulting to a lower concentration of ether groups in the final network structure. Similar phenomena have been observed by other researchers [143, 144]. The FTIR findings were in agreement with the results obtained from the

DMTA analysis of the LY/HY5052/carbon composites, in which a 15°C difference in the β-transition peak temperature between the thermally and microwave cured composites was observed. The relative intensities of the absorption peaks in the IR spectra of both thermally and microwave cured LY/HY5052/carbon composites are presented below in Table 6.5.

Table 6.5: *Relative intensities of the infrared absorption peaks in both thermally and microwave cured LY/HY5052/carbon composites.*

Peak (cm^{-1})	Assignment	Relative Height	
		Conventional Thermal RTM	Microwave RTM
3350	Hydroxyl group	0.71	0.75
2922	Aliphatic hydrocarbon group	1	1
1244	Epoxide group	1.22	1.20
1103	Ether group	1.63	1.23
1024	Ether group	2.08	1.33

6.5.2 LY/HY5052/glass Composite System

Figures 6.18 and 6.19 show the normalised IR spectrum of the uncured LY/HY5052 resin superimposed on the normalised spectra of the conventionally and microwave cured LY/HY5052/glass composites, respectively. Similar with the carbon fibre composites, a large broad band at 3350 cm^{-1}, assigned to the hydroxyl group, appeared in the spectra of the glass fibre composites as a result of polymerisation. The epoxide ring absorption at 912 cm^{-1} decreased and was slightly shifted, appearing as a shoulder in the adjacent absorption of the ether group at 1026 cm^{-1}. The intensity of the band at 1244 cm^{-1}, also assigned to the epoxide ring, was reduced as well due to the epoxide molecules being consumed during the curing process.

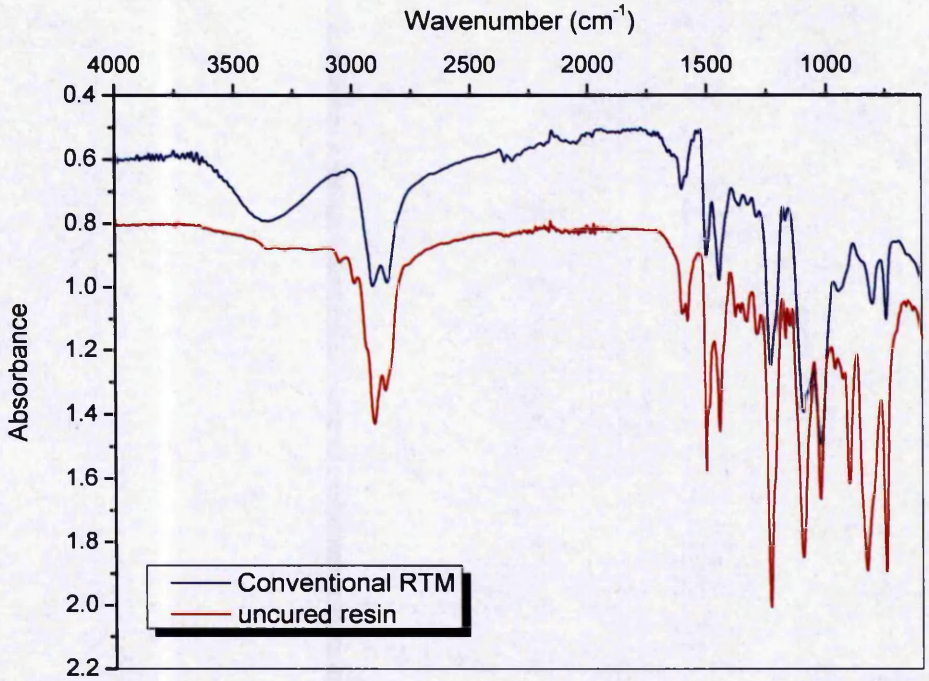

Figure 6.18: *Normalised IR spectra of the conventionally cured LY/HY5052/glass composites and the uncured LY/HY5052 resin system. The spectrum corresponding to the uncured resin is shifted for clarity.*

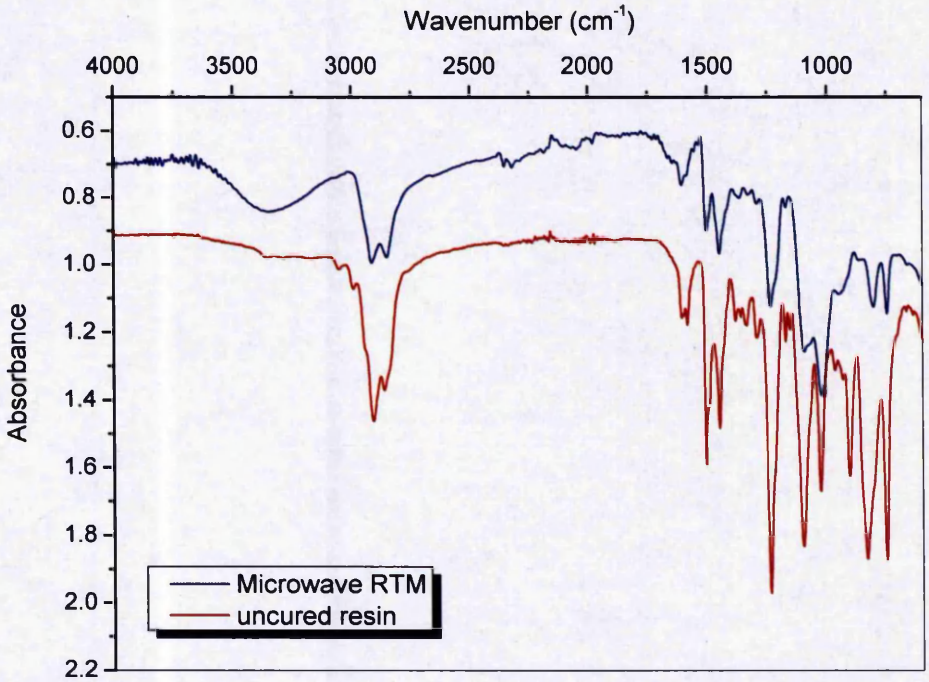

Figure 6.19: *Normalised IR spectra of the microwave cured LY/HY5052/glass composites and the uncured LY/HY5052 resin system. The spectrum corresponding to the uncured resin is shifted for clarity.*

In Figure 6.20 the normalised infrared spectra of the LY/HY5052/glass composites cured by both conventional thermal and microwave RTM processing are presented. The main appearance of the obtained spectra was found to be similar. In contrast with the carbon fibre composites, the difference in the intensity of the ether group absorption peaks at 1103 cm^{-1} and 1024 cm^{-1} between the thermally and microwave cured LY/HY5052/glass fibre composites was less prominent. The relative heights of these peaks were still increased in the conventionally cured composites compared to those cured using microwaves but to a smaller extent than their carbon fibre counterparts (Table 6.6). This is probably due to the presence of the glass fibres, considering that the same epoxy system was used in the fabrication of both composite types. Owing to their substantially lower dielectric loss, glass fibres absorbed less amount of microwave energy than carbon fibres during the curing process. As a result, more amount of microwave energy was available for the reactions taking place within the epoxy resin, which in turn may have improved the rate of the epoxy-hydroxyl etherification reaction. This was also consistent with the results obtained from the DMTA analysis which showed that the difference in the β-transition peak temperature between the thermally and microwave cured LY/HY5052/glass composites was only 4°C, as opposed to 15°C for the corresponding carbon fibre composites. Furthermore, the peaks at 816 cm^{-1} and 752 cm^{-1}, assigned to substituted benzene rings, appeared to have similar intensities in the spectra of the thermally and microwave cured LY/HY5052/glass composites, providing additional evidence of fewer differences in the network structure between the two types of glass fibre composites compared to those found between their carbon fibre counterparts. The relative intensities of the absorption peaks in the IR spectra of both thermally and microwave cured LY/HY5052/glass composites are summarised in Table 6.6.

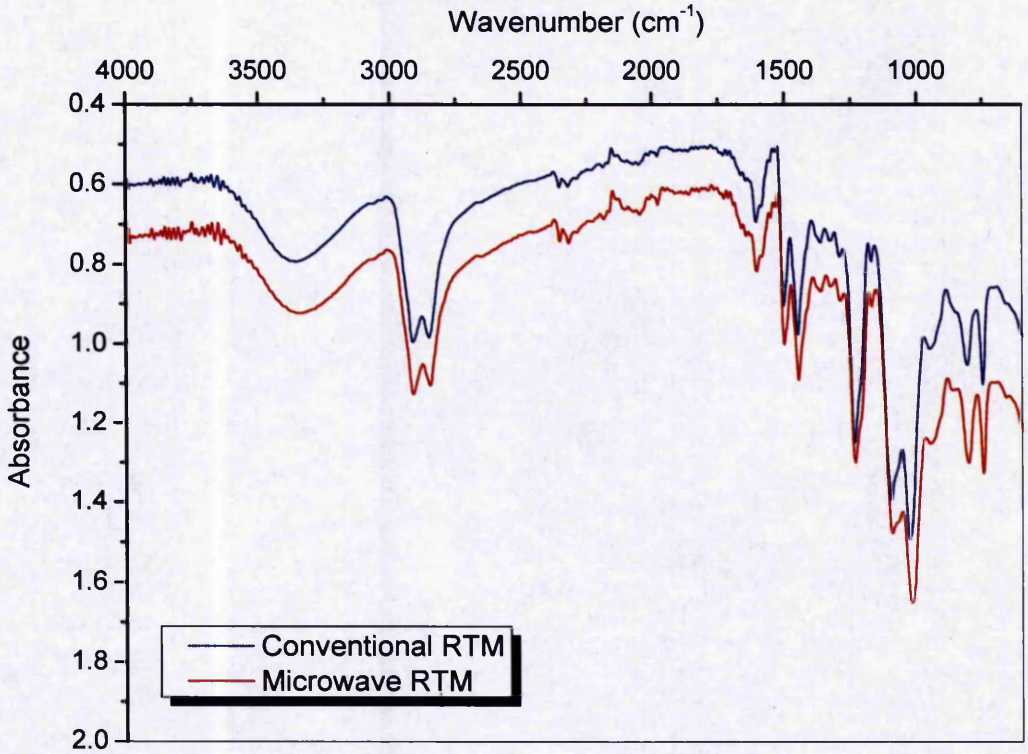

Figure 6.20: *Normalised infrared spectra of both conventionally and microwave cured LY/HY5052/glass composites. The spectrum corresponding to the microwave cured composites is shifted for clarity.*

Table 6.6: *Relative intensities of the infrared absorption peaks in both thermally and microwave cured LY/HY5052/glass composites.*

Peak (cm^{-1})	Assignment	Relative Height	
		Conventional Thermal RTM	Microwave RTM
3350	Hydroxyl group	0.81	0.83
2922	Aliphatic hydrocarbon group	1	1
1244	Epoxide group	1.25	1.22
1103	Ether group	1.39	1.25
1024	Ether group	1.50	1.38

6.6 Summary

The effectiveness of microwave RTM processing was assessed by determining the degree of cure across the manufactured composite panels using temperature modulated differential scanning calorimetry (TMDSC). The results indicated that both LY/HY5052/carbon and LY/HY5052/glass composites were fully cured, achieving a degree of cure of 99% and higher. The high average degree of cure values also verified that a uniform electric field distribution was achieved during the curing process. Furthermore, the dynamic mechanical properties of the produced composites were investigated. The carbon fibre composites exhibited similar T_g values. The glass transition, however, was more intense for the microwave cured samples compared to those cured conventionally. The intensity of the low temperature β-transition was found to be similar with a 15°C difference in the position of the β-transition peak detected between the two types of composites. On the other hand, the thermally and microwave cured LY/HY5052/glass composites exhibited similar T_g values, while the intensities of both glass transition and β-transition were also similar. The results, however, indicated a 4°C shift in the position of the β-transition peak to a higher temperature for the microwave cured composites compared to those cured thermally.

The molecular weight between cross-links (M_c) and cross-link density (v_e) of the fabricated composites were calculated in order to examine any variations in the network structure induced by the curing method employed. The microwave cured LY/HY5052/carbon composites exhibited higher M_c and lower v_e values than their thermally cured counterparts, which in turn suggests that a less packed network structure with a larger distance between cross-links was produced during microwave RTM processing. Conversely, similar extents of molecular packing were observed in the network structure of both thermally and microwave cured LY/HY5052/glass composites, as indicated by the comparable M_c and v_e values obtained. These findings were in agreement with the results from the DMTA analysis. In addition, Fourier transform infrared spectroscopy was also employed in order to investigate whether any differences existed in the curing path followed between thermal and microwave RTM processing by comparing the infrared spectra of the produced

composites. The results showed that the intensities of the absorption peaks at 1103 cm^{-1} and 1024 cm^{-1}, assigned to the ether group, were significantly increased in the thermally cured LY/HY5052/carbon composites compared to those cured using microwave heating, suggesting that the epoxide-hydroxyl etherification reaction occurred more readily during thermal curing than microwave curing. The difference, however, in the intensity of the ether group absorption peaks was found to be less prominent between the thermally and microwave cured LY/HY5052/glass fibre composites, which was also supported by the DMTA results.

CHAPTER 7

Mechanical and Physical Properties of Composite Systems

7.1 Introduction

This chapter focuses on the mechanical and physical properties of both thermally and microwave cured LY/HY5052/carbon and LY/HY5052/glass composites, as they are important for the evaluation of their performance. These properties are influenced by the fibre and void volume fractions of the produced composites hence they were obtained using matrix digestion with nitric acid and matrix digestion and optical microscopy, respectively. The mechanical performance in terms of flexural strength, flexural modulus and interlaminar shear strength of all the fabricated composite panels was assessed by means of four-point bending and short-beam testing. The fracture surfaces of the composite samples subjected to mechanical testing were also examined using scanning electron microscopy. Finally, other properties such as the dielectric properties of both the uncured LY/HY5052 epoxy resin and the cured composites are also discussed in this chapter.

7.2 Fibre and Void Volume Fraction

In order to perform an accurate comparison of the mechanical properties between thermally and microwave cured composite panels it is essential to determine first their fibre and void volume fractions, since the contribution of both fibre reinforcement and void content to the overall mechanical behaviour of a composite system are most significant. Whilst the former, subject to modulus, enhances the mechanical strength, the latter has a detrimental effect on the compressive, interlaminar shear and flexural properties of composite laminates, as established by several researchers [145-150]. For that reason, the fibre volume fractions of the composites manufactured by both curing methods were obtained using matrix digestion with nitric acid in a microwave oven according to the ASTM D 3171 standard [119], while their void contents were determined by means of both optical microscopy and matrix digestion. The relevant procedures are described in detail in Chapter 4, Sections 4.7 and 4.9, respectively.

As mentioned in Chapter 5, the microwave cured composite panels were slightly thicker than those cured thermally. The difference is attributed to the cavity of the Macor mould being deeper than that of the metal mould employed in conventional RTM processing. This had a direct effect on the fibre volume fraction of the produced composites, since the same amount of fibres was used to fabricate composites with both curing methods. In specific, the fibre volume fraction of the thermally cured composites was 6% higher compared to those cured using microwave heating. The overall average values of the fibre volume fraction for the microwave and thermally cured LY/HY5052/carbon and LY/HY5052/glass composites are summarised in Table 7.1.

The void content of the produced composites was determined by examining several optical micrographs of samples taken from different locations in the composite panels and dividing the void area by the overall area in each micrograph using image processing software. The results from optical microscopy were compared against those obtained from matrix digestion. The reported values were found to be in good agreement. Figures 7.1 and 7.2 show the general layout of the matrix area and fibre reinforcement for the thermally and microwave cured LY/HY5052/carbon and LY/HY5052/glass composite systems, respectively. A resin rich area can be clearly observed between the fibre tows in both composite systems. Figures 7.3 and 7.4 show optical micrographs of higher magnification used for void content determination. Example of micrographs showing voids are presented in Figure 7.3 (a) and 7.4(b). The overall average values of the void volume fraction for the manufactured composites are included in Table 7.1. The results indicated that all composites yielded minimal void contents (< 2%) with the conventionally cured LY/HY5052/carbon composites exhibiting the highest value.

Table 7.1: *Overall average values for the fibre and void volume fraction of the LY/HY5052/carbon and LY/HY5052/glass composites manufactured using both conventional and microwave RTM processing.*

Composite System	Average Fibre Volume Fraction (%)	Average Void Volume Fraction (%) (Matrix Digestion)	Average Void Volume Fraction (%) (Optical Microscopy)
CT-LY/HY5052/carbon	33	1.6	1.6
MW-LY/HY5052/carbon	27	0.6	0.5
CT-LY/HY5052/glass	26	0.7	0.8
MW-LY/HY5052/glass	20	0.5	0.6

(CT = Conventional Thermal RTM Processing; MW = Microwave RTM Processing)

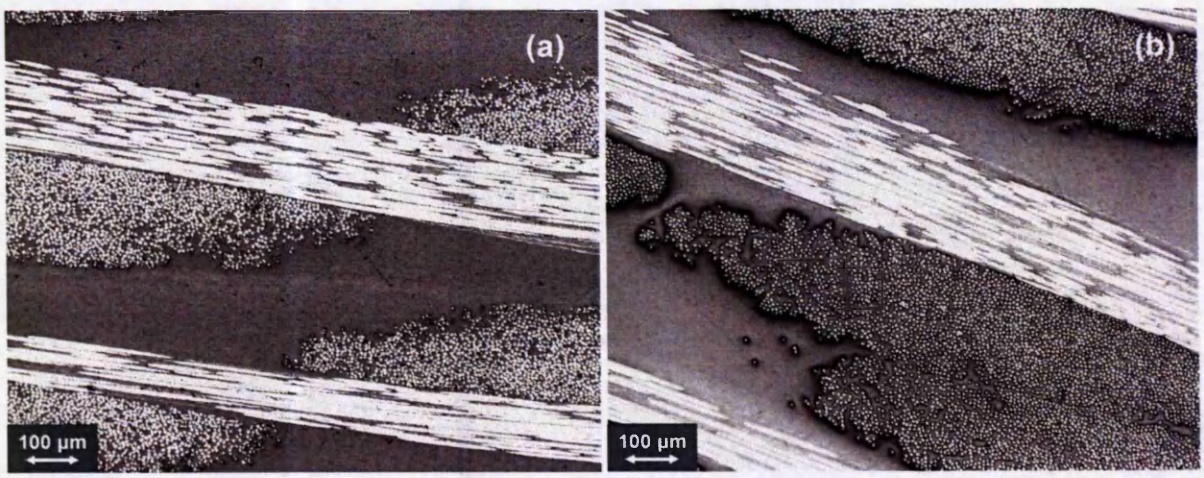

Figure 7.1: *Optical micrographs of the cross-section of the LY/HY5052/carbon composite system at x10 magnification; (a) conventionally cured specimen (b) microwave cured specimen.*

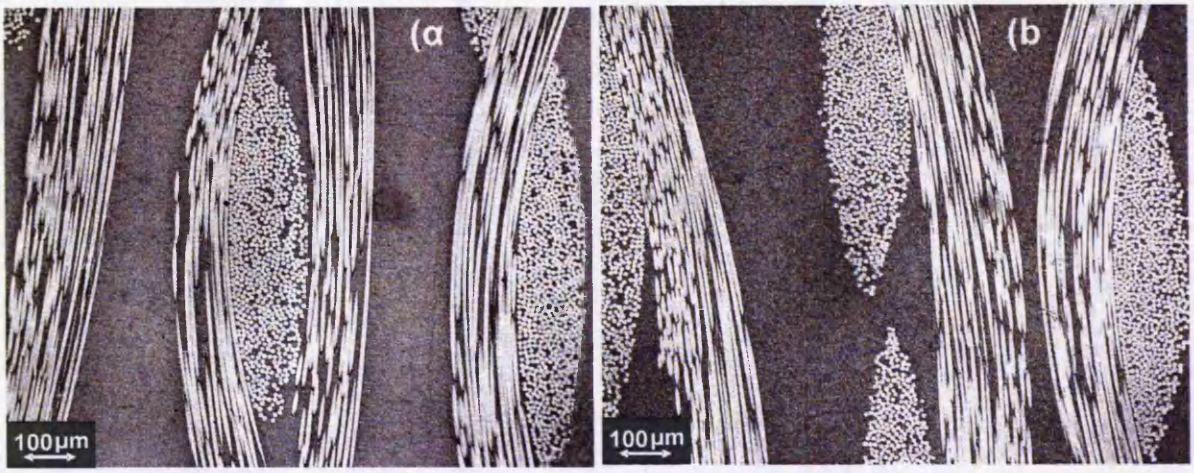

Figure 7.2: *Optical micrographs of the cross-section of the LY/HY5052/glass composite system at x10 magnification; (a) conventionally cured specimen (b) microwave cured specimen.*

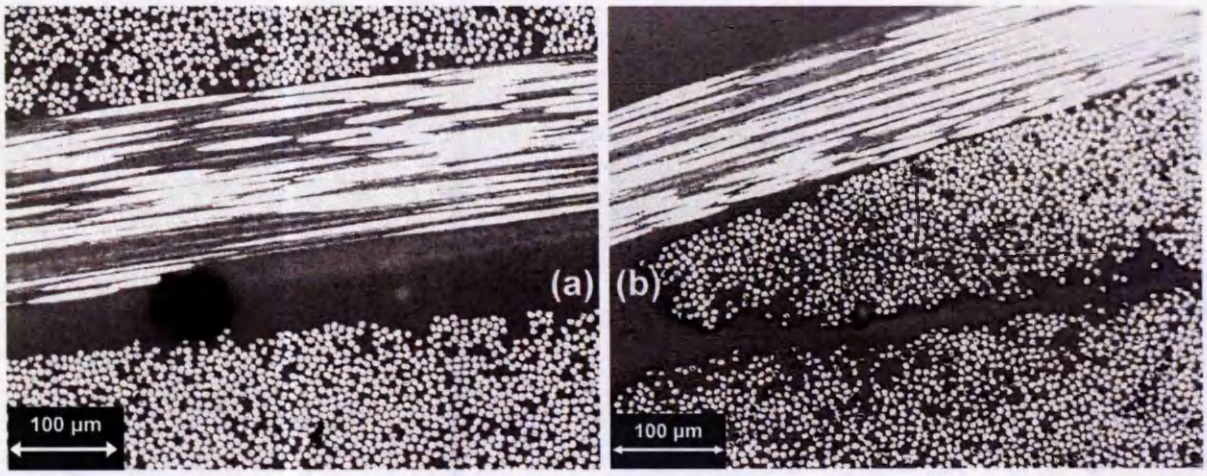

Figure 7.3: *Optical micrographs of the cross-section of the LY/HY5052/carbon composite system at x20 magnification; (a) conventionally cured specimen (b) microwave cured specimen.*

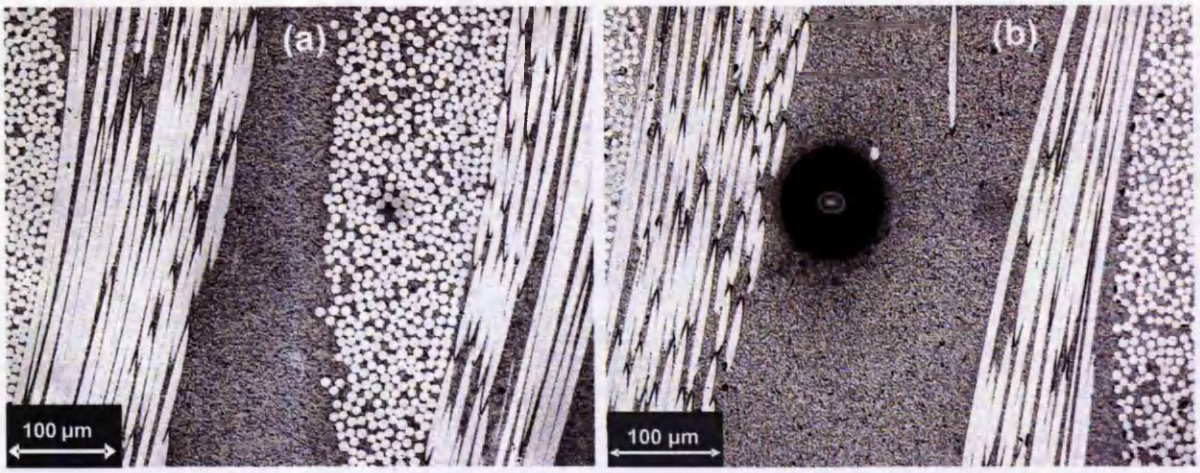

Figure 7.4: *Optical micrographs of the cross-section of the LY/HY5052/glass composite system at x20 magnification; (a) conventionally cured specimen (b) microwave cured specimen.*

7.3 Defects

Defects in a composite panel are mainly manifested as voids, delaminations, internal microcracks, fibre misalignments or areas of poor bonding due to lack of fibre wetting during resin injection. In this study, defects were examined using a jet probe inspection ultrasonic C-scan in through transmission mode. A jet probe inspection system uses a transducer to transmit sound waves along a column of water and into the component. Regardless of the complexity of a jet probe system, the theory of operation remains the same [151]. Two jets positioned on either side of the component must be maintained at a constant separation without any variation in the alignment of the jets. This allows a constant sound level, which is set as a maximum signal level, to get across from one transducer to the other. Any reductions in this signal level can only be caused by sound losses in the component, which in turn are due to the presence of defects. Further details of the technique are given in Chapter 4, Section 4.8. Ultrasonic C-scan is a non-destructive characterisation technique employed primarily for qualitative analysis of composite materials [152] and as such

it was used to assess the extent of defects in each composite panel, thus allowing a comparison of the overall quality between the cured laminates to be made.

7.3.1 LY/HY5052/carbon Composite System

The ultrasonic C-scan images obtained for both thermally and microwave cured LY/HY5052/carbon composite panels are illustrated below in Figures 7.5 and 7.6, respectively. The images were constructed by assigning a colour for each dB value, starting from white and progressing through successively darker tones of grey to black. The range of the signal attenuation was approximately 20 dB for both types of composites, from 5 to 25 dB and 7 to 27 dB for the thermally and microwave cured composites, respectively, as shown in the colour palette next to each image.

In general, no significant differences were observed between the thermally and microwave cured LY/HY505/carbon composite panels. Both types of composites exhibited minimal defects with small variations in the ultrasonic signal attenuation; hence the constructed two-dimensional images appear almost entirely light grey. This is also direct evidence that a uniform electric field distribution was established inside the applicator during microwave curing of the LY/HY5052/carbon composites which prevented localised hot spots from causing large temperature gradients and thus localised resin degradation or discrepancies in the degree of cure across the produced panels. Furthermore, the small variations in the signal attenuation verify that the thickness distribution of the manufactured laminates was uniform in both cases. As expected, based on the results from matrix digestion and optical microscopy, no distinctive dark areas indicating large voids or other defects were visible. The difference, however, in the void content between the thermally and microwave cured LY/HY5052/carbon composites was not apparent through ultrasonic C-scan inspection, as it was very small to be identified.

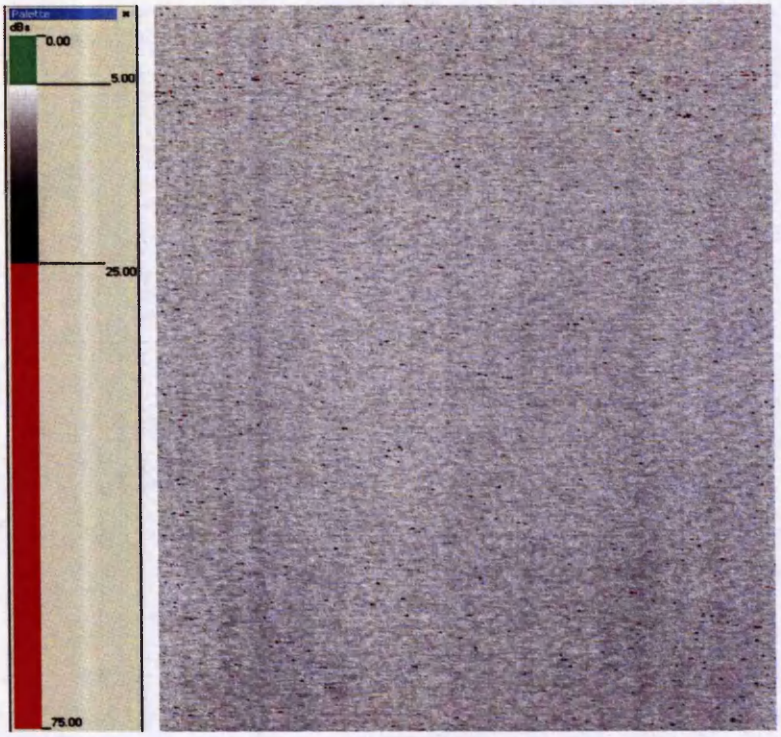

Figure 7.5: *Ultrasonic attenuation scan trace of a representative LY/HY5052/carbon composite panel manufactured using conventional thermal RTM processing.*

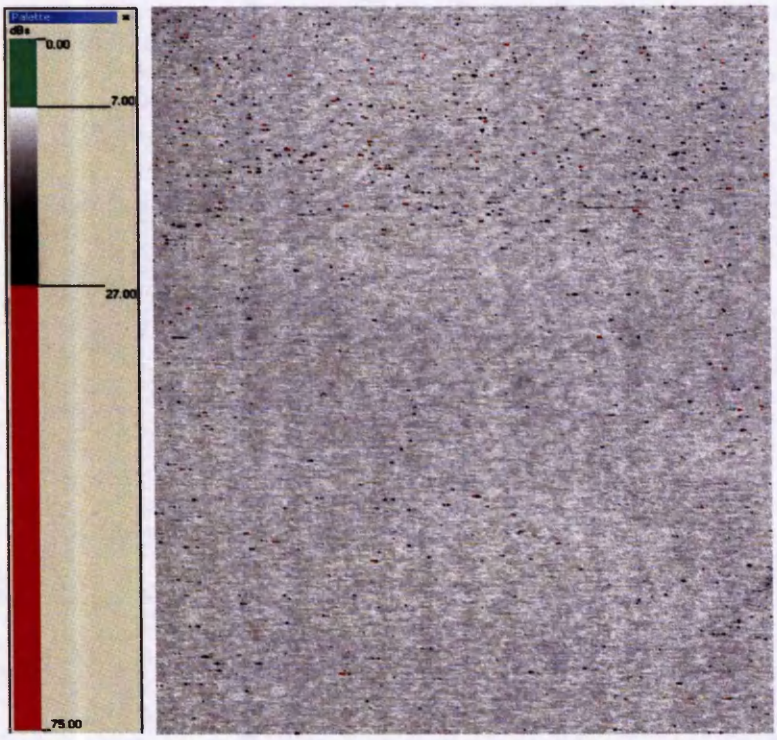

Figure 7.6: *Ultrasonic attenuation scan trace of a representative LY/HY5052/carbon composite panel manufactured using microwave RTM processing.*

7.3.2 LY/HY5052/glass Composite System

Similarly, Figures 7.7 and 7.8 show the ultrasonic C-scan images obtained for the thermally and microwave cured LY/HY5052/glass composites, respectively. The signal attenuation varied from 7 to 22 dB for the conventionally cured composites and from 10 to 25 dB for those cured using microwave heating. Both composite types yielded minimal defects with no significant differences identified between them. No dark areas indicating major defects or voids were observed, as anticipated by the low void content values measured previously. The multiple lines observed in the C-scan images were attributed to the milling marks obtained in the fabrication of the moulds. It appears that, especially in the case of the glass fibre composites, the C-scan was quite sensitive in detecting these milling lines located on the bottom surface of the produced panels. The small variations in the attenuation of the ultrasonic signal for the microwave cured LY/HY5052/glass composite panels once more indicate that the distribution of the electric field was sufficiently uniform during the curing process.

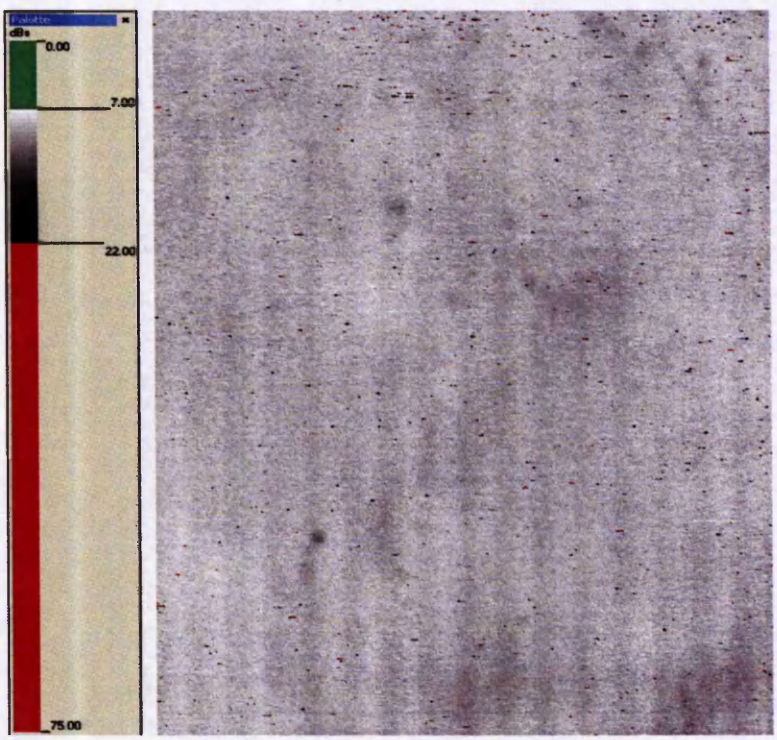

Figure 7.7: *Ultrasonic attenuation scan trace of a representative LY/HY5052/glass composite panel manufactured using conventional thermal RTM processing.*

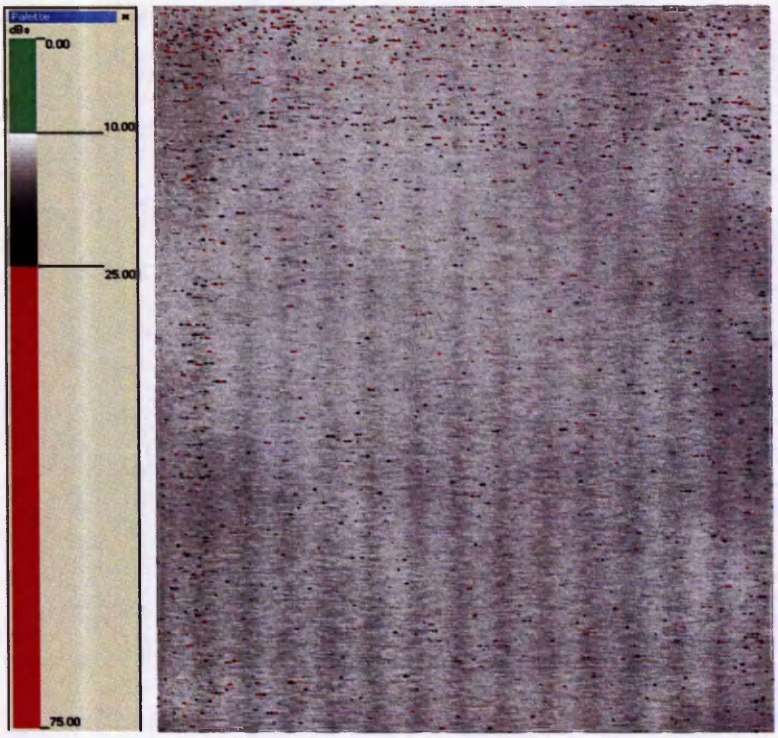

Figure 7.8: *Ultrasonic attenuation scan trace of a representative LY/HY5052/glass composite panel manufactured using microwave RTM processing.*

7.4 Mechanical Properties

The mechanical properties in terms of flexural modulus, flexural strength and interlaminar shear strength of the LY/HY5052/carbon and LY/HY5052/glass composites manufactured by both conventional thermal and microwave RTM processing were measured and compared against each other in order to detect differences in the mechanical performance due to the curing method employed. A minimum of ten samples were tested for each composite panel with the specimens being selected from different locations in the panels to ensure good representativity of the results. The failure surfaces of the composite samples subjected to mechanical testing were also investigated using scanning electron microscopy (SEM).

7.4.1 Flexural Properties

The flexural modulus and flexural strength of the produced composites were determined by means of four-point bending. In the four-point bending test, the sample rests on two cylindrical rollers while being loaded at two points, each an equal distance from the adjacent support point. The tests were carried out according to the ASTM D 6272 standard [113]. A detailed description of the method and the specifications used are given in Chapter 4, Section 4.3.1.

7.4.1.1 LY/HY5052/carbon Composite System

Figures 7.9 and 7.10 show typical stress-strain plots for the thermally and microwave cured LY/HY5052/carbon composites, respectively. The mechanical behaviour of the composites produced by both processing methods appeared to be similar. Failure occurred at a strain of 1.2 – 1.5 % for the thermally cured composites and 1.3 – 1.6 % for those cured using microwave heating. The stress-strain relationship was found to be almost linear until the point of failure for both types of composites. Table 7.2 shows the average values of the flexural modulus and flexural strength for the LY/HY5052/carbon composites manufactured by both conventional thermal and microwave RTM processing. The thermally cured composites yielded a flexural modulus of 44 ± 1 GPa and a flexural strength of 554 ± 44 MPa, as opposed to 37 ± 2 GPa and 493 ± 27 MPa, respectively, for those cured using microwave radiation. Since, however, the flexural properties of a composite system are largely dominated by the fibre reinforcement, the obtained values were normalised to an equivalent carbon fibre volume fraction (33% V_f). The normalisation was carried out assuming a linear relationship between fibre volume fraction and flexural strength and modulus. The results showed that both the flexural modulus and flexural strength of the microwave cured composites were similar to those of their conventionally cured counterparts.

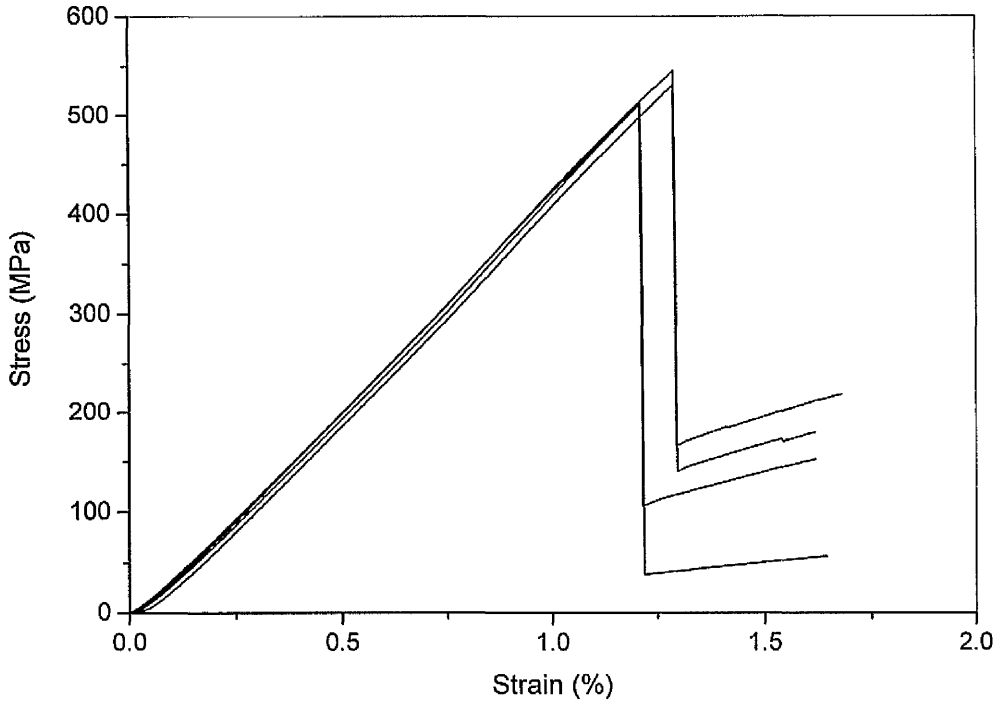

Figure 7.9: *Typical flexural stress-strain plots for the LY/HY5052/carbon composites manufactured using conventional thermal RTM processing.*

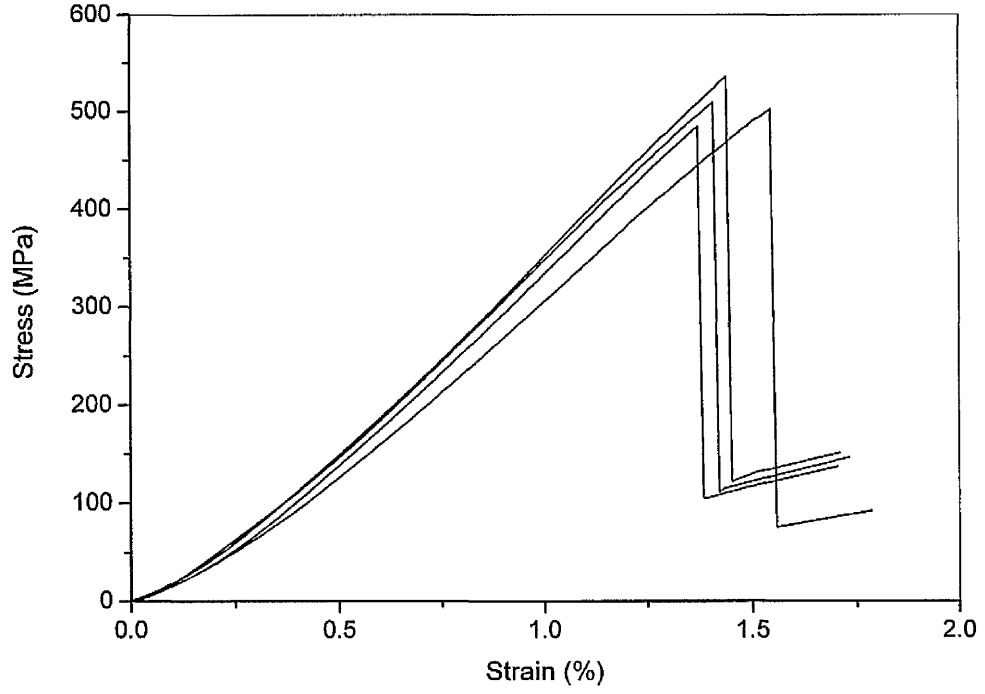

Figure 7.10: *Typical flexural stress-strain plots for the LY/HY5052/carbon composites manufactured using microwave RTM processing.*

Table 7.2: *Average values of flexural modulus and flexural strength for the LY/HY5052/carbon composites produced by conventional thermal and microwave RTM processing.*

Processing Method	Flexural Properties		Average Panel Thickness (mm)
	Flexural Modulus (GPa)	Flexural Strength (MPa)	
Conventional Thermal RTM	44 ± 1	554 ± 44	3.38 ± 0.08
Microwave RTM	37 ± 2	493 ± 27	3.74 ± 0.10
Microwave RTM (Normalised to 33% V_f)	45.2	602	-

The above findings are in agreement with the work of Fang and Scola [96] who investigated the application of microwave energy to the processing of carbon fibre reinforced phenylethynyl-terminated polyimide composites (PETI-5/IM7) using a variable-frequency microwave furnace. They reported that the flexural strength of both microwave and thermally cured composites were similar at room temperature, although the microwave cured composites exhibited slightly higher values of flexural modulus than the thermally cured composites. They also found that the interlaminar shear strength of the composites fabricated using microwave radiation was higher than that of their thermally cured counterparts, suggesting that better wetting of the fibres by the resin occurred during microwave curing.

Similar results were also reported by Tanrattanakul and Jaroendee [153] who compared the mechanical properties of epoxy-anhydride glass fibre reinforced composites cured by thermal and microwave heating. They found that incorporating a 2- and 3-step heating cycle in the microwave curing process resulted in composites with better mechanical properties compared to those obtained for the thermally and 1-step microwave cured composites. This was attributed to the slow increase in temperature during the beginning of the microwave curing process, since a very low power level was applied in the first cycle of the multi-step heating process. This affected the slow rate of viscosity increment, resulting in better wetting of the glass fibres with enhanced interfacial adhesion achieved between the fibres and the resin.

The fracture surfaces of both thermally and microwave cured LY/HY5052/carbon composite samples subjected to four-point bending were examined using scanning electron microscopy (SEM). Representative features of the fracture surface morphology for the conventionally cured carbon fibre composites are shown in Figures 7.11 - 7.13. The principle failure modes identified were tensile and shear. In specific, Figure 7.11 shows an example of fibre breakage transverse to the applied load in a thermally cured carbon fibre composite sample, as a result of crack propagation through the fibre-matrix interface. The light colour regions on the right hand side in Figure 7.12 indicate brittle fracture of the matrix, while typical shear bands or hackle markings associated with fibre pull-out are evident on the left hand side. Figure 7.13 shows holes found in the composite indicating the presence of voids probably due to limited wetting of the carbon fibres during thermal curing.

Figures 7.14 – 7.16 show SEM micrographs of the fracture surfaces of microwave cured LY/HY5052/carbon composite samples subjected to four-point bending. Similar with the conventionally cured composites, the main failure modes observed in the microwave cured carbon fibre composites were tensile and shear. Figure 7.14 shows a group of broken fibres embedded in the resin. No empty spaces are observed around the fibre-matrix interface, while the exposed fibres are covered with resin debris. These features indicate that good adhesion between the fibres and the resin was achieved during microwave processing. Furthermore, Figure 7.15 shows a combination of shear failure resulting in fibre pull-out (right hand side) and fibre breakage as a result of tensile failure (left hand side). A characteristic region showing the direction of crack propagation in the matrix is also presented in Figure 7.16.

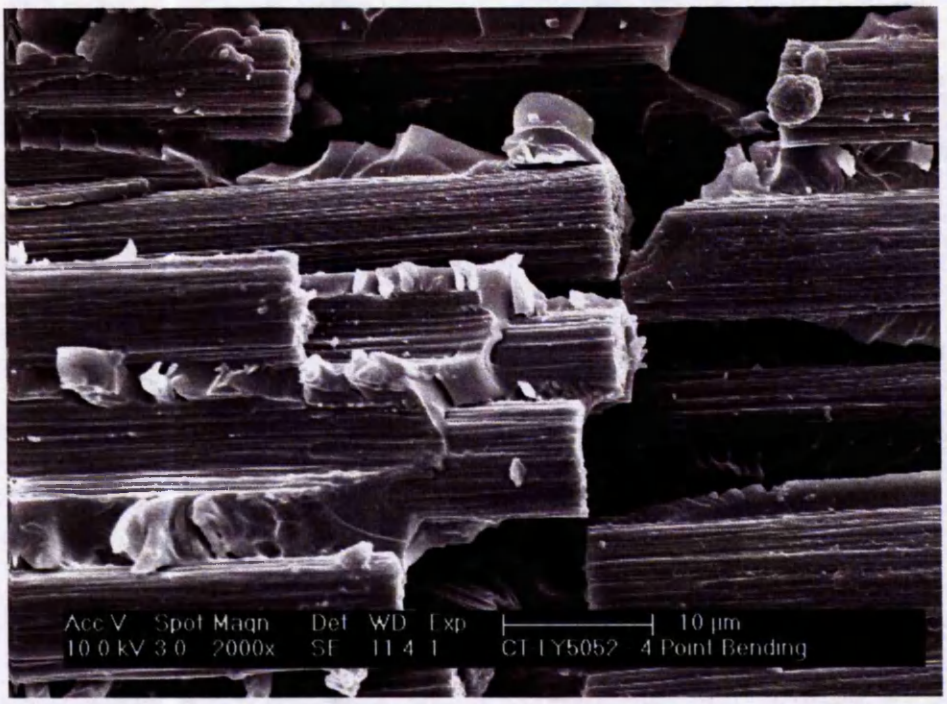

Figure 7.11: *Fracture surface of conventionally cured LY/HY5052/carbon composite subjected to four-point bending showing fibre breakage transverse to applied load.*

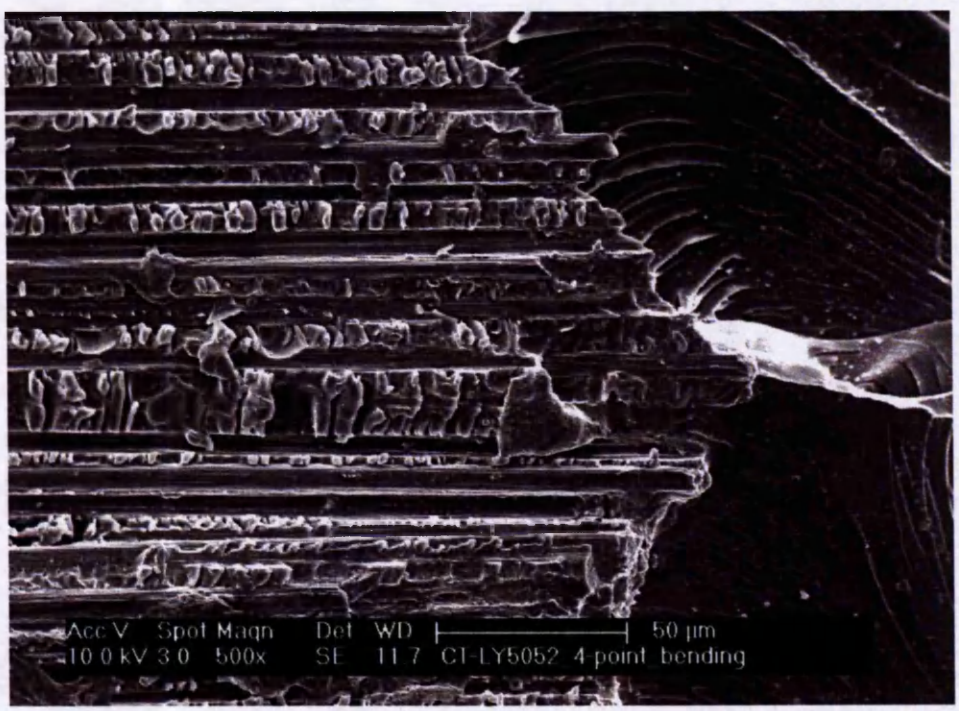

Figure 7.12: *Fracture surface of conventionally cured LY/HY5052/carbon composite subjected to four-point bending showing shear bands associated with fibre pull-out (left hand side) and brittle matrix fracture (right hand side).*

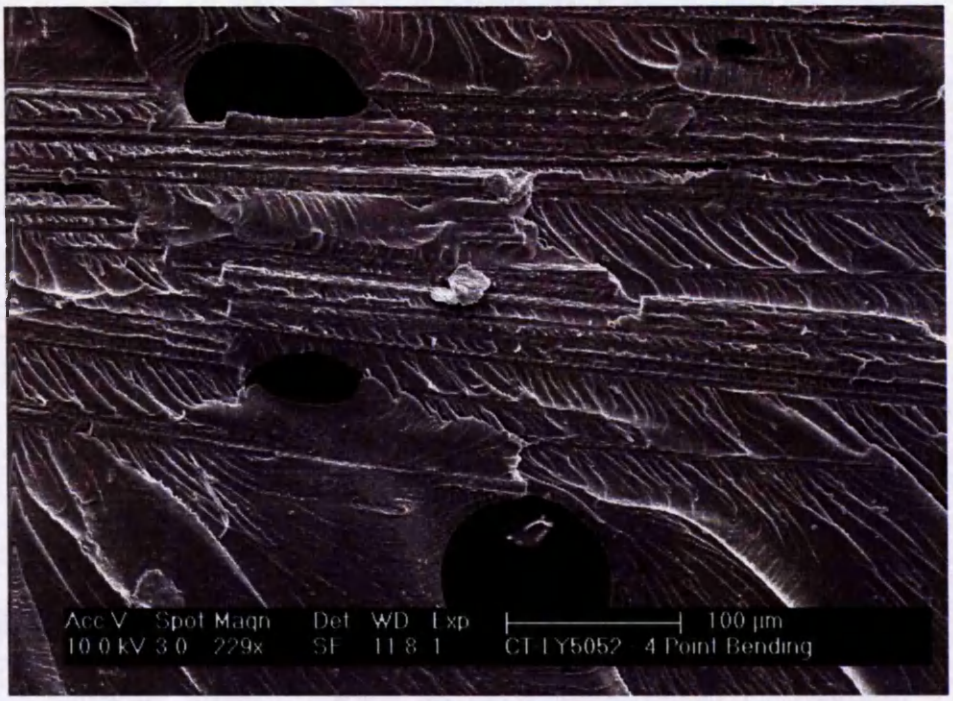

Figure 7.13: *Fracture surface of conventionally cured LY/HY5052/carbon composite subjected to four-point bending showing holes in the composite indicating the presence of voids.*

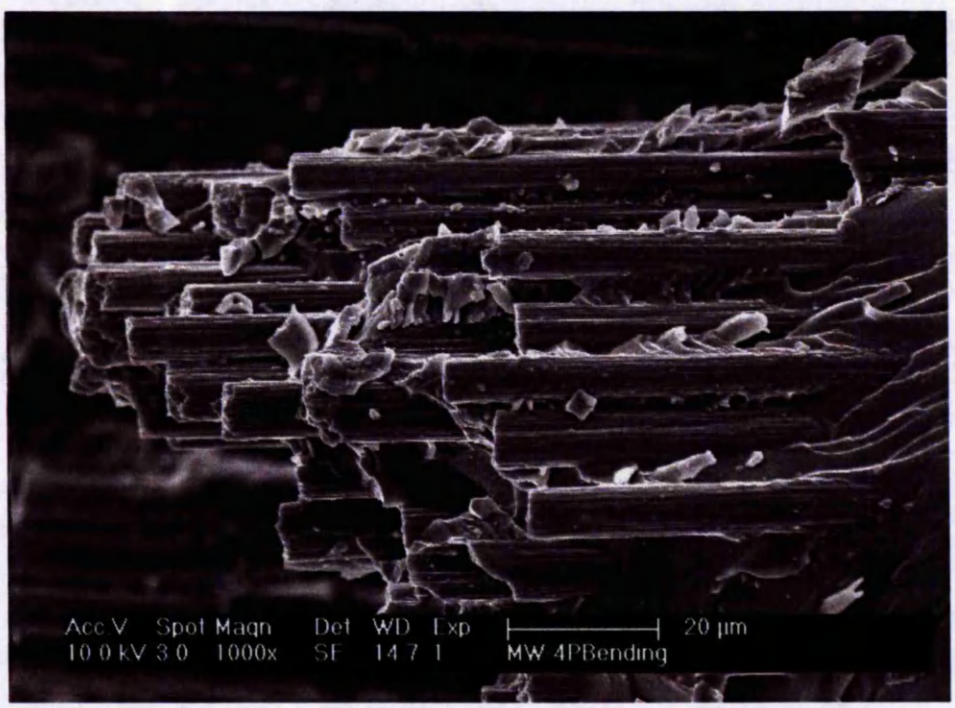

Figure 7.14: *Fracture surface of microwave cured LY/HY5052/carbon composite subjected to four-point bending showing good adhesion of the epoxy resin to the fibres.*

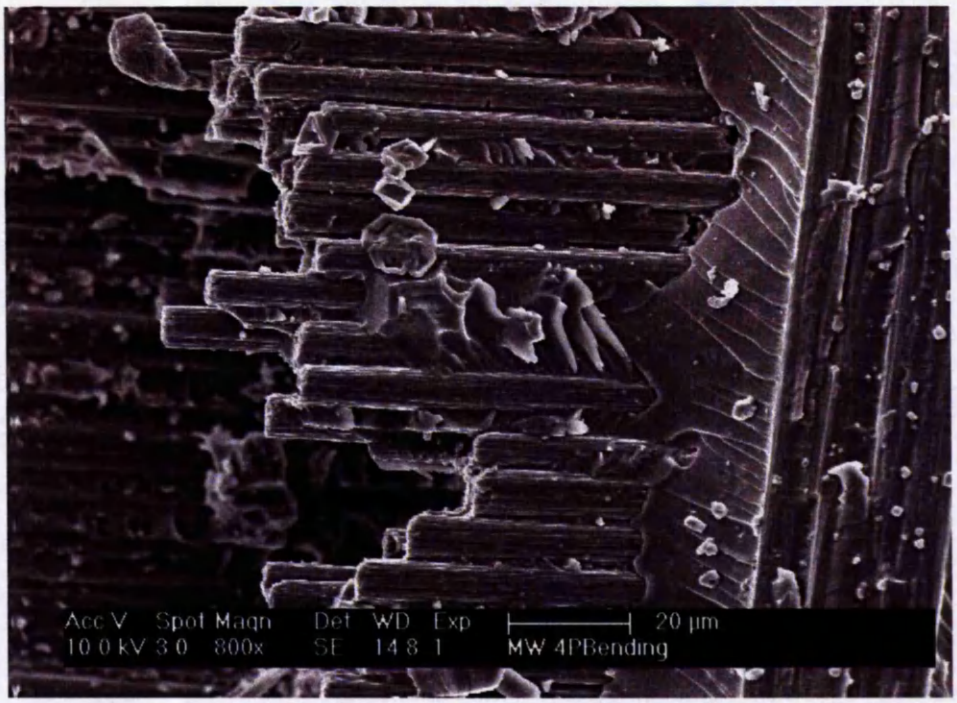

Figure 7.15: *Fracture surface of microwave cured LY/HY5052/carbon composite subjected to four-point bending showing fibre breakage (left hand side) and fibre pull-out (right hand side).*

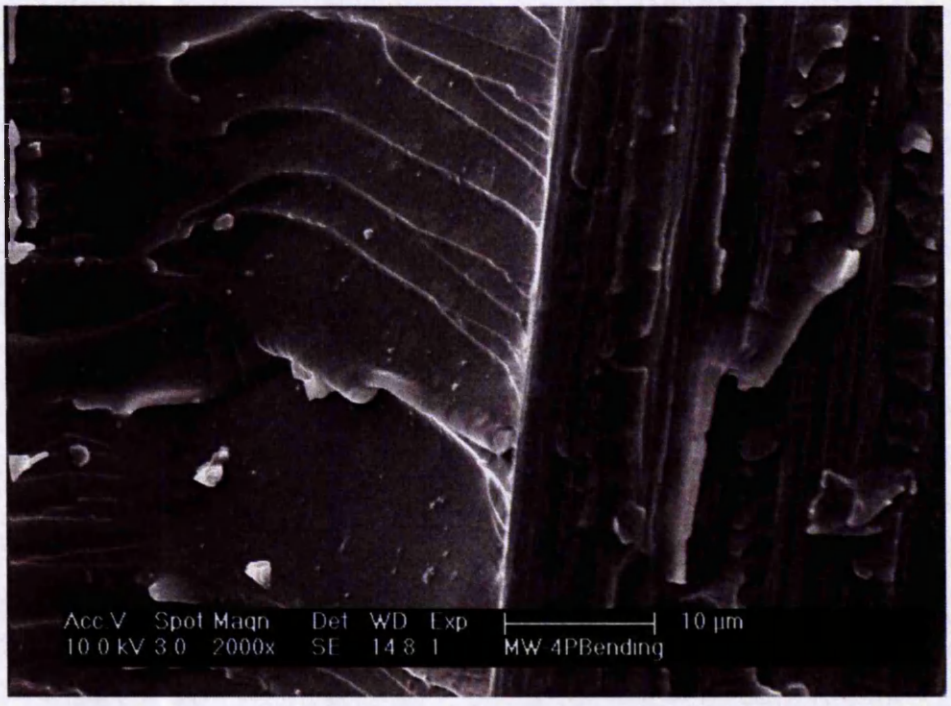

Figure 7.16: *Fracture surface of microwave cured LY/HY5052/carbon composite subjected to four-point bending showing crack propagation in the matrix.*

7.4.1.2 LY/HY5052/glass Composite System

Typical flexural stress-strain plots for the thermally and microwave cured LY/HY5052/glass composites are presented in Figures 7.17 and 7.18, respectively. Failure occurred at a strain of 1.6 – 1.8 % for the conventionally cured composites and 2.5 – 2.8 % for the microwave cured composites. Observing the stress-strain curves for the microwave cured LY/HY5052/glass composites, it appears that the mechanical behaviour was different compared to their thermally cured counterparts. Whilst the latter exhibited an almost linear stress-strain relationship up to the point of failure, the former exhibited a linear stress-strain relationship up to approximately 1.25 % strain followed by a series of small cracks and/or delaminations. Hence during the course of the four-point bending test, the load carried by the microwave cured samples momentarily dropped only to continue to rise again. This behaviour was repeated a few times before catastrophic failure occurred, suggesting a different failure mechanism between microwave and thermally cured LY/HY5052/glass composite samples.

The average values of the flexural modulus and flexural strength for the LY/HY5052/glass composites produced by both conventional thermal and microwave RTM processing are shown in Table 7.3. The load at failure for the microwave cured samples was taken just before the final large drop in the stress-strain curve (Figure 7.18). The thermally cured composites exhibited a flexural modulus of 23 ± 1 GPa and a flexural strength of 364 ± 20 MPa, while the corresponding values for the microwave cured composites were 17 ± 2 GPa and 322 ± 32 MPa, respectively. Nevertheless, normalisation of the flexural data to an equivalent glass fibre volume fraction (26 % V_f) yielded a flexural modulus of 22.1 GPa and a flexural strength of 418 MPa for the microwave cured composites, as shown in Table 7.3. The normalisation was carried out assuming a linear relationship between fibre volume fraction and flexural strength and modulus. The results indicated that the flexural properties were found to be similar between the two types of composites. These values were comparable with those reported by other researchers for similar glass fibre epoxy composite systems [154].

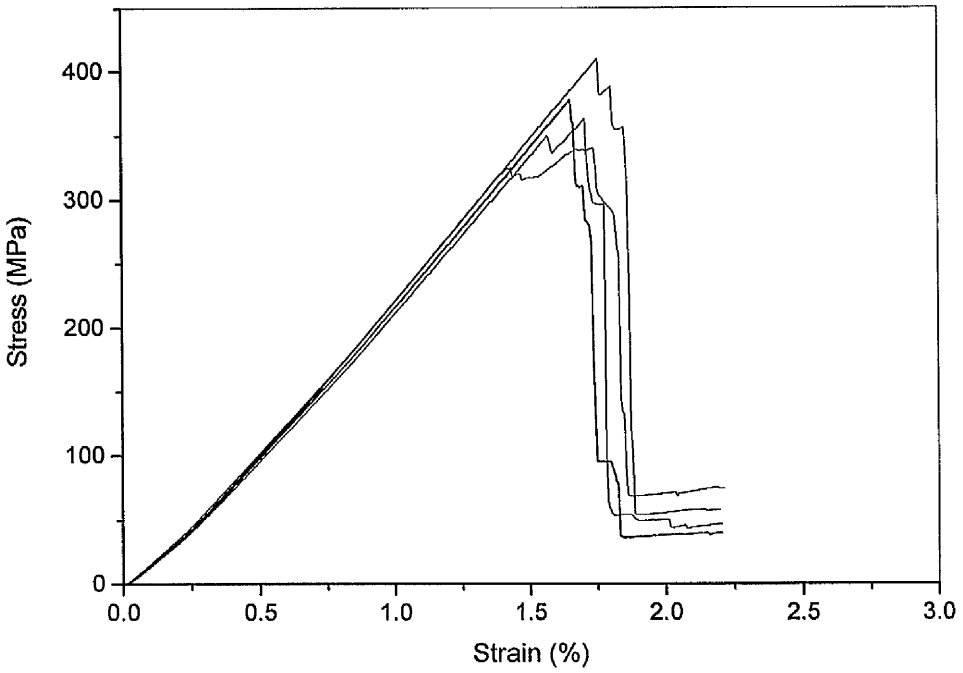

Figure 7.17: *Typical flexural stress-strain plots for the LY/HY5052/glass composites manufactured using conventional thermal RTM processing.*

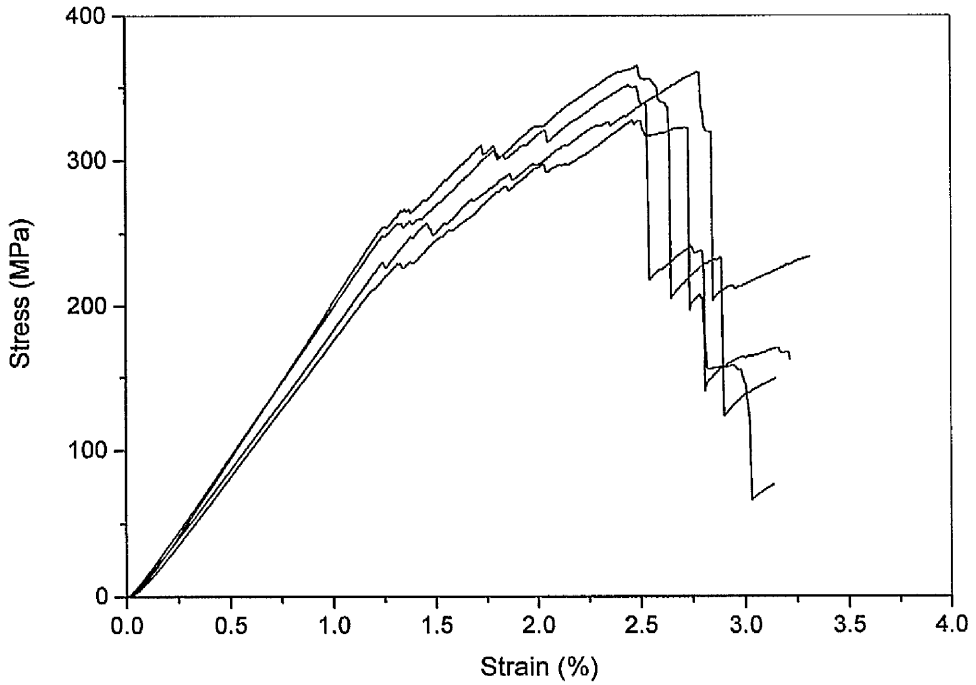

Figure 7.18: *Typical flexural stress-strain plots for the LY/HY5052/glass composites manufactured using microwave RTM processing.*

Table 7.3: *Average values of flexural modulus and flexural strength for the LY/HY5052/glass composites produced by conventional thermal and microwave RTM processing.*

Processing Method	Flexural Properties		Average Panel Thickness (mm)
	Flexural Modulus (GPa)	Flexural Strength (MPa)	
Conventional Thermal RTM	23 ± 1	364 ± 20	3.33 ± 0.03
Microwave RTM	17 ± 2	322 ± 32	3.79 ± 0.07
Microwave RTM (Normalised to 26% V_f)	22.1	418	-

Similar mechanical properties between thermally and microwave cured glass fibre-epoxy composites are also reported by other researchers. In specific, Mooteri et al. [92] studied the mechanical behaviour of glass fibre-epoxy composites microwave cured in a custom-built multi-mode microwave oven operating at a frequency of 2.45 GHz. They reported that the mechanical performance of the glass fibre-epoxy composites produced by microwave curing under tension, compression and flexure was in close comparison, and sometimes even better, compared to their thermally cured counterparts. Their study also demonstrated that microwave processing was twenty times more energy efficient and thirty times faster than the equivalent thermal process.

Furthermore, research carried out by Tanrattanakul and SaeTiaw [89] on the tensile, impact resistance and flexural properties of epoxy-anhydride resins cured with conventional and microwave heating showed that equivalent or better properties were obtained by microwave curing. Microwave processing also resulted in an equivalent degree of conversion at a shorter cure time, while the glass transition temperatures between the thermally and microwave cured resins were found to be comparable, as indicated by dynamic mechanical thermal analysis. Equivalent mechanical properties between glass fibre-epoxy composites produced thermally and by microwave curing were also reported by Tanrattanakul and Jaroendee [153], as mentioned previously in Section 7.4.1.1.

The fracture surfaces of both thermally and microwave cured LY/HY5052/glass composite samples subjected to four-point bending were examined by means of scanning electron microscopy (SEM). Representative features of the fracture surface morphology for the conventionally cured composites are presented in Figures 7.19 – 7.21. The main failure modes identified after observation of the entire fracture surface area of the samples were tensile and shear. Figure 7.19 shows fibre breakage due to tensile failure in a conventionally cured specimen. Good adhesion is achieved between the fibres in the bundle, as residual resin is still attached to some of the fibres. Figure 7.20 shows typical shear bands or hackle patterns associated with fibre pull-out, while in Figure 7.21 signs of a mixed failure mode due to both tensile (brittle matrix fracture) and shear failure (fibre pull-out) are evident.

Figures 7.22 – 7.24 show SEM micrographs of the fracture surfaces of microwave cured LY/HY5052/glass composites subjected to four-point bending. Similar to the thermally cured glass fibre composites, the principle failure modes identified in the microwave curd composites were tensile and shear. In specific, Figure 7.22 shows a group of broken fibres due to tensile failure. Some resin debris is evident on the surface of the fibres, indicating good fibre-resin adhesion. Figure 7.23 shows characteristic shear bands, similar to those in Figure 7.20, as a result of fibre pull-out. Finally, the light colour regions on the left hand side in Figure 7.24 indicate brittle fracture of the matrix, while signs of shear failure are also present on the right hand side.

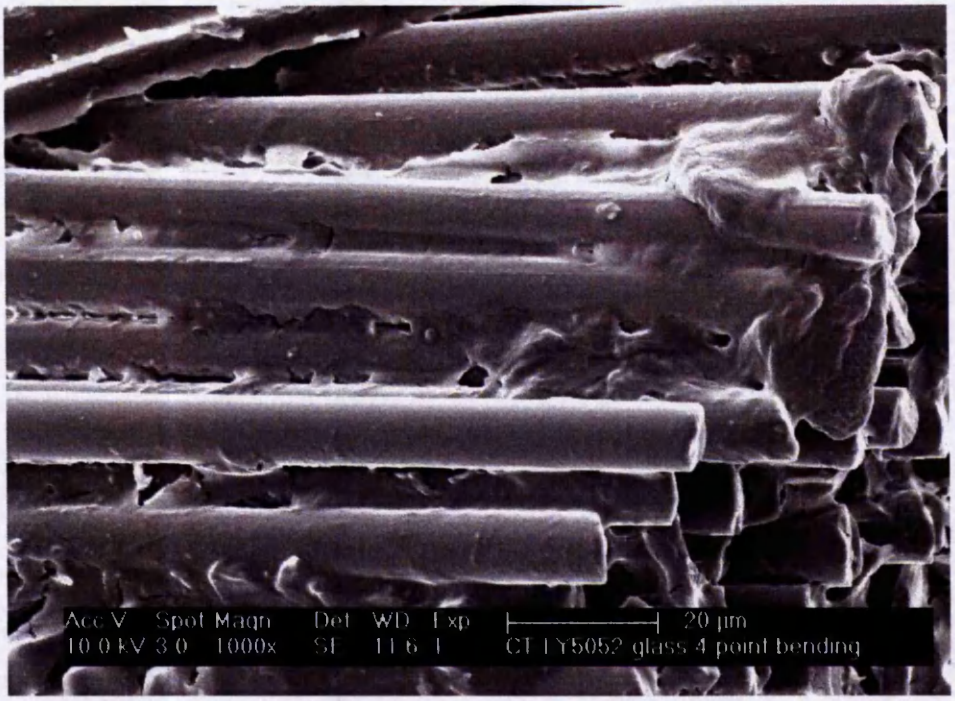

Figure 7.19: *Fracture surface of conventionally cured LY/HY5052/glass composite subjected to four-point bending showing fibre breakage due to tensile failure.*

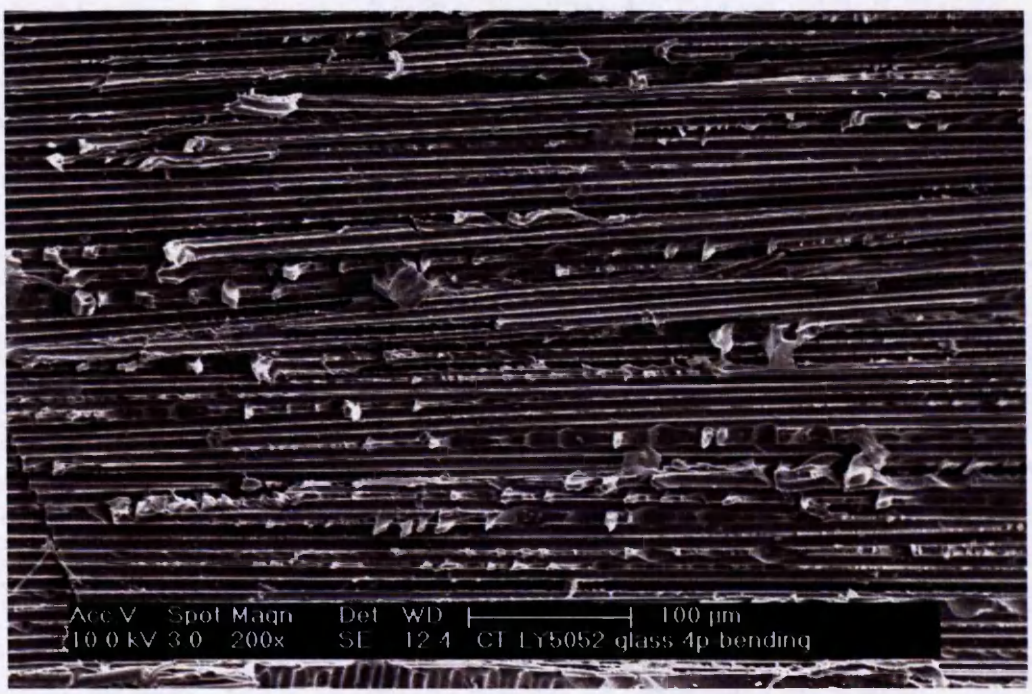

Figure 7.20: *Fracture surface of conventionally cured LY/HY5052/glass composite subjected to four-point bending showing shear bands associated with fibre pull-out.*

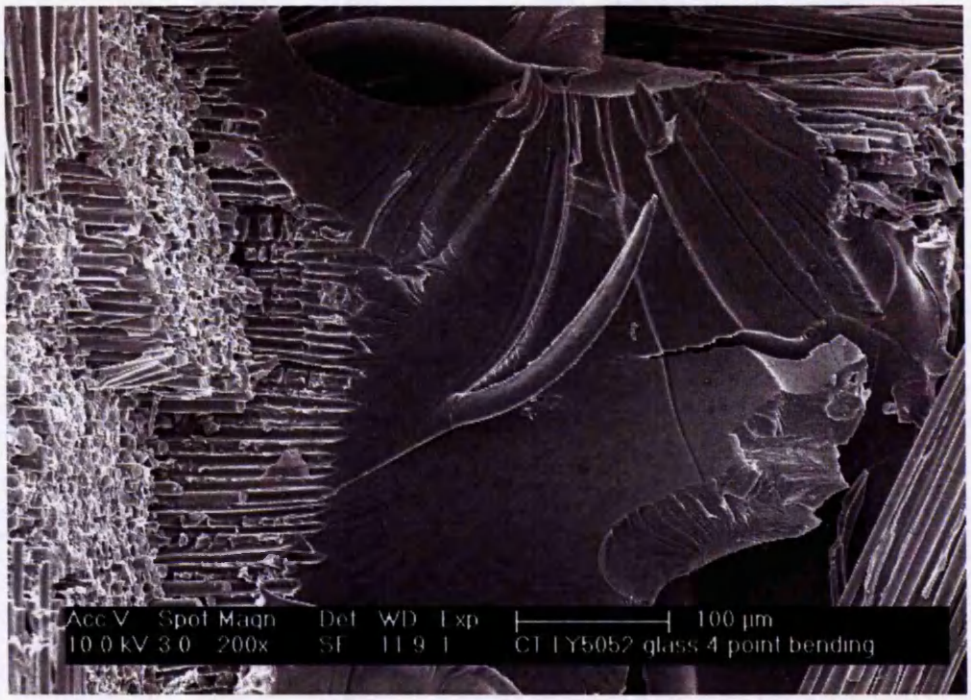

Figure 7.21: *Fracture surface of conventionally cured LY/HY5052/glass composite subjected to four-point bending showing fibre pull-out (left hand side) and brittle matrix fracture (right hand side).*

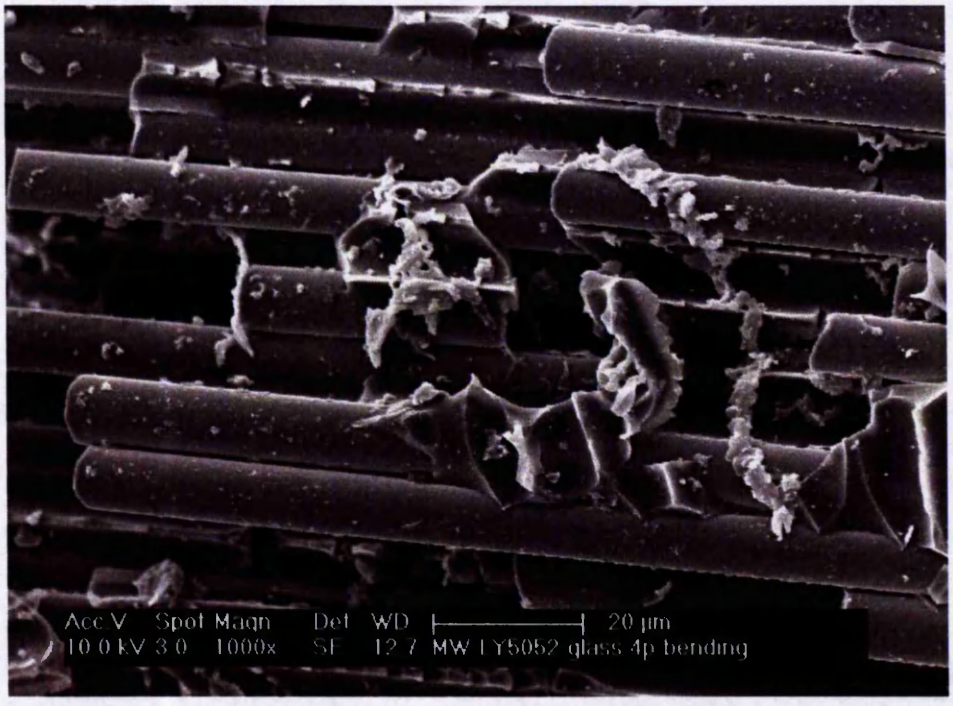

Figure 7.22: *Fracture surface of microwave cured LY/HY5052/glass composite subjected to four-point bending showing fibre breakage due to tensile failure.*

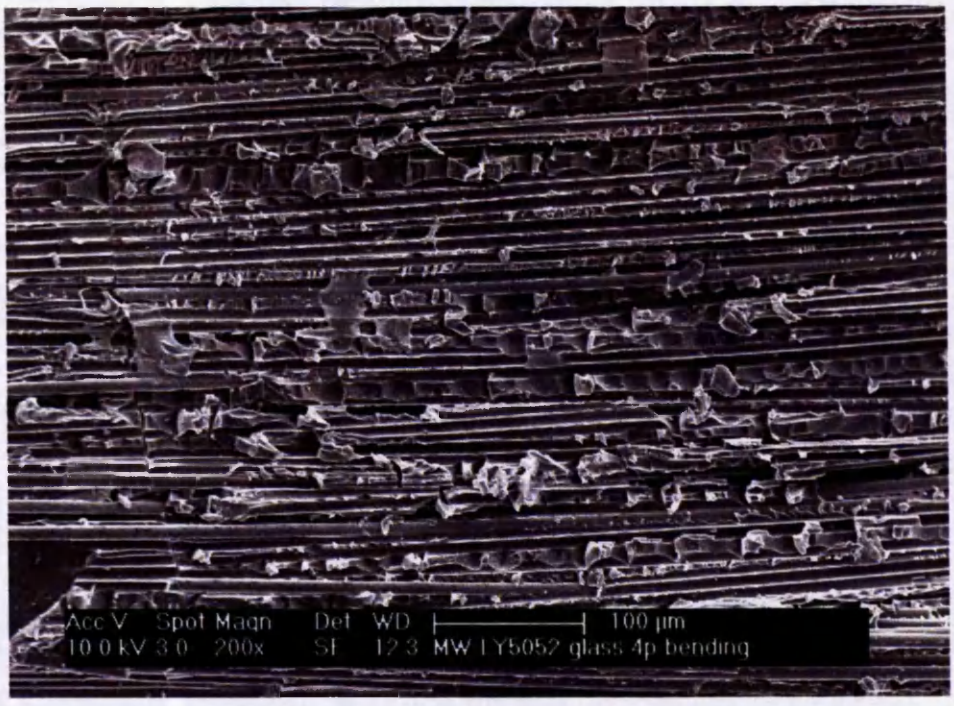

Figure 7.23: *Fracture surface of microwave cured LY/HY5052/glass composite subjected to four-point bending showing shear bands associated with fibre pull-out.*

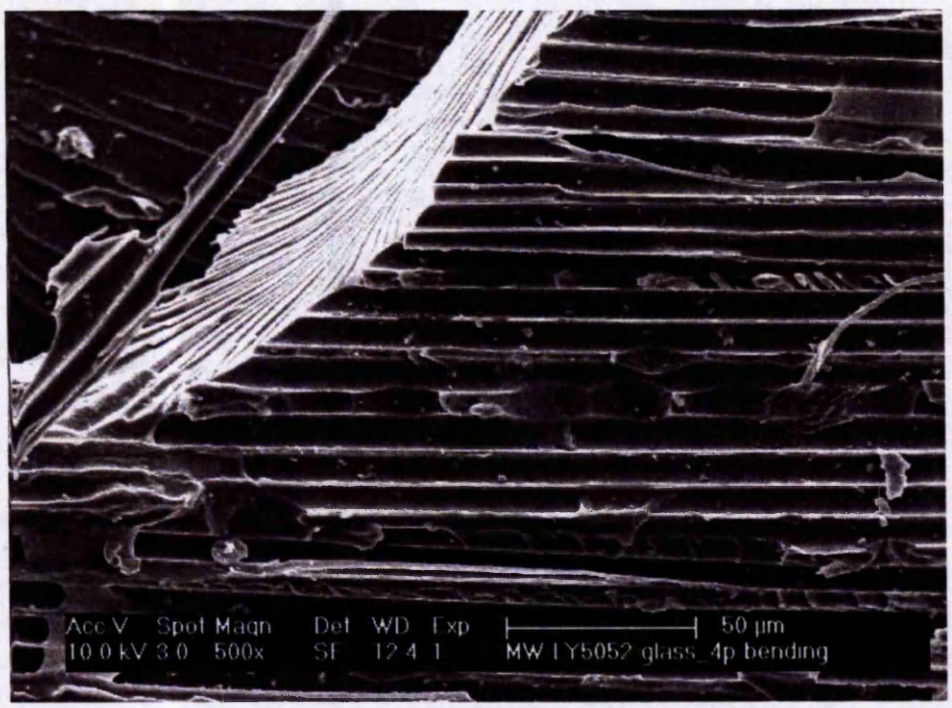

Figure 7.24: *Fracture surface of microwave cured LY/HY5052/glass composite subjected to four-point bending showing fibre pull-out (right hand side) and brittle matrix fracture (left hand side).*

7.4.2 Interlaminar Shear Strength

The interlaminar shear strength of the fabricated composites was determined by means of short-beam shear testing. This test is quite similar to three-point bending with the only difference that a smaller span-to-thickness ratio (4:1) is employed in order to encourage interlaminar shear failure in the samples. The tests were carried out according to ASTM D 2344/D 2344M standard [114]. The relevant details are given in Chapter 4, Section 4.3.2.

7.4.2.1 LY/HY5052/carbon Composite System

Figures 7.25 and 7.26 show typical interlaminar shear load-displacement plots for the thermally and microwave cured LY/HY5052/carbon composites, respectively. The relationship between load and displacement appears to be almost linear until the maximum load was reached and failure occurred. The point of failure was observed at a displacement of 0.65 – 0.73 mm for the thermally cured composites and 0.68 – 0.77 mm for those cured using microwave heating. The microwave cured composites exhibited a higher interlaminar strength than their thermally cured counterparts. In specific, the interlaminar shear strength of the conventionally cured composites was 50 ± 1 MPa, as opposed to 54.5 ± 1 MPa for the microwave cured composites.

The above results are consistent with those found by Nightingale and Day [93] who compared the mechanical properties of two carbon fibre reinforced epoxy composites cured in three different ways: autoclave curing, partial autoclave curing and microwave post-curing, and microwave curing. They found that the autoclave cured composites yielded the best flexural and interlaminar shear strength properties followed by the microwave cured composites. The mechanical properties of the latter were nevertheless better compared to those of the microwave post-cured composites, suggesting that under the correct conditions microwave curing has the potential to enhance the mechanical properties of composites matching those obtained from autoclave curing but in a much shorter time. A stronger fibre-resin interface in microwave cured carbon fibre composites is also reported by other researchers [96, 155].

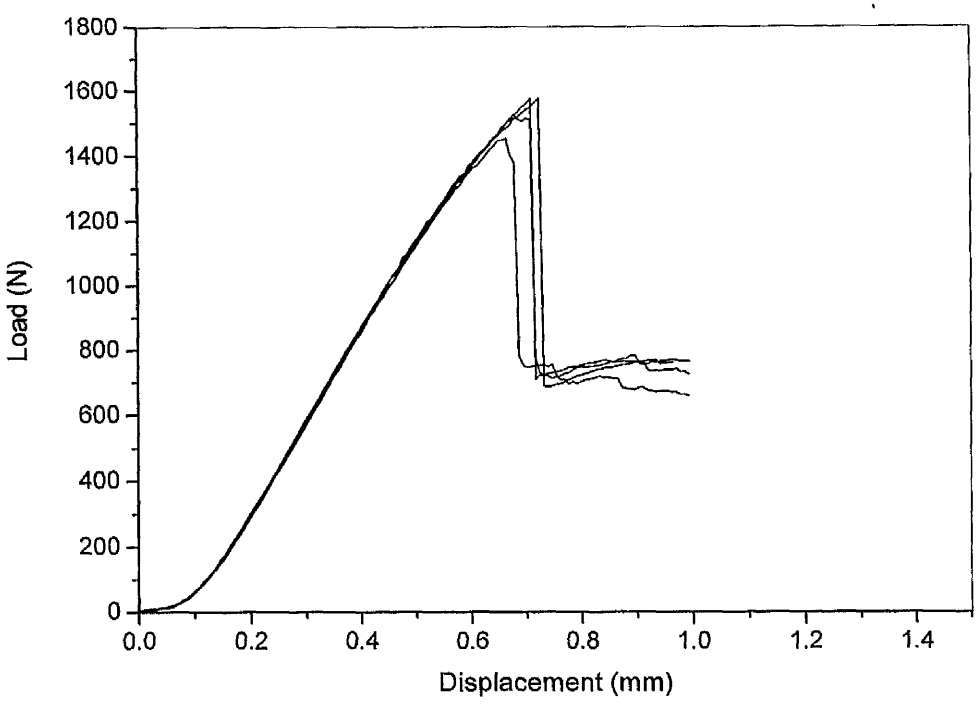

Figure 7.25: *Typical interlaminar shear load-displacement plots for the LY/HY5052/carbon composites manufactured using conventional thermal RTM processing.*

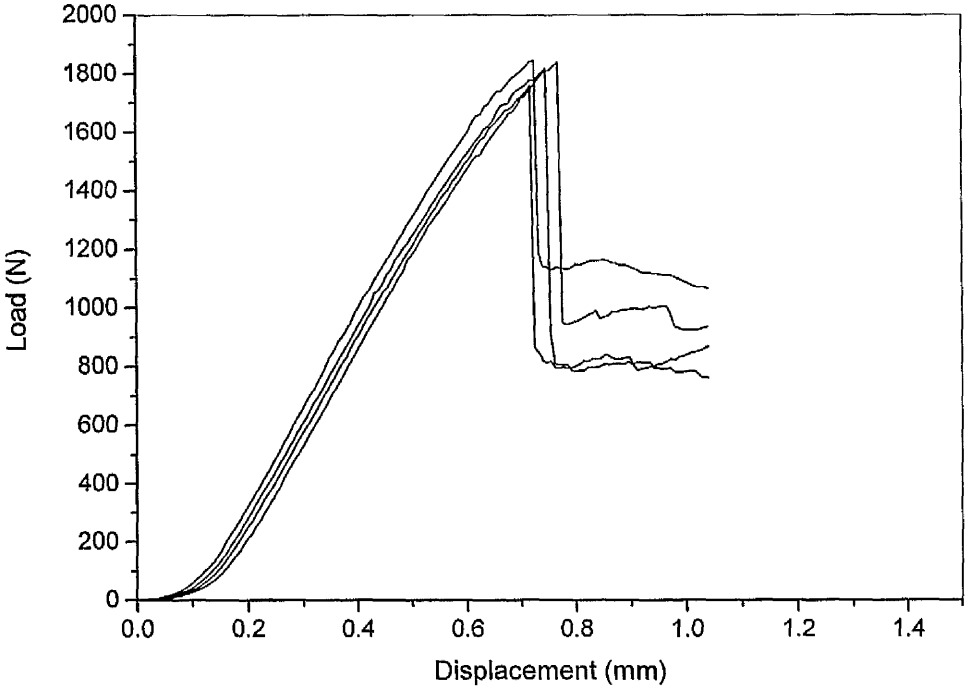

Figure 7.26: *Typical interlaminar shear load-displacement plots for the LY/HY5052/carbon composites manufactured using microwave RTM processing.*

Liu et al. [95] investigated the microwave curing of neat polyimide resin (RP-46), glass fibre and hybrid glass fibre-graphite fibre reinforced polyimide composites using a microwave oven operating at a frequency of 2.45 GHz. They noted that the electrically conducting fibres, such as graphite and carbon fibres, absorb microwave energy more efficiently than the non-conducting materials. Thus, microwave heating of composites containing conducting fibres could result in inside to outside solidification, which may also enhance the bonding between resin and fibres. The importance of an inside to outside solidification was also emphasized in the work of Thostenson and Chou [156]. It was concluded that, although thermal gradients during processing can not be avoided, microwave processing offers greater control over the spatial solidification of thick composite laminates. This was reflected in the cross-section of the autoclave fabricated laminates, in which matrix cracks were visible due to outside to inside solidification, while no cracks were observed in the cross-section of the microwave processed laminates.

Generally, microwave heating is regarded as a volumetric heating technique in which the microwaves interact with the material and heat is generated directly as a result. Hence heating is efficient, because energy is deposited directly into the material and the effects of convective and conduction heat transfer are less significant than with some other heating techniques. In carbon fibre composites, however, the situation is probably more complicated. As described in Chapter 2, the attenuation of the electromagnetic field in microwave processing is expressed by a penetration depth, which is inversely proportional to both the applied frequency and the dielectric loss of the processed material. Due to the high dielectric loss of carbon fibres and the high frequency range used in this work, the penetration depth is expected to be quite small. Thus, the microwaves do not penetrate a long way into the composites at all frequencies. They interact instead with a surface layer. This means that there is still good heat transfer into the surface of the composite. Within the composite it is likely that the microwave electric field generates an electric current in the carbon fibres and thus resistive heating.

Kim and See [157] studied the electrical properties of unidirectional carbon fibre-epoxy composites in the frequency range of 1.7 to 10 GHz. They found that, regardless of the fibre volume fraction, the composites for the longitudinal direction can be considered as good conductors even at higher frequencies. Since the frequency range employed for microwave curing of the composites in the present work was 4 – 8 GHz, it can be assumed that good electrical conductivity was achieved throughout the curing process. It is thus postulated that the epoxy resin is heated through dielectric heating at the surface of the composite, while within the bulk it is heated due to resistive heating of the carbon fibres and through thermal conduction. The additional heat passing on from the carbon fibres to the surrounding resin within the bulk is suggested to have initiated a higher heating rate in the resin compared to that achieved in thermal processing, which in turn would result in a decrease in the resin viscosity.

Figure 7.27 shows the change of viscosity with respect to time at three different heating rates (2°C/min, 5°C/min and 10°C/min) for the uncured LY/HY5052 resin system. As the heating rate increased, the minimum viscosity of the neat resin decreased considerably from 0.12 Pa-s to 0.068 Pa-s and finally to 0.043 Pa-s. A decrease in the resin viscosity would facilitate resin flow, especially at the early stages of the curing process, hence making it easier for the resin to impregnate the carbon fibre surface and improve the interfacial bonding and mechanical interlocking between the resin and the fibres, which in turn was manifested as increased interlaminar shear strength.

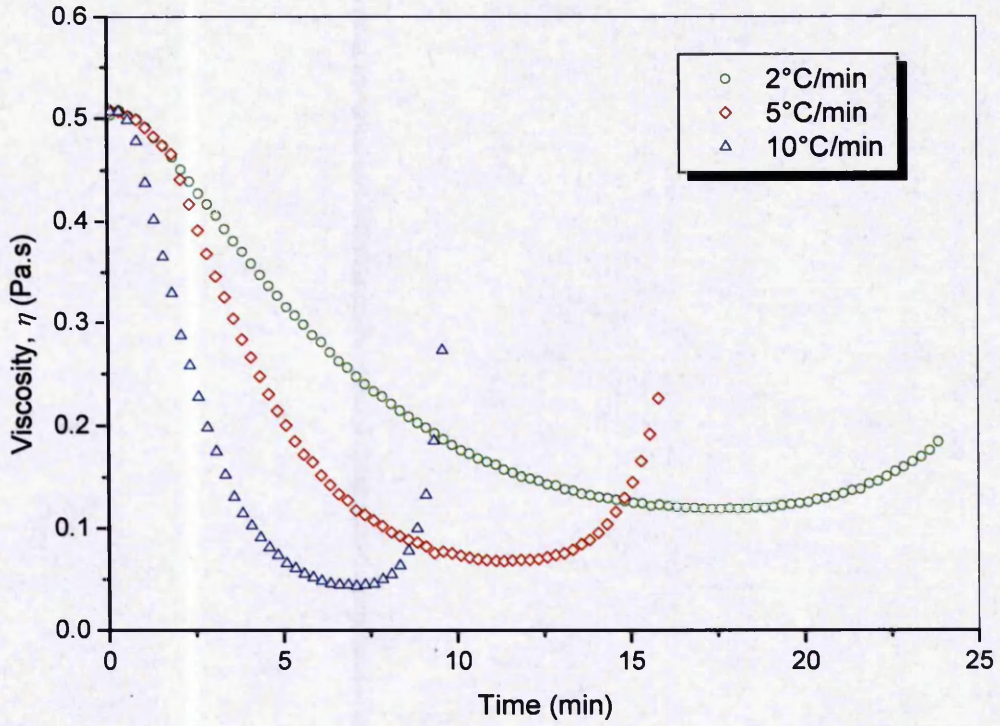

Figure 7.27: *Viscosity versus time at 2°C/min, 5°C/min and 10°C/min for the neat LY/HY5052 resin system.*

The fracture surfaces of both thermally and microwave cured LY/HY5052/carbon composite samples subjected to interlaminar shear testing were examined using scanning electron microscopy (Figures 7.28 – 7.31). Careful examination of the fracture surface morphology revealed some differences between the two types of composites. Figure 7.28 shows a significant amount of clean fibres present in a thermally cured sample with shear bands or hackle patterns evident as a result of fibre pull-out. Figure 7.30, on the other hand, shows the fracture surface of a microwave cured sample at the same magnification, in which the fibres are thoroughly coated with resin and no distinct shear bands are identified. Comparing Figures 7.28 and 7.30, it appears that the conventionally cured LY/HY5052/carbon composites exhibited poorer interfacial bonding and more extensive fibre pull-out compared to that of their microwave cured counterparts. This is also consistent with the interlaminar shear strength results obtained for the two types of composites. Furthermore, regions of brittle matrix fracture were also observed for both thermally and microwave cured samples, as shown in Figures 7.29 and 7.31, respectively.

Figure 7.28: *Fracture surface of conventionally cured LY/HY5052/carbon composite subjected to interlaminar shear testing showing clean fibres.*

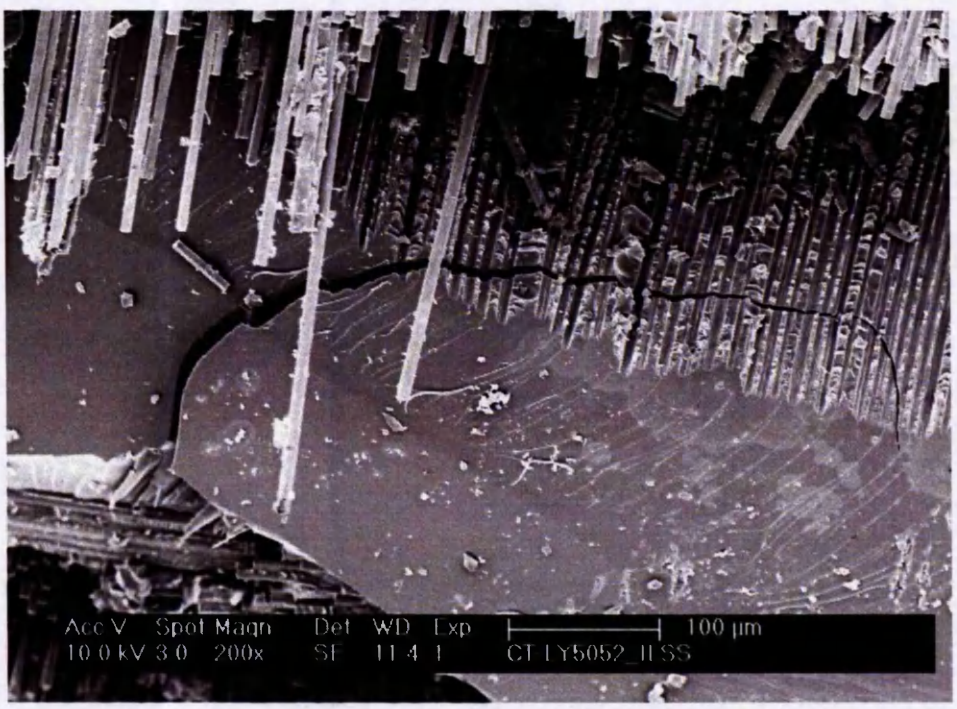

Figure 7.29: *Fracture surface of conventionally cured LY/HY5052/carbon composite subjected to interlaminar shear testing showing brittle matrix fracture.*

Figure 7.30: *Fracture surface of microwave cured LY/HY5052/carbon composite subjected to interlaminar shear testing showing fibres coated with resin.*

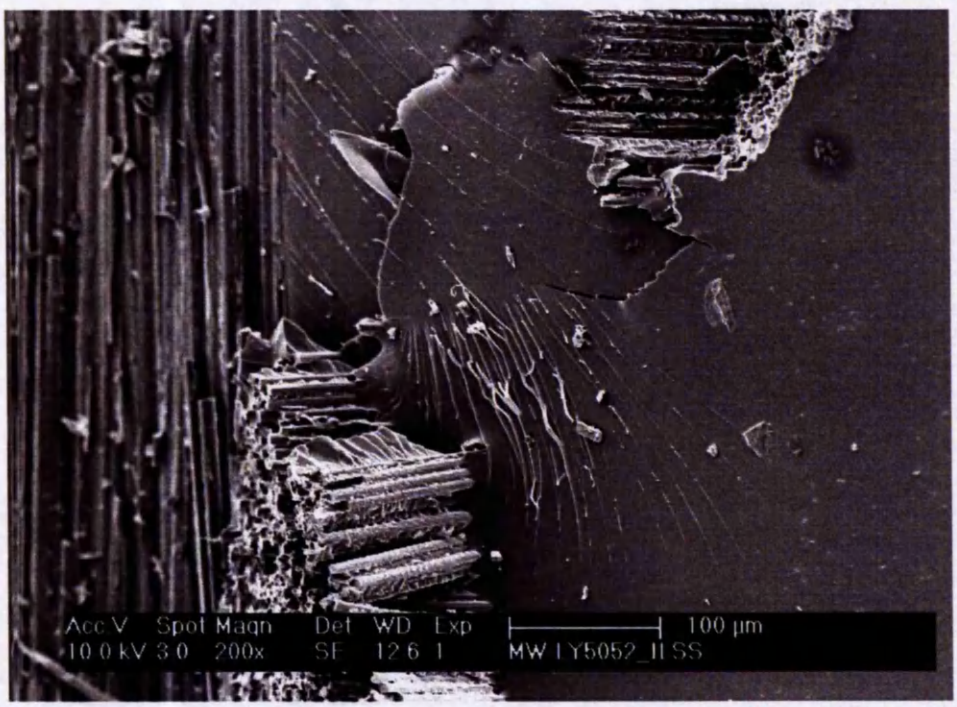

Figure 7.31: *Fracture surface of microwave cured LY/HY5052/carbon composite subjected to interlaminar shear testing showing brittle matrix fracture.*

7.4.2.2 LY/HY5052/glass Composite System

Figures 7.32 and 7.33 show typical interlaminar load-displacement plots for the thermally and microwave cured LY/HY5052/glass fibre composites, respectively. The load-displacement relationship was almost linear for both types of composites with failure occurring at a displacement of 0.74 – 0.89 mm for the conventionally cured composites and 0.91 – 1.04 mm for those cured by microwave heating. The interlaminar shear strength of the thermally cured glass fibre composites was found to be comparable to those of their microwave cured counterparts. The corresponding interlaminar shear strength values were 48 ± 2 MPa and 45 ± 2 MPa, respectively.

These findings are in agreement with the work of Rao et al. [102] who investigated the effect of thermal and microwave curing on the thermo-mechanical properties of 3 mm thick glass fibre epoxy-amine laminate systems. They found that the tensile and interlaminar shear strength properties of the microwave cured composites were similar or superior to those of their thermally cured counterparts (51.1 to 37.8 MPa and 49.8 to 46.9 MPa for low and high temperature cure cycles respectively). Additionally, it was established that microwave curing produced composites with high uniformity of cure at substantial energy savings (energy consumption was reduced to $1/20^{th}$ of that required for thermal curing) and reduced cure cycle time (cure cycle time was reduced from 28hours to 20 minutes for low temperature curing and to about $1/10^{th}$ of the high temperature thermal curing cycle). Furthermore, Bai and Djafari [99] reported that the fibre-matrix interface of microwave cured glass fibre-epoxy composite samples was stronger than that of the thermally cured samples, although the former had more voids. Analysis of the mechanisms of rupture revealed that matrix damage occurred prior to interfacial debonding in the microwave cured samples and not in those cured thermally, signifying that the interface of the former was more resistant. Higher interfacial shear strength in microwave cured glass fibre-epoxy composites was also reported by Boey and Yue [100].

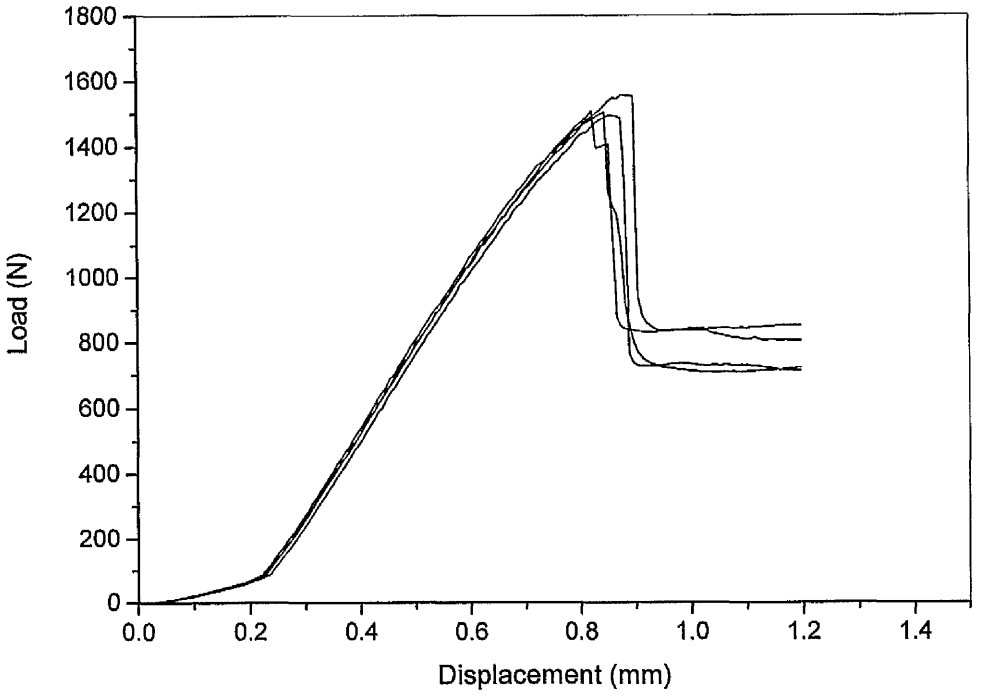

Figure 7.32: *Typical interlaminar shear load-displacement plots for the LY/HY5052/glass composites manufactured using conventional thermal RTM processing.*

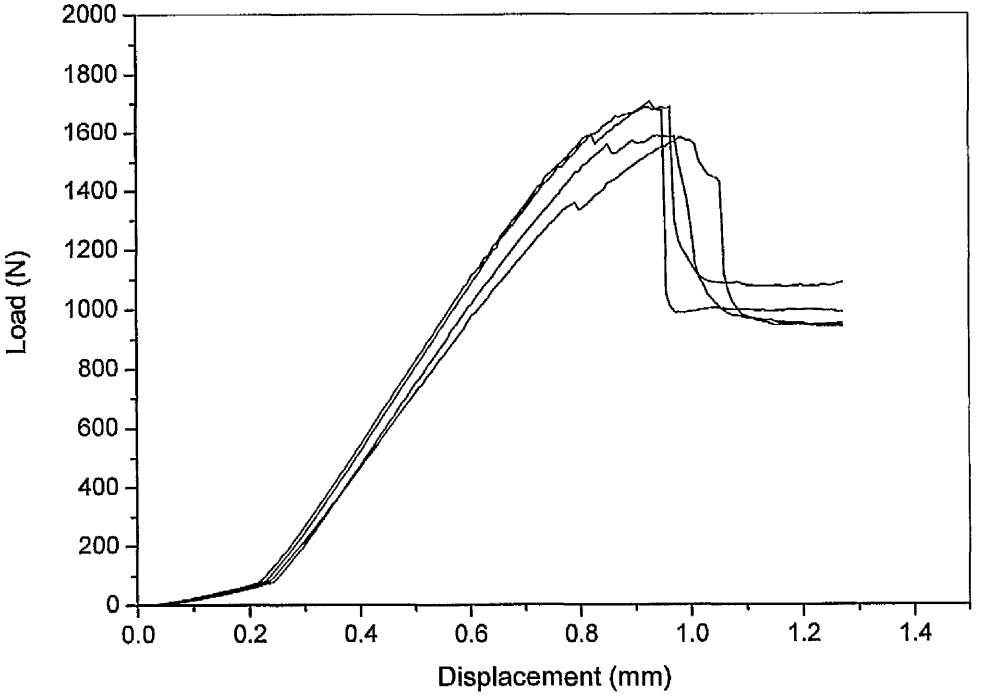

Figure 7.33: *Typical interlaminar shear load-displacement plots for the LY/HY5052/glass composites manufactured using microwave RTM processing.*

As suggested by Sirgia and Hawley [158], who investigated the effectiveness of microwave curing of natural fibre (including glass) reinforced epoxy composites, the epoxy resin is primarily heated during the initial stages of the microwave curing process owing to its significantly higher dielectric loss compared to that of the glass fibres. The dielectric constant of the glass fibres is low and would not affect the microwave processing of the composites. As the cure of the epoxy resin progresses, however, its dielectric loss factor decreases. The loss factor of the epoxy would eventually drop below that of the glass fibres, at which point the fibres would be preferentially heated by microwaves. Comparing the heating mechanism during microwave processing between carbon and glass fibre composites, the penetration depth of the microwaves is expected to be considerably higher in the latter due to the lower dielectric loss of glass fibres. Hence dielectric heating of the resin within its bulk is expected to be more pronounced. As a result, although the cure cycle time in microwave processing was reduced to half of that employed in conventional processing, the interfacial properties of the microwave cured LY/HY5052/glass composites were comparable to those of their thermally cured counterparts.

The fracture surfaces of both thermally and microwave cured LY/HY5052/glass composite samples subjected to interlaminar shear testing were examined using scanning electron microscopy (Figures 7.34 – 7.37). No significant differences regarding the fracture surface morphology were observed between the two types of composites. Figure 7.34 shows a group of fibres covered in resin debris after failure in a thermally cured sample, indicating good adhesion between the glass fibres and the matrix. Similarly, Figure 7.36 shows the debris formation on the glass fibre surface in a microwave cured sample at the same magnification. Furthermore, Figures 7.35 and 7.37 show examples of crack propagation through the fibre-matrix interface in thermally and microwave cured composite samples, respectively. This indicates that a good interface was formed during the curing process in both cases, allowing the crack front to propagate through the interface as a result of good stress transfer from the matrix. The above observations are also in agreement with the interlaminar shear strength results obtained for both types of glass fibre composites.

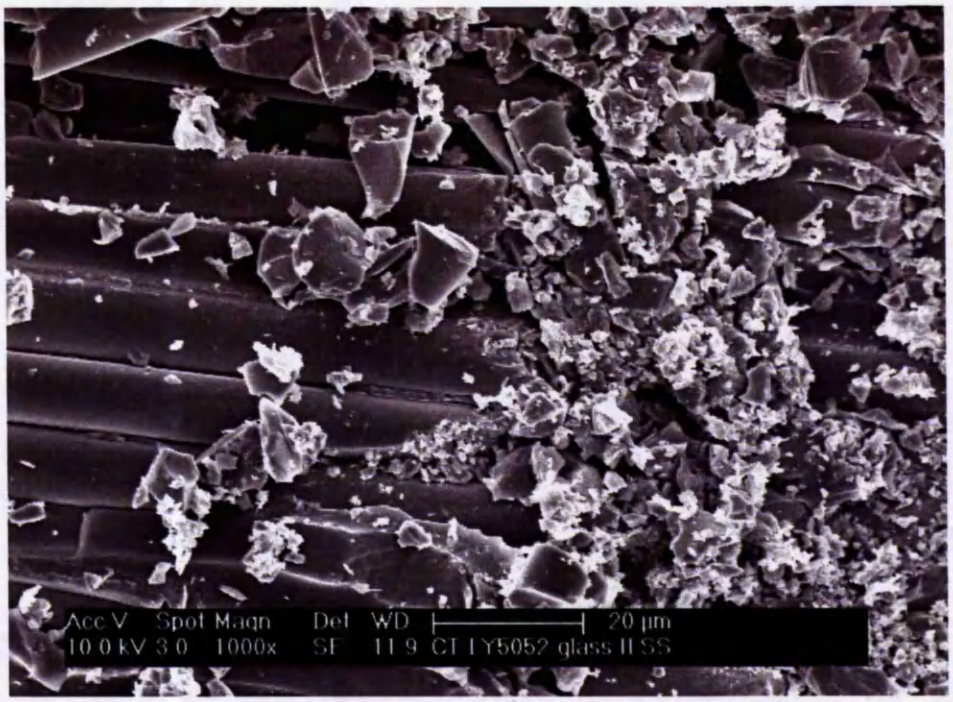

Figure 7.34: *Fracture surface of conventionally cured LY/HY5052/glass composite subjected to interlaminar shear testing showing resin debris on the glass fibre surface.*

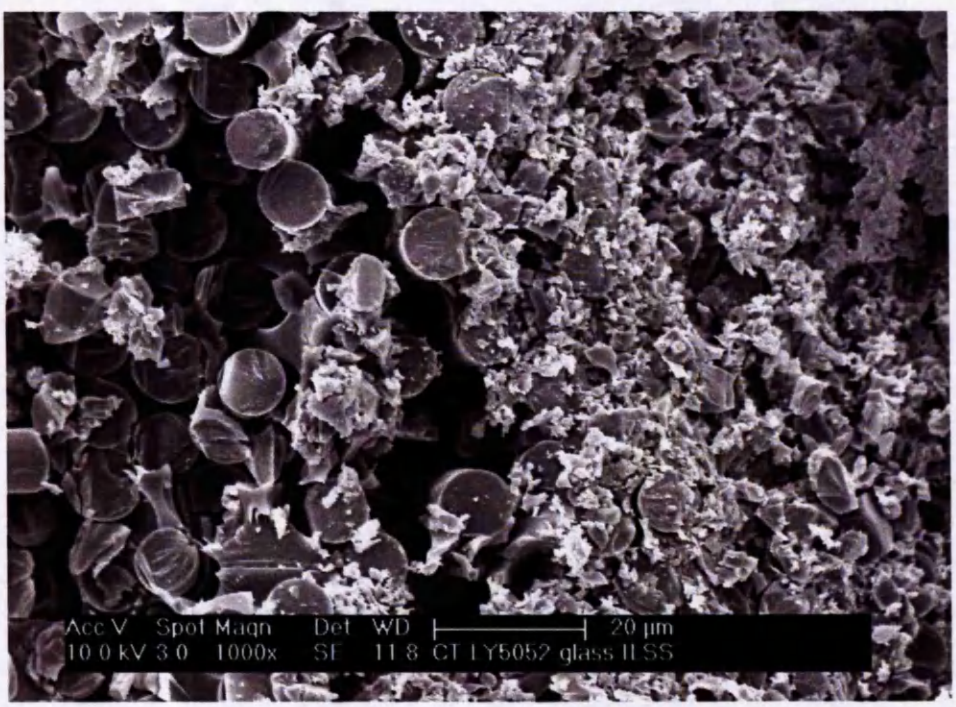

Figure 7.35: *Fracture surface of conventionally cured LY/HY5052/glass composite subjected to interlaminar shear testing showing crack propagation through the fibre-matrix interface.*

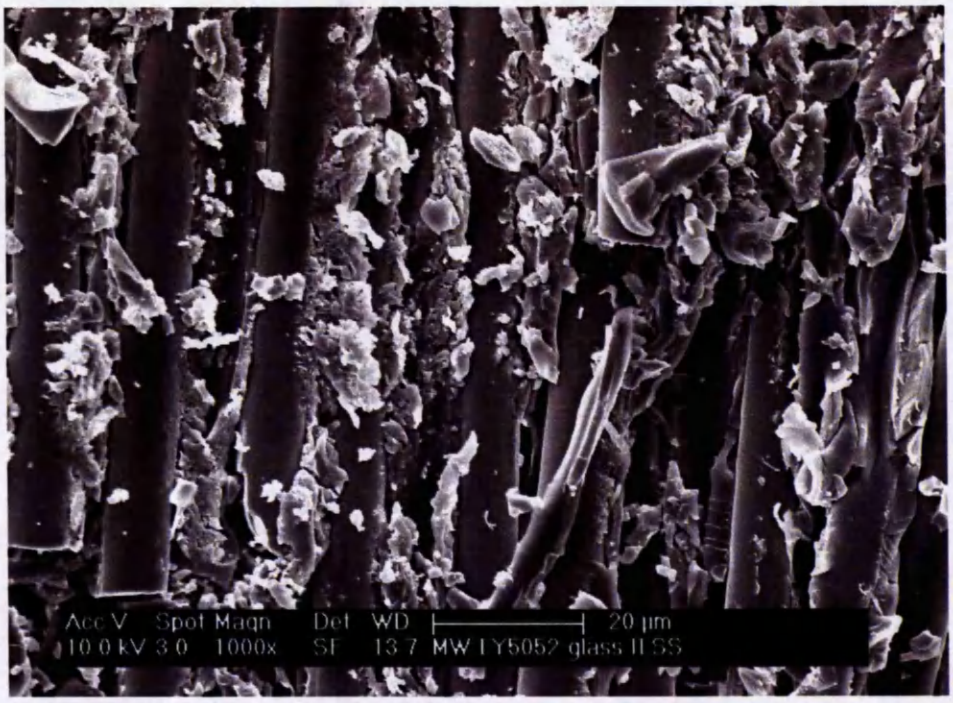

Figure 7.36: *Fracture surface of microwave cured LY/HY5052/glass composite subjected to interlaminar shear testing showing resin debris on the glass fibre surface.*

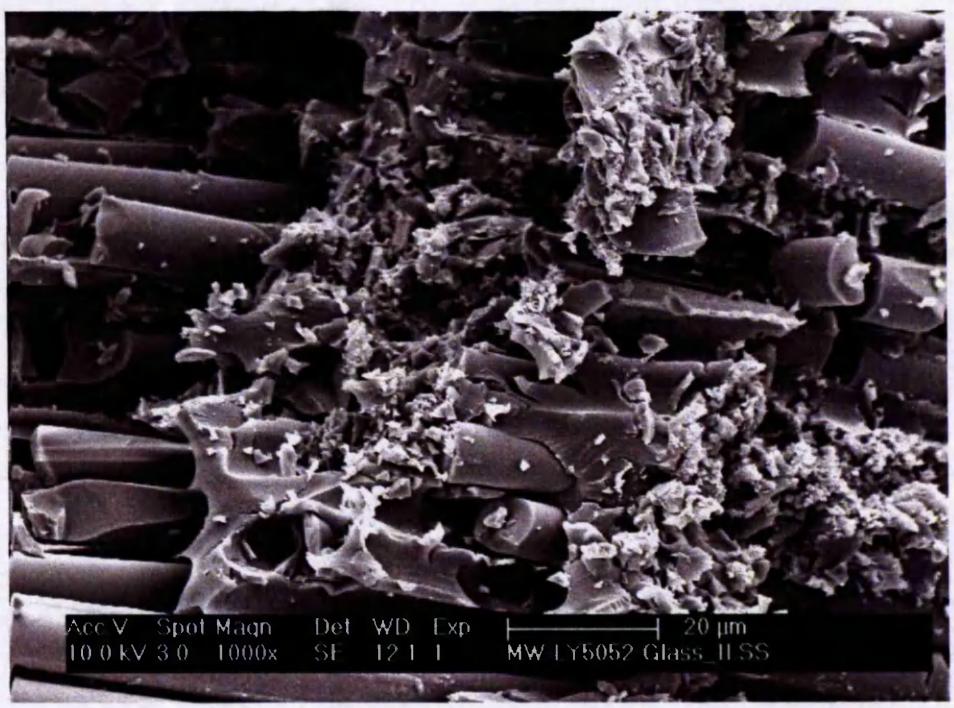

Figure 7.37: *Fracture surface of microwave cured LY/HY5052/glass composite subjected to interlaminar shear testing showing crack propagation through the fibre-matrix interface.*

7.5 Dielectric Properties

The dielectric properties of the uncured LY/HY5052 epoxy resin were determined using the cavity perturbation method. The technique is described in detail in Chapter 4, Section 4.11. The dielectric constant (ε') and dielectric loss (ε'') of the uncured epoxy resin were measured during microwave curing at 2.45 GHz from room temperature until 200°C at 5°C/min and 10°C/min, as shown in Figures 7.38 and 7.39 respectively. The dielectric properties of the neat resin were also measured isothermally at the selected cure temperature of 100°C and are plotted as a function of time in Figures 7.40 and 7.41, respectively.

In general, the dielectric properties of an epoxy resin increase with temperature and decrease as the extent of cure increases [159, 160]. The dielectric behaviour of the curing resin depends not only on the change in the dipolar groups present as a result of the chemical reactions taking place but also on the rapid decrease in the molecular mobility due to the formation of a cross-linked network [16]. The dielectric constant and dielectric loss initially increased as the sample temperature reached that of the sample holder and then started to decrease with the onset of the curing process, as shown in Figure 7.40. The decrease in the dielectric properties is caused by the disappearance of the epoxy and amine groups in the reactants as well as the increase of resin viscosity during cross-linking. Figure 7.41 shows the evolution of tan Delta against time. Tan Delta is the ratio of the dielectric loss over the dielectric constant and as such it reflects the ability of the resin to convert any absorbed amount of microwave energy into heat. Hence it can be directly linked to the extent of cure. Therefore, as the curing progressed tan Delta decreased exponentially levelling out after a certain period of time, which signified the end of the curing process.

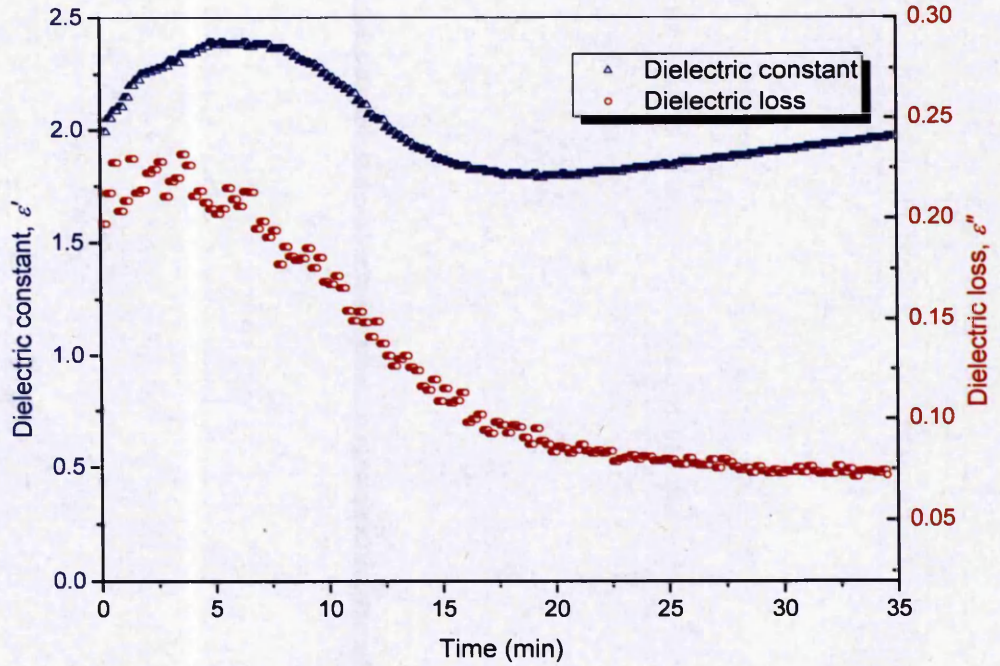

Figure 7.38: *Dielectric constant and dielectric loss of the uncured LY/HY5052 epoxy resin against time during microwave heating at 5°C/min.*

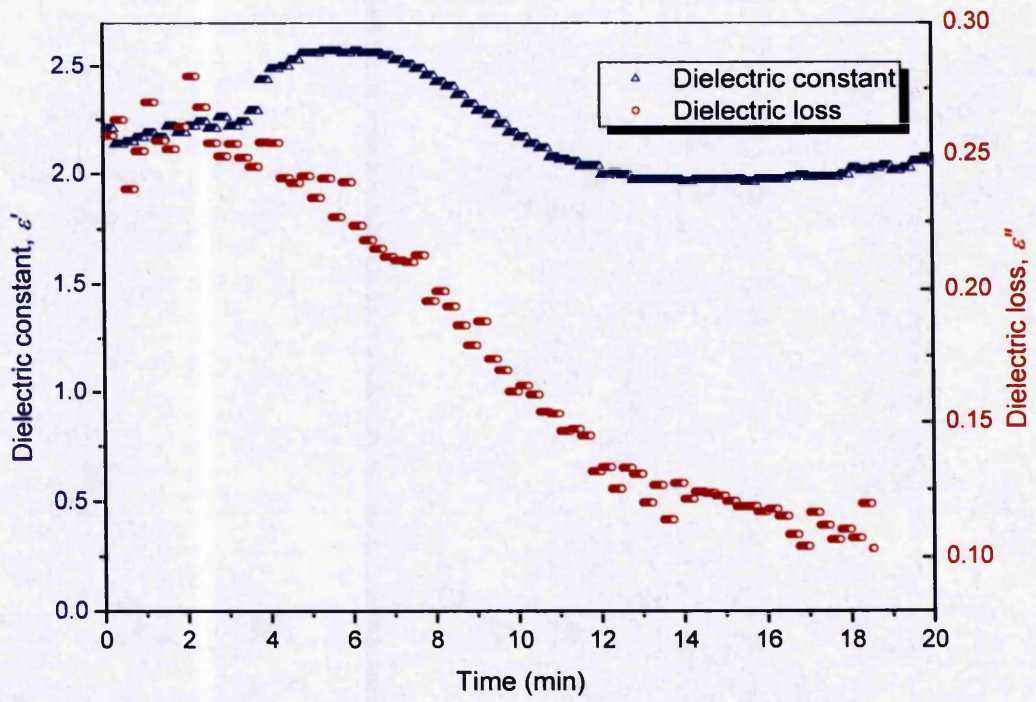

Figure 7.39: *Dielectric constant and dielectric loss of the uncured LY/HY5052 epoxy resin against time during microwave heating at 10°C/min.*

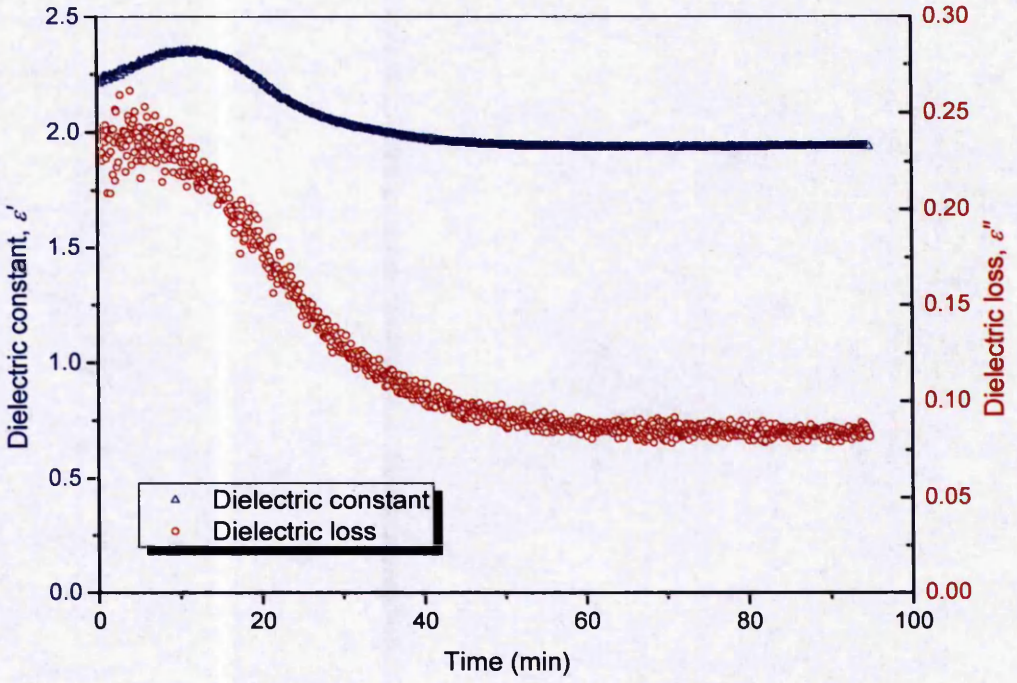

Figure 7.40: *Dielectric constant and dielectric loss of the uncured LY/HY5052 epoxy resin as a function of time during microwave heating at 100°C.*

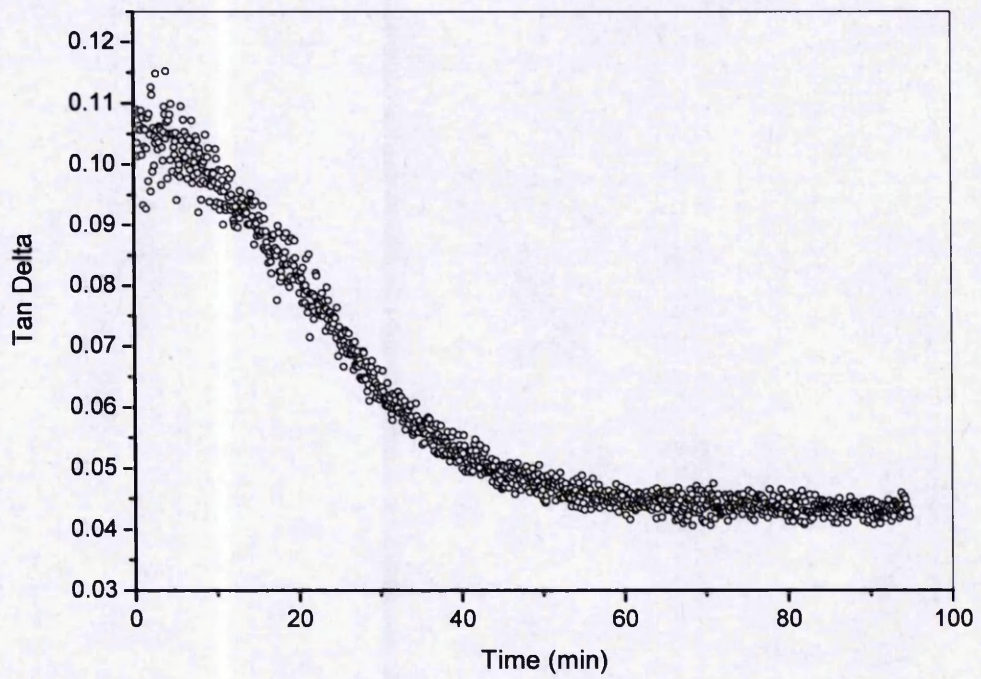

Figure 7.41: *Tangent Delta of the uncured LY/HY5052 epoxy resin as a function of time during microwave curing at 100°C.*

The dielectric properties of both thermally and microwave cured LY/HY5052/carbon and LY/HY5052/glass composites were also measured at room temperature using the cavity perturbation method. The obtained values are given below in Table 7.4. The results showed that the conventionally cured carbon fibre composites yielded the higher dielectric constant value, probably due to their higher carbon fibre volume fraction. Conversely, the dielectric properties of the glass fibre composites produced both thermally and by microwave heating were found to be similar.

Table 7.4: *Average dielectric constant and dielectric loss values for both thermally and microwave cured LY/HY5052/carbon and LY/HY5052/glass composites.*

Composite System	Dielectric Constant (ε')	Dielectric Loss (ε'')
CT-LY/HY5052/carbon	6.14 ± 0.4	$0.024 \pm 5 \times 10^{-3}$
MW-LY/HY5052/carbon	5 ± 0.2	$0.020 \pm 4 \times 10^{-3}$
CT-LY/HY5052/glass	2.8 ± 0.1	$0.038 \pm 4 \times 10^{-3}$
MW-LY/HY5052/glass	2.75 ± 0.1	$0.042 \pm 2 \times 10^{-3}$

(CT = Conventional Thermal RTM Processing; MW = Microwave RTM Processing)

7.6 Summary

The fibre volume and void volume fractions of both thermally and microwave cured LY/HY5052/carbon and LY/HY5052/glass composites were determined by means of matrix digestion with nitric acid in a microwave oven and both optical microscopy and matrix digestion, respectively. The results indicated that all composites exhibited minimal void contents (< 2%) with the thermally cured LY/HY5052/carbon composites exhibiting the highest value. Defects in the produced composites were examined using a jet probe inspection ultrasonic C-scan in through transmission mode. No significant differences were identified between the thermally and microwave cured LY/HY505/carbon and LY/HY5052/glass composite panels, respectively. Both types of composites exhibited minimal defects with small variations in the ultrasonic signal attenuation. The latter also verified that the distribution of the electric field within the applicator was sufficiently uniform during microwave curing of the composites.

The mechanical properties of the fabricated composite panels were evaluated by means of four-point bending and short-beam shear testing. The overall average values of the flexural modulus, flexural strength and interlaminar shear strength for the LY/HY5052/carbon and LY/HY5052/glass composites cured both thermally and by microwave heating are summarised below in Table 7.5. The results revealed that the flexural properties of the microwave cured LY/HY5052/carbon composites were similar, if not slightly superior, to those of their conventionally cured counterparts. The interlaminar shear strength of the former was also found to be higher. On the other hand, both flexural properties and interlaminar shear strength were similar between the thermally and microwave cured LY/HY5052/glass composites.

These findings were supported by observations of the fracture surface morphology of the composite samples subjected to mechanical testing using scanning electron microscopy. Furthermore, dielectric measurements of the uncured LY/HY5052 epoxy resin via the cavity perturbation method showed that the dielectric constant, dielectric loss and tan Delta of the neat resin decreased exponentially with time during the curing process. The dielectric properties of the cured composites were also determined. The thermally cured LY/HY5052/carbon fibre composites yielded a higher dielectric constant compared to those cured by microwave heating, possibly due to the higher fibre volume fraction of the former. The dielectric properties of both conventionally and microwave cured LY/HY5052/glass fibre composites were similar.

Table 7.5: *Overall average values of flexural properties and interlaminar shear strength for the LY/HY5052/carbon and LY/HY5052/glass composites manufactured by both conventional thermal and microwave RTM processing.*

Composite System	Flexural Modulus (GPa)	Flexural Strength (MPa)	Interlaminar Shear Strength (MPa)
CT-LY/HY5052/carbon	44 ± 1	554 ± 44	50 ± 1
MW-LY/HY5052/carbon	37 ± 2 45.2*	493 ± 27 602*	54.5 ± 1
CT-LY/HY5052/glass	23 ± 1	364 ± 20	48 ± 2
MW-LY/HY5052/glass	17 ± 2 22.1**	322 ± 32 418**	45 ± 2

(CT = Conventional Thermal RTM Processing; MW = Microwave RTM Processing)

* Normalised values to an equivalent carbon fibre volume fraction of 33%.

** Normalised values to an equivalent glass fibre volume fraction of 26%.

CHAPTER 8

Conclusions and Future Work

8.1 Conclusions

The conclusions derived from this work are summarised in this chapter. In particular, the microwave assisted RTM technique was successfully employed for the manufacture of both carbon fibre and glass fibre reinforced epoxy composites. A new moulding tool was constructed from Macor, a machinable glass ceramic, and was used in microwave RTM processing as a substitute of the standard metal mould used in conventional thermal RTM processing. Macor appeared to be a good choice for a mould material, due to its suitable mechanical stiffness and dielectric properties. The composite panels fabricated by microwave heating exhibited minimal thickness variation across their surface. The average thickness of the microwave cured composites, however, was slightly higher than that of their thermally cured counterparts due to the difference in the depth of the cavity between the Macor and the metal mould.

The temperature profiles recorded during microwave processing indicated that the employed control system was able to maintain a stable cure temperature and achieve uniform heating of the composite samples during microwave processing. The latter was also verified by the high degrees of cure of the fabricated composite samples, as shown by TMDSC analysis, and the small variations in the ultrasonic signal attenuation of the composite panels, as indicated by C-scan inspection. Temperature stability was provided by adjusting the microwave power and uniformity of the electric field distribution within the applicator was achieved by varying the excitation frequency between 4 – 8 GHz. The maximum amplifier power output used during microwave heating was 250 W, while the power available for conventional thermal heating was 4 KW.

Dynamic and isothermal DSC analysis on the uncured LY/HY5052 resin system indicated that the optimal cure cycle for conventional processing was 3 hours at 100°C. The cure cycle, however, was reduced to 90 minutes at 100°C for microwave processing, based on measurements of the dielectric properties of the uncured resin. As a result, a 50% reduction in the cure cycle time was achieved through microwave

heating. For comparative reasons, the same cure temperature was used in both curing methods.

The degrees of cure across the produced composite panels were determined using TMDSC. The results showed that both LY/HY5052/carbon and LY/HY5052/glass composites were fully cured, achieving a degree of cure of over 99%. The dynamic mechanical properties of the fabricated composites were also investigated using DMTA. Although both types of LY/HY5052/carbon composites yielded similar T_g values, the glass transition appeared to be more intense for the microwave cured samples than their thermally cured counterparts. The intensity of the β-transition, however, was found to be similar between thermally and microwave cured LY/HY5052/carbon composites, while the position of the β-transition peak was shifted by 15°C to a higher temperature for the microwave cured samples. On the other hand, the T_g values and intensities of the glass and β-transition for both thermally and microwave cured LY/HY5052/glass composites were similar. Nevertheless, a smaller 4°C shift in the position of the β-transition to a higher temperature was observed this time for the microwave cured composites. These differences suggest possible alterations in the cross-linking path, and thus the molecular structure formed, between microwave and conventional thermal curing.

The molecular weight between cross-links (M_c) and cross-link density (v_e) of the produced composites were calculated in order to examine any variations in the network structure as a result of the curing method employed. The microwave cured LY/HY5052/carbon composites exhibited higher M_c and lower v_e values than those cured thermally, suggesting that microwave curing resulted in a less packed network structure with a larger distance between cross-links. The M_c and v_e values, however, were comparable for both thermally and microwave cured LY/HY5052/glass composites, indicating similar extents of molecular packing between the two types of composites. These findings were consistent with the results from the DMTA analysis.

The effect of the curing method upon the cross-linking path was evaluated by comparing the infrared spectra of the produced composites. The latter were obtained using Fourier transform infrared spectroscopy (FTIR). The intensities of the ether

group absorption bands at 1103 cm^{-1} and 1024 cm^{-1} were considerably increased in the IR spectra of the conventionally cured LY/HY5052/carbon composites compared to those of their microwave cured counterparts, indicating that the epoxide-hydroxyl etherification reaction was more prominent during thermal curing than microwave curing. This increase, however, was found to be less prominent between the conventionally and microwave cured LY/HY5052/glass composites.

The fibre volume and void volume fractions of the fabricated composites were determined by matrix digestion with nitric acid and by optical microscopy. All composites yielded minimal void contents (< 2%), with the conventionally cured LY/HY5052/carbon composites exhibiting the highest value. The fibre volume fractions of the thermally cured composites were higher than those cured by microwaves, owing to the difference in the cavity depth between the metal and the Macor mould employed. Furthermore, the overall quality and defects of the produced panels were assessed through ultrasonic C-scan inspection. The C-scan traces obtained revealed that all composites had minimal defects and no significant differences were observed between the thermally and microwave cured LY/HY5052/carbon and LY/HY5052/glass composite panels, respectively.

The mechanical performance of the produced composites was evaluated by four-point bending and interlaminar shear testing. The results indicated that the flexural strength and flexural modulus of the microwave cured LY/HY5052/carbon composites were similar, if not slightly superior, to those of their thermally cured counterparts, while the interlaminar shear strength (ILSS) of the former was found to be higher. Conversely, mechanical testing showed comparable flexural strength, flexural modulus and interlaminar shear strength values between the thermally and microwave cured LY/HY5052/glass composites.

The above findings were also supported by observations of the fracture surface morphology of the composite samples subjected to mechanical testing using scanning electron microscopy (SEM). The main failure modes in four-point bending for both thermally and microwave cured LY/HY5052/carbon and LY/HY5052/glass composites, respectively, were tensile and shear. Examination of the fracture surface of samples failed in interlaminar shear testing revealed a significant amount of clean

fibres for the thermally cured LY/HY5052/carbon composites, as opposed to fibres thoroughly coated with resin for their microwave cured counterparts, which in turn indicates a stronger fibre-matrix interface for the latter. No significant differences, however, were observed regarding the fracture surface morphology between the thermally and microwave cured LY/HY5052/glass composite samples subjected to interlaminar shear testing.

The cavity perturbation method was used to measure the dielectric properties of the uncured LY/HY5052 resin system. The results showed that the dielectric constant, dielectric loss and tan Delta of the neat resin initially increased, as the temperature was raised, and then decreased exponentially with time during microwave curing. The dielectric properties of the cured composites were also determined. The thermally cured LY/HY5052/carbon composites exhibited a higher dielectric constant compared to those cured by microwave heating, while the dielectric properties of both conventionally and microwave cured LY/HY5052/glass composites were found to be similar.

As mentioned in Chapter 2, the acceleration of the cure kinetics of thermosetting resins is one of the most commonly reported "microwave effect". Whether, however, this is a result of a specific microwave effect or not is still under consideration, as some researchers have shown favourable results while others have reported the opposite. One of the models proposed so far, assumes that while the reaction time is considerably reduced through the use of microwaves, the kinetics or mechanism of the reaction is not altered. The reduction in the reaction time is caused by the drastic enhancement of the system temperature, and hence the reaction rate, due to thermal dielectric heating induced by microwave irradiation. On the other hand, the alternative model suggests that the reaction rate enhancement is caused by a specific activation effect due to microwave radiation in addition to dielectric heating. In this work, the duration of the cure cycle was reduced by 50% through microwave processing. The overall mechanical properties of the microwave cured composites, however, were found to be similar, and in some cases slightly superior, to those of their thermally cured counterparts. This highlights the effectiveness of microwave radiation as an alternative power source and is postulated to be predominantly due to dielectric heating of the resin system during the curing process, resulting in

composites with comparable mechanical properties in significantly less cure cycle time. Small differences, however, were detected in the network structure between thermally and microwave cured composites, as indicated by the DMTA and FTIR results, which suggests that microwave heating may have also affected to a certain extent the cross-linking path followed. Hence the results presented in this work are not conclusive as to whether there is a specific microwave induced activation effect or just dielectric heating during microwave curing of fibre reinforced polymer composites.

8.2 Future Work

The results presented in this work underline the potential of microwave heating in improving composite processing and manufacture. Further research, however, is necessary in order to supplement our understanding on how microwave processing affects the overall properties of composites and hence expand its ability to be implemented into current composite manufacturing techniques.

In order to use resin systems that require a higher cure temperature, a higher amplifier power output could be used. This could also enable a higher heating rate to be achieved during the curing process, effectively reducing further the cure cycle. The possibility, however, of generating large exotherms which could degrade the resin should be considered.

Other microwave cavities could be also designed to further improve the electric field distribution. Provided a source of higher microwave power is available, the cavities could be larger in size, allowing larger composite samples of more complicated shapes to be cured. In the case of microwave RTM processing, this means that more complicated mould tools would have to be constructed. In particular, a mould tool of variable thickness could be constructed and used in microwave RTM processing in order to investigate the ability of microwaves to penetrate composite layers of different thickness within the same panel.

Composite samples with higher fibre volume fractions could be cured using microwave RTM processing. This could be initially attempted with glass fibre composites, due to the desirable dielectric properties they possess, and subsequently with carbon or aramid fibre composites. As the fibre volume fraction of the composite sample increases, however, the internal pressure applied to the mould tool increases as well, as a result of the increase in the resin injection pressure in order to achieve proper wetting of the fibres.

Since carbon fibre epoxy composites are largely tailored for aerospace applications, the aging properties of the microwave cured composites could be assessed by comparing them against those obtained from conventional thermal processes. This is usually done by exposing composite samples to specific conditions (approximately 70°C temperature and 80% humidity) for a predetermined period of time and then evaluating their mechanical and physical properties.

Finally, recent research showed that the resin/hardener ratio in order to obtain the maximum T_g in a resin system may not be the same for both thermal and microwave curing [161]. Thus, the resin formulation in commercial systems could be manipulated in such way that a higher T_g is obtained through microwave curing than thermal curing, resulting in fibre reinforced composites with superior mechanical and physical properties.

REFERENCES

REFERENCES

1. J. Zhou, et al., "Research on the technology and the mechanical properties of the microwave processing of polymer", *Journal of Materials Processing Technology,* **137**(1-3), pp. 156-158 (2003).
2. J. Mijovic and J. Wijaya, "Review of cure of polymers and composites by microwave energy", *Polymer Composites,* **11**, pp. 184-191 (1990).
3. H. S. Ku, et al., "Productivity improvement through the use of industrial microwave technologies", *Computers & Industrial Engineering,* **42**(2-4), pp. 281-290 (2002).
4. Y. V. Bykov, et al., "High-temperature microwave processing of materials", *Journal of Physics D: Applied Physics,* **34**(13), pp. R55-R75 (2001).
5. E. T. Thostenson and T.-W. Chou, "Microwave processing: fundamentals and applications", *Composites Part A: Applied Science and Manufacturing,* **30**(9), pp. 1055-1071 (1999).
6. R. J. Agrawal and L. T. Drzal, "Effect of Microwave Processing on Fibre-Matrix Adhesion in Composites", *Journal of Adhesion,* **29**, pp. 63-79 (1989).
7. S. M. Singer, et al., "Effects of Processing on Tensile Properties of an Epoxy/Amine Matrix: Continuous Electromagnetic and/or Thermal Curing", *SAMPE Quarterly,* **20**(2), pp. 14-18 (1989).
8. N. S. Strand, "Fast Microwave Curing of Thermoset Parts", *Modern Plastics,* **57**(10), pp. 64-67 (1980).
9. P. L. Mallick, *Fibre-Reinforced Composites: Materials, Manufacturing and Design*, 2nd ed., Marcel Dekker Inc., New York, 1993.
10. P. L. Ku, "Epoxy Resins: Their Manufacture and Applications", *Advances in Polymer Technology,* **8**(1), pp. 81-91 (1988).
11. D. Feldman and A. Barbalata, *Synthetic Polymers: Technology, Properties, Applications*, 1st ed., Chapman & Hall, London, 1992.
12. I. Skeist, *Handbook of Adhensives*, 2nd ed., Van Nostrand Reinhold, New York, 1977.
13. Greenlee, *Manufacture of Epoxide Resins*, 1954, Vol. 2.
14. Wynstra, "The Chemistry of Epoxy Resins", *American Chemical Society,* (1956).

15. H. Lee and K. Neville, *Epoxy Resins: Their Applications and Technology*, McGraw-Hill Book Company, Inc., 1957.
16. E. Marand, et al., "Comparison of Reaction Mechanisms of Epoxy Resins Undergoing Thermal and Microwave Cure from in Situ Measurements of Microwave Dielectric Properties and Infrared Spectroscopy", *Macromolecules,* **25**(8), pp. 2243-2252 (1992).
17. R. Yusoff, "Microwave assisted RTM processing of carbon/epoxy composites", *PhD Thesis,* (The University of Manchester, 2004).
18. M. H. Geier, *Quality Handbook of Composite Materials*, Chapman & Hall, London, 1994.
19. K. K. Chawla, *Composite Material and Engineering*, 2nd ed., Springer-Verlag, New York, 1998.
20. D. R. Askeland, *The Science and Engineering of Materials*, 2nd ed. PWS-Kent, 1989, p. 591.
21. C. D. Rudd, et al., *Liquid Moulding Technologies*, 1st ed., Woodhead Publishing Limited, Cambridge, 1997.
22. E. Fitzer, in *Carbon Fibers Filaments and Composites*, edited by J. L. Figueiredo, C. A. Bernardo, R. T. K. Baker, and K. J. Huttinger, eds. (Kluwer Academic Publishers, Dordrecht, 1990), pp. 3-41.
23. G. M. Jenkins and K. Kawamura, *Polymeric carbons-carbon fibre, glass and char*, Cambridge University Press, 1976.
24. G. Dorey, "Carbon fibres and their applications", *Journal of Physics D: Applied Physics,* **20**(3), pp. 245-256 (1987).
25. D. D. L. Chung, *Carbon fiber composites*, Butterworth-Heinemann, 1994.
26. P. J. Goodhew, et al., "A review of the fabrication and properties of carbon fibres", *Materials Science and Engineering,* **17**(1), pp. 3-30 (1975).
27. S. Damodaran, et al., *Journal of the Textile Institute,* **81**(4), pp. 384-420 (1990).
28. E. Fitzer and W. Frohs, *Chemical Engineering & Technology,* **13**(1), pp. 41-49 (1990).
29. W. W. Wright, *Compos. Polym.,* **3**(4), pp. 231-257 (1990).
30. C. E. Knox, *Handbook of composites*, Van Nostrand Reinhold, 1982.
31. E. P. Pleuddemann, *Silane Coupling Agents*, 2nd ed., Plenum Press, New York, 1992.

32. A. T. DiBenedetto, "Tailoring of Interfaces in Glass Fiber Reinforced Polymer Composites: A Review", *Materials Science and Engineering, Part A,* **302**(1), pp. 74-82 (2001).

33. J. M. Berthelot, *Composite Materials Mechanical Behaviour and Structural Analysis*, Springer, New York, 1998.

34. H. F. Mark, et al., *Encyclopedia of Polymer Science and Engineering*, 2nd ed., John Wiley and Sons, New York, 1986.

35. C. T. Chou and L. S. Penn, "Chemical bonding and physical interaction by attached chains at the fiber-matrix interface", *Journal of Adhesion,* **36**, pp. 125-133 (1991).

36. L. S. Penn, et al., "The study of reactive functional groups in adesive bonding at the aramid-epoxy interface", *Journal of Adhesion,* **23**, pp. 163-172 (1987).

37. Y. Wu and G. C. Tesoro, "Chemical modification of Kevlar fiber surfaces and of model diamides", *Journal of Applied Polymer Science,* **31**, pp. 1041-1050 (1986).

38. S. R. Wu, et al., "Kevlar fiber-epoxy adhesion and its effect on composite mechanical and fracture properties by plasma and chemical treatment", *Journal of Applied Polymer Science,* **62**, pp. 1347-1358 (1996).

39. J. Murphy, *Reinforced Plastics Handbook*, Elsevier Science Publishers Ltd., Oxford, 1994.

40. J. M. Charrier, *Polymeric Materials and Processing: Plastics, Elastomers and Composites*, Hanser Gardner Publications, 1991.

41. S. T. Peters, *Handbook of Composites*, Chapman & Hall, London, 1998.

42. K. Poter, *An Introduction to Composite Products-Design, Development and Manufacture*, Chapman & Hall, London, 1997.

43. K. D. Potter, "The early history of the resin transfer moulding process for aerospace applications." *Composites Part A: Applied Science and Manufacturing,* **30**(5), pp. 619-621 (1999).

44. C. D. Rudd, et al., "Effects of process variables on cycle time during resin transfer moulding for high volume manufacture", *Materials Science and Technology,* **6**, pp. 656-664 (1990).

45. N. R. L. Pearce, et al., "Improving the resin transfer moulding process for fabric-reinforced composites by modification of the fabric architecture",

Composites Part A: Applied Science and Manufacturing, **31**(12), pp. 1433-1441 (2000).

46. V. M. Karbhari and S. G. Slotte, "Effect of fiber architecture on manufacturability and crush performance of a stiffened plate type RTM structure", *Composite Structures,* **26**(1-2), pp. 83-93 (1993).
47. Y. Onur Kas and C. Kaynak, "Ultrasonic (C-scan) and microscopic evaluation of resin transfer molded epoxy composite plates", *Polymer Testing,* **24**, pp. 114-120 (2005).
48. G. Lebrun, et al., "Experimental investigation of resin temperature and pressure during filling and curing in a flat steel RTM mould", *Composites Part A: Applied Science and Manufacturing,* **27**(5), pp. 347-355 (1996).
49. N. Pearce, et al., "A study of the effects of convergent flow fronts on the properties of fibre reinforced composites produced by RTM", *Composites Part A: Applied Science and Manufacturing,* **29**(1-2), pp. 141-152 (1998).
50. S. Bickerton, et al., "Fabric structure and mold curvature effects on preform permeability and mold filling in the RTM process. Part I. Experiments", *Composites Part A: Applied Science and Manufacturing,* **31**(5), pp. 423-438 (2000).
51. N. C. W. Judd and W. W. Wright, "Voids and their effects on the mechanical properties of composites - an Appraisal", *SAMPE Journal,* **14**(1), pp. 10-14 (1978).
52. J. Varna, et al., "Effect of voids on failure mechanisms in RTM laminates", *Composites Science and Technology,* **53**(2), pp. 241-249 (1995).
53. R. V. Decareau, *Microwaves in the Food Processing Industry,* Academic Press Inc., London, 1985.
54. D. E. Clark, et al., "Processing materials with microwave energy", *Materials Science and Engineering A,* **287**(2), pp. 153-158 (2000).
55. R. V. Decareau and R. A. Peterson, *Microwave Processing and Engineering,* Ellis Horwood Series in Food Science and Technology, Ellis Horwood Ltd. and VCH Verlagsgesellschaft mbH, 1986.
56. J. B. Wei, et al., "Recent progress in microwave processing of polymers and composites", *Trends in Polymer Science,* **4**, pp. 18-24 (1996).
57. K. F. Sander, *Microwave Components and Systems,* Addison-Wesley Publishing Company, Inc., 1987.

58. R. Meredith, *Engineers Handbook of Industrial Microwave Heating*, Power Series 25, Herts, 1998.

59. H. E. Thomas, *Handbook of Microwave Techniques and Equipment*, Prentice-Hall, Inc. & Englewood Cliffs, N.J., 1972.

60. S. Zhou and M. C. Hawley, "A study of microwave reaction rate enhancement effect in adhesive bonding of polymers and composites", *Composite Structures,* **61**(4), pp. 303-309 (2003).

61. L. A. Fellows and M. C. Hawley, "Experimental Design and Preliminary Results of Microwave Heating of Complex Shapes by Mode-Switching Techniques", *Proceedings of 37th International SAMPE Symposium and Exhibition*, p. 914 (1992).

62. Q. L. Van and A. Gourdenne, "Microwave Curing of Epoxy Resins with Diamino DiphenylMethane-I. General Features", *European Polymer Journal,* **23**(10), pp. 777-780 (1987).

63. A. Gourdenne, et al., "Cross-linking of Thermosetting Resins by Microwave Heating Quantitative Approach", *Polymer Preprints,* **20**(2), pp. 471-477 (1979).

64. A. Gourdenne and Q. L. Van, "Intimate Study of Microwave Curing", *Polymer Preprints,* **22**(2), pp. 125-127 (1981).

65. A. D. Surrett, et al., "Polymer curing using variable frequency microwave processing", in *Microwave Processing of Materials IV,* Materials Research Society Proceedings, edited by M. F. Iskander, R. J. Lauf, and W. H. Sutton, eds. (San Francisco, 1994), pp. 691-696.

66. M. T. Demuse and A. C. Johnson, "Variable frequency microwave processing of thermoset polymer matrix composites", in *Microwave Processing of Materials IV,* Materials Research Society Proceedings, edited by M. F. Iskander, R. J. Lauf, and W. H. Sutton, eds. (San Francisco, 1994), pp. 723-727.

67. J. Mijovic and J. Wijaya, "Comparative Calorimetric Study of Epoxy Cure by Microwave vs. Thermal Energy", *Macromolecules,* **23**(15), pp. 3671-3674 (1990).

68. M. C. Finzel, "Comparison of Multimode Microwave and Thermal Methods for Curing Epoxy/Amine Systems", presented at the AICHE Conferenece of

Emerging Technologies in Materials, Minneapolis, Minnessota, August, 1987.

69. B. Fu and M. C. Hawley, "Comparative Study of Continuous-Power and Pulsed-Power Microwave Curing of Epoxy Resins", *Polymer Engineering and Science,* **40**(10), pp. 2133-2143 (2000).
70. E. Karmazsin, et al., "Use of continuous and pulsed microwaves for quick polymerization of epoxy resins: Study of some thermomechanical properties", *Thermochimica Acta,* **93**, pp. 305-309 (1985).
71. J. Jacob, et al., "Review Thermal and non-thermal interaction of microwave radiation with materials", *Journal of Materials Science,* **30**, pp. 5321-5327 (1995).
72. J. Wei, et al., "Comparison of Microwave and Thermal Cure of Epoxy resins", *Polymers Engineering and Science,* **33**(17), pp. 1132-1140 (1993).
73. J. Wei and M. C. Hawley, "Utilization of microwaves in processing of polymer composites - past, present and future", *Polymeric Materials Science and Engineering,* **66**, p. 478 (1992).
74. J. Wei, et al., "Kinetics Modeling and Time-Temperature-Transformation Diagram of Microwave and Thermal Cure of Epoxy Resins", *Polymer Engineering and Science,* **35**(6), pp. 461-470 (1995).
75. F. Y. C. Boey, et al., "Microwave curing of epoxy-amine system - effect of curing agent on the rate enhancement", *Polymer Testing,* **18**, pp. 93-109 (1999).
76. D. A. Lewis, et al., *Polymer Preprints,* **28**(2), p. 330 (1987).
77. J. C. Hedrick, et al., *Polymer Preprints,* **29**, p. 363 (1988).
78. K. R. Baker, et al., "Dielectric constant measurement of polymers undergoing cure", *Polymeric Materials Science and Engineering,* **66**, pp. 474-475 (1992).
79. M. Wallace, et al., "Investigation of the microwave curing of an epoxy resin system", *Tech. Report No. TP01PUB20* (Society of Manufacturing Engineers, 2001).
80. J. Mijovic, et al., "Mechanistic Modeling of Epoxy-Amine Kinetics. 2. Comparison of Kinetics in Thermal and Microwave Fields", *Macromolecules,* **25**, pp. 986-989 (1992).
81. J. Mijovic, et al., "Mechanistic Modeling of Epoxy-Amine Kinetics. 1. Model Compound Study", *Macromolecules,* **25**, pp. 979-985 (1992).

82. J. Mijovic, et al., "*In Situ* Real-Time Study of Crosslinking Kinetics in Thermal and Microwave Fields", *Polymers for Advanced Technologies,* **9**(4), pp. 231-243 (1998).

83. D. J. T. Hill, et al., "A Systematic Study of the Microwave and Thermal Cure Kinetics of the DGEBA/DDS and DGEBA/DDM Epoxy-amine Resin Systems", *Polymers for Advanced Technologies,* **13**, pp. 353-362 (2002).

84. J. Mijovic, et al., "A Study of Reaction Kinetics by Near-Infrared Spectroscopy. 2. Comparison with Dielectric Spectroscopy of Model and Multifunctional Epoxy/Amine Systems", *Macromolecules,* **28**(8), pp. 2797-2806 (1995).

85. D. G. Rogers, et al., "Anomalies between microwave and thermal cure kinetics of epoxy-amine resin systems", *High Performance Polymers,* **11**, pp. 27-39 (1999).

86. E. Karmazsin, et al., presented at the III European Symposium on Thermal Analysis and Calorimetry, Interlaken, Switzerland, 1984.

87. S. L. Bai, et al., "A comparative study of the mechanical behaviour of an epoxy resin cured by microwaves with one cured thermally", *European Polymer Journal,* **31**(9), pp. 875-884 (1995).

88. C. Jordan, et al., "Comparison of Microwave and Thermal Cure of an Epoxy/Amine Matrix", *Polymer Engineering and Science,* **35**(3), pp. 233-239 (1995).

89. V. Tanrattanakul and K. SaeTiaw, "Comparison of Microwave and Thermal Cure of Epoxy-Anhydride Resins: Mechanical Properties and Dynamic Characteristics", *Journal of Applied Polymer Science,* **97**, pp. 1442-1461 (2005).

90. W. I. Lee and G. S. Spriner, "Microwave curing of composites", *Journal of Composite Materials,* **18**, pp. 387-409 (1984).

91. F. Y. C. Boey and W. L. Lee, "Microwave radiation curing of a thermosetting composite", *Journal of Materials Science Letters,* **9**, pp. 1172-1173 (1990).

92. P. S. Mooteri, et al., "Studies on Mechanical Behavior of Microwave and Thermally Cured Glass Fiber Reinforced Polymer Composites", *Journal of Reinforced Plastics and Composites,* **25**(5), pp. 503-512 (2006).

93. C. Nightingale and R. J. Day, "Flexural and interlaminar shear strength properties of carbon fibre/epoxy composites cured thermally and with

microwave radiation", *Composites Part A: Applied Science and Manufacturing,* **33**(7), pp. 1021-1030 (2002).

94. Y. Qiu and M. Hawley, "Composite Material Processing in a Single Mode Cavity with Variable Frequency Microwaves", presented at the 12th International Conference on Composite Materials, Paris, France, July, 1999.
95. Y. Liu, et al., "Microwave Irradiation of Nadic-End-Capped Polyimide Resin (RP-46) and Glass-Graphite-PR-46 Composites: Cure and Process Studies", *Journal of Applied Polymer Science,* **73**, pp. 2391-2411 (1999).
96. X. Fang and D. A. Scola, "Investigation of Microwave Energy to Cure Carbon Fiber Reinforced Phenylethynyl-Terminated Polyimide Composites, PETI-5/IM7", *Journal of Polymer Science: Part A: Polymer Chemistry,* **37**, pp. 4616-4628 (1999).
97. J. Wei, et al., "Microwave Processing of Crossply Continuous Graphite Fibre/Epoxy Composites", *SAMPE Journal,* **27**(1), pp. 33-39 (1991).
98. S. W. Lye and F. Y. C. Boey, "PC-based Monitoring and Control System for Microwave Curing of Polymer Composites", *Material and Manufacturing Processes,* **9**, pp. 851-868 (1994).
99. S. L. Bai and V. Djafari, "Interfacial properties of microwave cured composites", *Composites,* **26**(9), pp. 645-651 (1995).
100. F. Y. C. Boey and C. Y. Yue, "Interfacial strength of a microwave-cured epoxy-glass composite", *Journal of Materials Science Letters,* **10**, pp. 1333-1334 (1991).
101. R. J. Day and S. H. C. Yau, "Investigation of the Effect of Microwave Curing upon the Micromechanics of Kevlar/epoxy Composites", in *Proceedings of the 10th International Conference on Composite Materials*, edited by (ICCM Society, Vancouver, 1995), pp. 705-710.
102. R. M. V. G. K. Rao, et al., "Studies on Tensile and Interlaminar Shear Strength Properties of Thermally Cured and Microwave Cured Glass-Epoxy Composites", *Journal of Reinforced Plastics and Composites,* **25**(7), pp. 783-795 (2006).
103. L. T. Drzal, et al., "Enhanced Chemical Bonding at the Fiber-Matrix Interphase in Microwave Processed Composites", *Materials Research Society Proceedings,* **189**, pp. 449-454 (1991).

104. K. J. Hook, et al., "Effects of Microwave Processing on Fiber-Matrix Adhesion. II. Enhanced Chemical Bonding of Epoxy to Carbon Fibers", *Journal of Adhesion,* **32**, pp. 157-170 (1990).

105. F. Y. C. Boey and T. H. Lee, "Electromagnetic radiation curing of an epoxy/fibre glass reinforced composite", *Radiation Physics and Chemistry,* **38**(4), pp. 419-423 (1991).

106. C. Y. Yue and H. C. Looi, "Influence of thermal and microwave processing on the mechanical and interfacial properties of a glass/epoxy composite", *Composites,* **26**(11), pp. 767-773 (1995).

107. F. L. Paulaskas and T. T. Meek, "Processing of Thermoset Prepreg Laminates via Exposure to Microwave Radiation", *Materials Research Society Symposium Proceedings,* **347**, pp. 743-752 (1994).

108. R. J. Day and E. Samoladas, "Micromechanics of model carbon/epoxy composites cured using microwave heating", *Science and Engineering of Composite Materials,* **7**(12), pp. 23-50 (1998).

109. M. S. Johnson, et al., "Microwave assisted resin transfer moulding", *Composites Part A: Applied Science and Manufacturing,* **29**(1-2), pp. 71-86 (1998).

110. A. R. Rahmat, "Microwave Assisted Resin Transfer Moulding", *PhD Thesis,* (UMIST, 2002).

111. D. R. Suckley, "Microwave processing of the araldite LY5052:HY5052 epoxy resin system", *PhD Thesis,* (UMIST, 2000).

112. J. M. Hodgkinson, *Mechanical Testing of Advanced Fibre Composites*, Woodhead Publishing Ltd and CRC Press LLC, 2000.

113. ASTM D 6272, "Standard test method for flexural properties of unreinforced and reinforced plastics and electrical insulating materials by four-point bending", (2002).

114. ASTM D 2344/D 2344M, "Standard test method for short-beam strength of polymer matrix composite materials and their laminates", (2000).

115. P. J. Haines, *Principles of Thermal Analysis and Calorimetry*, The Royal Society of Chemistry, 2002.

116. TA Instruments DMA Q800, Product Brochure.

117. P. J. Haines, *Thermal Methods of Analysis: Principles, Applications and Problems*, Blackie Academic & Professional, 1995.

118. ABT 1-0018, "Airbus UK Test Specification", (2003).

119. ASTM D 3171, "Standard test method for constituent content of composite materials", (1999).

120. R. Halmshaw, *Non-destructive Testing*, Edward Arnold, 1987.

121. P. J. Goodhew and F. J. Humphreys, *Electron Microscopy and Analysis*, Taylor & Francis, 1988.

122. A. Nesbitt, et al., "Development of a microwave calorimeter for simultaneous thermal analysis, infrared spectroscopy and dielectric measurements", *Measurement Science and Technology,* **15**(11), pp. 2313-2324 (2004).

123. J. B. Lambert, et al., *Organic Structural Spectroscopy*, Prentice-Hall, Inc., 1998.

124. Thermo Electron Nicolet 5700 spectometer, User's Guide.

125. "Macor properties", retrieved 15/7/2007, http://www.precision-ceramics.co.uk/mprop.htm.

126. J. Wei, et al., "Modelling and controlling during microwave and thermal processing of composites", *Materials Research Society Symposium Proceedings,* **269**, pp. 439-445 (1992).

127. S. Montserrat, et al., "Vitrification and dielectric relaxation during the isothermal curing of an epoxy-amine resin", *Polymer,* **44**(1), pp. 101-114 (2003).

128. T. Murayama and J. P. Bell, "Relation between the Network Structure and Dynamic Mechanical Properties of a Typical Amine-Cured Epoxy Polymer", *Journal of Polymers Science: Part A-2,* **8**, pp. 437-445 (1970).

129. M. Ochi, et al., "Mechanical and dielectric relaxations of epoxide resins containing spiro-ring structure", *Journal of polymer science. Polymer physics edition,* **24**(10), pp. 2185-2195 (1986).

130. G. A. Pogany, "Gamma relaxation in epoxy resins and related polymers", *Polymer,* **11**(2), pp. 66-78 (1970).

131. M. Shimbo, et al., "Mechanical relaxation mechanism of epoxide resins cured with acid anhydrides", *Journal of Polymer Science Polymer Physics Edition,* **22**(8), pp. 1461-1470 (1984).

132. P. Guerrero, et al., "Influence of cure schedule and stoichiometry on the dynamic mechanical behaviour of tetrafunctional epoxy resins cured with anhydrides", *Polymer,* **37**(11), pp. 2195-2200 (1996).

133. M. Ochi, et al., "Mechanical relaxation mechanism of epoxide resins cured with aliphatic diamines", *Journal of Polymer Science Polymer Physics Edition,* **20**(4), pp. 689-699 (1982).

134. A. Vazquez, et al., "Interphase modification in unidirectional glass-fibre epoxy composites", *Composites Science and Technology,* **58**, pp. 549-558 (1998).

135. X. Gong, "The Dynamic Mechanical Behavior of Random-in-Plane Short Fiber-reinforced Epoxy Resin Composites", *Polymers for Advanced Technologies,* **7**, pp. 141-145 (1995).

136. J. S. Chen, et al., "Controlled degradation of epoxy networks: analysis of crosslink density and glass transition temperature changes in thermally reworkable thermosets", *Polymer,* **45**, pp. 1939-1950 (2004).

137. L. E. Nielsen and R. F. Landel, *Mechanical Properties of Polymers and Composites*, 2nd ed., Marcel Dekker, Inc., New York, 1994.

138. V. M. Karbhari, "Dynamic Mechanical Analysis of the Effect of Water on E-glass-Vinylester Composites", *Journal of Reinforced Plastics and Composites,* **25**(6), pp. 631-644 (2006).

139. A. N. Fraga, et al., "Relationship between dynamic mechanical properties and water absorption of unsaturated polyester and vinyl ester glass fibre composites", *Journal of Composite Materials,* **37**(17), pp. 1553-1574 (2003).

140. M. Sánchez-Soto, et al., "Curing FTIR study and mechanical characterization of glass bead filled trifunctional epoxy composites", *Composites Science and Technology,* **67**, pp. 1974-1985 (2007).

141. L. Xu and J. R. Schlup, "Etherification versus amine addition during epoxy resin / amine cure: An in situ study using near-infrared spectroscopy", *Journal of Applied Polymer Science,* **67**(5), pp. 895-901 (1998).

142. K. Fryauf, et al., "Curing of glycidyl ethers with aromatic amines: model studies on the effects of tertiary amines as accelerators", *Polymer,* **34**(2), pp. 323-327 (1993).

143. M. Wallace, et al., "Investigation of the microwave curing of the PR500 epoxy resin system", *Journal of Materials Science,* **41**, pp. 5862-5869 (2006).

144. P. Navabpour, et al., "Comparison of the curing kinetics of the RTM6 epoxy resin system using differential scanning calorimetry and a microwave-heated calorimeter", *Journal of Applied Polymer Science,* **99**, pp. 3658-3668 (2006).

145. S. F. M. Almeida and Z. S. N. Neto, "Effect of void content on the strength of composite laminates", *Composite Structures,* **28**, pp. 139-148 (1994).

146. K. J. Bowles and S. Frimpong, "Void effects on the interlaminar shear strength of unidirectional graphite-fiber-reinforced composites", *Journal of Composite Materials,* **26**(10), pp. 1487-1509 (1992).

147. A. R. Chambers, et al., "The effect of voids on the flexural fatigue performance of unidirectional carbon fibre composites developed for wind turbine applications", *International Journal of Fatigue,* **28**, pp. 1389-1398 (2006).

148. M. L. Costa, et al., "The influence of porosity on the interlaminar shear strength of carbon/epoxy and carbon/bismaleimide fabric laminates", *Composite Science and Technology,* **61**, pp. 2101-2108 (2001).

149. H. Jeong, "Effect of voids on the mechanical strength and ultrasonic atteuation of laminated composites", *Journal of Composite Materials,* **31**(3), pp. 276-292 (1997).

150. M. R. Wisnom, et al., "Reduction in interlaminar shear strength by discrete and distributed voids", *Composite Science and Technology,* **56**, pp. 93-101 (1996).

151. Midas-NDT presentation, "Through Transmission Inspection: The Truths & The Myths", (2007).

152. W. H. M. van Dreumel, "Ultrasonic scanning for quality control of advanced fibre composites", *NDT International*, pp. 233-235 (October 1978).

153. V. Tanrattanakul and D. Jaroendee, "Comparison Between Microwave and Thermal Curing of Glass Fiber-Epoxy Composites: Effect of Microwave-Heating Cycle on Mechanical Properties", *Journal of Applied Polymer Science,* **102**, pp. 1059-1070 (2006).

154. Y. Cao and J. Cameron, "Flexural and Shear Properties of Silica Particle Modified Glass Fiber Reinforced Epoxy Composite", *Journal of Reinforced Plastics and Composites,* **25**(4), pp. 347-359 (2006).

155. R. J. Argawal and L. T. Drzal, "Effect of Microwave Processing on Fibre-Matrix Adhesion in Composites", *Journal of Adhesion,* **29**, pp. 63-79 (1989).

156. E. T. Thostenson and T.-W. Chou, "Microwave and Conventional Curing of Thick-Section Thermoset Composite Laminates: Experiment and Simulation", *Polymer Composites,* **22**(22), pp. 197-212 (2001).

157. H. C. Kim and S. K. See, "Electrical properties of unidirectional carbon-epoxy composites in wide frequency band", *Journal of Physics: Part D:Applied Physics,* **23**, pp. 916-921 (1990).

158. N. Sgriccia and M. C. Hawley, "Thermal, morphological, and electrical characterization of microwave processed natural fiber composites", *Composite Science and Technology,* **67**, pp. 1986-1991 (2007).

159. L. Zong, et al., "Dielectric studies of three epoxy resin systems during microwave cure", *Polymer,* **46**, pp. 2638-2645 (2005).

160. S. Carrozzino and G. Levita, "Calorimetric and Microwave Dielectric Monitoring of Epoxy Resin Cure", *Polymer Engineering and Science,* **30**(6), pp. 366-373 (1990).

161. O. Pinprayoon, "Microwave Processing of TGDDM/DDS resin system", *MSc Thesis,* (The University of Manchester, 2007).

APPENDIX

PUBLICATIONS

1. D. A. Papargyris, R. J. Day, A. Nesbitt, D. Bakavos, "Comparison of the mechanical and physical properties of a carbon fibre epoxy composite manufactured by resin transfer moulding using conventional and microwave heating", Accepted for publication in *Composites Science and Technology* in 02/12/2007.

2. D. A. Papargyris, R. J. Day, A. Nesbitt, "Effect of microwave heating on the mechanical and physical properties of a glass fibre epoxy composite produced by resin transfer moulding", (For submission to *Composite Science and Technology*).